Tahribatsız ve Hızlı Yöntemlerle Gıdalarda Kalite Kontrolü

Proje No: 106E057

Prof.Dr. Yasemin Yardımcı Çetin
Yrd.Doç.Dr. Pervin Başaran

ŞUBAT 2009 ANKARA

ÖNSÖZ

Bu projede Türkiye'nin önemli ihracaat kalemlerinden olan fındık ve kırmızı biberdeki aflatoksin maddesinin tespitine yönelik yöntemler geliştirilmiştir. Geliştirilen tahribatsız ve hızlı tespit yöntemlerinin doğruluğu kimyasal analiz sonuçlarına uyumluluk ile ölçülmüştür. Fındık için çeşitli ihracaat kipleri ayrı ayrı ele alınarak her kipe yönelik farklı yöntemler tasarlanmıştır. Kabuklu fındıklarda dış kabuğun küf sporlarına bariyer oluşturması dolayısıyla aflatoksin oluşumuna engel olduğu tespit edilmiş, çarpma seslerine dayalı bir yöntemle esasen çatlak ve kırık fındıkların tespiti için yöntem geliştirilmiştir. İç fındıklar için görüntü işleme yöntemleri üzerinde durulmuş, özellikle hiperspektral görüntülemeye dayalı yöntemler ile başarılı sonuçlar alınmıştır. Bizzat aflatoksinli fındıkların tespiti yerine küflenmiş ve dolayısıyla aflatoksin içermesi hayli muhtemel olan fındıkların tespitinde daha başarılı olunduğu tespit edilmiştir. Bu sonuçlar, literatürde şam fıstığı ve mısır için geçerli olduğu söylenen aflatoksin ve ışınım arasında bire bir ilişki olmadığı saptaması ile uyumludur.

Kırmızı biberde piyasadan uluslararası normlara uygun sağlıklı biber temininde zorluk çekilmiş, yapay küflendirmeye gidilmeden piyasadan alınan biberlerin doğrudan kullanılması tercih edilmiştir. Bu biberler üzerinde hiperspektral görüntü işlemeye dayalı yöntemler sınırlı başarı getirmiştir.

Proje çerçevesinde ODTÜ'de bir doktora, bir yüksek lisans tezi, Süleyman Demirel Üniversitesi'nde bir yüksek lisans tezi yapılmıştır. Projede elde edilen bulgular çeşitli dergi ve konferans yayınına dönüştürülmüştür. Bu konuda yaptığımız çalışmalar hem ülkemizin sorunlarını çözerken hem de uluslararası camiada bir vizibilite sağlamıştır. Bu proje uluslararası işbirliklerine temel oluşturmuş, gıda güvenliği alanındaki bir FP7 ve FAO konsorsiyumu içinde yer alınmıştır.

Bu proje TUBİTAK EEEAG tarafından 1001 projeleri kapsamında 106E057 kodu ile desteklenmiştir.

İÇİNDEKİLER

ŞEKİLLER

TABLOLAR

ÖZET

Aflatoksin kontaminasyonu hem insan sağlığı açısından hem de dış ticaret açısından büyük problemler oluşturmaktadır. Bu projede aflatoksin içeren ve/veya aflatoksin içerme ihtimali yüksek olan küflü fındıkların ses sinyalleri ve hiperspektral görüntüleri kullanarak; aflatoksin içeren kırmızı biberlerin ise hiperspektral görüntüler kullanılarak tespit edilmesi üzerine yöntemler geliştirilmiştir. Kabuğu çatlak fındıkların ayrımında çarpma sesi kullanılmış ve bu ses sinyallerinden Yerel Ayırtaç Tabanları (YAT) yöntemi kullanılarak elde edilen öznitelikler ile %96.5'lik bir doğru sınıflandırma oranına ulaşılmıştır. Kavrulmuş fındıkların sınıflandırılmasında 2B YAT yaklaşımı geliştirilmiş ve bu yöntemle çıkarılan öznitelikler kullanılarak yaklaşık %97'lik bir sınıflandırma doğruluğuna elde edilmiştir. Naturel fındıklarda ise sınıflandırma başarısı yaklaşık % 85 civarında kalmıştır. Kırmızı biberde de hiperspektral görüntüler üzerinde 2B YAT yaklaşımı kullanılarak yaklaşık %80'lik bir sınıflandırma oranına ulaşılmıştır.

Anahtar Kelimeler: Hiperspektral Görüntüleme, Akustik Sinyal İşleme, Yerel Ayırtaç Tabanları, Gıda Güvenliği, Aflatoksin

ABSTRACT

Aflatoxin contamination leads to serious problems in both human health and external trade. In this project, methods were developed to detect the hazelnuts that are either aflatoxin contaminated or prone to contamination by using acoustic and hyperspectral images; and to detect aflatoxin contaminated chili peppers by using hypespectral images. A Local Discriminant Bases (LDB) based algorithm is developed and used to cracked shell hazelnut kernels and a classification accuracy of 96.5% was obtained. A 2D LDB algorithm is developed for the roasted hazelnuts and a classification accuracy of 97% is achieved by the features obtained by this method. The accuracy for the naturel hazelnuts has remained around 85%. The 2D LBD approach is also used for chili peppers images and a classification accuracy of 80% was obtained.

Keywords: Hyperspectral Imaging, Acoustic Signal Processing, Local Discriminant Bases, Food Safety, Aflatoxin

1. GİRİŞ

Fındık ve kırmızı biberde küf oluşması yaygın olup, gelişmeleri insan ve hayvan sağlığı için önemli bir risk oluşturmaktadır. Küflenme bu iki tarım ürünündeki raf ömrünü kısaltan etkenlerden en önemli etkenlerdendir. Küf gelişimi bahçede başlamakta, hasat ve yetersiz uygun olmayan kurutma koşulları nedeniyle gelişebilmekte, depolama ve taşıma sırasında da büyüyebilmektedir. Gıdalarda aflatoksin oluşumu ortam bağıl nemi (ya da ürünün su aktivitesiyle) ilgilidir. Aflatoksinler (B1, B2, G1, G2), Aspergillus türü küfler (A. flavus, A. parasiticus vb. gibi) tarafından belli sıcaklık ve nem koşullarında sentezlenmektedir.

Aflatoksinler karaciğer kanserine neden olduklarından gıdalarda bulunmasına izin verilen miktarları WHO, FDA, EU gibi uluslararası otoriteler tarafından 4-10 (EU) ve 20 (USA) ppb ile sınırlandırılmaktadır.

Ülkemiz koşullarında fındık ve kırmızı biberde aflatoksin oluşumunun önlenmesi veya sınırlandırıması için hasata kadar "iyi tarım pratikleri" ve hasat sonrası "iyi üretim teknikleri" kurallarına uyulması gereklidir. Ancak bu önlemler gerek tek başlarına yeterli olmadıklarından gerekse yaygın olarak uygulanamadığından dolayı aflatoksin problemi tam olarak çözülebilmiş değildir.

Bilindiği üzere, fındık ülkemiz tarımında özellikle de dış ticaretinde önemli bir paya sahiptir. Türkiye yıllara göre 350-600 bin ton yıllık üretimi ile dünya fındık üretiminin %75'ini, dünya fındık ticaretinin ise %70-75'ini gerçekleştirmektedir. Önemli bir kısmı Avupa Birliği ülkelerine ihraç edilen fındığın aflatoksin kontaminasyon düzeyi ihraç edildiği ülkeler tarafından sürekli denetlenmektedir. Yasal limitlerin üzerinde aflatoksin içerdiği belirlenen fındıkların geri dönmesi ve/veya imha edilmesi önemli bir ekonomik kayba neden olmaktadır. Bu tip sorunların engellenmesi için iç/dış piyasaya sunulan fındıkların aflatoksin içeriklerinin düzenli olarak kontrol edilmesi gerekmektedir. Aflatoksin analizleri halen sıvı kromatografik teknik kullanılarak gerçekleştirilmektedir. Ancak bu tür kimyasal teknikler kullanılarak aflatoksin analizinde en önemli problem homojen bir örnekleme yapılmasındaki güçlüklerdir. Uygulamada iki tonluk bir fındık grubu içerisinden herbiri 300 gr olan 40 ayrı örnek alınarak analiz edilmektedir. Analiz sonuclarinda bu örneklerde belirli seviyede aflatoksine rastlanması halinde ise örneğin temsil ettiği fındık grubunun ihracı durdurulmaktadır. Fakat bu duruma alınan örnekler içerisinde yer alan bir kaç yüksek aflatoksin içerikli fındık bile sebep olabilmektedir. Ayrıca kimyasal analizi yapılan fındıkların geri dönüşümü mümkün olmamaktadır. Bu sebepten dolayı ihraç edilecek veya tüketime sunulacak olan fındıkların hızlı ve tahribatsız yöntemlerle incelenip aflatoksin içeren veya içerme potansiyeli yüksek olanların tespit edilip ayıklanması gerekmektedir. Yapay görmeye ve ses bilgisine dayalı tekniklerden yararlanılarak fındıklardaki küflenme ve aflatoksin kontaminasyonunun hızlı ve çok düşük bir maliyetle tespit edilebilmesinin mümkün olduğu düşünülmektedir..

Benzer problemler kırmızı biber üretimi için de geçerlidir. Bilindiği üzere ülkemiz seksenli yıllarda Avrupanın en büyük kırmızı biber üreticisi konumundaydı. Fakat 1993 yılında ihraç ettiğimiz kırmızı biberlerde aflatoksin maddesine rastlanmasıyla beraber kırmızı biber ihracatımız sekteye uğramıştır. Bu günden sonra eski konumuna gelememiş ve bu yüzden üreticilerimiz büyük maddi kayıba ugramıştır. İkiyüz milyon dolarlık kırmızı biber piyasası Meksikalı üreticilerin hakimiyeti altına girmiştir. Ayrıca ürettiğimiz biberlerin aflatoksin içerip içermediğine bakılmaksızın ülke genelinde tüketimi yapılmaktadır.

Bu projede aflatoksin içeren ve/veya aflatoksin içerme ihtimali yüksek olan küflü fındıkların ses ve görüntü işleme yöntemlerine dayanılarak ayrıştırılması; aflatoksin içeren kırmızı biberlerin ise görüntü işleme yöntemleri kullanılarak tespit edilmesi üzerine yöntemler geliştirilmiştir. Geliştirilen yöntemler, üzerinde çalışılan gıda ürünü ve çeşitlerine göre farklılık göstermekte olup diğer tür gıda ürünlerinde de kullanılabilicek özelliktedir.

2. FINDIK ÜZERİNE YAPILAN ÇALIŞMALAR

Projede ele alınan fındık örneklerinin ihraç edilmekte olan fındık formuna uygunluğunu sağlayabilmek için Fındık Tanıtım Grubunun ihracaat verileri dikkate alınmıştır. Bu verilere göre fındık hasat sonrasında üç farklı şekilde (kabuklu, iç, işlenmiş)

ihraç edilmekte ve/veya ülke içi tüketime sunulmaktadır (Figure 1). Her üç grup fındık yapısal ve fiziksel olarak farklı olduklarında ayrı ayrı ele alınmıştır. Bu alandaki çalışmalara ilk olarak DÜZCE'de faliyet gösteren KARIN GIDA A.Ş'nin fındık işleme fabrikasına ziyaret ile başlandı. Fındık işleme prosedürü, işleme ve depolamadaki kritik noktalar tespit edildi ve gelişitirilecek yöntemlerde bu kritik noktalarda entegre edilebilecek ayıklama sistemlerine uyumlu yaklaşımlar benimsendi. Söz konusu fabrikadan çalışmalarımız için gerekli fındık temin edildi. İleriki dönemlerde ise Ordu yöresinden temin edilen fındıklar ile çalışmalar yapıldı. Fındık üzerine yapılan çalışmalar planlanan farklı kimyasal deneyler ile beraber yürütülmüştür.

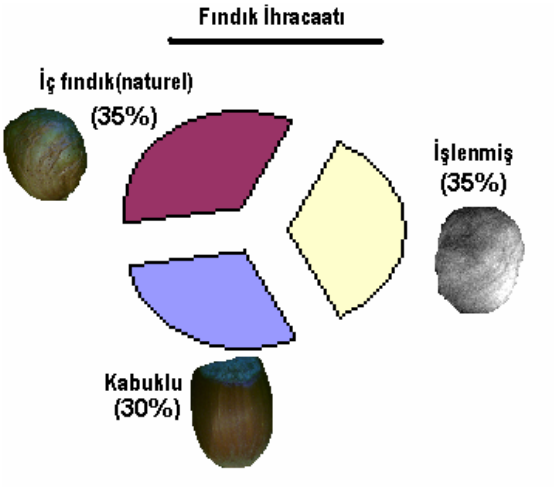

Şekil 1. Yıllık ihraç edilen fındık oranları

DENEY 1: Kabuk özelliklerinin küflenmeye olan etkisinin araştırılması

Fındık ihracatının %30'u kabuklu olarak yapılmasına rağmen, fındıkların kabuklu olarak depolaması oranın çok daha yüksektir. Depolanmış fındıklar ihracaat öncesinde kırılarak nakliye masraflarında düşüş sağlanmaktadır. Bu deneyde fındık kabuğunun ve kabuk üzerinde gerek hasat öncesi, gerekse hasat ve işlenme sırasında oluşan kırık ve çatlak gibi hasarların fındık küflenmesine olan etkisi araştırılmıştır. Bunun için temin edilen fındıklar aşağıdaki dört farklı gruba ayrılmıştır (Şekil 2).

Şekil 2. Deney 1 için kullanılan fındık çeşitleri, a) iç dındık, b) kabuğu çatlak fındık, c) kabuğu kırık fındık, d) kabuğu sağlam fındık

Bu fındıklarda deney yapmak üzere aflatoksin oluşturulması için gerekli olan A.parasiticus küfleri 2 farklı suş (NRNL 2999 ve NRNL 465) olarak ABD Ziraat Bakanlığı Laboratuvarlarından temin edilmiştir. Yukarıda gruplanan fındıklardan her gruptan 800' er

adet alınmış ve A.parasiticus küfüne maruz bırakılmak üzere geçmişte fındıklarda küflenme-zaman ilişkisini inceleyen çalışmaları bulunan Namık Kemal Üniversitesi öğretim üyesi Yrd. Doç. Dr. Muhammed Arıcı' ya gönderilmiştir. Burada küf sporu çoğaltıldıktan sonra fındıklara inkübe edilmiş ve fındıklar 90% nem ortamında ve 28 ^{0}C'lik ortamda 18 gün bekletilmiştir. Küflenen fındıkların bir kısmı kabuğun fiziksel durumu ve buna bağlı olarak küflenmeye karşı oluşturduğu bariyerin tespiti için Tubitak Ankara Test Analiz Laboratuvarına gönderilmiş ve HPLC kullanılarak analizi yapılmıştır. Analizler sonucunda elde edilen verilere bakıldığında (Tablo 1) kabuğun fındıkta küflenmeye karşı bir bariyer oluşturduğu fakat kabuk üzerindeki, büyüklüğüne ve özelliğine bakılmaksızın, çatlak veya kırığın bu bariyer özelliğini ortadan kaldırdığı açığa çıkmıştır. Bu yüzden depolama öncesinde fındıklar çatlak/kırık ve sağlam kabuklu ayrımına tabi tutulmalı ve bu gurupların ayrı ayrı depolanmalıdır. Kabuğu çatlak olan fındıklar işlenmede öncelikli olmalı ve bu sınıftaki fındıkların aflatoksin içerme potansiyellerinin yüksek olduğu dikkate alınmalıdır.

Tablo 1. Dört gruba ait aflatoksin analiz sonucları

Örnek grubu	Toplam Aflatoksin (ng/g)
Kabuğu sağlam fındık	43,16
Kabuğu çatlak fındık	2730
Kabuğu kırık fındık	2467
İç fındık	2494

Bu durumda kabukları sağlam olan fındıklar ile kabuğu hasarlı veya kabuksuz fındıkların ayrıştırılmasının aflatoksin oluşumunu sınırlamak adına yapılması gereken bir çalışma olduğu konusundaki inancımız pekişmiştir. Bu gelişme ışığında kabuğu sağlam olan fındıklar ile çatlak olanların ayrıştırılması için görüntü işleme, ses işleme veya her ikisinin eş zamanlı çalışmasına dayalı yöntemler incelenmiştir. Küflenmenin kabukta değil de iç fındıkta oluşmasından ve dolayı görüntüye dayalı dayalı sistemler bu fındıklar için uygun olmadığı anlaşılmıştır. Bu sebepten dolayı bu fındıkların ayrıştırılmasında çarpma sesine dayalı yöntemler geliştirilmiştir.

2.1 Çarpma sesi kullanılarak kabuğu çatlak olan fındıkların ayıklanması

Kabuğu çatlak olan fındıklar potansiyel olarak yüksek oranlarda aflatoksin içerebileceğinden bu fındıklar kabuğu sağlam olanlardan ayıklanmalıdır. Bu amaçla fındıkların çarpma sesleri aşağıda verilen ses sistemi (Şekil 3) aracılığı ile alınmıştır. Bu sistemde fındıklar yere 120 ^{0}C lik bir açı ile duran metal bir plaka üzerine bırakılıp ve çarpma anında açığa çıkan ses mikrofon vasıtası ile bilgisayar ortamına aktarılıp incelenmiştir. Yapılan ön incelemelerde çatlak kabuklu fındıkların sağlam olanlara göre farklı özellikte ses sinyalleri yaydığı tespit edilmiştir.

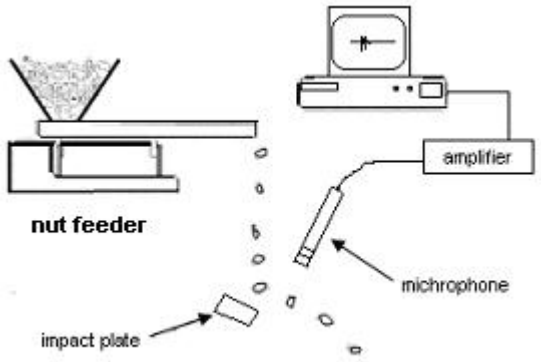

Şekil 3. Çarpma sesi alım sistemi

Bu çarpma sinyalleri dalgacık dönüşümü ile alt zaman-frekans bantlarına bölünüp ve bu bantlardan elde edilen özniteliklerin sen iyi sınıflandırma sonucunu veren öznitelik vektörü tespit edilmiştir. Bu öznitelik vektörleri kullanilarak bir doğrusal sınıflandırma sistemi eğitilmiştir. Bu çalışma proje öncesinde yapılmış olup İrlanda'nın Dublin şehrinde düzenlenen "IEEE Conference on Machine Learning for Signal Processing" çalıştayında sunulmuştur [1]. Çalıştay sırasında değişik ülke araştırmacıları bu çalışmaya ilgi göstermiş ve kendi laboratuvarlarında çalışmak üzere kullandığımız ses veri tabanını taleb etmişlerdir.

Proje kabulunden sonra ABD'ın "University of Minnesota" Elektrik-Elektronik Mühendisliği araştırmacı ve öğretim üyesi ile beraber yürüttüğümüz çalışma ile yüksek sınıflandırma potansiyeli taşıyan özniteliklerinin zaman frekans düzleminde bulundukları konumların otomatik olarak tespit edilmesi için bir algoritma geliştirilmiş ve sınıflandırma oranı daha önce deneme yanılma yöntemi ile tespit edilen özniteliklere göre daha yüksek doğruluğa sahip sonuçlar alınmıştır. Bu çalışmada ses sinyalleri zaman-frekans ekseninde ağaç yapısında küçük parçalara bölündü ve ayrımsallık potansiyelleri dikkate alınarak bu ağacın dalları budandı. Bu budama işlemi bize ayrımsallığı en yüksek olan bilginin ses sinyalindeki konumunu vermektedir. Ses sinyalinin belirlenen bu konumlarından elde edilen öznitelikler ile yapılan sınıflandırma da %96.5 lik bir doğru sınıflandırma oranına ulaşılmıştır. Bu algoritma saniyede 32 fındık işleyebilecek kapisede olduğundan fındık işleme tesislerinde ayıklama amaçlı dizayn edilecek bir sistemde kullanılabilir özelliktedir.

Bu çalışma sonucunda elde edilen verilerle iki adet uluslararası dergi yayını [2, 3]; ikisi uluslararası olmak üzere üç konferans bildirisi [4, 5, 6] yapılmıştır.

DENEY 2: Düşük nem ortamında küflenmiş fındıkların hazırlanması

Deney 1'de hazırlanan fındık örnekleri nemli ortamda bekletildiğinden dolayı ileri seviyede küflenmeye maruz kalmıştı. Bu fındıklar üzerinde oluşan küf sporları fındıkların görünümünü belirgin olarak değiştirmektedir. Fakat bu projede hedeflenen ise görünüşte normal gözüken fakat gerçekte toksin içeren veya içerme potansiyeli yüksek olan fındıkların tespit edilmesidir.

Temelde sınıflandırma problemi olan bu ayrıştırmayı yapabilecek bir sistem geliştirilmesi için elimizde aflatoksin içeren ve içermeyen fındıklar olması gerekmektedir. Doğada aflatoksin içeren fındıklara çok sık rastlanmadığından, fındıkların tane olarak

kimyasal analizi hem pahalı hem de fındığı tekrar kullanılamaz duruma getirdiğinden ve bu fındıklar kimyasal olmayan yöntemlerle tespit edilemediğinden bu fındıkların temini için yapay olarak aflatoksine sebep olacak şeklide küflendirilmesi işlemine gidilmiştir. Bu deney için ORDU yöresinden fındık temin edilmiştir. Bulaştırmada kullanılarak oluşturulacak fındıkların bulaştırma öncesinde temiz olması bulaştırmanın etkisini tam olarak görebilmek açısından önemlidir. Bu yüzden küflenmede kullanılacak olan yığında doğal olarak aflatoksin içeren fındıkların olma ihtimaline karşı, fındıklar Türkiye Atom Enerjisi Kurumunda 8 saat boyunca yüksek dozda Gama ışınına tabi tutulmuşlardır. Bu işlem gıdada var olabilecek aflatoksini parçalamaktadır.

Laboratuvar ortamında yapılacak olan çalışmada kullanılacak fındıklarda doğal olarak küflenen fındıklara benzer ölçüde küflenme gerçekleştirilmesi gerekmektedir. Fakat bunun hangi çevre koşulları ve sürede gerçekleşebileceği üzerine ortak bir kanı bulunmamaktadır. Bu yüzden küflenme işleminin kontrollu yapılması gerekmektedir. Bunun için küflenmeye bırakılacak olan fındıklardan her gün aynı saatte örneklerin alınıp bu fındıkların görüntüleri alındıktan sonra vakit kaybetmeden kimyasal analizinin yapılması işlemine geçilmesi planlanmıştır. Çalışmada kullanılacak olan fındıklar üç gruba ayrılmıştır;

- Kabuğu çatlak olan fındıklar
- Kabuğu sağlam olan fındıkar
- İç fındıklar

Çalışma sonunda fındık küflendirmesi için uygun olan gün belirlenmesinin yanında kabuğun küflenmeye olan etkisinin belirlenmesi hedeflenmekteydi. Bu fındıkların görüntülerinin alınması ve işlenmesi ile de multispekral görüntüler ile aflatoksin içeriği arasındaki ilişki kurulması hedeflenmiştir.

Küflenme için aflatoksine sebep olan A. Parasiticus türü küf sporu çoğaltılmış ve fındık örnekleri küfe bulaştırıldıktan sonra her güne 15 iç fındık, 10 çatlak fındık, 10 kabuklu fındık gelecek şekilde ayrı ayrı petri kaplara konulmuş ve 28 ^{0}C lik sıcaklıkta aflatoksin üremesi için beklemeye konulmuştur. Küflenmenin hızlı gerçekleşip fındık yüzeyini fındığı tanınmayacak hale getirmesini engellememek Deney 1'de olduğu gibi ortama extra nem verilmemiştir.

Küflenmenin başladığından itibaren, 1, 2, 3, 4, 5, 6, 7, 8, 9, 10, 11, 14 ve 21. günlerde fındıklar alınarak Odtü Enformatik Enstitüsü'nde kurmuş olduğumuz laboratuvarda 400 nm den başlayıp 640 nm bandına kadar 10nm band genişliğinde filtreler kullanarak multispektral görüntüleri alınmıştır. Görüntüleri alınan fındık taneleri aynı gün içinde Tubitak-Atal laboratuvarında kimyasal analize (HPLC) alınmıştır. Yapılan kimyasal analizlerdeki ortalama aflatoksin seviyelerine bakıldığında iç fındıkda diğerlerine göre daha fazla oranda aflatoksin ürediği görülmüştür (Şekil 4). Günlük artışa bakıldığında ilk 2 günde iç fındıkta görülen yüksek oranda aflatoksin seviyesi uzmanlar tarafından açıklanamamış, kimyasal deney sonuçlarının ve yaptığımız küflendirme işleminindeki uygulanan sistematiğin gözden geçirilip değerlendirilmesine sebep olmuştur. Buna ek olarak kullanılan kameranın hiperspektral görüntüleme için yeterli ve uygun olmadığı ve belirlediğimiz sınırlı nem koşullarının fındık yüzeyinde küf artışını engellediği görülmüştür. Bu deneyimler ışığında uygun küflendirme koşullarının tespit edilip fındıkların tekrar küflendirilmesi gerektiği kanısına varılmıştır. Bu sebepten dolayı nemli ortamda kontrollu kuflendirme için yeni bir **Deney 3** tasarlanmıştır.

Şekil 4. Kabuklu (sağlam) , kabuğu çatlak ve iç fındıkların farklı günlerde alınmış örneklerindeki ortalama aflatoksin kontaminasyonu

Şekilden den de görüldüğü üzere özellikle iç fındıkda ilk iki gün yüksek miktarda aflatoksin olmasına karşın bu miktar sonrasında düşüşe geçmiştir. İlk iki gündeki beklenmeyen durumun anlaşılabilmesi için iç fındıkta küflendirme deneyi ilk üç gün için tekrar edildir. Bu yeni deneyde hem fındıkların küflendirildiği besi yeri hem de fındıkların kendisi analiz edildi. Bu yeni deneyde fındıkların besi yerinden aflatoksin içeren parçacıklar alabildiği kanısına varıldı. Bu sebepten dolayı fındıkların besi yerinde çoğaltılan küflere temas ettirilerek değilde sıvı küf sporuna batırılılarak veya sıvı sporların püskürtülülerek küflendirilmesinin daha uygun olacağı kanısına varıldı.

DENEY 3: Nemli ortamda kontrollu küflendirme deneyi

İlk üç dönemde çeşitli şekilllerde yapılan küflendirme, görüntü alımı ve analizi çalışmaları değerlendi ve bu değerlendirme doğrultusunda iç fındıklar için Süleyman Demirel Üniversitesi Merkez Laboratuvarı'nda yeni bir pilot deney yapıldı. Bu deneyde incelenmek üzere aflatoksin içeren ve içermeyen iç fındıklar ile kavrulmuş fındıkların elde edilmesi hedeflendi. Bu pilot deney için 2007 mahsulü yaklaşık 600 adet iç fındık 2 gruba (Grup A, Grup B) bölünmüştür. Grup A'daki fındıklar ise kendi arasında 3 gruba (A1, A2, A3) bölündü (Tablo 1). A1 grubundaki fındıklara hiç bir işlem uygulanmadı ve sadece kontrol amacı için ayrıldı. A2 grubundaki fındıklar ise saf suya daldırıldıktan sonra bir kısmı 28 ^{0}C de %90 nem ortamında 9 gün; bir kısmı da aynı ortamda 18 gün beklemeye bırakıldı. A3 grubundaki fındıklar ise A2'den farklı olarak aflatoksin oluşumunu sağlayan Aspergillus Paraciticus küf solusyonuna batırıldı ve aynı sürelerde bahsedilen ortamda bekletildi. Bu süre sonunda bu gruptaki fındıklar görüntü alımı işleminden önce 140 ^{0}C de 15 dakika kavruldu. Kavurma işlemi fındık işleme fabrikalarında yapılan kavurma işlemine denk olacak şekilde yapılmıştır.

Tablo 2. Fındık grupları

	Kavrulmuş (Grup A)	Naturel (Grup B)
Kontrol	A1	B1
Saf su	A2	B2
Küf solusyonu	A3	B3

Elde edilen fındıkların hyperspektral görüntüleri (Şekil 5) alındıktan sonra kimyasal analize tabi tutuldu.

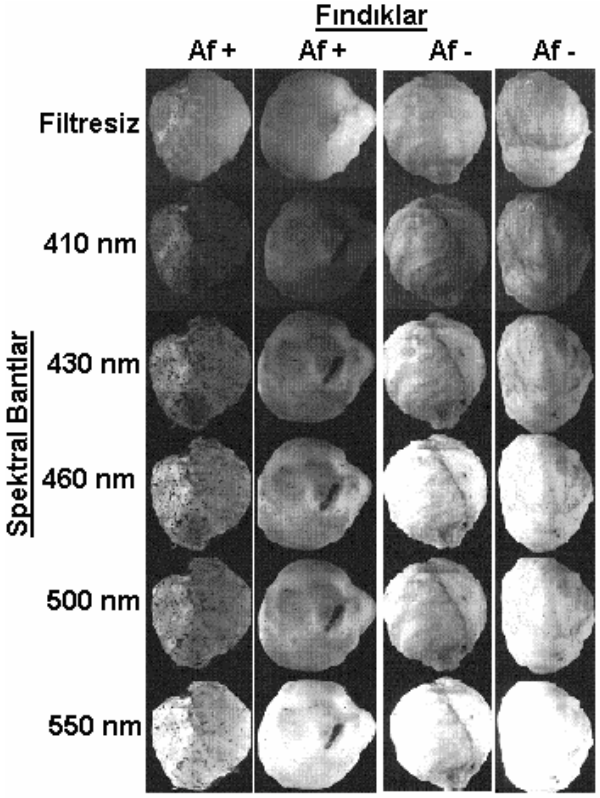

Şekil 5. Kavrulmuş fındıkların bazı spektral bantlarda alınmış görüntüleri. Birinci kolonda A3, ikinci kolonda A2, 3 ve 4. kolonlarda ise A1 grubunda rastgele seçilmiş fındıklardan elde edilen görüntüler yer almaktadır.

Grup B' deki fındıklar da Grup A'daki gibi üç gruba bölündü (B1, B2, B3) ve aynı işlemlere tabi tutuldu (Tablo 2). Fakat Grup A' daki fındıklardan farklı olarak kavrulma işlemine tabi tutulmadılar. Grup B' daki fındıklar kavrulmadığından iç zar korunmuştur.

Yapılan incelemeler sonucunda 18 günlük küflendirme süresinin fındıklarda şekilsel bozukluğa sebep olduğu kanısına varıldı. 18 gün boyunca sıcak ve nemli ortamda bekletilen fındıklarda aşırı derece küflenme olduğu tespit edildi. Görsel olarak ayrıştırılması olabildiğince kolay olmasına rağmen pratikte karşılaşılacak küflenmenin çok ötesine geçtiği için 18 gün boyunca bekleyen fındıklar kullanılmadı. 9 gün bekletilen fındıkların gerçek hayatta karşılaşılan görünümde küflenmeye sebep olduğu düşünüldüğünden görüntü analizi işlemi bu fındıklar üzerinde yapıldı.

Küfe batırılan (A3, B3) fındıkların yanısıra saf su solusyonuna batırılan fındıklarda da (A2, B2) küf oluşumu gözlendi. Yapılan analizlerde bu gruplardaki fındıkların birçoğunda

belirlenen seviyenin (4 ppb) üzerinde aflatoksine rastlandı. Bu fındıkların aflatoksin haricinde farklı zararlı maddeler içerme ihtimali yüksektir. Bu sebepten dolayı bu fındıklar tüketilmemesi gereken fındıklar olarak değerlendirildi. A3 ve B3 grubundaki fındıkların tamamında yüksek seviyede (>800 ppb) aflatoksine rastlandı. Bu fındık gruplarından sadece A1 ve B1 tüketilebilecek özellikte olan fındıklardır.

Yapılan pilot deney sonucunda elde edilen fındıklar istenilen seviyede fındıklar olasından dolayı aynı şartlarda daha fazla fındık küflendirilerek daha geniş bir deney seti oluşturulmuştur. Bu fındıklar kullanılarak aflatoksin içeren veya içerme potansiyeli yüksek olan fındıklar ile içermeyenler araşında ayrım yapabilecek algoritmaların geliştirilmesine başlanmıştır.

2.2 Hyperspektral görüntüler kullanılarak fındıkların histogram tabanlı öznitelikler ile sınıflandırılması

Deney 3' te ilk etapta yapılan pilot küflendirme sonucunda elde edilen kavrulmuş fındıkların hiperspektral görüntülerden histogram tabanlı öznitelikler ile sınıflandırılması yapılmıştır. Bunun için spektral görüntülerden ilk etapta ortalama filtre kullanılarak gürültüden arındırıldı, Sonrasında ise fındık görüntüsü arkaplandan ve kavrulma sonrasında fındık yüzeyinde kalan zarlı bölgelerdenden temizlendi (Şekil 6-c). Bu temizleme için fındığın 550 nm'deki görüntüsü kullanılarak elde edilen maskeden faydalanıldı (Şekil 6-a). Maskeleme işlemi için diğer 480-510nm gibi spektral bantlar da kullanılabilir.

-a- -b- -c-

Şekil 6. a-) Fındığın 550 nm dalgaboyundaki görüntüsü, b-) maske, c-) maskelenmiş görüntü

Temizlenen fındık görüntülerinin histogramları iki farklı eşik değeri (t_1, t_2) kullanılarak 3 farklı bölgeye ($B0\_t_1$, $Bt_1\_t_2$, Bt_2_255) bölündü. Her spektral bantın yeğinlik dağılımı birbirinden farklı olduğundan herbiri için Tablo 3'deki eşik değerleri histogram üzerinde belirlenerek histogramlar Şekil 7'deki gibi 3 bölgeye ayrıldı.

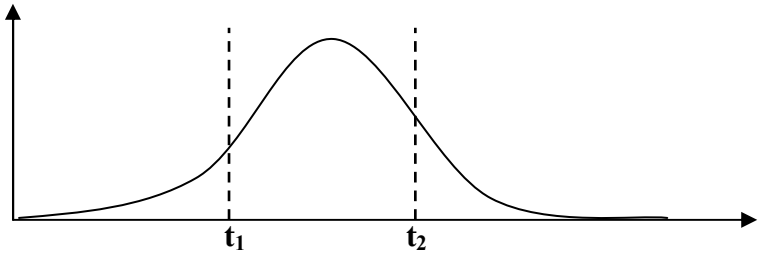

Şekil 7. Üç bölgeye ayrılmış bir yeğinlik histogram eğrisi örneği

Tablo 3. Hiperspektral görüntülerin deneysel olarak tespit edilen histogram eşik değerleri

Spektral Bantlar	t_1	t_2
Filtresiz, 400, 420, 510, 550, 600	120	180
410, 430, 440, 450, 460, 470, 480, 490	60	90
500	230	250

Histogramdaki her üç bölgedeki örneklerin ortalama değeri, μ_s^b, ile değişinti değeri , υ_s^b, öznitelik olarak hesaplandi. Burada ***b*** histogram bölgesini; ***s*** ise spektral bantı göstermektedir. Bu değerler kullanılarak hesaplanan 90 boyutlu öznitelik vektörünün her elemanının ***f*** karekökü alındıktan sonra normalize edildi ve sınıflandırmada kullanıldı.

$$f = \left\{\mu_{400}^1, \mu_{400}^2, \mu_{400}^3, \ldots \mu_{600}^3; \upsilon_{400}^1, \upsilon_{400}^2, \upsilon_{400}^3, \ldots \upsilon_{600}^3\right\}^{1/2}$$

Sınıflandırma için doğrusal sınıflandıcı tercih edildi ve öznitelik vektöründeki herbir öznitelik ayrımsallık potansiyeline göre sıralanarak sınıflandırıcıda kullanıldı. Sonuçlar incelendiğinde en iyi ortalama sınıflandırma oranı olan %97.5 lik sonuca ilk en iyi 31 öznitelik ile ulaşıldı. İlk 31 öznitelik incelendiğinde bunların çoğunluklukla 450, 460, 470, 480, 490, 500 ve 550 nm merkez frekansına ait olan spektral bantlardan seçildiği tespit edildi. Bu sınıflandırma işlemi için daha az sayıda öznitelik kullanılması yöntemin pratiğe dökülebilmesi açısından önemlidir. Bu çalışma IEEE SIU 2008 konferansında sunulmuştur [7].

2.3 Hyperspektral görüntüler kullanılarak fındıkların 2B LDB tabanlı öznitelikler ile sınıflandırılması

Deney 3 kapsamında yapılan pilot çalışma ile elde edilen görüntülere ek olarak yeni findik örneklerinin görüntüleri de alıinarak veri setimiz genişletilmiştir. Görüntü alımı sonrasında fındıklar zaman geçirilmeden aflatoksin analizine tabi tutulmuşlardır. Naturel (Grup B) ve kavrulmuş (Grup A) grubu için elde edilen fındık sayısı ve bunlara ait ortalama aflatoksin kontaminasyon değerleri Tablo 4' te verilmiştir.

Tablo 4. Naturel ve kavrulmuş fındıklar, aflatoksinli ve aflatoksinsiz olanların sayısı ve ortalama aflatoksin değerleri

KAVRULMUŞ FINDIKLAR (Grup A)			
	A1 (Kontrol)	**A2 (Saf su)**	**A3 (A.parasiticus)**
Aflatoksinli sayısı	2	15	79
Aflatoksinsiz sayısı	102	87	0
Ort. aflatoksin seviyesi	0,7	7,47	2227

NATUREL FINDIKLAR (Grup B)			
	B1 (Kontrol)	**B2 (Saf su)**	**B3 (A.parasiticus)**
Aflatoksinli sayısı	1	4	49
Aflatoksinsiz sayısı	81	100	0
Ort. aflatoksin seviyesi	0,36	26,25	3418

Bu guruplarda yer alan fındıklardan alınan bazı spektral bantlardaki görüntüsü Şekil 8'de verilmiştir

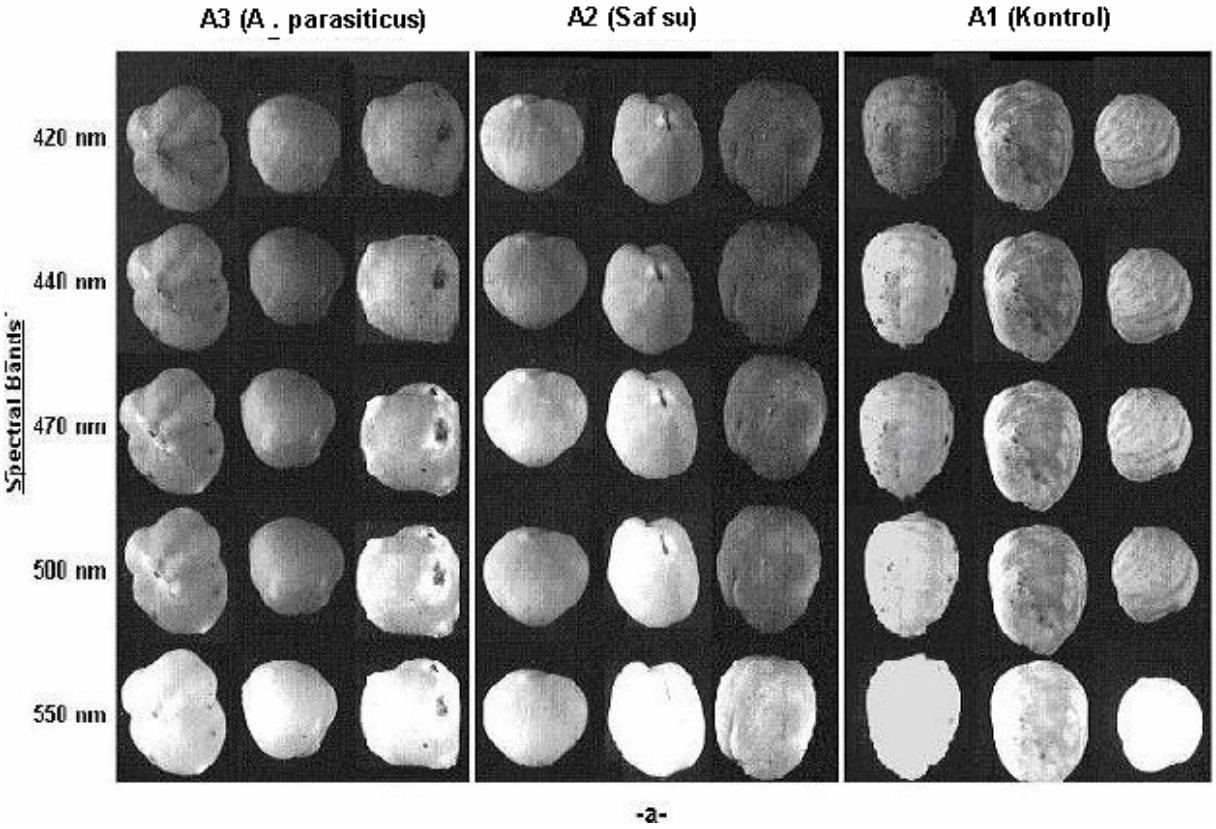

-a-

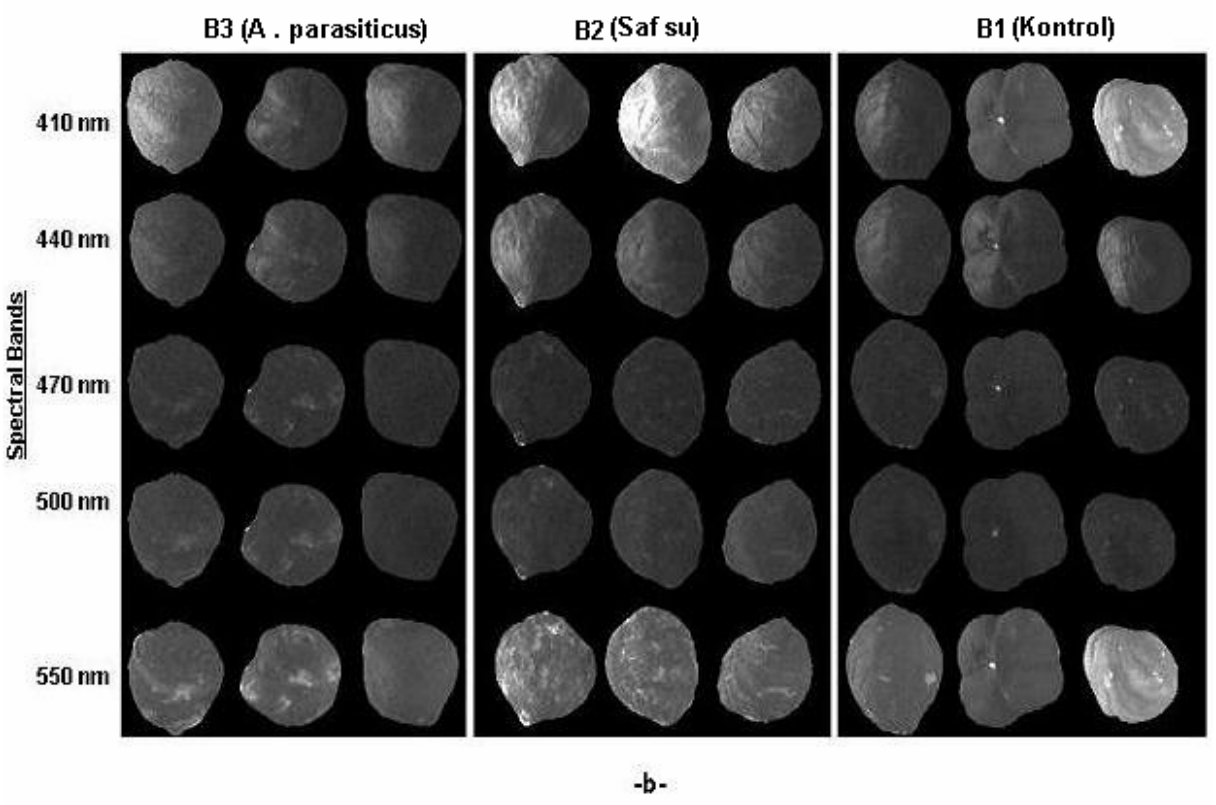

Şekil 8. a) Kavulmuş, b) Naturel fındıklar içerisindeki üç gruba fındıklar içerisinden alınan 3'er fındığa ait bazı spektral bant görüntüleri.

Spektral görüntüler gürültü ve arkaplandan ayırt edilebilmesi için ön işleme tabi tutuldular. Bu ön işlemde görüntü üzerinde bulunan gürültüler ortalam filtre ile temizlendi. Arka plan ve kavrulmuş fındıklar üzerinde yer alan zarlı bölgenin ve naturel fındıkar üzerindeki zarsız bölgelerin görüntüler üzerinden ayrılması için bir maske oluşturulmuştur. Bu maske için ilk önce görüntüler üzerinde eşik değeri belirlenerek görüntüler ikili sayı formatına getirilip açma ve kapama işlemleri uygulanmıştır. Elde edilen maske aynı fındığa ait bütün spektral bantlar için kullnılmıştır. Fındık görüntüleri değişik boyuttaki pencerelere bölündü ve her bir pencere için ayrı ayrı inceleme yapılmıştır. Şekil 9'de arkaplan ve zarlı bölgesinden ayıklanmış ve sonrasında 51x51 'lik pencerelere bölünmüş bir kavrulmuş fındık görüntüsü vardır.

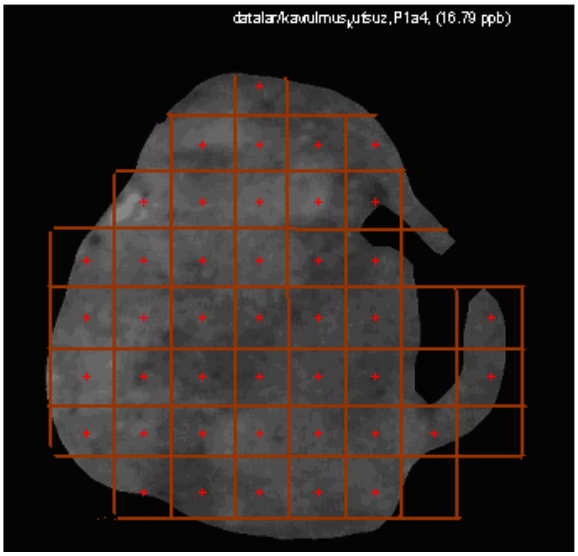

Şekil 9. 51x51 boyutlu pencerelere bölünmüş olan temizlenmiş fındık görüntüsü

Bu işlem sonrasında sınıflandırma için hangi spektral bantların ve bu spektral bandların hangi özelliklerinin kullanılacağının tespiti için iki boyutlu (2B) Yerel Ayırtaç Tabanları (YAT) yöntemi geliştirilmiştir. Bu yöntem uygun spektral bant seçiminde bazı bantları eleyebildiği gibi tek başlarına önem taşımayan bantları birleştirerek sınıflandırma açısından önemli bantlar oluşturabilir. Bu özellik sayesinde yüksek sınıflandırma oranına az sayıda spektral bant kullanılarak ulaşılmış olacaktır. Kullanılacak spektral bant sayısının az olması geliştirilecek algoritmaların gıda işleme üretim hattına kurulacak olan bir cihaz üzerinde çalışabilmesine imkan tanıyacaktır. 2B YAT yöntemi ilk olarak spektral ve uzamsal-frekans ekseninde öznitelik ağaçlarının oluşturulur. Bu öznitelik ağaçları sonrasında budanarak sınıflandırma açısından önemli olan özniteliklerini ve bu özniteliklerin elde edildiği spektral uzamsal-frekans alt bantı kombinasyonunu verir. Elde edilen öznitelikler elemeye tabi tutularak katkı sağlamayanların ayıklanması sağlanır.

2.3.1 Spektral ve uzamsal-frekans ekseninde öznitelik ağaçlarının oluşturulması

İlk olarak spektral eksende 4 seviyeli ikili öznitelik ağacı oluşturuldu (Şekil 10). Bunun için spektral bant (SB) imgelerinin yansıma enerjileri ağaç yapısındaki en alt seviyedeki düğümlere yerleştirildi. Üst seviyedeki anne düğümlerin enerjisi ise çocuklarının enerjileri toplanarak elde edildi. Bu işlem bütün spektral bantların toplanmasıyla oluşan en üstteki tek düğüme ulaşılıncaya kadar devam etti. Kullanılabilir olarak aynı özelliklere sahip 12 spektral bant imgesi (400nm ile 510nm arasında) olduğundan ikili spektral bant ağacındaki en alt seviyedeki son dört düğüme "0" degeri atandı.

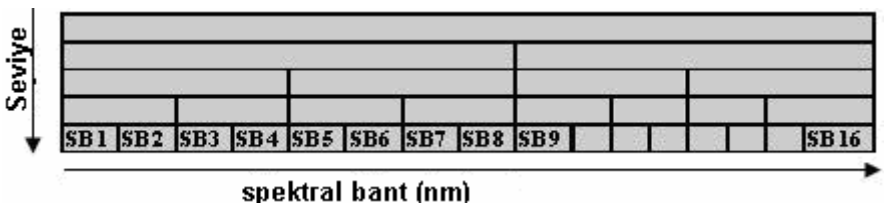

Şekil 10. 4 seviyeli ikili spektral bant öznitelik ağacı

Benzer bir öznitelik ağacı ise her bir spektral bant imge için uzamsal-frekans ekseninde oluşturuldu. Tam dalgacık dönüşümü kullanılarak oluşturulan ağaç yapısı diğerinden farklı olarak dörtlü yapıya sahiptir (Şekil 11). Dalgacık dönüşümü ile alt bantlara inilirken imge ilk olarak sıra bazında yüksek (H) ve alçak (L) geçiren filtrelerden; daha sonrada kolon bazında bu filtrelerden geçirilir.

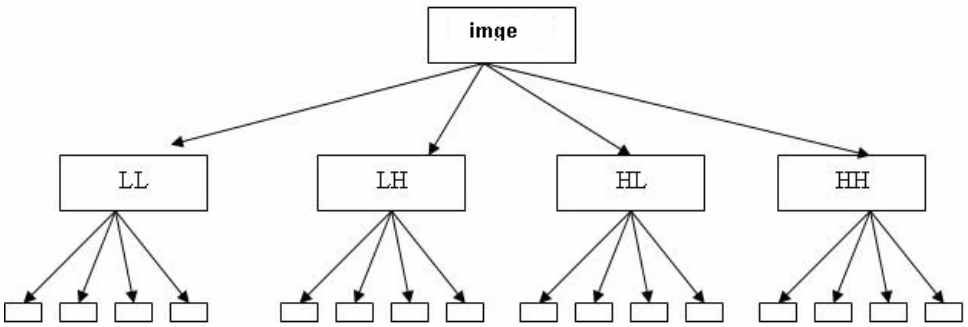

Şekil 11. 2 seviye tam dalgacık dönüşüm ağacı

Bütün fındık hiperspektral görüntüleri ikili ağaç yapısıyla öznitelik uzayında 16x21=252 boyutlu bir öznitelik vektörü haline getirilmiştir.

2.3.2 Öznitelik ağaçlarının budanması

Şekil 10'da yer alan ağaç yapısındaki her bir düğümün ayrımsallık değeri kümülatif dağılım fonksiyonları arasındaki Öklit uzaklığı hesaplandı ve ağaç yapısı içerisindeki anne düğümlerin en alttan başlamak suretiyle çocuk düğümler ile karşılaştıma süretiyle yapıldı. Budama algoritmasında anne düğüm aysrımsallığı çocuklarından büyük olması durumunda tutulur; aksi durumda alt (çocuk) düğümlere bölünür. Şekil 12'de budanmış bir spekral bant ağacı görülmektedir. Görüldüğü üzere 440 ile 470 nm arası; ve 480 nm ile 510 nm arasındaki spektral bantlar birleştirilirken ilk 4 spektral bantın ayrı olaral kalması algoritma tarfından tercih edilmiştir.

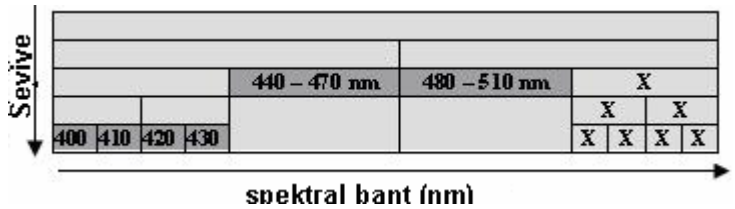

Şekil 12. Budanmış spektral bant öznitelik ağacı

Aynı yöntemle uzamsal-ferakans eksenindeki 4'lü ağaç yapısı budanmıştır. Spektral eksendeki budanma algoritmasından farklı olarak anne düğümler 4 çocuk düğüm ile karşılaştırılmıştır. Bu iki budama işlemi sonucunda spektral ve uzamsal-frekans ekseninde aşağıdaki (Şekil 13) gibi bir öznitelik haritası oluşmuştur.

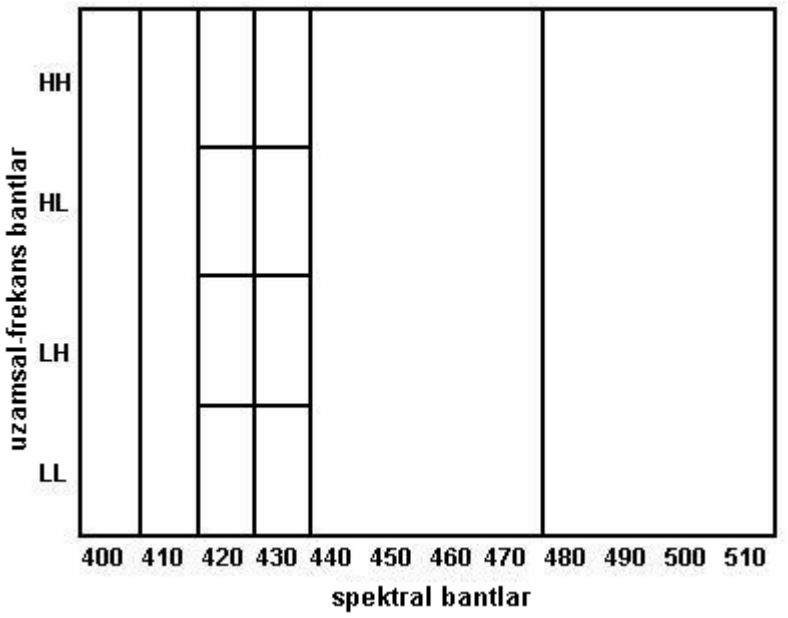

Şekil 13. Spektral uzamsal-frekans düzlemindeki en ayrımcı özniteliklerin konumunu gösterem öznitelik haritası

2.3.3 Öznitelik seçimi

İki farklı düzlemde yapılan budama işlemleri (Bölüm 2.3.1 ve 2.3.2) alinan hiperspektral veri içeririnde yer alan en ayırt edici özniteliklerin konumunu belirler, fakat bunları kendi içinde sıralamaz. Ortaya çıkarılan bu özniteliklerinde en önemli olanlarını tespit etmek için Fisher uzaklık, İlinti, Temel Bileşen Analizi ve "Wrapper" tabanlı öznitelik seçme algoritmaları kullanılmıştır. Şekil 13'deki öznitelik haritası Fisher uzaklık tabanlı öznitelik seçini algoritmasına göre sıralandığında en iyi özniteliğin 430 nm spektral bandındaki "LL" uzamsal-frekand altbandında olduğu anlaşılmaktadır (Şekil 14). Şekilde özniteliklerin önem sırası üzerindeki rakamlar ve renklerin koyuluğu ile de gösterilmiştir.

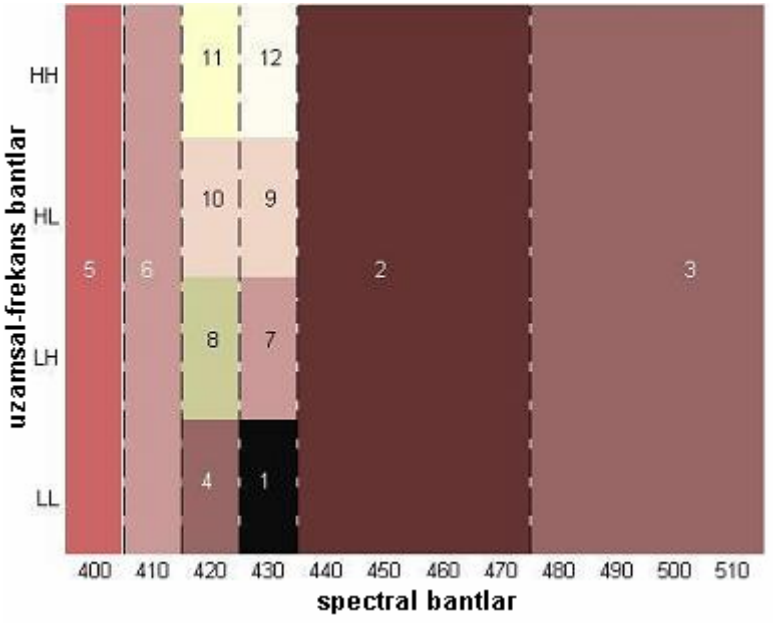

Şekil 14. Önem sırasına göre özniteliklerin sıralandığı öznitelik haritası

2.3.4 Sınıflandırma

Sınıflandırıcı olarak "Doğrusal Ayırtaç Analizi" kullanılmış ve bu sınıflandırıcının eğitimi eldeki veri setinin ¾' ü ile yapılıp , testi de geri kalan ¼ lük set ile yapıldı. Bu işlem her seferinde test setinin değiştirilmesi suretiyle 4 kere tekrarlanmıştır. Fındıktaki her bölge ayrı ayrı sınıflandırılmış (Şekil 15) ve bu bölgeler için verilen kararlar ile "çoğunluk oylaması" prensibine göre fındık sınıflandırıldı. Şekil 15' de yer alan fındık örüntüleri üzerindeki kırmızı ile işaretli bölgeler küflü, mavi ile işaretli bölgeler ise küfsüz olarak karar verilen bölgelerdir. Doğru sınıflandırma oranları her testte elde edilen sınıflandırma oranlarının ortalaması olarak alındı

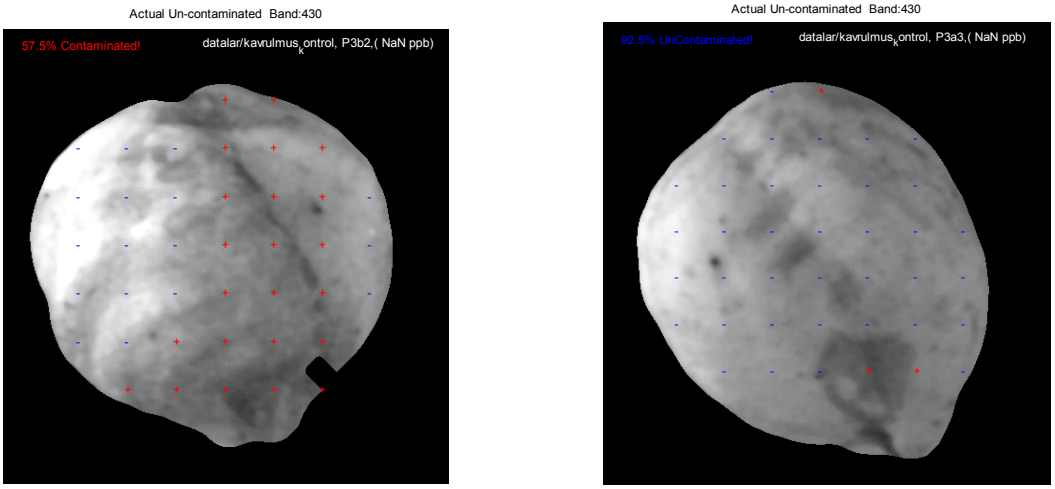

-a- **-b-**

Şekil 15. a) Gerçekte kontrol sınıfında olupta a) %57.5 ihtimalle küflü olarak b) %92.5 kontrol grubu olarak karar verilmiş fındıklar.

2.3.5 Kavrulmuş (Grup A) Fındıklarının Sınıflandırılması

Tablo 2 'de de görüldüğü üzere Kontrol grubundaki findiklardan çok azı; su ile kontamine edilenlerden bir kaçı ve küf ile kontamine edilenlerin tamamı aflatoksin içermektedir. Fındık üzerine yapılan çalışmalarda iki farklı sınırlandırma problemi tanımlandı. Birinci problemde **Kontrol** grubundaki fındıklar (104 tane) ile saf su veya A. Parasiticus solüsyonuna batırılan **Küflü** fındıklar (181 tane) arasında sınıflandırma yapılmıştır. Bu problemde elde edilen veri seti ile yapılan çalışmada geliştirilen algoritma 252 boyutlu öznitelik uzayını 12 boyutlu vektor haline getirmiştir. Bu 12 öznitelik de kendi arasında sıralanıp sınıflandırıcıda kullanıldı. Elde edilen sınıflandırma sonuçlarına bakıldığında en düşük hata oranı olan 2,6% hata oranı ile "wrapper" yöntemi ile sıralanmış en iyi ilk 4 öznitelik ile ulaşılmıştır (Tablo 5).

Tablo 5. Dört farklı öznitelik seçimi algoritması ile sıralanmış öznitelikler ile elde edilen en düşük küflü-küfsüz sınıflandırma hatası.

	Fisher (5)	İlinti (5)	TBA(2)	Wrapper(4)
Hata (%)	4,35	4,35	3,00	2,60

Fisher ile yapılan hata oranı baz alındığında 104 Kontrol fındığından 3'ü; 181 Küflü fındıktan 10'u hatalı karar verilmiştir. Başlanğıçta ortalama alatoksin seviyesi 608 ppb olan test fındıklarının sınıflandırılması sonucunda oluşturulan ve kufsuz olarak tanımlanan fındıkların aflatoksin seviyesi 0.7 ppb olmuştur. Bu da geliştirilen algoritmanın incelenen fındıklar içerisinden küflü ve dolayısıyla aflatoksinli olanları yüksek başarım oranı ile tespit edebildiğini göstermektedir.

Kavrulmuş fındıklarda ikinci bir deney ise küflü küfsüz ayrımı yapılmaksızın sadece aflatoksin miktarına bakılarak yapılmıştır. Aflatoksin seviyesi 4 ppb'nin üzerinde olan 89 fındık aflatoksinli (Afla+); 4 ppb'den düşük olan 189 fındık ise aflatoksinsiz (Afla-) olarak değerlendirilip 2 farklı sınıf oluşturulmuştur. Bu veri seti ile yapılan analizler sonucunda 252 boyutlu öznitelik vektörü 13 boyuta indirgenmiştir. Elde edilen sınıflandırma sonuçlarına bakıldığında en düşük sınıflandırma hatası oranı olan %7.69 değerine wrapper yöntemi ile sıralanan en iyi ilk öznitelik ile ulaşılmıştır (Tablo 6).

Tablo 6. Dört farklı öznitelik seçimi algoritması ile sıralanmış öznitelikler ile elde edilen en düşük Afla+ Afla- sınıflandırma hatası.

	Fisher (4)	İlinti (4)	TBA(6)	Wrapper(3)
Hata (%)	10,34	10,34	10,34	7,69

Fisher uzaklığına göre seçilen öznitelikler ile elde edilen 10,34'lük sınıflandırma değeri incelendiğinde 96 Afla- fındıktan 3'ü; 189 Afla- fındıktan ise 39 tanesi hatalı karar verilmiştir. Fakat hatalı olarak Afla+ olarak karar verilen 39 fındık incelendiğinde bunların 38'inin su ile kontamine olan sınıftan olduğu tespit edilmiştir. Dolayısıyla algoritma fındıkları aflatoksin miktarına göre değil de küflü olup olmadıklarına göre sınıflandırmakya başarılı olmaktadır. Böyle bir ayrımda hem % 2,6'lik bir hata oranına ulaşabildiğimiz gibi hem de aflatoksin içeren veya içermemesine rağmen küflü olan fındıkların tespiti yapılmış olacaktır.

2.3.6 Naturel (Grup B) Fındıklarının Sınıflandırılması

Kavrulmuş fındıklar üzerine yapılan çalışma ihracatımızın %35'lik bir kısmını oluşturan naturel, zarlı, fındıklar üzerinde de tekrarlandı. Işlenme sonrasında oluşan Şekil 8-b'de de görüldüğü üzere naturel fındık görüntüleri kavrulmuşlara göre daha düşük kalitededir. Fındık üzerindeki ayrıntılar yetersiz yansımadan dolayı görülememektedir. Bunun yanısıra, fındık üzerindeki kahverengi zar fındık içinin yansımasını da engellemektedir. Ne var ki aflatoksinin zar içinde oluştuğu bilinmektedir. Natural fındıklar da kavrulmuşlarda olduğu gibi iki farklı problem tanımlandı. İlk problemde sadece küflü (150 adet) ve küfsüz (89 adet) oluşumuna göre veri seti ayrıştırıldı ve algoritma çalıştırıldı. Naturel fındık imgeleri üzerine yapılan analizde oluşturulan öznitelik ağaçlarında çok fazla budama yapılmadığı ve 252 boyutlu oznitelik vektorunun ancak 120'ye indirgenebildiği görüldü. Çıkarılan bu özniteliklerde yine öznitelik seçimi algoritmaları ile sıralandı ve sınıflandırıcıda kullanıldı. Naturel fındık gurubunda küflü–küfsüz ayrımı için en düşük sınıflandırma oranı olan %15.85 değerine "wrapper" yönemi ile belirlenmiş iki öznitelikle ulaşılmıştır (Tablo 7).

Tablo 7. Naturel fındıklarda dört farklı öznitelik seçimi algoritması ile sıralanmış öznitelikler ile elde edilen en düşük küflü-küfsüz sınıflandırma hatası.

	Fisher (2)	İlinti (2)	TBA(78)	Wrapper(2)
Hata (%)	18,88	18,88	18,02	15,85

Naturel fındıklarda ikinci bir sınıflandırma problemi için fındıklar kavrulmuşlarda olduğu giği küflü-küfsüz ayrımına bakılmaksızın sadece aflatoksin içeriğine göre ayrıştırıldı. Bu şekilde yapılan denemede de geliştirilen algoritmanın öznitelik ağaçlarını beklendiği kadar budamadığı ve 252 boyutlu öznitelik ağacını 115'e kadar düşürdüğü görülmüştür. Bu özniteliklerin sıralanması ve sonrasında yapılan sınıflandırmada en düşük hatası olan %17'lik değere yine "wrapper" yöntemi ile sıralanmış iki öznitelik ile ulaşılmıştır (Tablo 8).

Tablo 8. Naturel fındıklarda dört farklı öznitelik seçimi algoritması ile sıralanmış öznitelikler ile elde edilen en düşük Afla+ Afla- sınıflandırma hatası.

	Fisher (95)	İlinti (18)	TBA(115)	Wrapper(2)
Hata (%)	37	38	30	17

Naturel fındık imgelerinde yansıma enerjisi düşük olduğu için çoğunlukla uzamsal-frekans duzlemin yüksek frekanslı bölgelerindeki öznitelikler seçilmiştir. Bu gurup fındıklar için daha farklı aydınlatma koşullarında ve kameralar ile hiperspektral imge alınması durumunda daha iyi sınıflandırma sonuçlarına ulaşılabileceği düşünülmektedir. Bu konudaki ayrıntılı bilgiyi proje araştırmacılarından olan Habil Kalkan 'ın doktora tezinde bulabilirsiniz [8]. Geliştirdiğimiz 2B YAT yöntemi [9] uluslararası "Pattern Recognition" dergisine gönderilmiş olup bu konuda yapılan bir bildiri de uluslararası bir konferansta sunulmuştur [10].

Naturel fındıklarda yapılan çalışmalara ek olarak fındıklar gün ışığında ve yüksek çözünürlüklü bir fotoğraf makinesi ile de imgelenmiş ve elde edilen sonuçlar ayrıca Bölüm 2.3.7'de verilmiştir.

2.3.7 Naturel fındıkların gün ışığında alınan imgelerle sınıflandırılması

Naturel fındıklar hiperspektral görüntülemeye ek olarak daha basit gün ışığı altında yüksek çözünürlüklü fotoğraf makinası ile alınan görüntüler ile de incelenmiştir. Bunun için Naturel fındıklar içerisinden alınan B1(Kontrol) ve B3 (A.Praciticus) fındıkları kullanılmıştır. B3 grubu fındıklar üzerinde yüksek miktarda küf sporları gözlenmiştir. Bu küf sporları fındık yüzeyi görünümünü önemli derecede değiştirdiği için bu fındıklar göz ile de kolaylıkla ayırt edilebilmektedir. Bu gruptaki fındıkların bir kısmı üzerlerindeki küf sporlarından silme ile arındırılarak incelenmiştir. Bu yeni grup fındıklar B4 olarak adlandırıldı (Şekil 16).

-a- **-b-** **-c-**

Şekil 16. Naturel fındıklardan a) kontrol, b) küflü (B3) ve c) küfden arındırılmış (B4) grubu fındıklara ait gün ışığında alınmış görüntüler

Bu görüntülerden de Şekil 11' daki gibi 2 boyutlu dalgacık dönüşümü ile öznitelikler çıkartıldı ve bir çok bant çiftinin benzer sonuçlar verdiği tespit edildi. Örnek bir çift olarak "HL" ve "HLLH" dalgacık altbandına ait olan saçılma grafiği Şekil 17' da verilmiştir. Burada görüldüğü üzere üzeri küf sporu ile kaplı olan (B3) ile kontrol grubu (B1) fındıklar %100'e yakın bir değerde birbirlerinden ayrılmaktadır. Bu ayrımsallık değeri küf sporlarından arındırılmış (B4) fındıkları ile konrol grubu B1 fındıkları arasında %85 civarındadır (Şekil 17-b).

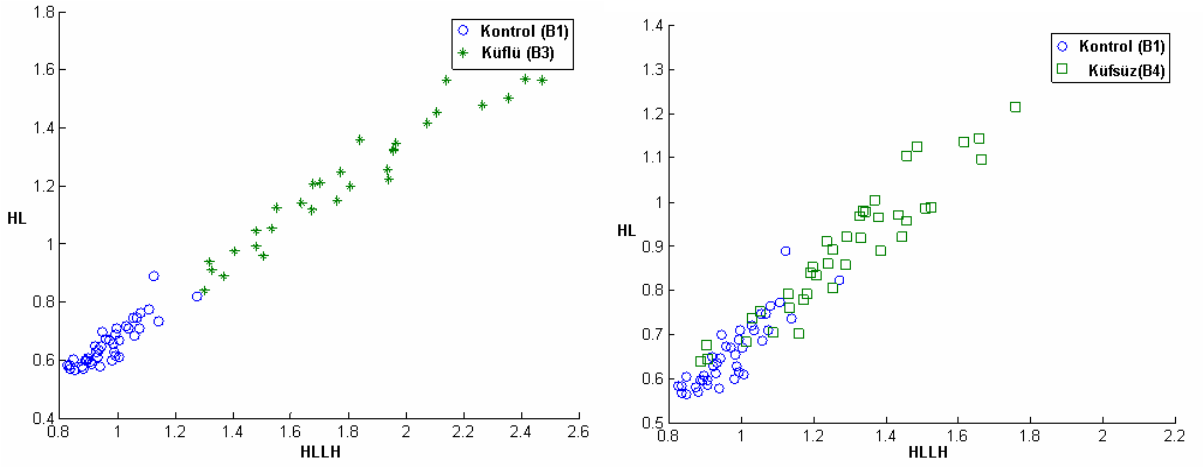

-a- -b-

Şekil 17. İki farklı naturel fındık grubu arasındaki ayrımsallık grafiği

3. BİBER ÜZERİNE YAPILAN ÇALIŞMALAR

İlk aşamada ülkenin değişik bölgelerinden paketli veya paketsiz satılan toplam 32 adet biber örnegi üzerinde çalışıldı. Bu veri setindeki aflatoksinsiz biberlerin sayısının yeterli olmadığına karar verilip 8 adet biber örneği daha temin edildi. Yeni alınan biber örnekleriyle birlikte toplam 40 biber örneği üzerinde çalışılmıştır. Biber örneklerinin temin edildikleri şehirler Tablo 8'deki gibidir. (örnekler aflatoksin miktarına göre azdan çoğa doğru sıralanmıştır.)

Tablo 9. Biber örneklerinin temin edildikleri şehirler

Biber No	Şehir	Aflatoksin miktarı (ppb)	Biber No	Şehir	Aflatoksin miktarı (ppb)	Biber No	Şehir	Aflatoksin miktarı (ppb)
1	Ankara	1,31	15	Ankara	8,48	29	Diyarbakır	43,96
2	Kahramanmaraş	2,56	16	Ankara	9,90	30	İstanbul	49,40
3	Ankara	2,65	17	İzmir	17,90	31	Antalya	52,10
4	Diyarbakır	2,93	18	Ankara	19,67	32	Sivas	55,75
5	Erzincan	3,12	19	Kahramanmaraş	20,91	33	Hatay	62,81
6	Ankara	3,63	20	Kahramanmaraş	24,37	34	Ankara	71,83
7	Ankara	4,46	21	Antalya	25,25	35	Antalya	78,42
8	Erzincan	4,88	22	İzmir	27,21	36	Antalya	84,07
9	Ankara	5,16	23	Ankara	27,72	37	Ankara	84,57
10	Kahramanmaraş	5,49	24	Kahramanmaraş	29,90	38	Ankara	97,30
11	Kahramanmaraş	5,49	25	Kahramanmaraş	32,32	39	Kahramanmaraş	188,90
12	Kahramanmaraş	6,46	26	İstanbul	33,88	40	Diyarbakır	244,41
13	Hatay	8,10	27	Kahramanmaraş	36,17			
14	Diyarbakır	8,27	28	Antalya	38,50			

40 adet biber örneğinin görüntüleri 400 nm dalgaboyundan başlayıp 510 nm'ye kadar 10 nm'lik, 550 nm için 70 nm'lik ve 600 nm için 40 nm'lik band aralıklarında alınmıştır. Her biberin 3 farklı bölgesinden 3 ayrı görüntüsü alınarak 40 adet biber örneğinden toplam 120 biber görüntüsü elde edilmiştir. Görüntüleri alınan biberler ilk etapta Tübitak ATAL'a ve bunu takiben Süleyman Demirel Üniversitesi Merkez Laboratuvarına kimyasal analize gönderilmiştir. Bu biberlerden biri uzmanlar tarafından sağlıksız ve kontamine görünüme sahip olarak değerlendirilmekle beraber kimyasal analiz sonucunda aflatoksin miktarı çok düşük çıkmaktaydı. Daha sonraki güneydoğu yöresinden uzmanlar ile yapılan görüşmelerde biberlere aflatoksinin kimyasal analizde belirlenmesini engelleyen bazı maddeler (Silisyum) katılarak hile yapıldığı ve bu pratiklerin çiftçiler tarafından kullanılabildiği anlaşılmıştır. Sözkonusu örnek biber Tarım Bankanlığı Ankara Laboratuvarı'nda silisyum analizine gönderilmiş ve içerisinde bir miktar silisyuma rastlanmıştır. Daha sonradan temin edilen 8 biber örneği Süleyman Demirel Üniversitesi Merkez Laboratuvarında kimyasal olarak analiz edilmiştir. Diğer biber örnekleri de zaman içerisinde küf miktarlarında bir değişim olabileceği göz önünde bulundurularak Süleyman Demirel Üniversitesi'nde tekrar analiz edilmiştir. Analizler sonucunda elde edilen aflatoksin kontaminasyonu Şekil 18 ve Tablo 8'de verilmiştir.

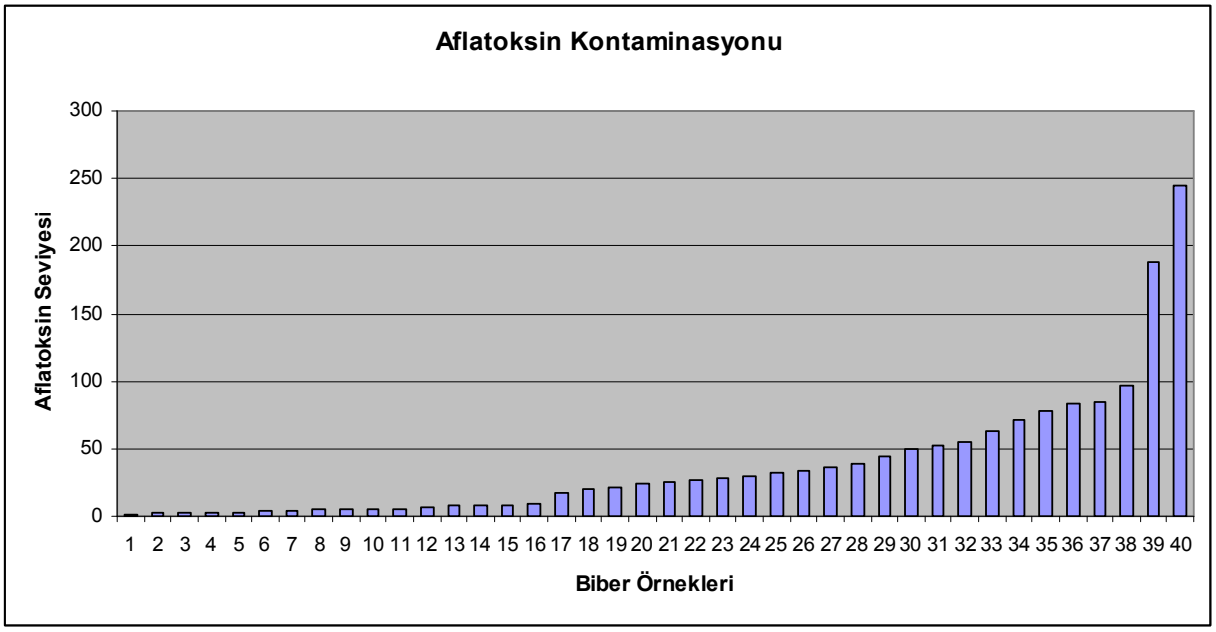

Şekil 18. Biber örneklerinin aflatoksin kontaminasyonu

Aflatoksin miktarı 10 ppb'nin üzerinde olan biberler aflatoksinli, 10 ppb'nin altında olan biberler aflatoksinsiz olarak kabul edilmiştir. Bu durumda, ilk aşamada piyasadan temin edilen 32 biber örneğinin 23 tanesi aflatoksinli, 9 tanesi aflatoksinsiz olarak belirlenmiştir. Sonradan temin edilen 8 biberin de katılmasıyla aflatoksinli biber sayısı 24'e, aflatoksinsiz biber sayısı da 16'ya yükselmiştir.

Aflatoksinli ve aflatoksinsiz biberler arasından seçilen birer biber örneğinin spektral görüntüleri sırasıya Şekil 19 ve Şekil 20'te verilmiştir.

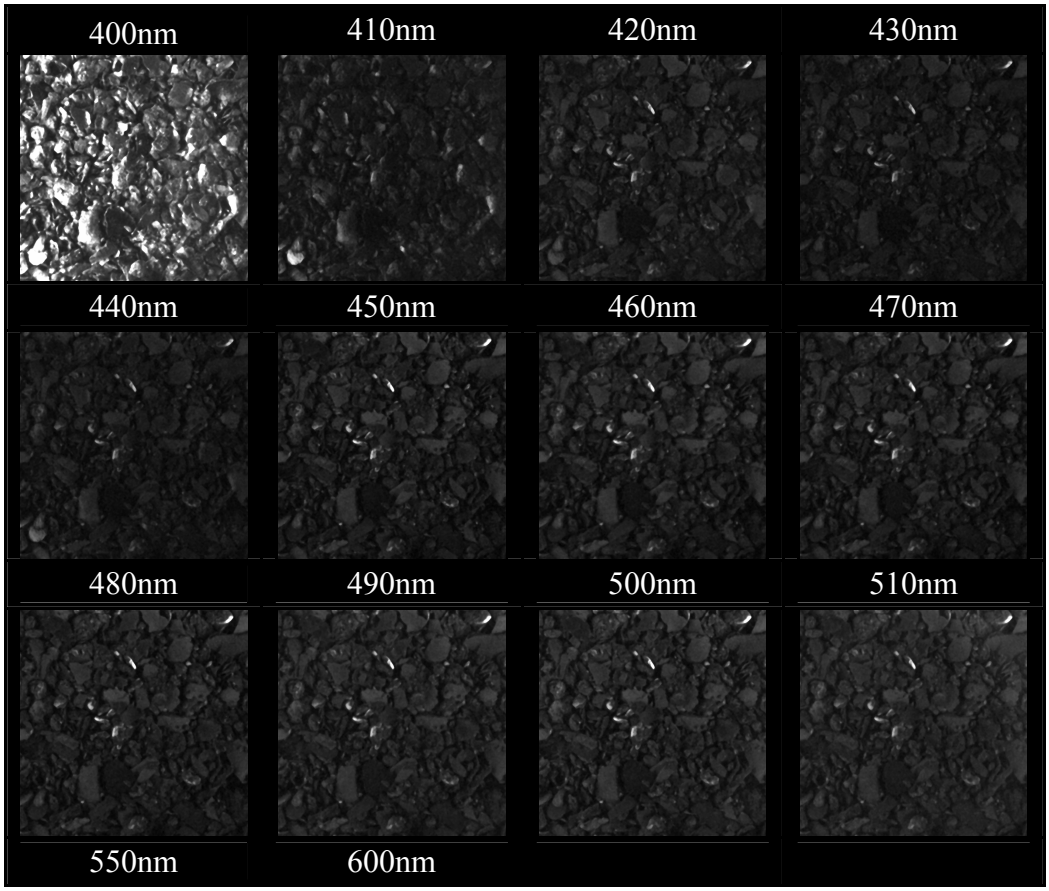

Şekil 19.Aflatoksinli biber örneğinin spektral görüntüleri

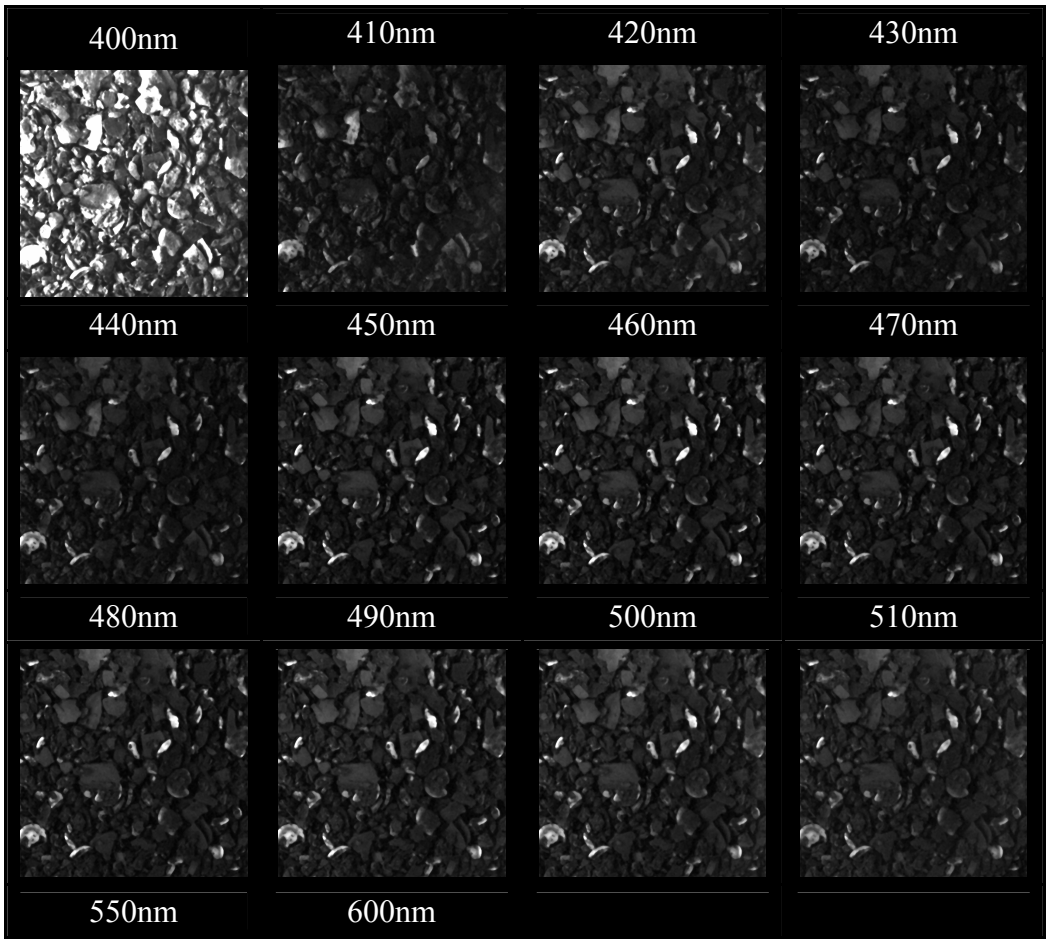

Şekil 20. Aflatoksinsiz biber örneğinin spektral görüntüleri

Aflatoksinli ve aflatoksinsiz biberleri ayırt edebilmek amacıyla iki farklı yöntem kullanılmıştır. İlk yöntemde birinci dereceden istatistiksel öznitelikler ve eş oluşum matrisinden elde edilen öznitelikler kullanılarak sınıflandırma yapılmıştır. Bu çalışmada 32 biberden oluşan veri seti kullanılmıştır. İkinci yöntemde, fındık üzerinde de uygulanmış olan Yerel Ayırtaç Tabanları yaklaşımı kullanılmıştır. Bu çalışma toplam 40 biberin hiperspektral görüntüleri üzerinde yapılmıştır.

3.1 Hyperspektral görüntüler kullanılarak biberlerin birinci dereceden öznitelikler ile sınıflandırılması

İlk aşamada 14 biber örneğinin 400 nm'den başlayarak 510 nm'ye kadar 10 nm aralıklarla alınmış olan hyperspektral görüntüleri üzerinde çalışılmıştır.

Biber görüntülerinden ortalama yeğinlik değerleri hem imgeyi bir bütün olarak ele alarak hem de biber imgeleri 400 parçaya bölünerek 24x32 lik imgeler üzerinden hesaplanmıştır. Lokal öznitelikler hesaplanırken her bir pencere için öznitelikler hesaplanmış ve sınıflandırma sonunda 400 pencere için alınan kararlar üzerinde çoğunluk oylaması yapılarak biber coğunluğun verdiği karara göre aflatoksinli veya aflatoksinsiz olarak sınıflandırılmıştır. Her spektral bant için ortalama yeğinlik değerleri ile öznitelik vektörü oluşturulmuştur. Bu öznitelikler yapay sinir ağı sınıflandırıcısına verilmiştir. 11 kere farklı

başlangıç noktalarından hareket edecek şekilde sınıflandırıcıya verildiğinde her biber için elde edilen hata sayıları Tablo 10'da verilmiştir.

Tablo 10. Lokal ve global hata sayıları

	km1	f13	fm3	f33	f23	km3	km2	km 5	h7	km 6	k1	F43	B1	h2
Aflatoksin Miktarı (ppb)	0.13	0.18	0.54	0.92	2.71	3.29	6.57	7.47	11.1	13.3	42.3	54.6	58.3	84.4
Toplam Hata (Lokal)	10	0	0	0	0	0	0	0	1	0	0	5	0	0
Toplam Hata (Global)	5	4	6	0	9	10	0	0	1	0	3	0	4	1

Lokal öznitelikler kullanılarak daha iyi sonuçlar elde edilmiştir. Bu çalışmanın sonuçları IUPAC [11] konferansında sunulmuştur.

3.2 Hyperspektral görüntüler kullanılarak biberlerin Birinci Dereceden İstatistiksel ve Eş Oluşum Matrisi öznitelikleri ile sınıflandırılması

32 biber örneginin tüm spektral bant görüntülerinden ilk sıra istatistiksel öznitelikler ortalama, varyans, çarpıklık ve basıklık değerleri hesaplanmıştır.

Eş oluşum matrisi imge gri seviyelerinin belirli bir yön (θ) ve uzaklıkta (d) birlikle bulunma dağılımlarını verir. En çok kullanılan dört yön θ = 0°, 45°, 90°, 135° dir. Bu çalışmada, komşuluk uzaklığı 1 olarak seçilerek bu 4 yön için eş oluşum matrisleri oluşturulmuştur.

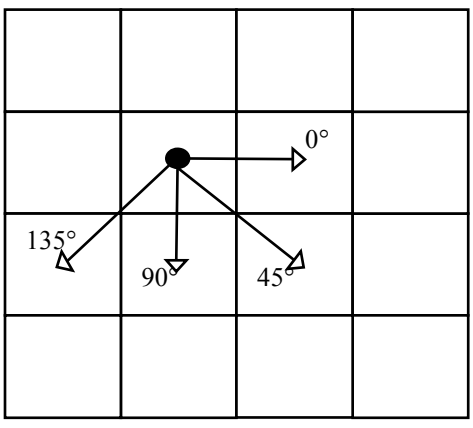

Şekil 21. Komşuluk uzaklığı d=1 için en çok kullanılan yönler

Ancak biberlerdeki yönsellik bilgisi önemli olmadığı için bu dört eş oluşum matrisindeki değerlerin ortalaması alınarak tek matriste birleştirilmiş ve öznitelikler bu matris kullanılarak hesaplanmıştır. Bu matristen elde edilen öznitelikler homojenlik, kontrast, enerji, entropi, ters fark momenti, ençok olasılık ve korelasyondur.

Birinci derece istatistiksel öznitelikler ve eş oluşum matrisi öznitelikleri birleştirildiğinde her spektral görüntü için toplam 11 öznitelik elde edilmiştir. 14 spektral bant için toplam 154 öznitelik çıkarılmıştır.

Bu 154 öznitelikten en ayırt edici olanları seçmek amacıyla, her seferinde 1 biber veri setinden çıkarılarak diğer biber örnekleri bir eğitim seti olarak kullanılmıştır. Bu eğitim seti için aflatoksinli ve aflatoksinsiz biber sınıfları arasındaki Fisher uzaklıkları hesaplanmıştır. Bu işlem çıkarılan biber veri setine eklenip bir başka biber çıkarılarak tekrarlanmıştır. Tüm eğitim setleri için elde edilen Fisher uzaklık değerleri kullanılarak her öznitelik için bir genel öznitelik skoru hesaplanmıştır. Bu skorlar büyükten küçüğe sıralanarak en iyi 10 öznitelik belirlenmiştir. Seçilen en iyi öznitelikler ve ait oldukarı spektral bantlar Tablo 11'de verilmiştir.

Tablo 11. Genel öznitelik skoruna göre en iyi 10 öznitelik

Spektral Bant	**Öznitelik**		
400	homojenlik	kontrast	enerji
480	basıklık		
490	basıklık		
500	basıklık	enerji	
510	ortalama	basıklık	
550	homojenlik		

Aflatoksinli ve aflatoksinli biberleri sınıflandırmada kullanılacak en iyi spektral bantları ve öznitelikleri elde etmek amacıyla iki farklı öznitelik seçim yöntemi kullanılmıştır. Birinci seçim yöntemi olan filtre yönteminde, daha önceki aşamada seçilen 10 en iyi öznitelik skorlarına göre en iyiden başlayarak doğrusal sınıflandırıcıya her defasında bir öznitelik daha ekleyerek verilmiştir. İkinci seçim yöntemi olan wrapper yönteminde, tüm öznitelik kombinasyonları doğrusal sınıflandırıcıya verilmiştir. Elde edilen sınıflandırma eğrileri Şekil 22'da verilmiştir.

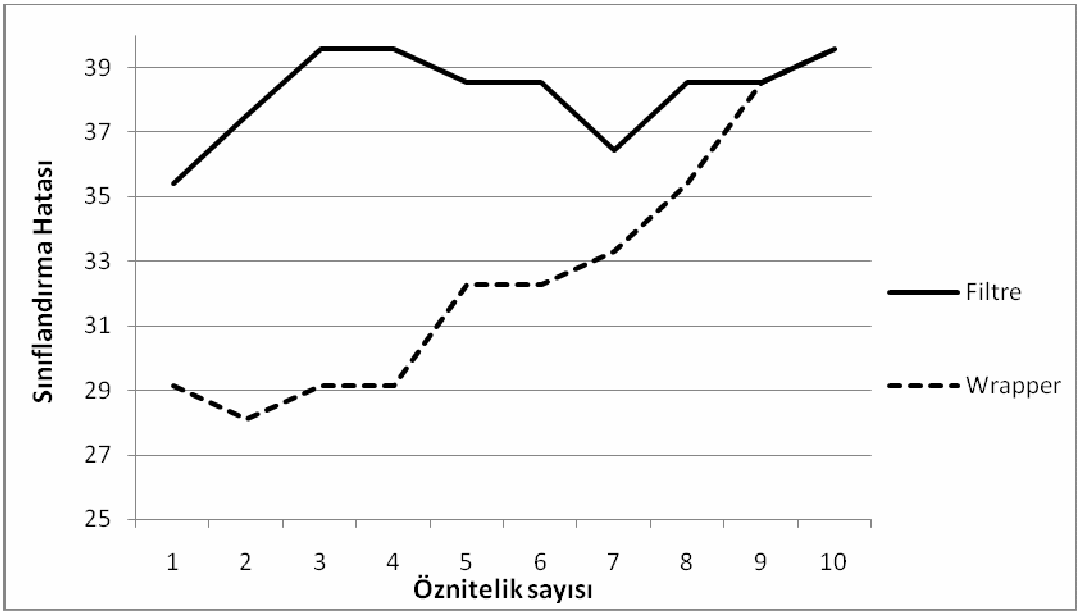

Şekil 22. İstatistiksel yöntemle elde edilen özniteliklerin filtre ve wrapper seçim yöntemleri için sınıflandırma eğrileri

Yapılan sınıflandırma sonucunda en iyi sınıflandırma doğruluğu wrapper seçim yöntemi kullanılarak seçilen iki öznitelik kullanılarak yaklaşık % 72 olarak bulunmuştur.

3.3 Hyperspektral görüntüler kullanılarak biberlerin 2B YAT tabanlı öznitelikleri ile sınıflandırılması

2B YAT tabanlı özniteliklerin çıkarılmasında kullanılan aşamalar fındıkla ilgili bölümde açıklanmıştı.

Biber için yapılan çalışmada önce spektral bantlar için bir ikili ağaç oluşturuldu ve tüm bantların yansıma enerji değerleri bu ağacın tabanına yerleştirildi. 550 ve 600 nm bantların bantgenişliği daha geniş olduğu için birleştirilmeleri istenmediğinden bu bantlar ağaç tabanına yerleştirilmedi.

Bir diğer ağaç dörtlü ağaç yapısında uzamsal-frekans ekseninde oluşturuldu. 3 seviye dalgacık paket ayrıştırması ile her spektral bant imgesi için 85 altbant imgesi elde edildi. Öznitelik olarak bu altbant imgelerinin enerji değerleri kullanıldı ve dörtlü yapıdaki ağaç üzerine yerleştirildi. 14 spektral bant için 1190 öznitelik elde edilmiş oldu.

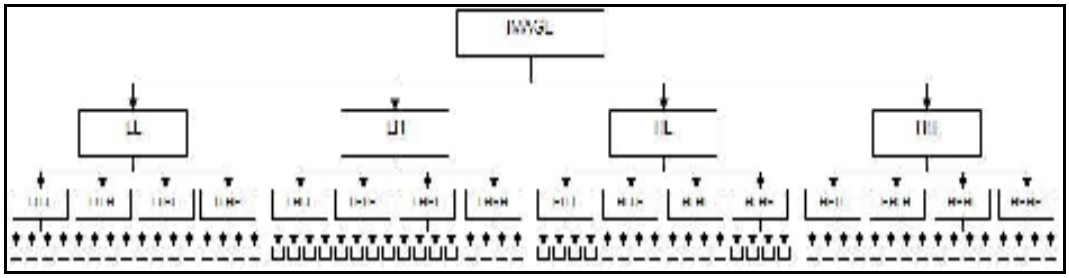

Şekil 23.3 seviye dalgacık dönüşümü ayrıştırması

Daha sonra bu iki ağaç da budanarak öznitelik haritası elde edildi. Genel öznitelik hartitası Şekil 24'te verilmiştir.

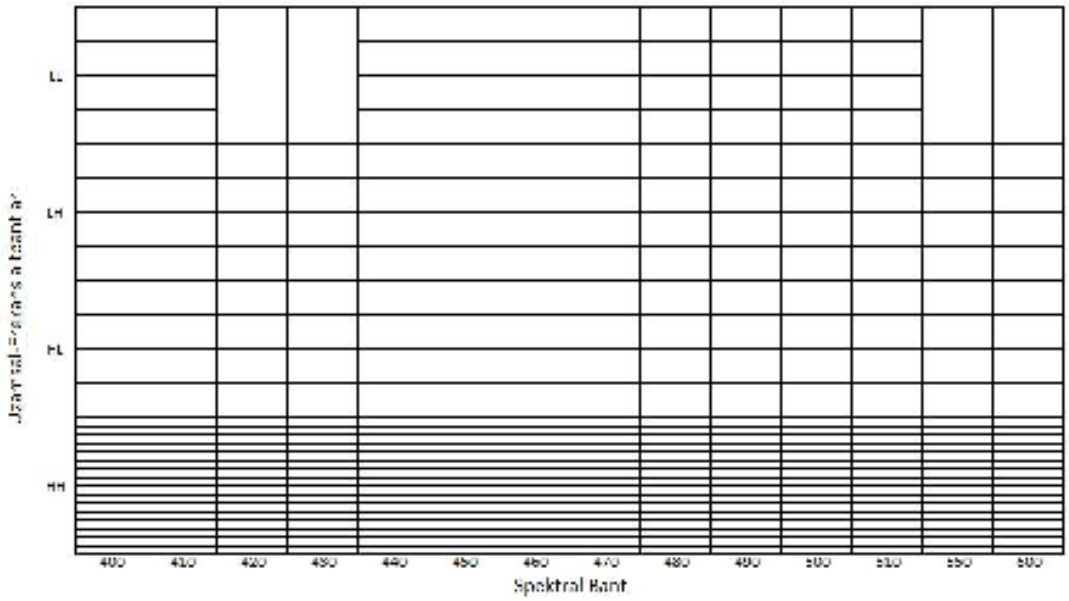

Şekil 24.Genel öznitelik haritası

Bu 1190 öznitelikten en ayırt edici olanları seçmek amacıyla, her seferinde 1 biber veri setinden çıkarılarak diğer biber örnekleri bir eğitim seti olarak kullanılmıştır. Bu eğitim seti için öznitelik haritası çıkarılmıştır. Bu işlem çıkarılan biber veri setine eklenip bir başka biber çıkarılarak tekrarlanmıştır. Tüm eğitim setleri için elde edilen haritalardaki öznitelikler için Fisher uzaklığı hesaplanmıştır ve Fisher uzaklığı en yüksek olan 20 öznitelik kaydedilmiştir. Bu değerler kullanılarak her öznitelik için Fisher uzaklığına göre sırası ve tüm öznitelik haritasında bulunma sayısı göz önünde bulundurularak bir genel öznitelik skoru hesaplanmıştır. Bu skorlar büyükten küçüğe sıralanarak en iyi 11 öznitelik belirlenmiştir. Bu öznitelikler Şekil 25'ta verilmiştir.

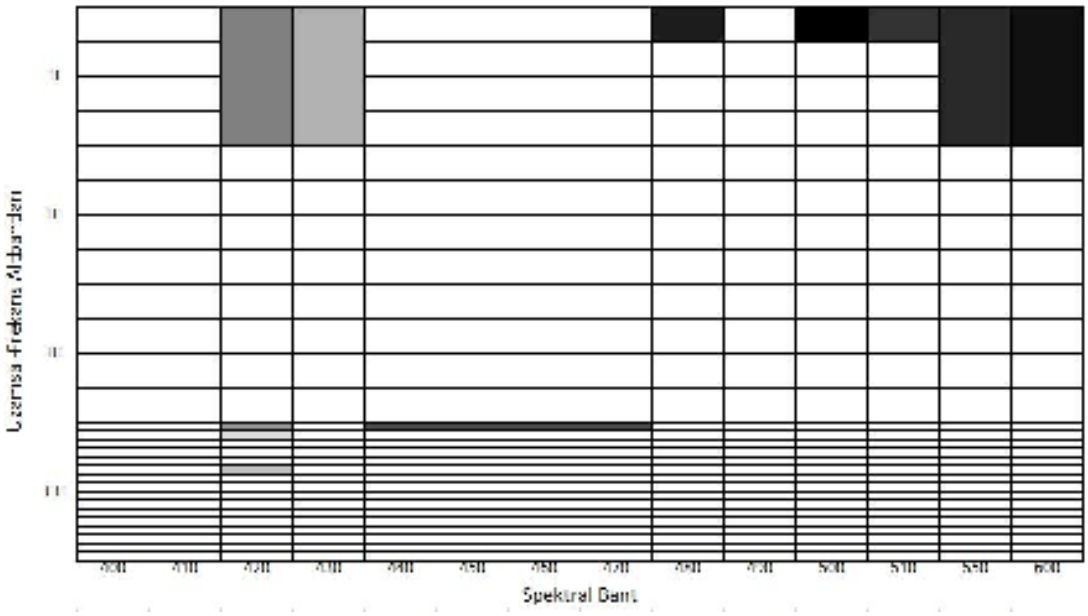

Şekil 25. Spektral ve uzamsal-frekans düzlemindeki en ayırt edici 11 öznitelik.

Aflatoksinli ve aflatoksinli biberleri sınıflandırmada kullanılacak en iyi spektral bantları ve öznitelikleri elde etmek amacıyla iki farklı öznitelik seçim yöntemi kullanılmıştır. Filtre yönteminde, daha önceki aşamada seçilen 11 en ayırt edici öznitelik skorlarına göre en iyiden başlayarak doğrusal sınıflandırıcıya her defasında bir öznitelik daha ekleyerek verilmiştir. Wrapper yönteminde, tüm öznitelik kombinasyonları doğrusal sınıflandırıcıya verilmiştir. Elde edilen sınıflandırma eğrileri Şekil 26'da verilmiştir.

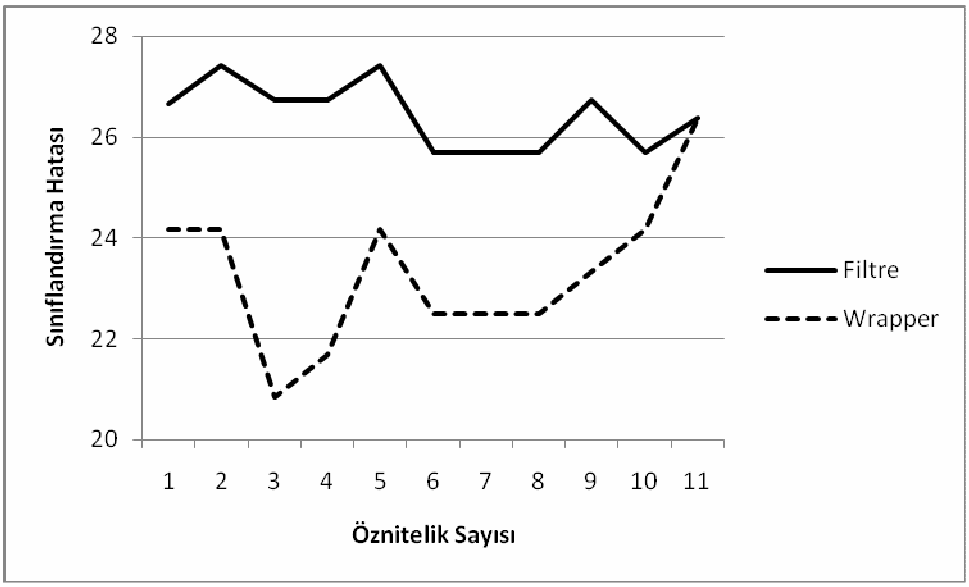

Şekil 26. 2B YAT yöntemiyle elde edilen özniteliklerin filtre ve wrapper seçim yöntemleri için sınıflandırma eğrileri

En iyi sınıflandırma doğruluğu %79,17 olarak bulunmuş ve wrapper öznitelik seçim yöntemi ile seçilen 3 özniteliğin kullanılması ile elde edilmiştir. Bu öznitelikler 420, 430 ve 600 nm spektral bantlarının düşük frekans altbantlarından elde edilen özniteliklerdir. Bu

yöntemle 72 aflatosinli biberin 15 tanesi ve 48 aflatoksinsiz biberin 10 tanesi yanlış sınıflandırılmıştır. Veri setinden aflatoksinli olarak sınıflandırılan tüm biberlerin atılmasıyla ortalama aflatoksin seviyesi 38,26'dan 15,93'e düşmüştür.

En ayırt edici özniteliklerin düşük frekans altbantlardan seçilmesi aflatoksinli ve aflatoksinsiz sınıfların yeğinlik değerlerine göre sınıflandırıldığının bir göstergesidir. Veri seti incelendiğinde aflatoksinli biberlerin genellikle daha karanlık, aflatoksinsiz biberlerin ise genellikle daha aydınlık olduğu gözlemlenmiştir. Bu gözlem sonucunda, biberlerin yeğinlik değerlerine göre aydınlık ve karanlık olarak iki sınıfa ayrılmasına ve 2B YAT yönteminin bu iki grup için ayrı ayrı uygulanmasına karar verilmiştir.

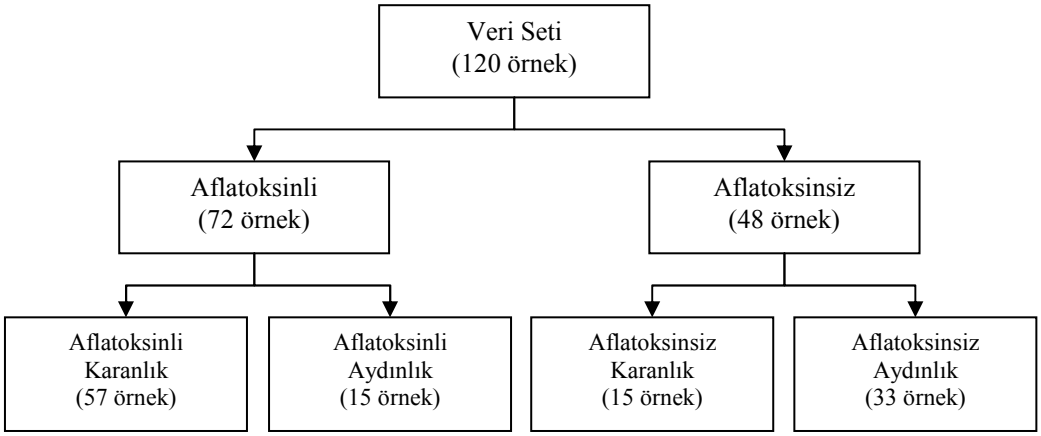

Şekil 27 . Yeğinlik tabanlı veri setleri ve örnek sayıları

2B YAT yöntemi karanlık ve aydınlık biberler üzerinde ayrı ayrı uygulandığında seçilen an ayırt edici 12 öznitelik karanlık biber grubu için Şekil 28'de, aydınlık grup için Şekil 29'da verilmiştir.

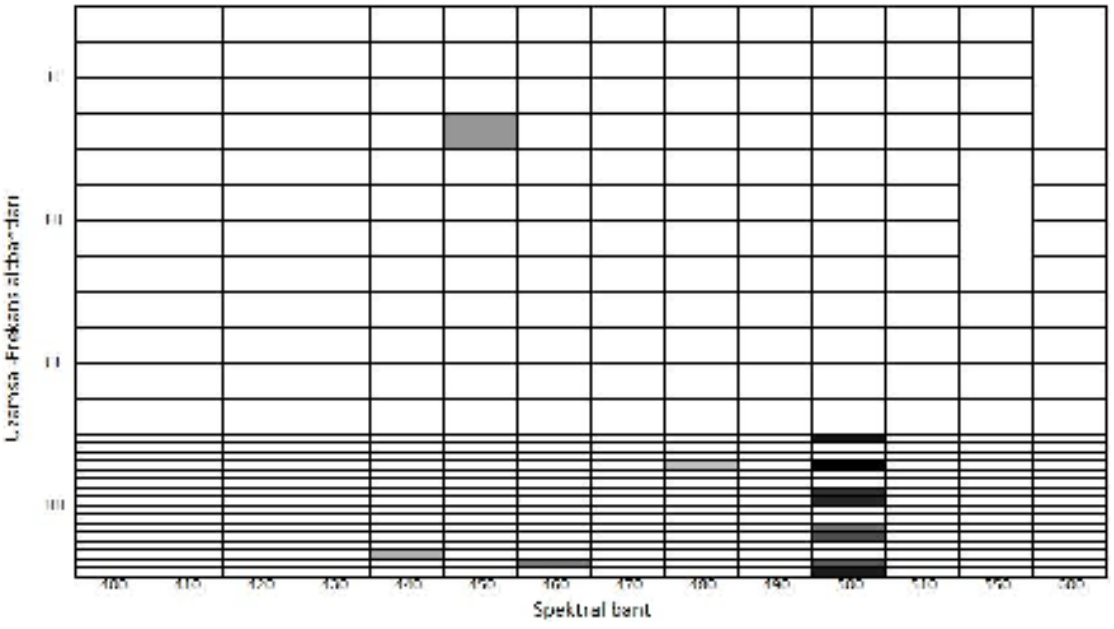

Şekil 28. Karanlık biberler için en ayırt edini 12 öznitelik

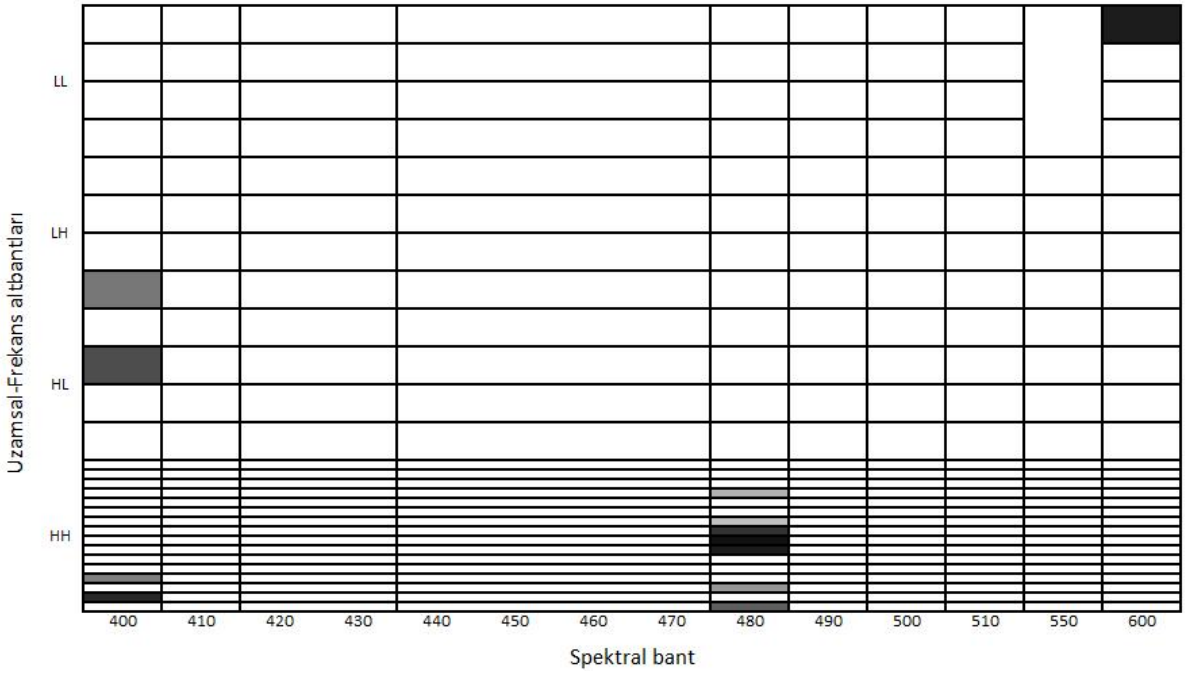

Şekil 29. Aydınlık biberler için en ayırt edini 12 öznitelik

Bu öznitelikler daha önce kullanılan seçim yöntemleri ile değerlendirildiğinde, elde edilen en düşük sınıflandırma hataları Tablo 12'da verilmiştir.

Tablo 12. Aydınlık ve karanlık biberler için sınıflandırma hataları

	Filtre		Wrapper	
	Karanlık	Aydınlık	Karanlık	Aydınlık
Öznitelik Sayısı	8	2	4	2
Hata(%)	32.77	39.72	26.39	14.58
Ortalama Hata(%)	36.25		20.83	

Aydınlık ve karanlık biberlerin ayrı ayrı ele alınmasıyla %79,17 lik bir sınıflandırma doğruluğu elde edilmiştir. 72 aflatoksinli biberin 17 tanesi ve 48 aflatoksinli biberin 8 tanesi yanlış sınıflandırılmıştır. Sınıflandırma sonucunda aflatoksinli olarak belirlenen örneklerin veri setinden çıkarılması ile veri setinin ortalama aflatoksin seviyesi 38,26'dan 29,24'e düşmüştür. Biber konusunda elde edilen veriler ve sonuçlar ODTÜ Enformatik Enstitüsü'nden Pelin Beriat [12] ve Süleyman Demirel Üniversitesi Gıda Mühendisliği'nden Meltem Özcan tarafından tez çalışması haline getirilmiştir [13].

Bu proje uluslararası işbirliklerine temel oluşturmuş, gıda güvenliği alanındaki bir FP7 konsorsiyumu içerisinde yer alınmıştır. Yapılan proje önerisi en iyi eşik üstü 3 proje arasına 2. olarak girmiş fakat sadece 1 projenin desteklenmesinden dolayı sunulduğu çağrıda kabul edilmemiştir. Bunu takiben FAO tarafından açılan proje çağrısına bir öneri yollanmış, proje desteklenmeye değer bulunmuş fakat BM tarafından kaynak temin edilemediğinden desteklenmemiştir. Bu deneyimler bu alandaki çalışmalara duyulan ihtiyacı ortaya çıkarmaktadır. Bu proje sonrasında bir SANTEZ projesi ile prototip geliştirme üzerinde çalışılması planlanmaktadır.

REFERANSLAR

[1] KALKAN, H., YARDIMCI, Y., *"Classification of Hazelnut Kernels by Impact Acoustics"*, IEEE MLSP, Dublin (2006)

[2] KALKAN, H., İNCE, F., TEWFİK, A., H., YARDIMCI, Y. PEARSON, T., *"Classification of Hazelnut Kernels by Using Impact Acoustic Time- Frequency patterns",* EURASIP Journal on Advances in Signal Processing, V: 2008, Article ID 247643 (2008)

[3] INCE, F,. ONARAN, I., PEARSON, T., TEWFIK, A., CETIN, A.E., KALKAN, H., YARDIMCI, Y.,, Identification of Damaged Wheat Kernels and Cracked Hazelnuts with Impact Acoustics Time Frequency Patterns, Transactions of the ASABE, 51(4): 1461-1469(2008).

[4] INCE, F, ONARAN, I., TEWFIK, A., KALKAN, H., PEARSON, T., CETIN, A.E., YARDIMCI, Y., *"Wheat and Hazelnut Inspection with Impact Acoustics Time-Frequency Patterns"*, ASABE Annual International Meeting, Minneapolis, USA (2007)

[5] KALKAN, H., YARDIMCI, Y., İNCE, F., TEWFİK, A., SENYUVA, H., ARICI, M., H. Senyuva, M. Arici, PEARSON, T., CETIN, A.E., ONARAN, I., *"Separation of damaged shell hazelnut by impact acoustics'"*", XII International IUPAC Symposium on Mycotoxins and Phycotoxins, Istanbul (2007)

[6] KALKAN, H., İNCE, F., TEWFİK, A., H., YARDIMCI, Y. PEARSON, T., "Extraction of Optimal Time-Frequency Plane Features for Classification", IEEE SIU, Eskisehir (2007)

[7] KALKAN, H., YARDIMCI, Y., "Detection of Contaminated Hazelnuts by Hyperspectral Imaging", IEEE SIU, Didim (2008)

[8] KALKAN, H., *Feature Extraction from Acoustic and Hyperspectral Data by 2D Local Discriminant Bases Search*(PhD Thesis), Informatics Institute, METU (2008)

[9] KALKAN, H., YARDIMCI, Y., *"Feature Extraction from Hyperspectral Data by 2D Local Discriminant Bases",* Submitted to Pattern Recognition (Elsevier-2008)

[10] KALKAN, H., YARDIMCI, Y., "Extraction of Discriminative Features from Hyperspectral Data", IEEE SSTDM Workshop on International Conference on Data Mining, Pisa, Italy (2008).

[11] KALKAN, H., ÖZCAN, M., YARDIMCI, Y., *BASARAN, P., BERİAT, P.,*, *"A Novel Prospective Technological Approach: Machine Vision Techniques for Noninvasive Aflatoxin Detection in Chilly Peppers"*, XII International, IUPAC Symposium on Mycotoxins and Phycotoxins, Istanbul (2007)

[12] BERIAT, P., Non-destructive Testing of Textured Foods (Master Thesis), Informatics Institute, METU (2009)

[13] ÖZCAN, M., *Tahribatsız ve Hızlı Yöntemlerle Kırmızı Biber ve Fındıkta Kalite Kontrolü*, (Yüksek Lisans Tezi), Süleyman Demirel Üniversitesi (2008)

TÜBİTAK
PROJE ÖZET BİLGİ FORMU

Proje No: 106E057

Proje Başlığı:

Tahribatsız ve Hızlı Yöntemlerle Gıdalarda Kalite Kontrolü

Proje Yürütücüsü ve Araştırmacılar:

Prof.Dr.Yasemin Yardımcı (Yürütücü)

Yrd. Doç.Dr. Pervin Başaran (Yrd. Araştırmacı)

Projenin Yürütüldüğü Kuruluş ve Adresi:

Enformatik Enstitüsü, 06531, ODTÜ, Ankara

Destekleyen Kuruluş(ların) Adı ve Adresi:

Projenin Başlangıç ve Bitiş Tarihleri: 01.07.2006- 31.12.2008

Öz (en çok 70 kelime)

Bu projede fındık ve kırmızı biberlerin kanserojen aflatoksin maddesi barındıranlarının görüntü ve ses işlemeye dayalı yöntemlerle tespit edilmesi üzerine algoritmalar geliştirilmiştir. Kabuklu fındıklar için kabuğu sağlam ve çatlak olanlar çarpma sesine dayalı olarak; iç fındıklar (kavrulmuş veya naturel) ve kırmızı biberler ise hiperspektral görüntülerine dayalı olarak ayırt edilmiştir. Bu ayrıştırma için alınan ses ve görüntü sinyallerinden çeşitli öznitelikler çıkartılmış ve en yüksek başarımı verenler tespit edilmiştir. Geliştirilen algoritma ile kabuklu fındıklar %96, kavrulmuş fındıklar %97, naturel fındıklar %85, kırmızı biberlerde %80 lik başarım oranları ile sınıflandırılmıştır.

Anahtar Kelimeler:

Hiperspektral görüntü işleme , akustik sinyal işleme, öznitelik çıkarımı ve seçimi, gıda güvenliği

Fikri Ürün Bildirim Formu Sunuldu mu **Evet** ☐ **Gerekli Değil** ☒

Fikri Ürün Bildirim Formu'nun tesliminden sonra 3 ay içerisinde patent başvurusu yapılmalıdır.

Projeden Yapılan Yayınlar:

- H. Kalkan, Y. Yardimci *"Feature Extraction from Hyperspectral Data by 2D Local Discriminant Bases",* Submitted to Pattern Recognition (Elsevier)
- H. Kalkan, F. Ince, A.Tewfik, Y. Yardimci, T. Pearson *"Classification of Hazelnut Kernels by Using Impact Acoustic Time- Frequency patterns",* EURASIP Journal on Advances in Signal Processing, V: 2008, Article ID 247643
- N. Ince, I. Onaran, T. Pearson, A.Tewfik, A.E.Cetin, H.Kalkan, Y.Yardimci, Identification of Damaged Wheat Kernels and Cracked Hazelnuts with Impact Acoustics Time Frequency Patterns, Transactions of the ASABE, 51(4): 1461-1469, 2008.
- H. Kalkan, Yasemin Yardımcı, "Extraction of Discriminative Features from Hyperspectral Data", IEEE SSTDM Workshop on International Conference on Data Mining 2008,Pisa, Italy.
- H. Kalkan, Y. Yardımcı, *"Classification of Hazelnut Kernels by Impact Acoustics"*, IEEE MLSP 2006,

Dublin

- Nuri F. Ince ,I. Onaran , A. H. Tewfik , H.Kalkan, T. Pearson, A.E. Cetin, Y.Yardimci, *"Wheat and Hazelnut Inspection with Impact Acoustics Time-Frequency Patterns"*, 2007 ASABE Annual International Meeting, Minneapolis, USA
- H. Kalkan, M. Özcan, Y. Yardımcı, P. Basaran,P. Beriat, *"A Novel Prospective Technological Approach: Machine Vision Techniques for Noninvasive Aflatoxin Detection in Chilly Peppers"*, XII International, IUPAC Symposium on Mycotoxins and Phycotoxins, Istanbul,2007
- H. Kalkan, Y. Yardimci, F. Ince, A. Tewfik, H. Senyuva, M. Arici, T. Pearson, E. Cetin, I. Onaran, *"Separation of damaged shell hazelnut by impact acoustics"*", XII International IUPAC Symposium on Mycotoxins and Phycotoxins, Istanbul, 2007
- H. Kalkan, F. Ince, A. Tewfik ,Y. Yardimci, T. Pearson, "Extraction of Optimal Time-Frequency Plane Features for Classification", IEEE SIU, Eskisehir, 2007
- H. Kalkan, Yasemin Yardımcı. "Detection of Contaminated Hazelnuts by Hyperspectral Imaging", IEEE SIU, Didim, 2008

FEATURE EXTRACTION FROM ACOUSTIC AND HYPERSPECTRAL DATA BY 2D LOCAL DISCRIMINANT BASES SEARCH

HABİL KALKAN

DECEMBER 2008

FEATURE EXTRACTION FROM ACOUSTIC AND HYPERSPECTRAL DATA BY 2D LOCAL DISCRIMINANT BASES SEARCH

A THESIS SUBMITTED TO
THE GRADUATE SCHOOL OF INFORMATICS
OF
MIDDLE EAST TECHNICAL UNIVERSITY

BY

HABİL KALKAN

IN PARTIAL FULFILLMENT OF THE REQUIREMENTS FOR THE DEGREE OF
DOCTOR OF PHILOSOPHY
IN
THE DEPARTMENT OF INFORMATION SYSTEMS

DECEMBER 2008

Approval of the Graduate School of Informatics:

_____

Prof. Dr. Nazife BAYKAL
Director

I certify that this thesis satisfies all the requirements as a thesis for the degree of Doctor of Philosopy.

_____

Prof. Dr. Yasemin YARDIMCI
Head of Department

This is to certify that I have read this thesis and that in my opinion it is fully adequate, in scope and quality, as a thesis for the degree of Doctor of Philosopy.

_____

Prof. Dr. Yasemin YARDIMCI
Supervisor

Examining Committe Members

Prof. Dr. Fatoş T. YARMAN VURAL	(METU, CENG)	_____
Prof. Dr. Yasemin YARDIMCI	(METU, II)	_____
Prof. Dr. Enis ÇETİN	(Bilkent Univ, EE)	_____
Assoc. Prof. Dr. Erkan MUMCUOĞLU	(METU, II)	_____
Asst. Prof. Dr. Erhan EREN	(METU, II)	_____

I hereby declare that all information in this document has been obtained and presented in accordance with academic rules and ethical conduct. I also declare that, as required by these rules and conduct, I have fully cited and referenced all materials and results that are not original to this work.

Name, Last name : **Habil Kalkan**

Signature : _____

ABSTRACT

FEATURE EXTRACTION FROM ACOUSTIC AND HYPERSPECTRAL DATA BY 2D LOCAL DISCRIMINANT BASES SEARCH

Kalkan, Habil
Ph.D., Department of Information Systems
Supervisor: Prof. Dr. Yasemin YARDIMCI

December 2008, 89 pages

In this thesis, a feature extraction algorithm based on 2D Local Discriminant Bases (LDB) search is developed for acoustic and hyperspectral data. The developed algorithm extracts the relevant features by both eliminating the irrelevant ones and/or by merging the ones that do not provide extra information on their own. It is implemented on real world data to separate aflatoxin contaminated or high risk hazelnuts from the sound ones by using impact acoustic and hyperspectral data. Impact acoustics data is used to sort cracked and intact shell hazelnuts with high classification accuracy. Hypespectral images of the shelled and roasted (SRT) hazelnuts are used for classification and the algorithm extracted the spectral and spatial-frequency features for that classification. Aflatoxin concentration of the SRT category hazelnuts is automatically decreased to 0.7 ppb from 608 ppb by eliminating the detected contaminated ones.

Keywords: LDB, feature extraction, acoustic, hyperspectral, food safety.

ÖZ

2B YEREL AYIRTAÇ TABANLARI ARAŞTIRMASI İLE AKUSTİK VE HYPERSPEKTRAL VERİDEN ÖZNİTELİK ÇIKARIMI

Kalkan, Habil
Doktora, Enformatik Enstitüsü
Tez Yöneticisi: Prof. Dr. Yasemin YARDIMCI

Aralık 2008, 89 sayfa

Bu tezde, akustik ve hyperspektral veriden 2B Yerel Ayırtaç Tabanları (YAT) araştırmasına dayalı bir öznitelik çıkarımı algoritması geliştirilmiştir. Geliştirilen algoritma gereksiz özniteliklerin atılması ve/veya tek başlarına fazladan bilgi taşımayanların birleştirilmesi sureti ile gerekli öznitelikleri çıkarır. Çarpma akustik verisi kullanılarak çatlak kabuklu fındıklar sağlam kabuklu olanlardan yüksek bir sınıflandırma oranı ile ayıklanmıştır. Kavrulmuş iç fındıkların (SRT) sınıflandırılmasında hyperspektral görüntüler kullanılmış ve algoritma bu sınıflandırma için spektral ve uzamsal-frekans özniteliklerini çıkarmıştır. Tespit edilen bozulmuş fındıkların ayıklanması ile SRT fındıklarındaki aflatoksin yoğunlugu otomatik olarak 608 ppb den 0.7 ppb'ye düşmüştür.

Anahtar Kelimeler: YAT, öznitelik çıkarımı, akustik, hyperspektral, gıda güvenliği.

To my parents

ACKNOWLEDGEMENTS

I would like to express my sincere gratitude to the following people for their contribution to the completion of my Ph.D. program.

First, I thank my supervisor Prof. Dr. Yasemin Yardımcı for her patient, valuable guidance, continuous support and friendly attitute throughout my research. Under her supervision, I have a chance to develop myself in both academic and personal subjects.

I have conducted some of my studies in University of Minnesota under the guidance of Dr. Nuri Fırat Ince and Prof. Dr. Ahmet Tewfik and Dr. Tom Pearson from USDA-ARS-GMPRC. I would like to thank to them for their support and valuable comments.

I would also like to thank Prof. Dr. Enis Çetin and Assoc. Prof. Dr. Erkan Mumcuoğlu for their valuable suggestions. I also thank to Prof. Dr. Fatoş Tünay Yarman Vural and Asst. Prof. Dr. Erhan Eren for reviewing my work.

This thesis work is supported by The Scientific and Technical Research Council of Turkey (TÜBİTAK) by the project of 106E057:"Food Safety with Noninvasive Methods".

Finally, I would like to express my deepest gratitude to my family for their unconditional support during my life. Special thanks goes to my wife, Nida, for her continuous support and understanding.

TABLE OF CONTENTS

LIST OF TABLES

LIST OF FIGURES

LIST OF ABBREVIATIONS

μ	:	mean
σ	:	standart deviation
H	:	Entropy
LDA	:	Linear discriminant analysis
PCA	:	Principal component analysis
LDB	:	Local discriminant bases
LCP	:	Local cosine packets
CFS	:	Correlation based feature selection
FFS	:	Fisher discriminant based feature selection
$SPCT$	:	Segmented principal component transformation
$STFT$	:	Short time fourier transform
SNR	:	Signal to noise ratio
DWT	:	Discrete wavelet transform
$UDWT$	:	Undecimated discrete wavelet transform
TF	:	Time-frequency
$NATF$	:	Non-adaptive time-frequency features
$NASB$	:	Non-adaptive subband features
$BGYF$	:	bright greenish-yellow fluorescence
ppb	:	part per billion
$HPLC$	:	High performance liquid chromatography
kNN	:	k-Nearest neighbor
SVM	:	Support vector machine
MLP	:	Multi layer perceptron
HMM	:	Hidden markov model

FuH	:	Fully developed hazelnut
EmH	:	Empty or undeveloped hazelnut
ReH	:	Fully developed hazelnut with regular shell
CrH	:	Fully developed hazelnut with cracked shell
BrH	:	Fully developed hazelnut with broken shell
InH	:	In-shell hazelnut
SRT	:	Shelled and roasted hazelnut
SHD	:	Shelled hazelnut
$UnCont$	:	Uncontaminated hazelnut
$FlavusCont$	:	Flavus incubated hazelnut
$WaterCont$	:	Pure water incubated hazelnut

CHAPTER 1

INTRODUCTION

The recent developments in electronics and computer technologies have made capturing and storing of images, signals or video in real-time easy and inexpensive. Machine learning algorithms analyze these data automatically. Feature extraction algorithms in machines learning focus on getting the useful and necessary content of the information. In this thesis a feature extraction technique based on Local Discriminant Bases (LDB) is developed to explore the location of the discriminative features for acoustic and hyperspectral data. The algorithm is tested on a real world problem in food safety field. The developed algorithm is robust and adaptive to other type of data and it is able to extract the relevant features which increase the performance of learning algorithms.

The feasibility of real-time food sorting and grading systems with satisfactory performance depends on how well the acquired data is represented with fewer number of features for classification. The data taken from food item may be high dimensional and low quality with low signal to noise ratio. High dimensional data is expected to increase the accuracy and effectiveness of classification algorithms. However, the increase in data dimension not only increases the computational complexity, but also decreases the classification accuracy, when a limited number of training data is available [1, 2]. Moreover, the high dimensional data increases the processing time which is inversely proportional to throughput of the system. Therefore, the data dimension should be reduced by either eliminating the irrelevant ones or by combining the features that do not provide extra information on their own.

The current dimensionality reduction algorithms are usually classified into two categories: feature extraction and feature selection. Feature selection is the process of moving to low dimensional feature space by eliminating the irrele-

vant features as much as possible and this process does not distort the original data by transformation. Unlike feature selection, feature extraction is defined as transforming to lower dimensional feature space by using various transformation methods. Although the reduction in dimension allows learning algorithms to operate faster, this may remove the significant interpretation of original data. Feature extraction is extensively studied by various researchers [3, 4, 5, 1].

Local Discriminant Bases (LDB) algorithm, which originated from Best Bases algorithm [6] is developed to extract local information from data by using a divide and conquer approach [7]. The original LDB algorithm searches discriminant bases, which are regarded as feature, of the 1D signals either in time or frequency axis. However, it has been shown that bases search in both axes is crucial for classification[8, 9, 10]. LDB algorithm is also adapted to hyperspectral data to get the relevant features by accepting the hyperspectral curve of pixels as a one dimensional signal [11, 12, 1]. In this thesis, LDB algorithm is applied to a practical nut sorting method to get the location of discriminative features in data.

1.1 Motivation

Hazelnuts are extensively used in the chocolate and confectionary industries. They are produced in Iran, USA and Mediterranean Countries such as Turkey, Italy, Spain, France, Greece and Portugal. However, Turkey is the major producer of hazelnuts in that 70% percent of the hazelnuts in worldwide is produced by Turkey and about 80% of the Turkish Hazelnut export is consumed by the European Union (EU) countries.

Unfortunately hazelnuts are prone to aflatoxin formation like many other natural products among which are corn, red pepper, almonds, and figs. The aflatoxins are a group of structurally related toxic compounds produced by certain strains of the fungi , Aspergillus Flavus and Aspergillus Parasiticus. Under favorable conditions of temperature and humidity, these fungi grow on certain foods and feeds, resulting in the production of aflatoxins. Aflatoxins produce acute necrosis, cirrhosis, and carcinoma of the liver on laboratory animals at low quan-

tities [13]. Due to the health risks they pose on humans; it is desirable to lower the aflatoxin levels in consumed food items. The present allowed level for aflatoxin contamination in seed is 20 ppb (ng/g) and 4 ppb in USA and EU, respectively.

The hazelnuts are subject to aflatoxin analysis before exporting. A total of 40 incremental samples of 300 gr each are taken from the lot of 2 tonnes and analyzed via chemical methods. A few highly aflatoxin contaminated kernels in the incremental sample may increase the aflatoxin concentration of the sample and finally may result the cancellation of export of the examined lot. In addition, the sample which has undergone chemical testing can no longer be consumed. Therefore, real-time passive screening procedures which do not destroy samples are highly desirable and can be used to detect and remove such contaminated samples.

For real time sorting systems, a classifier with maximum accuracy but with minimum feature vector dimension is desirable. In addition, the feature vector should be based on least amount of sensor data so that a simple and fast data acquisition system can be employed. Unlike the traditional feature extraction algorithm which use all the candidate features, LDB algorithm combines these features to obtaine a more compact feature set. These features are fed to the feature selection step to identify the most relevant part of the data.

In this thesis, we developed 2D "Local Discriminant Bases" based feature extraction algorithms to detect contaminated or potentially contaminated hazelnuts by non-invasive and rapid methods. We used impact acoustics and hyperspectral imaging data depending on the hazelnut kernels type and the developed algorithm is tested on both types of data. The algorithm s developed to

1.2 Thesis statement

In this thesis, we modified the original LDB algorithm to two dimensions to get the exact location of the discriminative features in data space. The bases search is performed in time and frequency axis of impact acoustic data, spectral and spatial-frequency axis for hyperspectral data. The developed algorithm decreases the feature dimension by either eliminating the irrelevant ones and/or combining

the ones that do not provide extra information on their own.

This algorithm is implemented on selecting the contaminated or potentially contaminated hazelnut kernels by using impact acoustic and hyperspectral data. It will be able to sort the hazelnut kernels by fewer number of features with high classification accuracy. It is also observed that prior to feature selection, feature extraction is a critical step on getting the discriminative features.

1.3 Thesis overview

Chapter 2 reviews the principle of feature extraction and selection algorithms and provides a brief overview on Best Bases algorithm and Local Discriminant Bases algorithm which the proposed feature extraction algorithm originates from. It also gives the shift invariance concept that is used for discussion of proposed algorithm. Some dissimilarity metrics and the classifier used in the study are given in Section 2.

Chapter 3 explains the aflatoxin problem in foods and especially in hazelnuts which is among the major export goods of Turkey. It also presents some non-invasive aflatoxin detection algorithm developed for specific food items. This section also describes impact acoustics sorter system and hyperspectral imaging systems which are also used to acquire data for our algorithm.

Chapter 4 presents the proposed feature extraction algorithm by 2D Local Discriminant Bases search for impact acoustic and hyperspectral data. Section 4.1 focuses on the algorithm for acoustic data whereas Section 4.2 focuses on hyperspectral data. Both algorithms are same in principle but have some minor differences depending on the data type.

Chapter 5 presents the data acquisition procedures for impact acoustic data and the signal acquired from hazelnuts. The weight of the hazelnut for different classes and the weight versus signal energy correlation are given in this Section 5.1. Section 5.2 gives the hyperspectral image acquisition procedures and the hyperspectral images of shelled hazelnuts. The aflatoxin concentration of the classes and the preprocessing of the hyperspectral images is also given in Section 5.2.

Chapter 6 begins by presenting the output of the steps of feature extraction algorithm developed for impact acoustic data. The classification results obtained with extracted features are compared to other type of features extracted from the same dataset in Section 6.1. The filter selection criteria and the effect of noise and shift invariance on classification are given in succeeding three sections. The relevance of extracted features for classification is compared to candidate feature set by two different feature selection algorithms.

Chapter 7 presents the findings of hyperspectral data classification on four different classification problems defined on separating the mold contaminated or aflatoxin contaminated kernels of two different hazelnut forms. The outputs of the spectral spatial-frequency feature extraction steps are given in detail for the mold detection of shelled&roasted hazelnut kernels. The summary of classsification results and the relevance of extracted features are given for each problem separately.

Chapter 8 presents conclusions and suggests future works.

CHAPTER 2

Literature Review and Background

2.1 Feature Extraction and Selection

In classification problems, it is expected that the high dimensional data should increase the accuracy and effectiveness of the classification. However, it is observed that the increase in the dimension decreases the classification accuracy when a limited number of training data is available [1]. When the dimension of the data increases the number of training samples should be increased exponentially in order to retain the accuracy of classifier. This is a common problem in hyperspectral data. In order to overcome this limitation, the number of dimension is reduced by eliminating the irrelevant ones or by combining features that do not provide extra information on their own [14, 5, 11].

The current dimensionality reduction algorithms are usually classified into two groups; feature extraction and selection. Feature extraction is defined as transforming to M dimensional feature space from N dimensional ($M<N$) measured data space [15] by using various transformation methods. Although the reduction in dimension allows learning algorithms to operate faster, this may remove the significant interpretation of original data.

Feature extraction algorithms are mostly developed depending on the problem and the data set. One of the common feature extraction algorithm is Principle Component Analysis (PCA) [4]. In PCA, new sequences of uncorrelated variables are generated by using Karhunen-Loeve transformation. The first M number of components are selected and used for classification or representation. This enables us to represent the high dimensional data by a few principle component.

One drawback of PCA is that it works with whole data set for transformation. Jia and Richards [5] segmented the PCA to remove the need for whole hyperspectral data set. They developed a PCA based feature extraction algorithm: Segmented Principle Component Transformation (SPCT). In SPCT, the highly correlated adjacent bands in hyperspectral data are grouped by edge detection. The principle components in each group are computed and each grouped is represented by a few components (eigenvectors) with high eigenvalues. The eigenvectors are then pruned according to their Bhattacharya distance between classes. However, the projection based dimension reduction methods are sensitive to noise. Therefore projection should be made using a large number of samples in order to overcome this problem. Although the simplicity and popularity of PCA, the features derived from PCA projection may not have better discrimination than the features in original data space [12]. Unlike to tranformation based algorithms, relevant features can be extracted by first order and second order statistics[3] or Best Bases Extraction algorithms [11] and etc..

Unlike feature extraction, feature selection is the process of moving to the K dimensional feature space from M ($K<M$) dimensional feature space by eliminating the irrelevant features as much as possible. The feature selection algorithms in the literature are usually performed [16] on four steps;

Step 1: Select an initial point in feature space

Start with an initial point in feature space. This selection is important because it may effect to find the solution in feature space.

Step 2: Search feature space

The search strategy of feature space is important because it determines the search direction. There exist 2^N possible feature subsets in N dimensional feature space. Generally speaking, there are two different search strategies for subset selection. The first one is *exhaustive search strategy* where all the subsets are investigated individually. This is an NP complete problem and suffers from computation complexity. The second one are *heuristic strategies*, which search the

feature space by heuristics methods. Basically, there are three types of heuristic method that is primarily works on addition or deletion approach [17].

Forward Selection starts with empty subset and successively expands by adding most relevant feature that will provide local improvement to the problem.

Backward Elimination starts with complete subset and successively deletes the most irrelevant feature from the current subset.

Stepwise Bidirectional Selection starts with null, full or randomly selected feature subset and adds the most relevant feature or removes the most irrelevant feature from the current subset.

Step 3: Evaluation of selected feature subset

The merit of the selected feature subset is evaluated by wrapper or filter model [Figure 2.1]. Evaluation functions which measure and determine the classification capability of individual features are used in filter model. In contrast, induction algorithm (learning accuracy) is executed to measure discrimination capability of the feature set in wrapper model. In wrapper model, data of the investigated feature subset is randomly divided into test and train set. An initial machine learning algorithm is trained with the train set and tested with the test set. The accuracy of the testing gives the merit of the investigated feature sub set. The wrapper model is slower than the filter function because the induction function is executed at every feature increment. However, this approach may give better results compared to filter models [18].

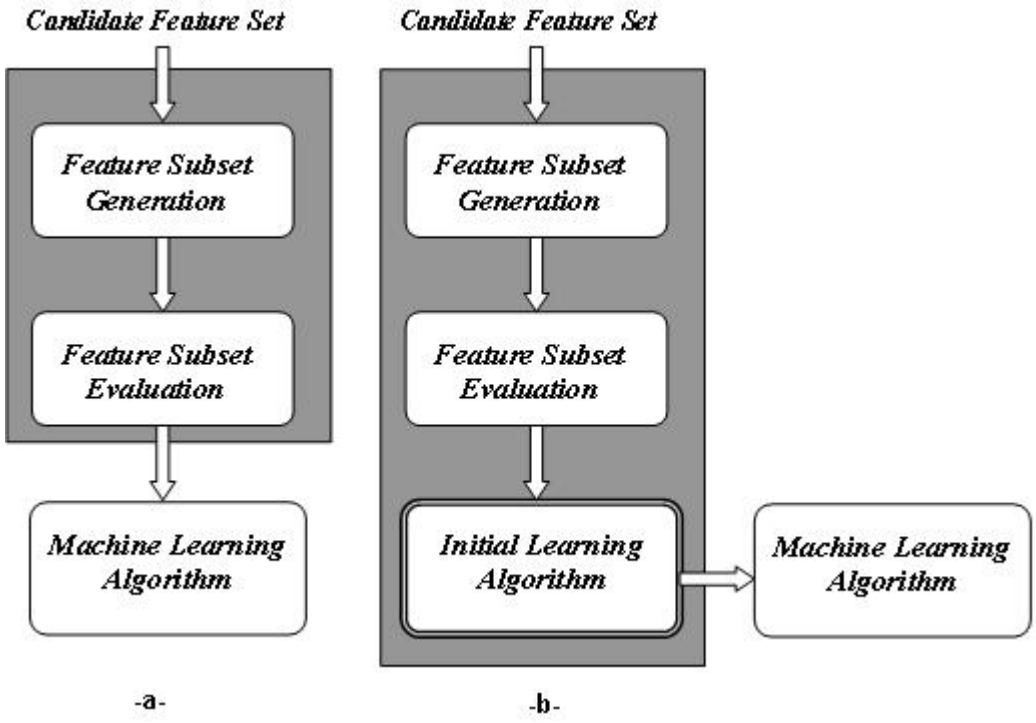

Figure 2.1: a) Filter and b) wrapper feature subset selection model

Step 4: Termination of feature selection

The feature subset selection process is terminated by predefined criteria. The process can be stopped when the addition of new feature does not improve the merit of feature subset (this is classification accuracy in wrapper model) or the process can be stopped at a given number feature subset size.

The critical step in feature selection algorithms is to evaluate the merit of the feature subset. Various evaluation functions may be used such as Mutual Information [19], Entropy, Information Gain, MDL, Gini, Relief, etc. [17, 16]. Hall [16] developed Correlation Based Feature Selection (CFS) based on the Pearson"s Correlation. In CFS algorithm, the initial feature subset of size $k-1$ is increased by the feature which gives the maximum merit M_s.

$$M_s = \frac{k\overline{r_{cf}}}{\sqrt{k + k(k-1)\overline{r_{ff}}}} \tag{2.1}$$

where $\overline{r_{cf}}$ is the mean class correlation and $\overline{r_{ff}}$ is the average feature-feature intercorrelation. The CFS algorithm aims to the find the feature subset including the features that are higly correlated with the class but uncorrelated with each other. The algorithm is terminated when the there is no improvement in the M_s value.

2.2 Best Bases Algorithm

Coifman and Wickerhauser developed a best basis algorithm for signal compression [6]. The best basis method firstly expands the signal into orthonormal wavelet or trigonometric basis in binary tree structure. Each basis vetor has different location in time-frequency axis and some of them may be redundant for signal representation. The importance of each basis (node at binary tree) is evaluated at the second step by using a defined minimization criterion, which is the entropy for signal compression. At the third step, the binary tree is pruned from bottom to top by using the entropy values of nodes. The best-basis algorithm can be summarized as follows,

Step 1: Define a decomposition method (wavelet or trigonometric) and expand the signal into orthonormal basis vectors in binary tree structure.

Step 2: Evaluate the information cost (entropy) of each node by using the expansion coefficients. The entropy H of a sequence {p} with $\sum p_i = 1$ can be calulated as

$$H(p) = -\sum_i p_i log(p_i) \tag{2.2}$$

Step 3: Prune the binary tree by mother and child node comparison.

The nodes at the level, right before the deepest level in tree are firstly selected as parent nodes. The parent node is discarded if its children nodes have less cumulative information and then the cumulative value of children are set to parent's

value. Otherwise, the children are destroyed and the parent is kept. This parent is set as a child for the higher level. The survived nodes at the end of the whole pruning operation are the nodes that are the best basis for signal compression.

2.3 Local Discriminant Basis Algorithm

As stated before, the best-basis algorithm [6] is developed to get local information for signal representation and compression. Entropy values of the nodes are used as information cost at pruning the binary tree. Saito and Coifman [7] adapted this best-basis algorithm for classification of signals and images. The local discriminant basis of the signals are evaluated and used for classification purposes. Instead of using the entropy, they proposed to use a dissimilarity cost function which will maximize the difference in time-frequency energy distributions of classes. The LDB algorithm first decomposes the signal into orthonormal basis (nodes) by using wavelet trigonometric packets in binary tree structure. Each basis vector has different time-frequency locations. The discrimination power of each node is calculated by using an appropriate dissimilarity measure. The best basis are detected by pruning the binary tree using divide and conquer algorithm. When pruning the binary tree, a parent node is split only if the cumulative discriminative power of its children is greater than the discrimination of the parent node. The parent node in that situation is destroyed and the cumulative discrimination power of children is transferred to the parent node. Whenever the cumulative discrimination power of children is smaller than the parent node the child nodes are destroyed and the parent node with its discrimination value becomes a child of a node at higher level. The resulting best basis vectors are ordered by their discrimination power and used for constructing the classification machine. The LDB algorithm can be summarized as follows:

Step 1: Define a decomposition method (wavelet or trigonometric) and expand the signal into orthonormal basis in binary tree structure up to level J.

Step 2: Construct the time-frequency (TF) energy map of classes.

Step 3: Construct discrimination power tree D from the TF energy map by using an appropriate dissimilarity measure.

Step 4: Prune the J level tree by the following rule:

- start from the nodes in j=*J-1* level

- for all k nodes in level j, do the following;

- if $D(k) > [D(k)_{child1} + D(k)_{child2}]$

- keep mother node, destroy chidren nodes

- else

- keep children nodes and set $D(k) = [D(k)_{child1} + D(k)_{child2}]$

Step 5: Order the selected best basis vectors (say M bases) by their discrimination value

Step 6: Use K<M basis for constructing classification machine.

2.4 Shift Invariance in Signal Classification

The real time signals are not always aligned in time (or space). Figure 2.2 shows two impact acoustics signals sequence for demonstration. The phase difference between acoustic signals are obvious in Figure 2.2.

For a shift varying system, a shift at the input signal may results a big difference at the output. Therefore, the developed signal classification algorithms that use the features extracted from the output signals may not have the highest

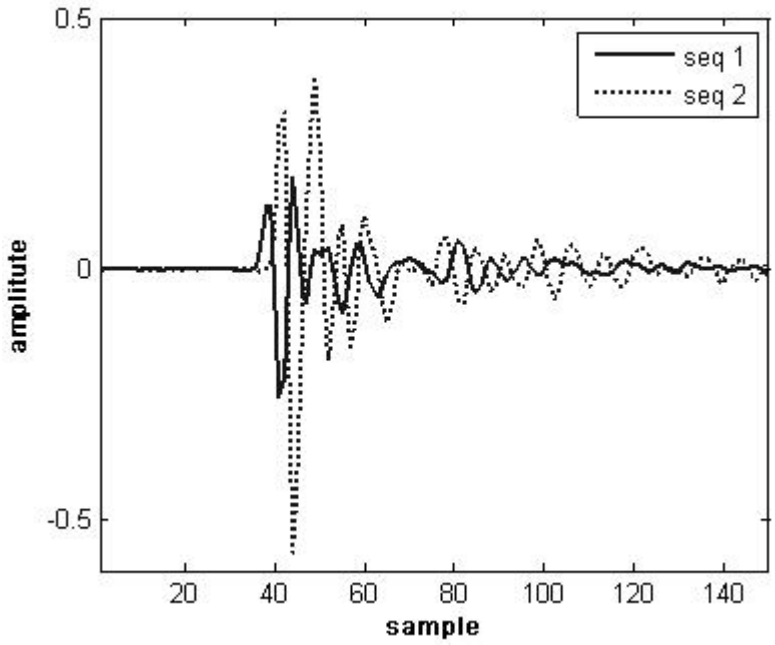

Figure 2.2: Two impact acoustic signal of hazelnut kernels from the same class.

accuracy. Shift invariance is usually introduced as requirement for robust classification. The importance of the shift invariance for classification is also emphasized in [7, 8, 20].

There are some shift invariant systems, but the wavelet and trigonometric packets that are used at LDB algorithm generates shift variant transformation. Some researchers used spin-cycle procedure to get shift invariance properties for signal classification purposes. [21, 22, 9]. In spin-cycle procedure, the input data set is expanded by shifting the original set in both directions in order to handle the possible shifts at the input signals. If the defined number of shift is τ then the data set is expanded by its $(-\tau, \tau+1, .., 0, .., \tau-1, \tau)$ versions and used as independent signals.

One drawback of spin-cycle procedure is increased computational complexity; because of the increased data size. This drawback must be taken account when the performance of the developed algorithm is considered.

Undecimated wavelet transform (UDWT) employed in this study; has shift invariance property. It is widely used in image denoising and enhancement ap-

plications [23, 24, 25]. It is also used for texture classification [26]. The UDWT can be used with the LDB algorithm to make it more robust against to the shifts for signal classification.

2.5 Dissimilarity Measure

The dissimilarity (distance) measure is used to compute the discrimination power of the basis vector(node). It has a direct effect on classification accuracy. Therefore, the best distance measure function should be investigated for a given problem. Let p and q are normalized energy distributions of signals belonging to *class 1* and *class 2*, respectively, where $\sum_{i=1}^{n} p_i = \sum_{i=1}^{n} q_i = 1$. The distance measure can be:

- The symmetric Kullback Leibler distance, which is also named as J-divergence

$$\begin{aligned} J(p,q) &= I(p,q) + I(q,p) \\ I(p,q) &= \sum_{i=1}^{n} p_i log(\tfrac{p_i}{p_i}) \end{aligned} \tag{2.3}$$

- Euclidean distance

$$D(p,q) = \left\| p_i - q_i \right\|^2 = \sum_{i=1}^{n} (p_i - q_i)^2 \tag{2.4}$$

- Hellinger Distance

$$H(p,q) = \sum_{i=1}^{n} (\sqrt{p_i} - \sqrt{q_i})^2 \tag{2.5}$$

- Fisher distance

$$F = \frac{\left| \mu_1 - \mu_2 \right|}{\sigma_1^2 + \sigma_2^2} \tag{2.6}$$

  where μ_i and σ_i are the mean and standard deviation of the corresponding feature for class i.

2.6 Classification

In pattern recognition problems, classification can be defined as assigning the test pattern to a learned class. Various types of classifier are used in literature such as Support Vector Machine (SVM), k-Nearest Neighbor (kNN), Multi Layer Perceptron (MLP), Linear Discriminant Analysis(LDA), Hidden Markov-Model(HMM), etc.. However the common point in these classifiers is the requirement to work with relevant and orthogonal features. The main objective of this study is the extraction of features for classification. Therefore, a single classifier, LDA, is selected and used for detailed analysis.

LDA is one of statistical classifiers commonly used in pattern recognition problems [27]. LDA generates the best hyperplane decision surface in M dimensional space. The orientation and location of the surface are determined by the vector w and bias w_0, respectively.

$$g(x) = w^t x + w_0 \tag{2.7}$$

The discriminant function $g(x)$ gives the distance of the test pattern x to the decision surface where $g(x)$ takes positive value when x is on the positive side and takes negative value when $g(x)$ is on the negative side of the surface. The detailed description of the LDA classifiers can be found at [27]. The surface weight vector w used in LDA for two classes is

$$w = (\sum_{1} + \sum_{2})^{-1}(\mu_1 + \mu_2) \tag{2.8}$$

where μ_i and $\sum_i$ are the mean vector and covariance matrix of the class i, respectively.

CHAPTER 3

Reduction of Aflatoxin in Hazelnuts by Impact Acoustics and Hyperspectral Imaging

3.1 Aflatoxin in Food Stuff

Aflatoxin that is caused by Aspergillus type molds (A. Flavus, A. Parasitius) is one of the defects affecting the chemical composition of the food item. Aflatoxin may cause porcine, pulmonary edema, liver cancer and esophageal hyptesia. It is estimated that in USA 58 to 158 people per year are inflicted with liver cancer because of aflatoxin consumption [13]. Therefore, aflatoxin contamination levels of seeds (corn, pistachios, hazelnuts, pepper, etc..) is restricted by legislations. The level for aflatoxin contamination in seed is 20 ppb (ng/g) and 4 ppb in USA and European Union (EU), respectively. Aflatoxin in foods can be detected by high-performance liquid chromatography (HPLC), mass spectroscopy (MS) and enzyme-linked immunosorbent assay (ELISA).

3.2 Detection of Aflatoxin Contaminated Food Items by Non-invasive Methods

Several studies have been conducted to detect aflatoxin contaminated foods by non-invasive techniques. A spectrophotometer is commonly used to detect compound of food items under inspection and it is also used to estimate aflatoxin contamination in food kernels. A spectrophotometer consists of a *spectrometer*

to produce light and a *photometer* to collect the reflected (R) or transmitted (T) light in various spectral bands. Pearson [28] used spectral reflectance ratio (R735nm/R1005nm) for detecting highly contaminated corn kernels (>100 ppb) from low contaminated (<10 ppb) or uncontaminated ones under illumination and reached 95% correct classification rate. Pearson could also distinguish the high contaminated (>100 ppb) yellow corn kernels at a rate of 98% by using spectral absorbance at 750 nm and 1200 nm [28]. Hirano [29] used transmittance ratio (T700nm/T1100nm) of peanuts for identification of contaminated kernels from uncontaminated ones. The imaging with spectrophotometer is time consuming. Therefore the non-invasive food safety algorithms developed with spectrophotometer is not suitable for real-time operations.

Aflatoxin may also be present inside the kernel. It that case, it may not be possible to visualize the moldy effects on the surface of the kernel. Nuclear Magnetic Resonance (NMR) and X-Ray Imaging can be used to detect internal aflatoxin contamination. However, these are highly expensive techniques and take more than 10 minutes to evaluate each kernel.

The mold of Aspergillus Flavus produces kojic acid which is observed to bright greenish yellow fluorescence (BGYF) compound by peroxidase in the plant. These plants exhibited BGY particles under UV radiation and this radiation can be detected by machine vision. The number of exhibited Bright Greenish Yellow (BGY) particles is taken as an indication of aflatoxin contamination. The BGY fluorescence is also used by Tyson and Clark [30] for detecting aflatoxin contaminated pecans. They soaked the pecan halves in aflatoxin solution for two days. They measured the BGY fluorescence or the pecan halves under UV light at 320 nm and used fluorescence ratios at 440nm/490nm and 450nm/490nm for classification. Fersai [31] used the same method for detecting aflatoxin contaminated pistachio nuts by using the fluorescence ratio of 420nm/490nm. Fersai stated that the peak emission occur at 490 nm for the BGY nuts. However, the human eye has only 30% percent sensitivity at 490nm compared to 550nm. This insensitivity causes fluorescence particles to appear as BGY although their peak sensitivities are at the region between blue and green not at yellow region. The BGY fluorescence is also used to detect aflatoxin contaminated corn kernel [32], figs [33, 34],

pistachio and Brazil nut [35, 36] and in some agricultural commodities [37].

However, Wilson detected that aflatoxin contaminated corn kernels do not exhibit BGY fluorescence all the time due to the insufficient amount of peroxidase in plant. Moreover, other types of fungi, besides the peroxidase, which don't produce aflatoxin, may yield kojic acid in foods and they may be regarded as aflatoxin contaminated foods when the BGY fluorescence is considered only. These findings are detailed in [38].

3.3 Aflatoxin Problem in Hazelnut

Tree nuts (almonds, pecans, pistachio, hazelnuts, etc) are used in food industry. However, environmental conditions and unsuitable processing procedures cause crack or damage to the nut shell. This damage decreases the nut quality and also increases the likelihood of mold infestation. For pistachio nuts, Pearson showed [39] that nearly all the aflatoxin contaminated pistachios are either damaged by birds or insects before harvesting or are early split ones. The damage at the shell of the kernels allows mold to diffuse into the kernels and cause aflatoxin. Pearson [40] used a machine vision system to classify pistachios nuts as stained (caused by early splitting), unstained or moderated stained with an average of 11% classification error rates. By removal of stained pistachio nuts aflatoxin contamination level of pistachio nut is reduced from 4.8- 8.6 interval to 0.04-2.5 ppb [41]. Unlike the pistachio nuts, hazelnut shell are damaged mostly at processing step before the drying phase which the contamination is mostly occured in. We categorized the hazelnut into four groups to investigate the physical properties of shell for aflatoxin contamination [42]. A sample hazelnut image from these groups are shown in Figure 3.1

100 hazelnut kernels from each group are pruned to aflatoxin producing molds and stored in high humidity environment with 28^0C temperature for 20 days. At the end of the 20 days these kernels are analyzed for aflatoxin contamination. The contamination results (Table 3.1) showed that the intact shell form strong barriers against mold contamination during storage. However, any type of damage at any size on the shell eliminates this capability. This can be seen from the

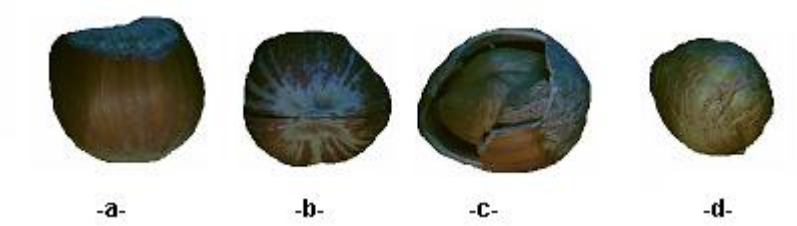

Figure 3.1: A sample image from a) Regular shell hazelnuts (ReH), b) Cracked shell hazelnuts (CrH), c) Broken shell hazelnuts (BrH) and d) In-shell hazelnuts (InH)

contamination level of the CrH, BrH and InH hazelnuts which are close the each other.

Table 3.1: The mean contamination levels of the hazelnuts from four groups

	ReH	CrH	BrH	InH
Cont.Level (ppb)	47	2730	2476	2494

Turkey is the major producer of hazelnut in the world. We produce 70% or the hazelnut in worldwide and we export 80% of this to European Union countries each year. The aflatoxin contamination in hazelnuts varies from year to year, and it is negligible in some years (2000-2003). In reality, 30 percent of the hazelnuts (Figure 3.2) are exported without any processing. The 35 percent is exported in shelled form and the 35 percent is exported after roasting and processing.

The hazelnuts in these three forms have different physical characteristics. Therefore, the hazelnut kernels in these categories should be investigated separately before storage or consuming. The risk for in-shell kernels can be eliminated by impact acoustic sorting systems. However, acoustic sorting can not be used for sorting the shelled kernels. A hyperspectral imaging system is used to address the risk of the shelled nuts (shelled, shelled&roasted) . The Shelled (SHD) and Shelled/Roasted (SRT) hazelnut kernels have different visual characteristics. Therefore these hazelnuts should be studied separately.

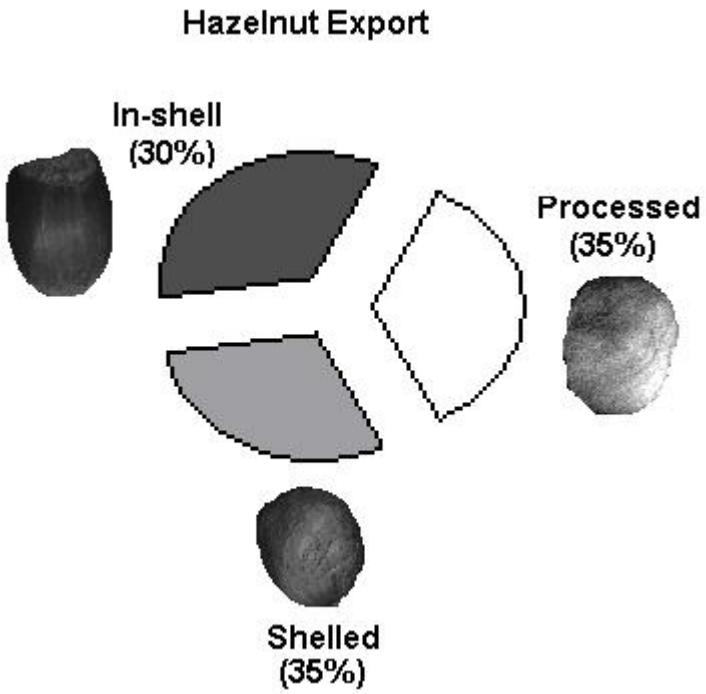

Figure 3.2: The forms of exported hazelnut in TURKEY

3.4 Impact Acoustic Sorter System

Pearson developed an impact acoustic sorter system to separate cracked and uncracked pistachio nuts. The system is currently working on pistachio processing assembly in California and also in Turkey. A similar system (Figure 3.3, modified from [43]) consisting of a pipe through which the nuts slide in, an impact plate that the nuts are dropped on, a microphone for impact sound acquisition and a PC for recording and processing the signals is used to get impact acoustic signal of hazelnut kernels.

A stainless steel plate with dimensions 7.5 x 15 x 2 cm is used as the impact plate. The impact plate is fixed to the ground with 120 ^0C. This angle prevents the nuts from making multiple impacts. A microphone, sensitive to frequencies up to 20 kHz, is placed 5 cm from the impact plate. The impact acoustic signal is sampled at 44.1 kHz, processed and used for decision making.

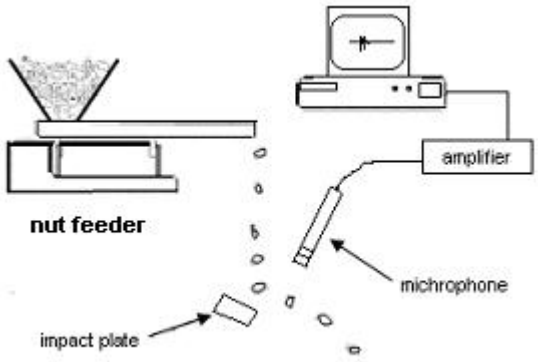

Figure 3.3: Schematic of experimental apparatus for collecting acoustic emissions from hazelnut kernels

This system is also used to separate empty hazelnuts from fully developed nuts in [44] by using 70 combined time and frequency features. Features that are widely used in speech processing algorithms are extracted from short time variances of signals, maximum signal amplitude, spectral peak locations and Weibull distribution parameters that fit to the envelope of the impact signal and used for classification. We called this feature set as non adaptive time-frequency (NATF) feature set.

Kalkan et.al [45] used impact acoustic signals for classifying cracked shell and regular shell hazelnuts by non-adaptive subband (NASB) features with 90% accuracy. In this work, impact acoustic signals were first decomposed into subbands by using undecimated wavelet transform. The subband signals were then divided into overlapping or non-overlapping segments of constant width. An energy feature was extracted for each segment in each subband. The relevance of features and the most relevant sub-bands for classification were investigated by wrapper or filter model. However, the non-adaptive feature extraction method may miss some of the relevant features for classification.

3.5 Multi/Hyperspectral Imaging System for Food Safety

A typical multi/hyperspectral imaging system consists of a CCD (charged coupled device) camera, a frame grabber device, a set of filters and an illumination system. The CCD cameras are solid state, silicon based devices. Some of the cameras have digital output. Frame grabber devices are used for the analog cameras in order to digitize the analog signal. Multiple images at different frequency bands are acquired by using a liquid crystal tunable filter, an acousto-optic tunable filter or by sequentially positioning band-pass filters in front of the lens of the camera.

In multi/hyperspectral imaging system, food items are usually visualized under UV (200-400nm), VIS (400-700nm) or NIR (700-2500nm) illumination. The light incident on the object is absorbed, reflected of transmitted through. These are accepted as the optical properties of the inspected material. The molecules of the objects are excited to higher energy states by absorbing the penetrating light. The excited molecules emit lights at higher wavelengths (fluorescence) when returning to their previous state. Some of the compounds in materials emit fluorescence in the visible region when exposed to UV illumination. The chemical properties of the investigated material are estimated by the properties of the reflected light (wavelength, intensity, etc...).

Tylor and McCure [46] used multispectral imaging system to detect leaf tissues. They stated the importance of three wavelengths 670, 800 and 990 for leaf tissue detection. Zeringue and Shih [47] used the reflectance at 435 nm for detecting the aflatoxin contaminated cotton lint. Park and Chen [48] stated the discriminative importance of the spectral image at 540 and 700 nm for separating the unwholesome carcasses from wholesome carcasses. The images at 566, 515 and 631 nm are used for fecal and ingesta detection at poultry carcasses [49]. Spectral image taken at 686 and 675nm are used for determining the main contamination and defect in apples [50].

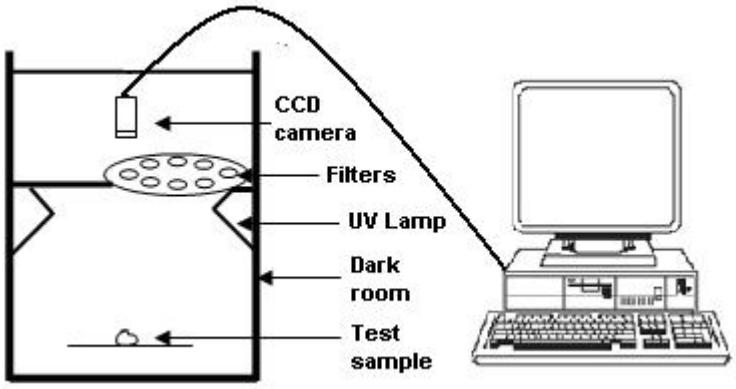

Figure 3.4: Hyperspectral imaging system with a rotating filter wheel

The hyperspectral imaging system (Figure 3.4) used in this study consists of

- An Imaging Source VIS DFK 41AF02 digital CCD camera
- 2 High Intensity Spectroline UV-A Lamps (peak intensity at 365 nm)
- A cabin to function as dark room
- A band pass filter set including the filters from 400 nm to 510 nm with 10 nm FWHM and 550nm and 600nm filters with 70 nm and 40 nm FWHM
- A computer for data acquisition and processing

chapter 4

Feature Extraction Algorithm Based on 2D LDB Search

In signal classification applications, depending on problem and the dataset, time (spatial in 2D) domain and and/or frequency domain features are extracted and used for learning. The original LDB algorithm decomposes the time axis by Local Cosine Packets or frequency axis by wavelet packets to locate the discriminative features of the data. However, it is observed that, especially for non-stationary signals (speech, acoustics, EEG, vibration, etc.), both time and frequency domain features are important for classification [43, 10, 51].

The original LDB algorithm is modified to 2D structure and adapted to impact acoustic and hyperspectral data to get the exact location of the discriminative features. For impact acoustic data, the time-frequency plane features are extracted by combining the Local Cosine Packets and Wavelet Packet analysis to obtain time and frequency adaptation in an off-line step. The introduced technique requires no prior information on the relevant time and frequency locations. Pruning in both axis extracts the most discriminative features by combining the ones which do not provide extra information on their own. The extracted features are then selected by feature selection algorithm are used in classification. Similar approach is used for hyperspectral imaging where the spectral axis is used instead of time axis. LDB is implemented to get the most relevant spectral and spatial-frequency features of hyperspectral data. The 2D LDB algorithm for one dimensional impact acoustics signals and three dimensional hyperspectral images are explained separately.

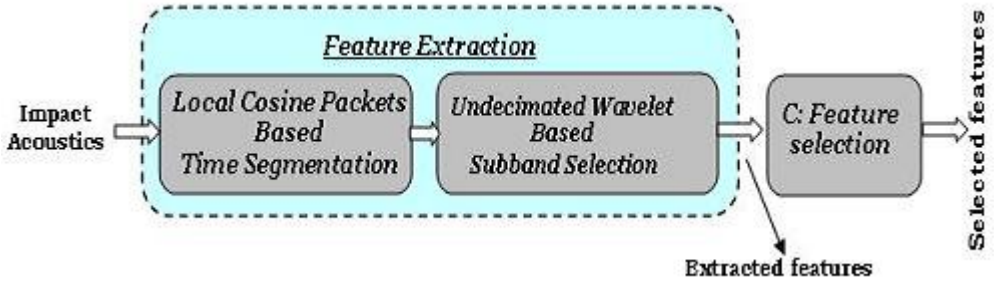

Figure 4.1: The block diagram of the 2D LDB based feature extraction for one dimensional signal

4.1 Feature Extraction from Acoustic Data by 2D Local Discriminant Bases Search

In 2D LDB algorithm, the time-frequency plane features are extracted by combining the Local Cosine Packets and Wavelet Packet analysis to obtain time and frequency adaptation in off-line step (Figure 4.1). The introduced technique requires no apriori information on the relevant time and frequency locations. It finds these locations automatically by pruning the time segments considering their discrimination potential. Then, the resulted time segment signals are decomposed into frequency subbands by undecimated wavelet transform. The extracted features are, then, selected by any feature selection algorithm and used for classification.

4.1.1 Adaptive segmentation and pruning in time axis

The non-stationary signals may have different characteristics in time. Therefore, these signals should be analyzed locally. In general, local information of the signal is extracted by Short Time Fourier Transform (STFT). This type of block transform generates side-lobe artifacts due to disjoint rectangular windows. On the other hand, usage of smooth windows removes the ortogonality. It is possible to construct orthogonal transforms with smooth and overlapping windows by trigonometric bases. Some researchers used Local Cosine Packets (LCP) because

of its advantages over STFT [52, 8]. Therefore, Local Cosine Packets (LCP) is used to partition the time axis in a dyadic binary tree structure (Figure 4.2).

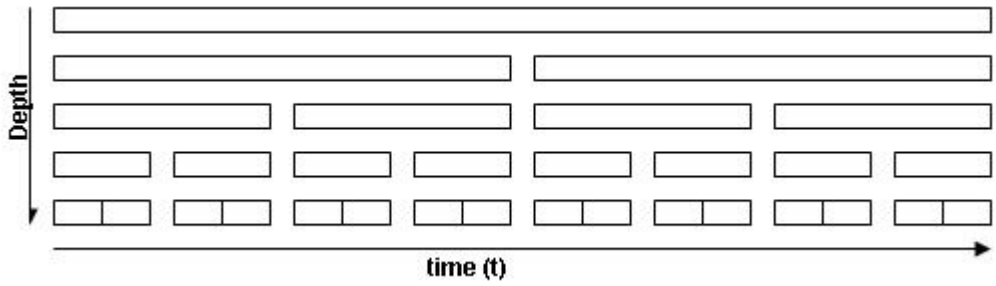

Figure 4.2: Time segmentation with LCP at 4 levels in dyadic tree structure

The LCP partition the time axis by using smooth bells [53] which are constructed using cut-off functions r(t) that satisfy

$$\left|r(t^2)\right| + \left|r(-t)^2\right| = 1 \quad for \quad all \quad t \in R \tag{4.1}$$

$$r(t) = \begin{cases} 0 & \text{if } t \leq -1 \\ 1 & \text{if } t \geq 1 \end{cases} \tag{4.2}$$

An example of such a function r(t) is

$$r(t) = \begin{cases} 0 & \text{if } t \leq -1 \\ sin\left[\frac{\pi}{4}\left(1 + sin(\frac{\pi t}{4})\right)\right] & \text{if } -1 < t < 1 \\ 1 & \text{if } t > 1 \end{cases} \tag{4.3}$$

Each signal is represented with Local Cosine Packets within smooth windows (as in Eq. 4.3) in the tree structure (Figure 4.3). The resulting expansion coefficients are squared and then averaged over the signals in the given class. This provides an averaged energy spectrum of each class in a given time segment within the pyramidal tree.

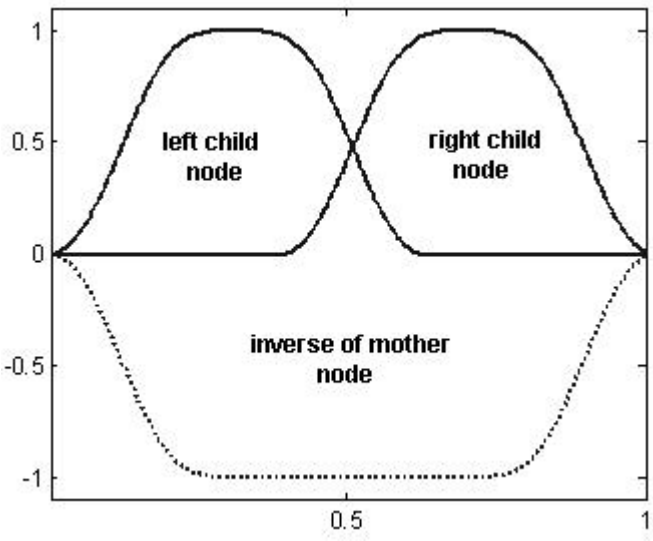

Figure 4.3: The smooth windows obtianed by LCP

Let p_i and q_i be the mean energy spectra of cracked and regular classes, in a given time segment respectively. The distance between the average spectra is calculated with the Distance criterion J (Section 2.4) where 'n' in Equation 2.2 corresponds to the total number of time samples in a given node. This way, the distance is accumulated along the spectrum within all subspaces to get a single value representing each node of the tree. The resulting binary tree is, then, pruned from bottom to top according the following rule to find the nodes with maximum discrimination power:

Pruning algorithm #1

if $J_{mother} \geq (J_{child1} + J_{child2})$

keep mother

else

keep children

where J_{mother} and J_{child} are the discrimination power of the mother and children node and are computed by the Kullback-Leibler distance criteria. The algorithm keeps the mother node if it captures the discriminative power of the children nodes; otherwise it keeps the children nodes. The algorithm may construct different tilings for different dataset. This may be regarded as a robustness measure of the algorithm.

4.1.2 Adaptive segmentation and pruning in frequency axis

The signal portion in time segments is divided into frequency bands to get the specific frequency content of the signals. This segmentation in frequency axis helps to find and analyze the local patterns in signals. Fourier Transform and Discrete Wavelet Transform are two of the methods to decompose the frequency axis. The methods for decomposition should be selected according to nature of the data set. In that aspect, shift invariant decomposition system is highly required when the obtained signals are not time aligned. The Undecimated Wavelet Transform has shift invariant property and for classification purposes it is firstly used for texture classification [26]. In this study, similar approach with a filter bank is used to analyze the impact signals for classification. A filter f that satisfies the quadrature mirror filter condition

$$F(z)F(z^{-1}) + F(-z)F(-z)^{-1} = 1 \tag{4.4}$$

used to construct the pyramidal filter tree (Fig. 4.4), where *F(z)* is the z-transform of f . The high-pass filter g is obtained by shift and modulation of f .

$$G(z) = zF(-z)^{-1} \tag{4.5}$$

The subsequent filters in the pyramidal tree are, then, generated by increasing the width of f and g at every step.

$$\begin{aligned} F_{i+1}(z) &= F(z^{2^i}) \\ G_{i+1}(z) &= G(z^{2^i}) \quad , i = 0, 1, 2, ...N \end{aligned} \tag{4.6}$$

In the signal domain, the filter generation can be expressed as

$$\begin{aligned} f_{i+1}(k) &= [f]_{\uparrow 2^i} \\ g_{i+1}(k) &= [g]_{\uparrow 2^i} \end{aligned} \tag{4.7}$$

where the notation $[]_{\uparrow m}$ denotes the up-sampling operation by a factor of m.

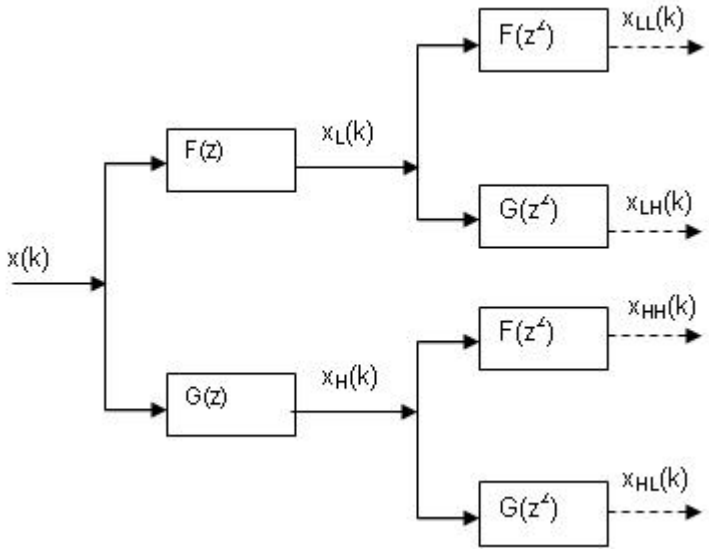

Figure 4.4: Pyramidal filter tree up to second level. L and H stands for Low and High band, respectively

The pyramidal filter tree is transformed into a filter bank (Figure 4.5) for which the filters are obtained by convolving the filters on the branch of the pyramidal tree.

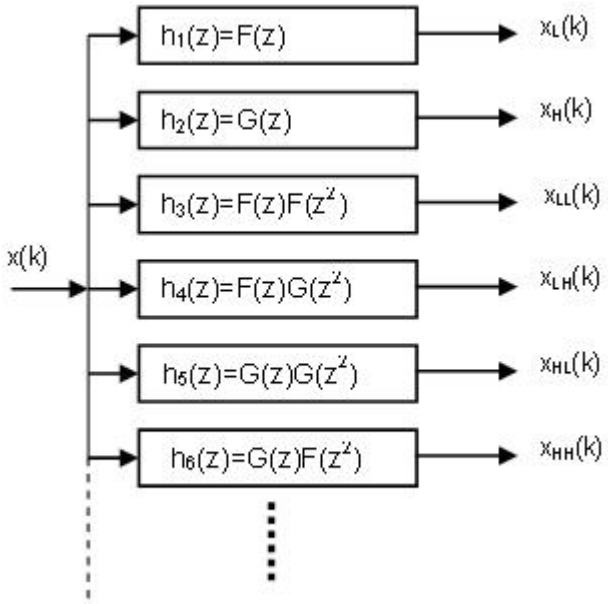

Figure 4.5: Filter bank

A third level filter band with Coiflet 5 tap wavelet and scale functions is shown in Figure 4.6.

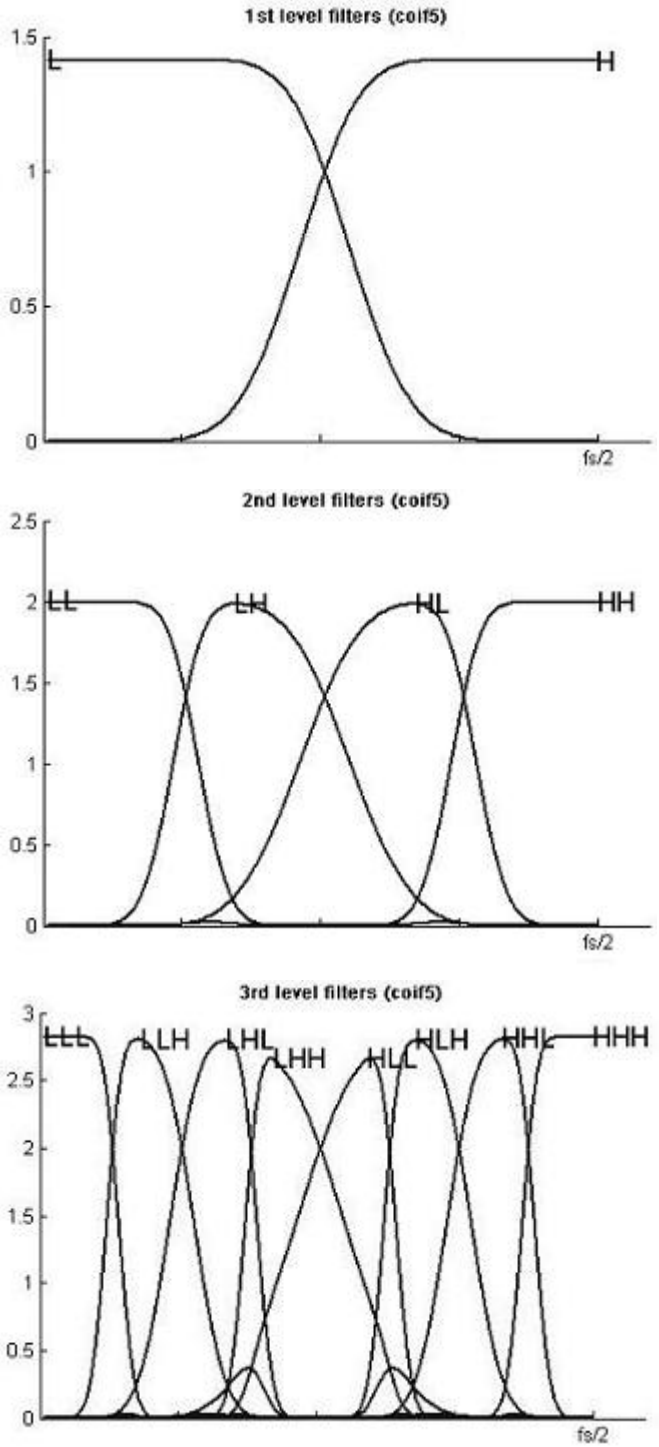

Figure 4.6: Undecimated filter banks up to third level decomposition

The obtained filter-bank is used to decompose the signals in time segments into sub-bands in frequency axis (Figure 4.7).

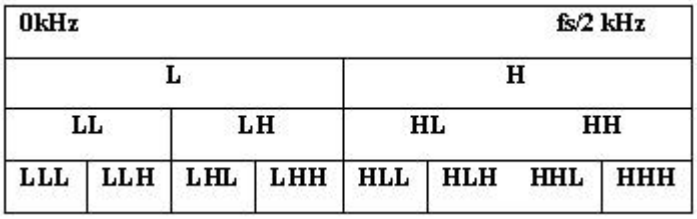

Figure 4.7: The 3 level full wavelet sub-band tree

The signals usually have different energy distribution in each sub-band. The Euclidean distance between cumulative probability distribution of subband energies in Equation 2.3 is chosen as the discriminative measure and the constructed pyramidal sub-band tree is pruned from bottom to top by the following rule:

Pruning algorithm #2
if $d_{mother} < max\{d_{child1}, d_{child2}\}$
set $max\{d_{child1}, d_{child2}\} as\ d_{mother}$
else
remove children

The characteristic of the filter may indirectly effect the discriminant band distribution. This may, also, change the classification accuracy of the system.

As a result, the discriminant time-frequency (TF) map is constructed by adaptive segmentation in time and frequency in order to localize the most discriminative patterns in signal.

4.1.3 Selection of extracted time-frequency features

The adaptive segmentation and pruning operation in both time and frequency axis by distance cost function revealed the location of the most discriminant energy features of the signals. This feature extraction step provides the best segmentation in two dimensions (time and frequency) but does not eliminate the irrelevant feature location. Therefore, the extracted features are then sorted by

feature selection algorithms and incrementally included to feature vector. These algorithms are Fisher Distance Based Feature Selection (FFS) and Correlation Based Feature Selection (CFS) algorithm [16]. The desired number of features is obtained when the minimum classification error is reached.

4.2 Feature Extraction from Hyperspectral Data by 2D Local Discriminant Bases Search

The LDB algorithm is also modified to 2D structure and applied to extract most discriminative features in hyperspectral data. A four step algorithm similar to the one in Section 4.4 is developed for hyperspectral data (Figure 4.8).

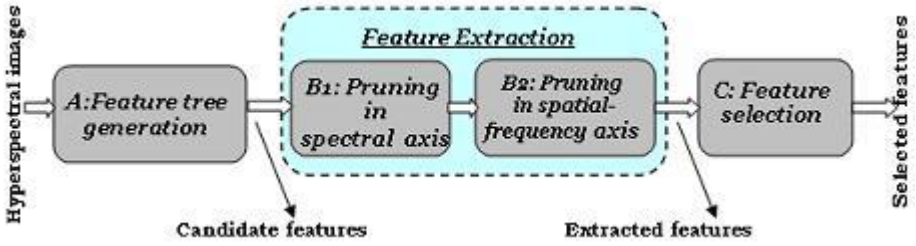

Figure 4.8: The block diagram of the 2D LDB based feature extraction for hyperspectral data

4.2.1 Feature Tree Generation

The first step in the algorithm is to obtain candidate feature set by generating two feature trees on spectral and spatial-frequency axis in order. In the first tree, the reflectance energies of spectral images are placed to the kth level of the tree from left to right. Figure 4.8 shows an illustration to k=4 levels binary spectral band tree with 16 spectral bands (SB). For the case of , the remaining nodes at the kth level can be set to null in order to complete the binary tree. The energy value of the mother nodes at the high levels were computed by summing the feature values of their branch nodes.

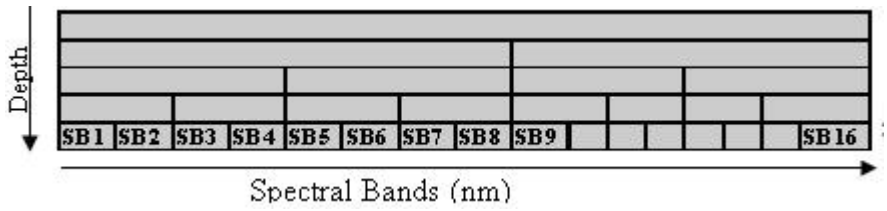

Figure 4.9: k=4 levels binary spectral band tree

The second feature tree is generated in spatial- frequency axis in quad tree structure by decomposing the raw spectral images into h level full wavelet subbands as in Figure 4.10. Wavelet transform retains the original image information and completely represents the image in subbands of (LL, LH, HL and HH) where first character shows the filtering (Low or High) through the x and second shows the filtering through the y direction of the image.

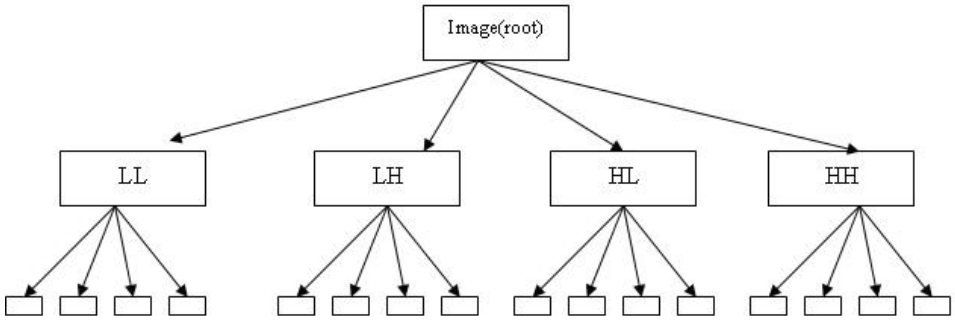

Figure 4.10: Full wavelet decomposition quad tree up to h=2 levels

The energy in each subband is computed and used as features for further analysis.

4.2.2 Adaptive Pruning in Spectral Axis

The feature extraction step (Figure 4.8) starts with pruning in spectral axis. The obtained binary spectral band feature tree (Figure 4.9) is pruned from bottom to top by the following rule:

Binary tree pruning algorithm

if $d_{mother} < max\{d_{child1}, d_{child2}\}$

set $max\{d_{child1}, d_{child2}\} as\ d_{mother}$

else

remove children

where d_i is the distance of the i_{th} node feature between classes. We used Euclidean distance between cumulative probability distribution of the nodes. However, other distance metrics can be used as well.

The algorithm prunes the spectral bands (branch node) if their discrimination potential is lower than their mother node. This process fuses some of the spectral bands for better classification accuracy. The frequency subband energies of the pruned spectral bands are averaged in parallel before pruning in the spatial-frequency axis.

4.2.3 Adaptive Pruning in Spatial-Frequency Axis

The pruning algorithm in Section 4.5.2 is modified to four children mode because of the quad tree structure (Figure 4.10) in spatial-frequency axis and applied to prune the quad tree in a bottom-up manner.

Quad tree pruning algorithm

if $d_{mother} < max\{d_{child1}, d_{child2}, d_{child3}, d_{child4}\}$

set $max\{d_{child1}, d_{child2}, d_{child3}, d_{child4}\} as\ d_{mother}$

else

remove children

where the *child1, child2,child3* and *child4* are the LL, LH,HL and HH wavelet subbands of the mother node, respectively. The algorithm keeps the mother node if its discrimination potential is higher than any of its four children nodes. Otherwise the children nodes survive as the nodes with high discrimination potential.

4.2.4 Selection of extracted spectral spatial-frequency features

The adaptive segmentation and pruning in both spectral and spatial-frequency axis based on the distance between the feature elements revealed the location of the discriminative features of the hyperspectral data. This feature extraction processes provides the best segmentation in both spectral and spatial-frequency axis but does not eliminate the irrelevant ones. Therefore, these features are also selected by feature selection algoritms (FFS, CFS and Wrapper) and fed into the classifier one by one to figure out the feature subset giving minimum classification error. In addition to these feature selection algorithm, a new feature set is generated by PCA algorithm and the tranformed features are used in the classifier.

CHAPTER 5

Datasets Used in Experiment

5.1 Acquisition of Impact Acoustics Data

'Levant' type in-shell hazelnuts, which were collected from an orchard in Akcakoca, Turkey in August 2003 are used for impact acoustic sorter. The weights of the hazelnuts are measured and the ones less than 0.9 gram are taken as empty or undeveloped (EmH) nuts. Hazelnuts with weights over 0.9 grams are accepted as fully developed (FuH). The shells of the fully developed nuts are visually inspected are further classified as nuts with regular shell (ReH) and nuts with cracked shell (CrH). The weight histogram of the randomly selected 180 nuts from each group is depicted in Figure 5.1. It is seen that the fully developed nuts with cracked shell have similar weights with the fully developed nuts with regular shell.

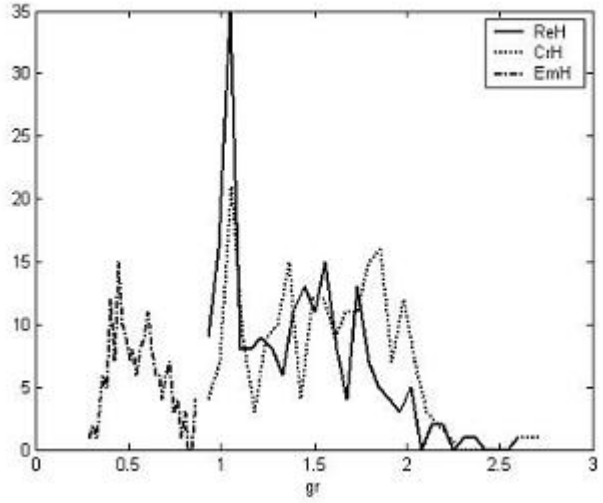

Figure 5.1: Weights of 'EmH', 'CrH' and 'ReH' hazelnuts

The impact acoustic data acquisition system is used to get impact acoustic signals of those classified hazelnuts. Typical signals of an empty or undeveloped hazelnut (EmH), a full hazelnut with regular (ReH) and cracked shell (CrH) are shown in Figure 5.2.

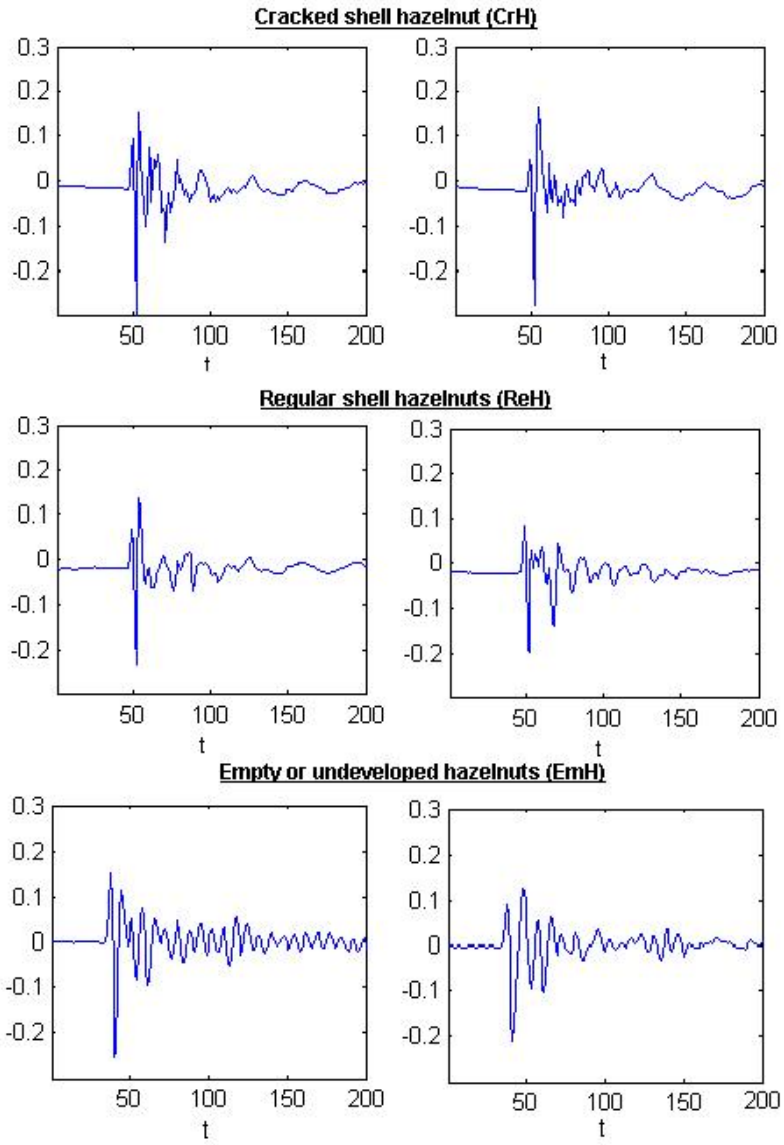

Figure 5.2: Typical impact acoustic signals of ReH, CrH and EmH hazelnuts

The impact instant of the acoustic signal is defined as the time of the first sample from left up to the sample whose amplitude is over the 15% of the absolute maximum amplitude. This impact instant is experimentally defined and the redundant samples before the impact instant are removed adaptively from the signals. The consecutive 768 samples from the impact instant are used as the impact acoustic signal for each hazelnut.

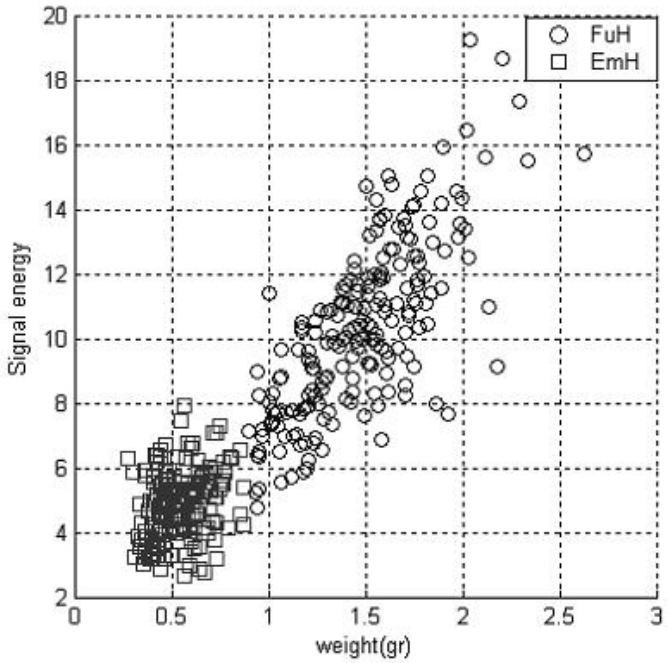

Figure 5.3: Signal energy of hazelnuts at various weights

It is observed that empty hazelnuts generate weaker signals compared to fully developed ones (FuH) and their impact signals tend to (computed by Equation 5.1) have lower energy values. The cracked hazelnut impact sounds have similar energy values to those with regular shell indicating similar weights but the cracked impact signals usually have a longer decay time due to the oscillations caused by the crack. Figure 5.3 shows the significant correlation between the nuts' weights and the total impact acoustic signal *x(j)* energy levels of the nuts computed by

$$e = \sum_{j} \left| x(j) \right| \qquad j = 1, 2, 3....M \tag{5.1}$$

where M is the total number of samples which is defined as 758.

It is possible to separate the EmH kernels from FuH ones at 96% classification accuracy by just using the raw signal energies as a feature. However, this is not valid for separation of ReH and CrH because they have similar weights and energy values. Therefore more advanced signal processing and feature selection techniques should be used to extract the relevant features for classification of ReH and CrH hazelnuts. The LDB algorithm is aimed to obtain such relevant features from the time-frequency domain of the signals (Figure 5.4). The impact acoustic signal of 1000 ReH and 1000 CrH hazelnuts were used for algorithm development.

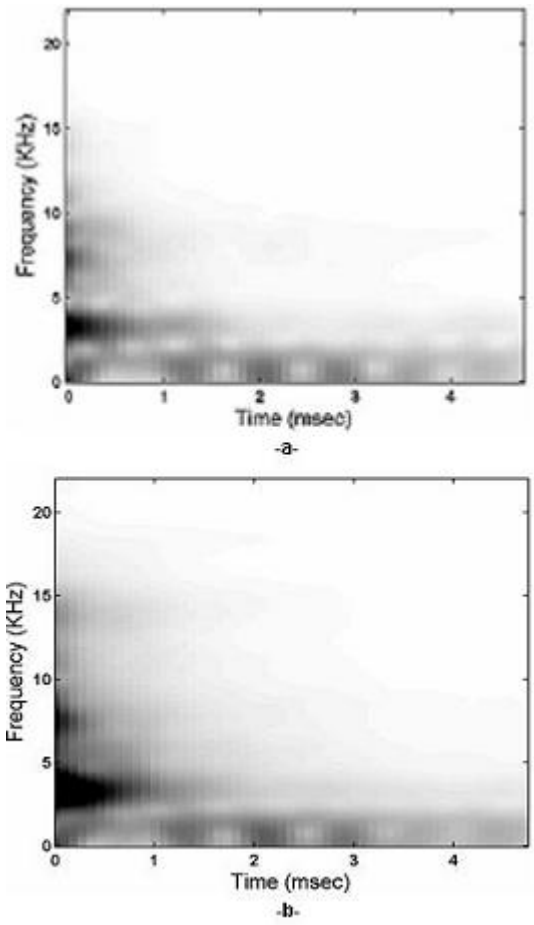

Figure 5.4: The averaged spectrogram of a) CrH and b) ReH hazelnuts

5.2 Acquisition of Hyperspectral Data

Shelled hazelnuts for hyperspectral imaging were collected from Ordu, Turkey in 2007. A few aflatoxin contaminated hazelnut kernels is encountered in the collected samples. Therefore an artificial contamination procedure is conducted to obtain aflatoxin contaminated hazelnut kernels. In stated in Section 3.2 that the in-shelled hazelnuts processed in two different category as Shelled (SHD)and Shelled/Roasted (SRT) nuts. The two types of hazelnuts have different visual characteristics because the roasting operation removes the inner skin of the InH hazelnuts.Therefore these hazelnuts were studied separately.The SHD and SRT hazelnuts were divided into three groups as shown in Figure 5.5. The first group was reserved for uncontaminated class *(UnCont)* where the second and third groups were artificially contaminated. The hazelnut kernels in the second group were incubated to aflatoxin producing molds *(FlavusCont)* whereas the kernels in the third group incubated to pure water *(WaterCont)*.

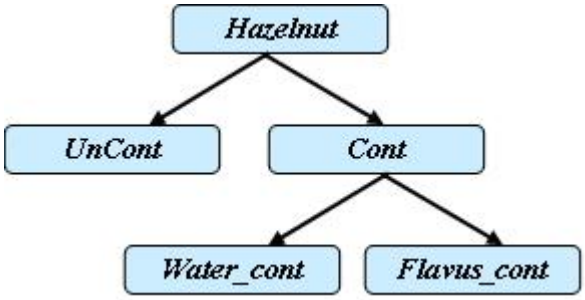

Figure 5.5: Categories of hazelnut used in the experiment

All the incubated kernels *(FlavusCont and WaterCont)* are kept in 28^0C with 90% humidity condition for 9 days. The mold infestation is observed at all the incubated hazelnuts. At the end of the 9th day, the hazelnuts in SRT category were roasted at 140^0C for 15 minutes. The roasting process removed the skin over the kernels. The hazelnuts in both SRT and SHD categories were sent to chemical analysis for aflatoxin contamination after hyperspectral image acquisition. The chemical analysis (Table 5.1 and Table 5.2) results showed high level of aflatoxin contamination at *FlavusCont* hazelnuts and respectively low level of aflatoxin at

some of the *WaterCcont* hazelnut of both categories. Aflatoxin over 4 ppb is detected in two UnCont hazelnuts from SRT and one UnCont hazelnuts from SHD category. All the kernels in *WaterCont* group are naturally mold infected and these hazelnuts should not be consumed although a few of them contain aflatoxin.

Table 5.1: Number of aflatoxin contaminated kernels and the mean aflatoxin level (ppb) of the three group SRT hazelnuts

	SRT_UnCont	SRT_FlavusCont	SRT_WaterCont
# of SRT_Afla+ kernel	2	79	15
# of SRT_Afla- kernel	102	0	87
Mean Aflatoxin Level	0.7	2227	7,47

Table 5.2: Number of aflatoxin contaminated kernels and the mean aflatoxin level (ppb) of the three group SDT hazelnuts

	SDT_UnCont	SDT_FlavusCont	SDT_WaterCont
# of SDT_Afla+ kernel	1	49	4
# of SDT_Afla- kernel	81	0	100
Mean Aflatoxin Level	0.36	3418	26,25

The hazelnut samples under UV-A light are screened by capturing the reflected light from the sample by using the hyperspectral imaging system. The spectral images are taken by IC Capture (Imaging Source Inc) image acquisition toll. The exposure time of the camera is set to 0.33 sec for SRT and 2 sec for SHDhazelnuts in order to capture sufficient reflectance light. The SHD category hazelnuts do not reflect sufficient light because of the inner skin and moisture. Therefore, we could not get high quality images although we increase the exposure time from 0.33 sec to 2 sec with the same hyperspectral imaging system. Figure 5.6 shows some of the band features of hazelnut kernels from SRT and SHD category, respectively. The first three columns show the *FlavusCont* hazelnut images, the second third columns show the *WaterCont* hazelnuts, whereas the last 3 columns show the *(UnCont)* hazelnut images. The kernels were also visualized without

any filter, at a filter 550 nm (70 nm FWHM) and 600 nm (40 nm FWHM). These images are used at image preprocessing but not used for algorithm development.

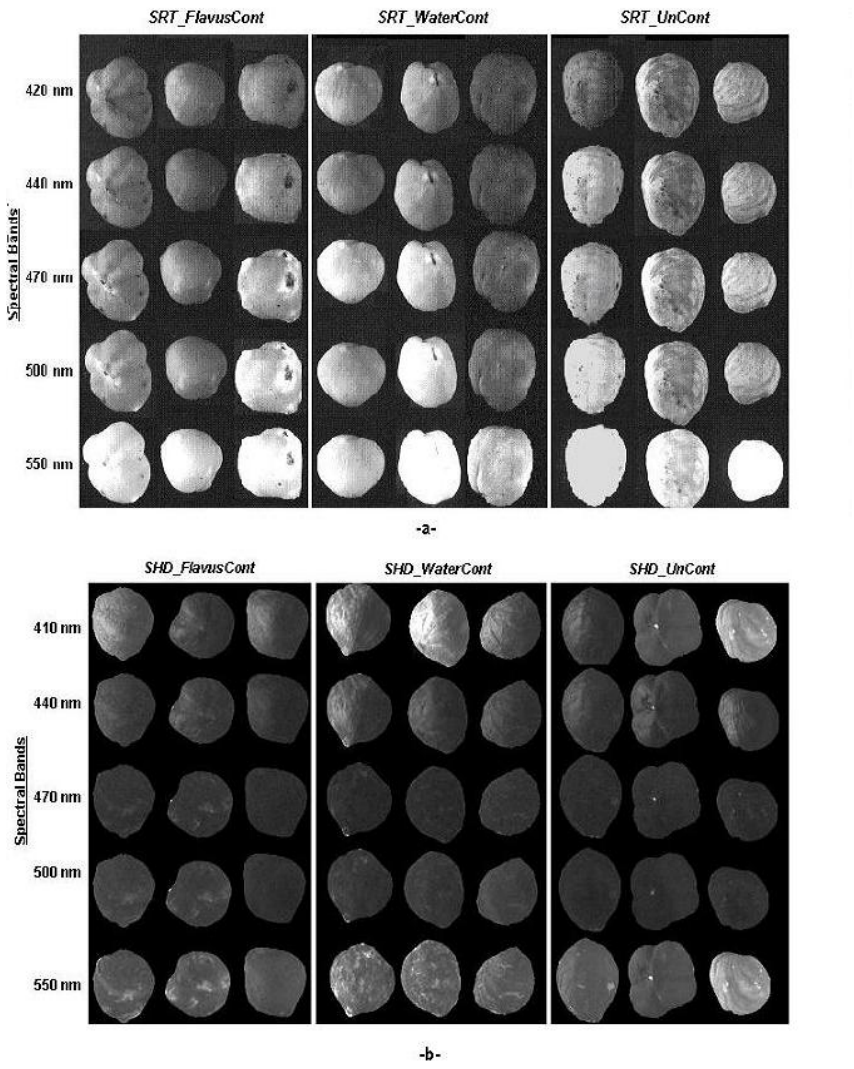

Figure 5.6: A few spectral band images for *FlavusCont*, *WaterCont* and *(UnCont)* group of a) SRT and b) SHD hazelnuts

5.3 Preprocessing the Hyperspectral Images

A median filter was applied to remove the noise at the spectral images (Fig 5.7-a). Secondly, a binary mask was generated to extract the hazelnut from background and the pixels of the regions which the inner skin was not removed during roasting. The images taken at 550 nm is appropriate for mask generation. This band clearly displays the distinction of the nut from background and unskinned region. The mask was further improved by erosion and dilation operation. These morphological operation removed the undesired defects due to thresolding. The generated mask was applied for all spectral images of the hazelnut (Fig 5.7-b).

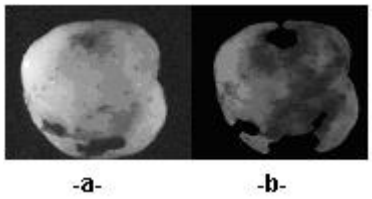

Figure 5.7: A raw spectral band image with unskinned region at the surface, b) masked image of 430 nm spectral band

Instead of a whole hazelnut image, the masked spectral images were divided into square regions (91x91 pixels) and each region was regarded as an independent sample and they were later on used for voting on the class membership of a given hazelnut kernel.

chapter 6

Results and Discussions on Impact Acoustic Data Classification

It is possible to separate the empty *EmH* kernels from the fully developed *FuH* ones with 96% classification accuracy by just using the raw signal energies as a feature for the linear classifier. However, a classification by raw signal energies does not separate the regular shell hazelnuts *ReH* and cracked shell hazelnuts *CrH* because they have similar weights and energy values. Therefore more advanced signal processing and feature selection techniques should be used to extract the relevant features for classification of *ReH* and *CrH*. The developed LDB based algorithm is aimed to obtain such relevant features from the time-frequency domain of the signals and the classification results of the extracted features are compared.

A total of one thousand ReH and one thousand *CrH* hazelnut kernels are used in this study. Each hazelnut is dropped on the metal plate and the resulting acoustic signal consisting of 768 time samples is recorded. The one thousand acoustic signals for each class are randomly divided into five non-overlapping sets, each consisting of 200 records. Five pairs of *ReH* and *CrH* sets are then randomly formed. Each pair is used to construct the adaptive time-frequency (T-F) segmentation and select features. The features identified are then used with the remaining 1600 acoustic signals to determine the performance of the classifier. This procedure is repeated five times with the five different pairs of *ReH* and *CrH* sets.

The acoustic signals were analyzed up to a tree depth of four resulting in a smallest segment size of 48 time samples in the time domain. It is empirically found that this level provides a healthy balance between transient waveforms and the required spectral resolution to distinguish between subbands with different behavior. The signals were first represented by using LCP (Figure 4.1) over the pyramidal tree structure (Figure 4.2). The pyramidal tree was pruned by using the pruning algorithm of Section 4.1.1 and the adaptive time segmentation for classification purpose was obtained for different sets of signals as indicated in Figure 6.1. It was observed that different sets of signals may cause different segmentation in time. The segmentation of Figure 6.1-a were used in further analysis. In this case, the time axis is divided into seven segments.

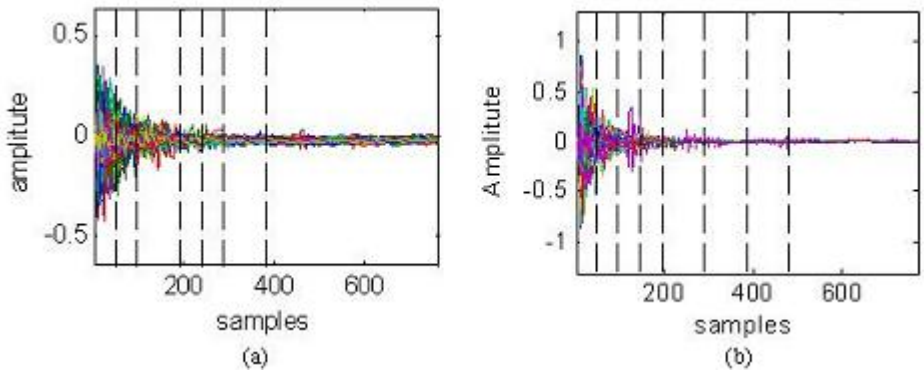

Figure 6.1: The adaptive time segmentation grids (dotted lines) of a-) of set1 and b-) of set2

In each time segment the signal was decomposed into sub-bands up to the fourth Wavelet decomposition level and the most relevant sub-bands were detected by using the procedures of Section 4.1.2.

A discriminative time-frequency map was generated in Figure 6.2 by combining the adaptively pruned trees both in time and frequency to visualize the most crucial T-F patterns.

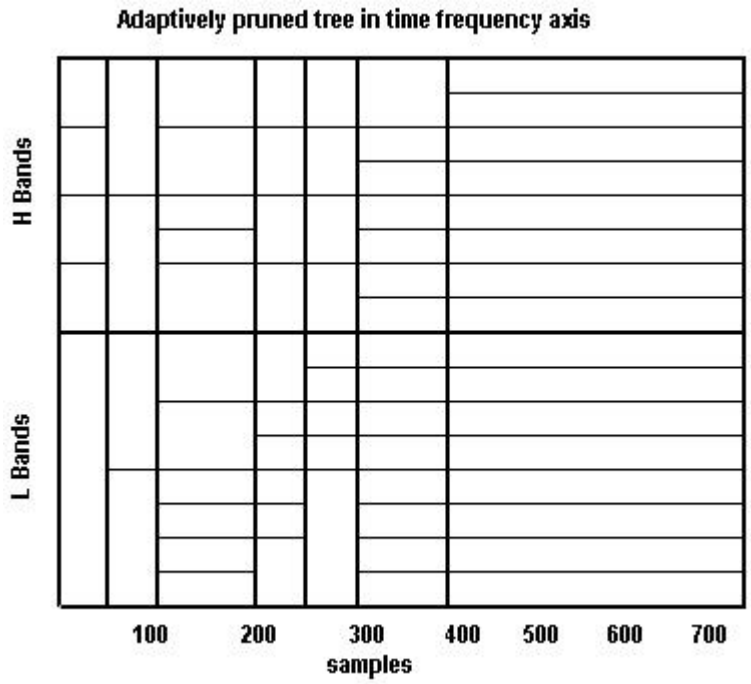

Figure 6.2: The location of most discriminative features in time-frequency axis

In our application, the algorithm usually generates a T-F map with around 70 sub-bands for various training data sets. For every signal in each training set, the energy value for each sub-band was computed resulting in two sets of feature vectors corresponding to cracked and healthy shell classes. The 70 features obtained were sorted by Fisher distance based (FFS) and Correlation Based Feature Selection (CFS) algorithms and then used for classification. We observed with all training data sets that the most discriminative feature locations (defined by FFS) were concentrated in the high frequency bands corresponding to the early and post impact regions as indicated in Figure 6.3. Among the 70 sub-bands, the 25 most discriminative ones are indicated by different shades of gray, with darker shades corresponding to higher discrimination levels.

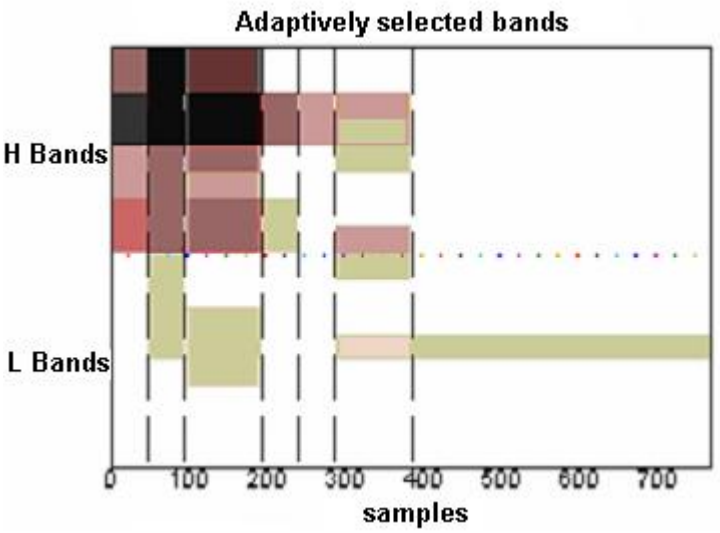

Figure 6.3: The time-frequency discrimination map of impact acoustic data. Darker regions indicate higher discrimination power

6.1 Classification

In order to assess the efficiency of the proposed algorithm, a comparison is made with the Non-Adaptive Time and Frequency features (NATF) [44], Non-Adaptive Sub-Bands features (NASB) and different order statistical features. Recall that in NATF method, 70 features were extracted from the short time variances of signal; maximum signal amplitude, spectral peak locations and Weibull distribution fit to the envelope of the impact signal and all are used for classification. In the NASB method, features were extracted from subband signals and the 20 most relevant features and the sub-bands including these features were manually selected. The time segmentation of Figure 6.1-a is employed to obtain a total of 28 statistical features including mean absolute energy, variance, skewness and kurtosis on each of the seven time segments.

The minimum number of features for classification was investigated by adding features one by one which were ranked by FFS and CFS feature selection algorithms. The feature selection step is repeated for all four different type of extracted feature sets. Related classification error curves are presented in Figure 6.4.

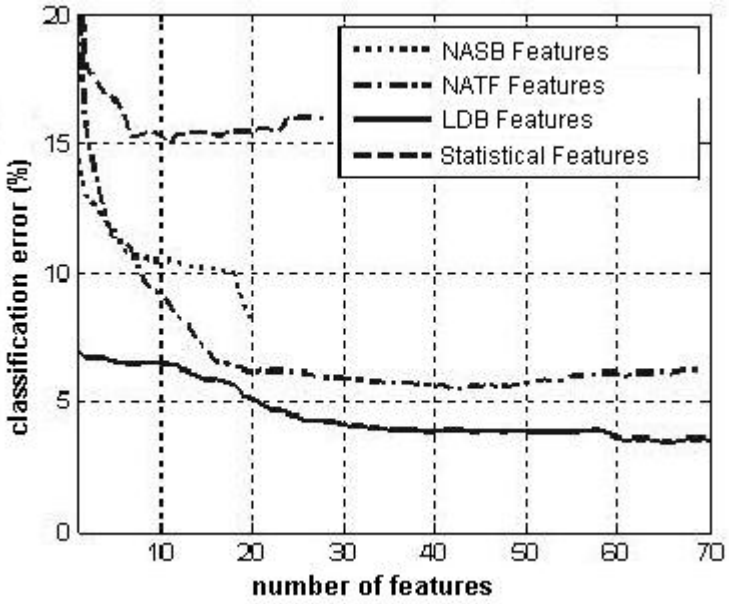

Figure 6.4: The classification error rates (%) with various numbers of features

The lowest classification error is achieved with the proposed LBD based approach. The minimal classification error rates achieved by each method are given in Table 6.1. It is observed that the lowest error is achieved by the first 64 features with an error level of 3.5% by our proposed approach. For the method of NATF, 43 out of 70 time and frequency domain features provided the minimum error level. Similarly, 20 features are used for the method of NASB. The statistical features gave poor classification error rates compared to other methods. The lowest error rate occurred when the first 7 features are used. Our proposed approach reaches an error rate around 4% after the first 30 features. Increasing the number of features provided marginal improvement of the error rate.

Table 6.1: Classification rate comparison of proposed LDB based method against the other methods

Method	Accuracy(%)
43 NATF features	94.47
7 statistical features	85.00
20 NASB features	91.80
64 LDB features	96.51

The ROC curves for the three methods are presented in Figure 6.5. It is observed that 64 and 30 dimensional LDB features provide higher detection of cracked hazelnuts for a given false alarm rate.

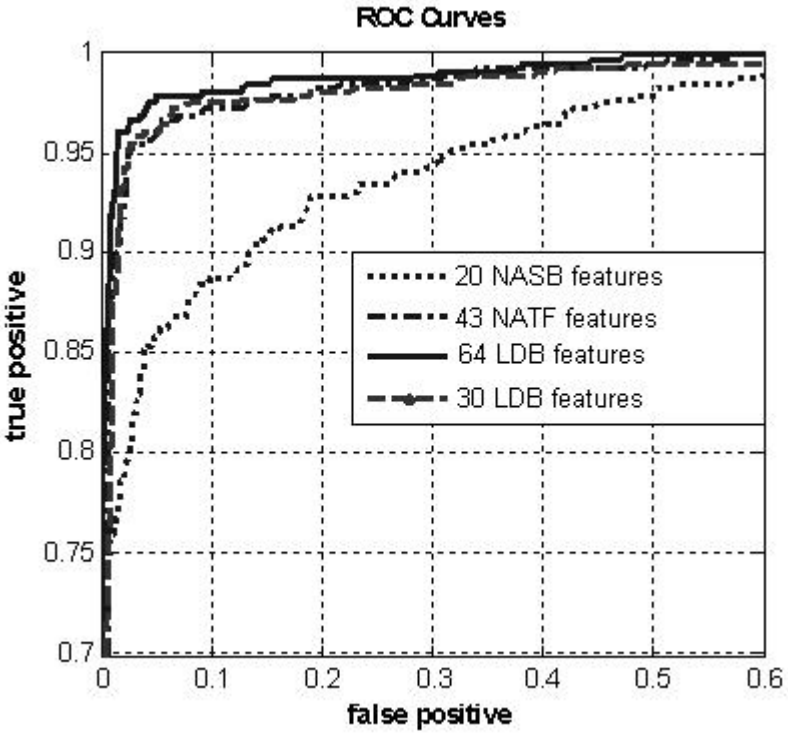

Figure 6.5: Receiver Operating Characteristics (ROC) curves

6.2 Filter Selection

Various types of wavelet filters (Daubechies, Coiflet, and Sym) are used for decomposition of the frequency axis and their effects on classification accuracy are observed. In Figures 6.6 (a) and (b) the classification error curves with various number of features are depicted in contour graphics format for the usage of various Daubechies and Coiflet Wavelets for frequency axis decomposition.

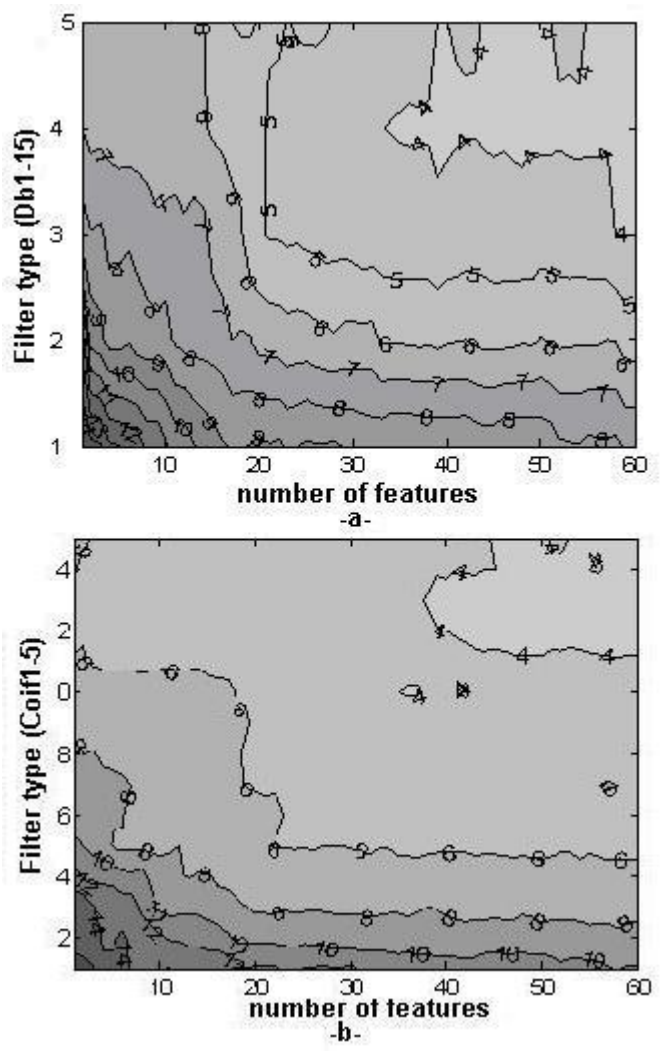

Figure 6.6: The effect of selected wavelets and feature dimension on classification accuracy. a) Daubechies, b) Coiflet

The x axis indicates the total number of features retained after sorting. The

y axis indicates the filter type used in subband decomposition. The numbers on the graph show the obtained classification accuracies (%). The higher filter types correspond to higher order filters. The darker regions in the contour graph give lower classification accuracy. It is observed that better classification error rates ($< 4\%$) are obtained when approximately 40 or more features are retained after decomposition with high order wavelet filters such as Daubechie's 12 to 15 tap and Coiflet's three to five tap filters. We selected one of the high order wavelet filters, Coiflet four tap, for further analysis. The discriminant band distribution of Figure 6.3 may slightly change depending on the wavelet filter.

6.3 Effect of noise on classification

In order to asses the robustness of our methods against disturbing effects, a zero mean Gaussian noise at various SNR level is added to the signal and classification performances are compared as shown in Figure 6.7.

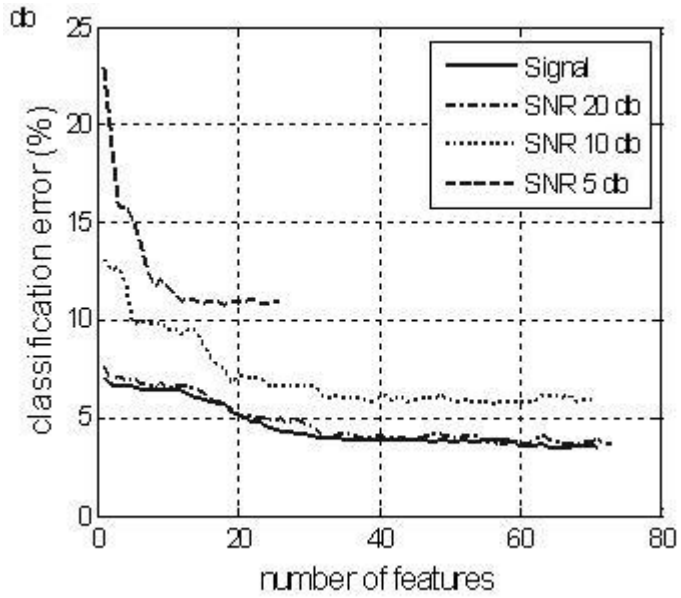

Figure 6.7: The classification error curves for noise disturbed impact acoustic signals

It is observed that the algorithm performs well for reasonable noise levels.

The algorithm usually selects low level subbands nodes when the signals are disturbed by high level noise. This can be justified by the fact that the energy of the impact acoustics is concentrated in the mid and lower bands of the spectrum as indicated in Figure 6.3. In order to keep the efficiency in classification, the algorithm selects features from lower bands with increasing noise level. This also results in a decrease in classification accuracy.

6.4 Effect of shift-invariance on classification

As indicated in the previous sections the main motivation for using UDWT against DWT is the shift invariance property of the UDWT. In order to justify our selection, the UDWT results with those obtained from the DWT and spin-cycle procedure of [Saito02] are compared. The spin-cycle procedure is introduced by [Saito02] to overcome the lack of shift invariance of the DWT and LCP. In particular, a signal is shifted to the left and right for a selected number of spins. For each shift, the signal is expanded into its DWT coefficients. These coefficients are either averaged or processed individually. It has been shown that the spin-cycle procedure provides significant improvements over the direct use of the DWT or LCP [Ince06, Saito02]. In The classification curves obtained from the DWT, the DWT with spin-cycle and the UDWT methods are shown in Figure 6.8.

As expected, the results obtained from DWT were poor. However, the DWT with spin-cycle and UDWT give better classification results. We note that the minimum error of spin-cycle method was slightly lower that UDWT but used more features. However, one should note that the data size of spin-cycle method is higher than that of UDWT. In real time applications it is difficult to obtain fast processing by this method.

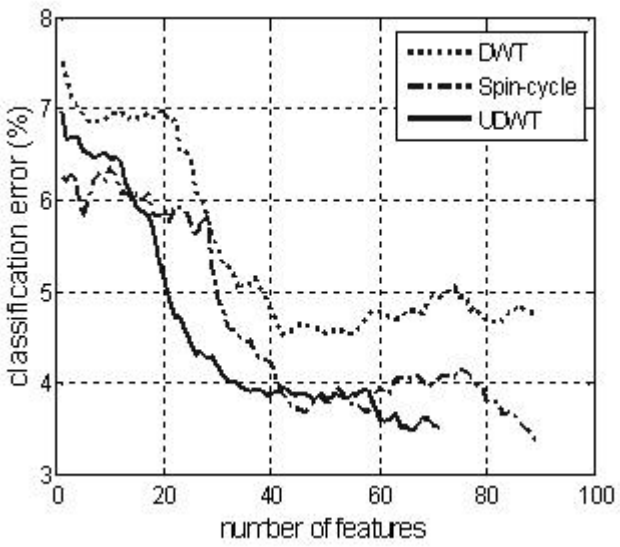

Figure 6.8: The classification error curves for evaluating the efficiency of shift invariance property. The spin-cycle curve stands for the results obtained from DWT supported 1-Spin-Cycle procedure

6.5 Effect of feature extraction algorithm on classification

A total of 210 features corresponding to 210 time-frequency bands are obtained before pruning both in time and frequency axis. The pruning operations not only extracted the most discriminative features; but also decreased the feature dimension from 210 to 70. The extracted features are also selected by FFS and CFS algorithms. Lower classification error curves are obtained with extracted feature set compared to candidate feature set of size 210 (Figure 6.9).

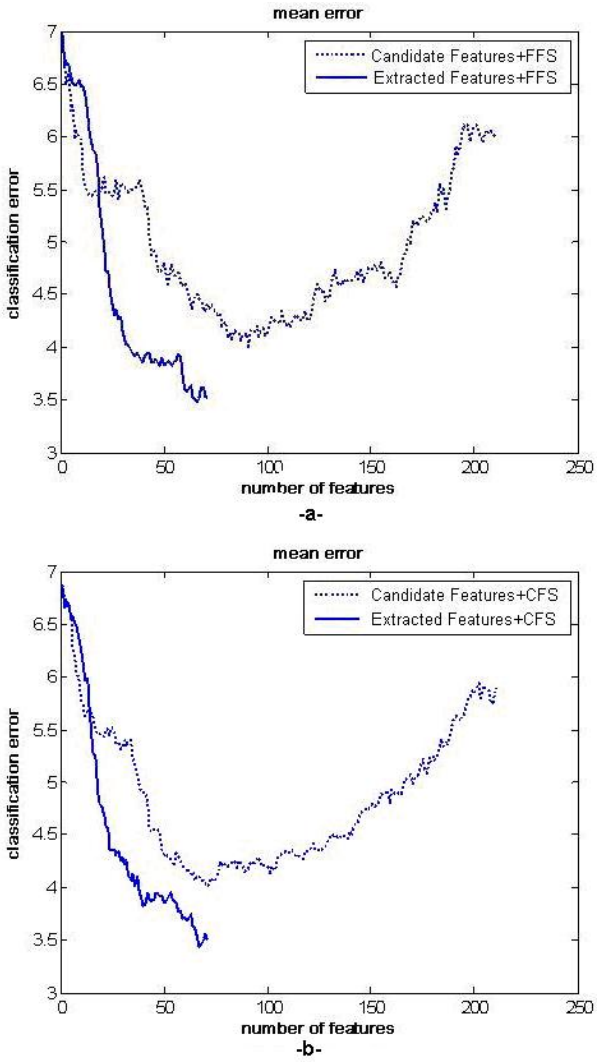

Figure 6.9: The classification error curves of a) FFS and b) CFS method with extracted and candidate feature set

The minimal error of 4% is achieved with around 70 candidate features and the classification error increased after addition of more features. This number coincides with the number of extracted features. It is observed from the Figure 6.9 that the proposed algorithm is successful at detecting relevant features in acoustic signals. Recall that the pruning algorithms in feature exraction merge the features in t-f axis for better classification. Therefore, lower classification error curves are achieved with 70 extracted features compared first 70 candidata features.

The feature selection algorithms of CFS and FFS on extracted feature set did not make a significant difference on classification error (Figure 6.10). However, the CFS has superior performance with the first 24 features.

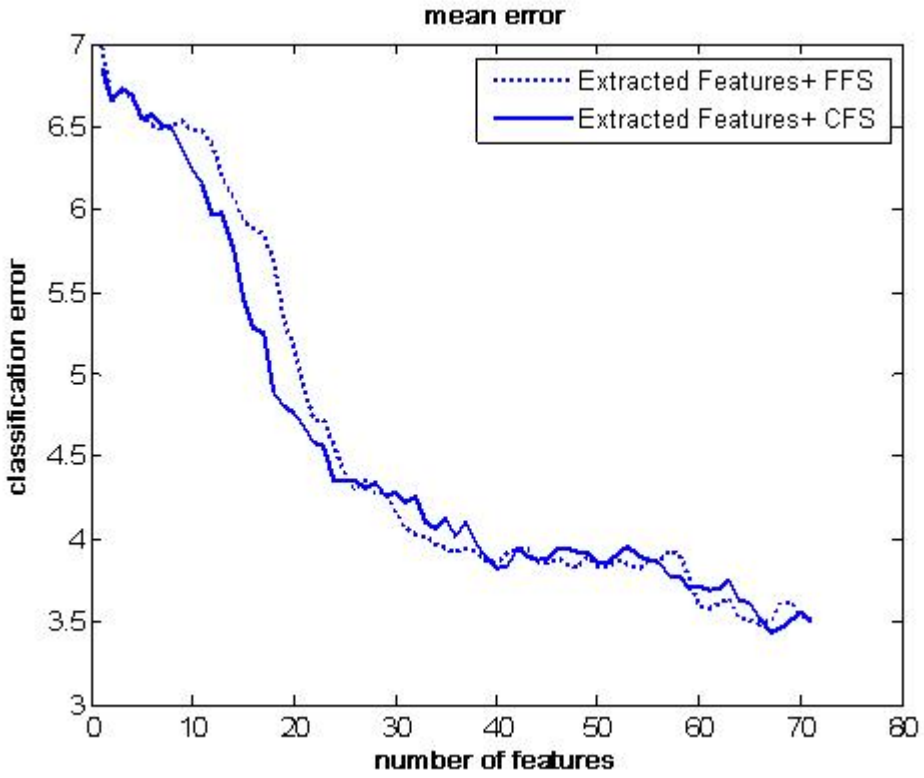

Figure 6.10: The classification error curves of CFS and FFS method with extracted feature set

6.6 Computational Complexity

Determining the best time-frequency segmentation of the signals and the bands to be retained for classification is relatively computationally demanding but this step has to be carried out only once, off-line. For online processing, the throughput of the algorithm in terms of nuts processed per second depends on the number of features used in classification. When the first 64 features providing the best classification rate is employed all 768 samples need to be processed. In this case 17.4 msec is required for signal acquisition of a single nut at a sampling rate of 44.1 kHz. The computations for feature extraction and classification require 13.1 msec on a dedicated P4 3GHz processor. In this case, up to 32 nuts can be processed in a second with classification error of 3.5%. In case an extra 0.5% classification error is tolerable, up to 45 nuts can be processed in a second with 30 features. We observed that only the first half of the signal is required to compute the first 19 features. The classification error achievable at this case is 5.3% and the throughput can be as high as 119 nuts/sec provided that the mechanical sorter system is able to keep up with signal processing.

chapter 7

Results and Discussions on Hyperspectral Data Classification

The developed algorithm is tested on Shelled (SHD) and Shelled/Roasted (SRT) hazelnut hyperspectral data, separately. The hazelnuts groups in both category (SHD and SRT) are considered for two different classification problems. In the first problem, the data sets (Table 5.1 and 5.2) are divided into mold contaminated *Cont (= FlavusCont + WaterCont)* and uncontaminated *(UnCont)* classes without considering the aflatoxin contamination (Figure 5.5). All of the kernels in *Cont* class are mold contaminated (but some of them do not contain measurable aflatoxin). In the second classification problem, we categorized the hazelnuts by just considering the aflatoxin contamination levels and the hazelnuts with over 4 ppb aflatoxin are accepted as aflatoxin contaminated *(Afla+)* and the remaining ones are accepted as aflatoxin free *(Afla-)*. All the kernels in *FlavusCont*; some of the kernels from *(WaterCont)* and *UnCont* groups are assigned to *Afla+* class and the remaining kernels from from *(WaterCont)* and *UnCont* were assigned to *Afla-* class as in Figure 7.1

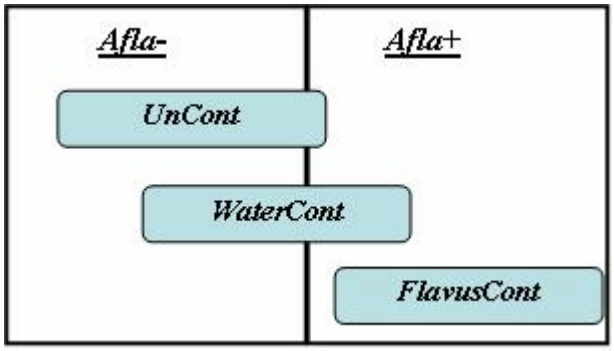

Figure 7.1: The schematic assigments of hazelnuts *Afla+* and *Afla-* groups

7.1 Problem 1: Classification of *SRT_Cont* and *SRT_UnCont* Hazelnuts

Initially, feature trees are generated first along the spectral then spatial-frequency axis. The reflectance energies of 12 spectral images (400-510) were placed on the 4^{th} level of the binary tree (Figure 4.8) from left to right. The remaining four spectral band nodes (SB13-SB16) at the 4^{th} level were set to null in order to complete the binary tree. Consequently, the spatial-frequency quad feature tree is generated by decomposing the spectral bands by full wavelet transform (Figure 4.9). We used Daubechies 8 tap filter for decomposition. Other wavelets can be used as well. For each spectral image, a total of 21 subband images are constructed by a two level decomposition (Figure 4.9). That gives a total of 252 spatial frequency patterns for 12 spectral bands. The nodes in trees are represented by their energies as features. The entropy distribution of the spatial-frequency features of spectral bands can be seen in Figure 7.2. It is observed that low spatial-frequency subbands have higher entropy than high frequency components.

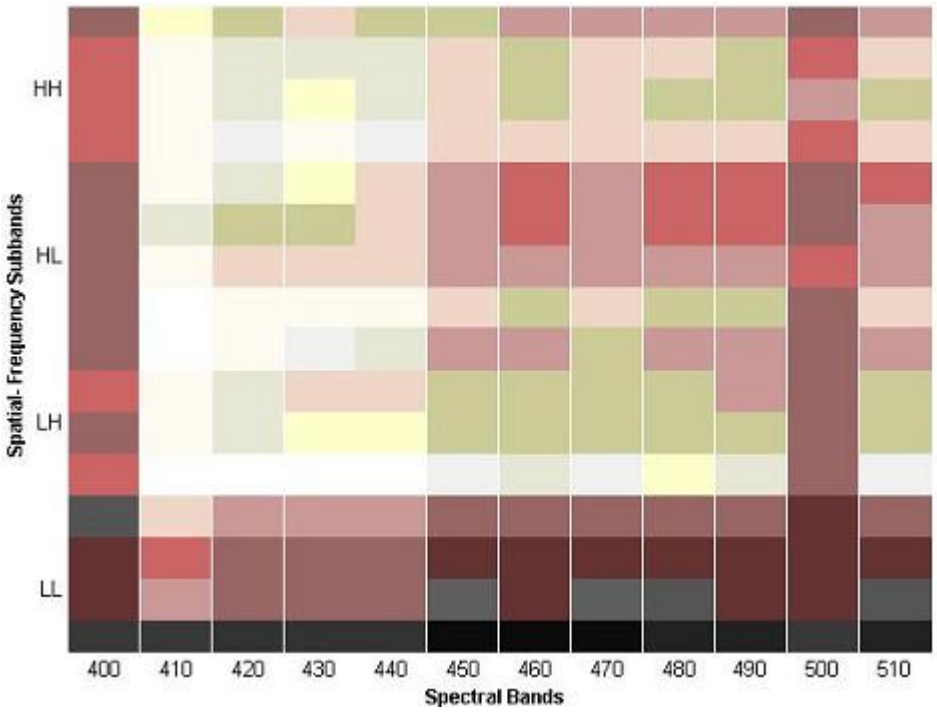

Figure 7.2: Entropy map of the spectral spatial-frequency features

After the generation of the feature trees, the feature extraction process is initiated by pruning the spectral bands (Section 4.2.2). Figure 7.3 shows the spectral band pruning. The spatial-frequency domain features (Figure 4.9) of the spectral bands are averaged according to the pruned tree in Figure 7.3 before pruning in spatial-frequency axis.

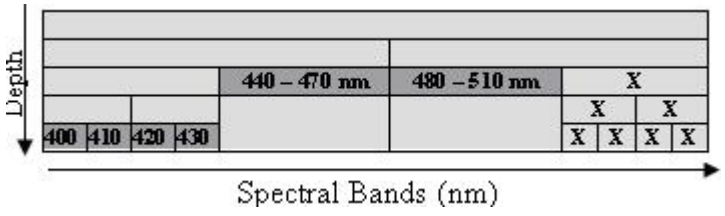

Figure 7.3: Spectral band pruning. The spectral bands (440-470) and (480 -510) are pruned. The null bands in the tree were ignored at pruning

The spatial-frequency subbands features are pruned after merging the frequency subband features of the pruned spectral bands (Section 4.2.3). The pruning in both axes revealed the location of the most discriminative features (Figure

7.4) of the hyperspectral data. A total of 12 spectral-frequency features were obtained after the pruning operations. These operations also decreased the feature dimension from 192 to 12. The location of 192 candidate features can be oberved in Figure 7.2.

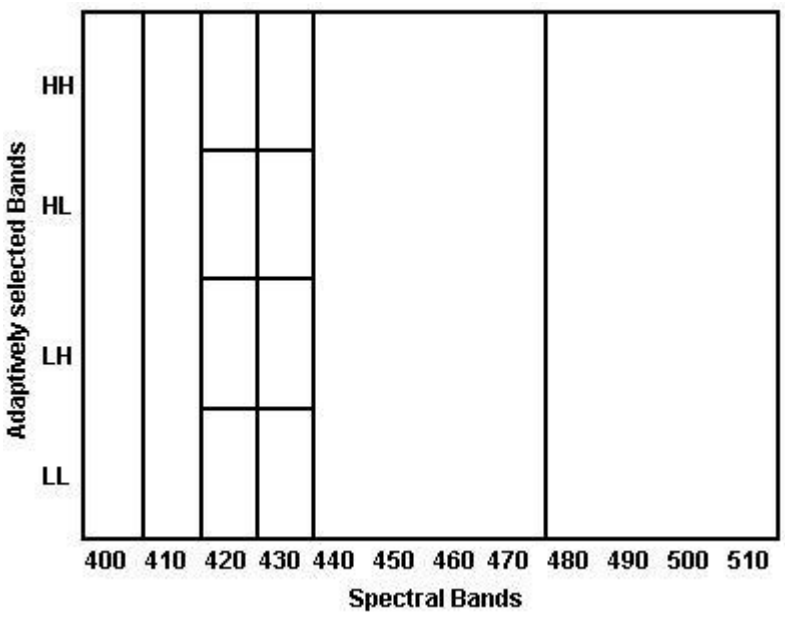

Figure 7.4: The location of the most discriminative features in spectral spatial-frequency axis

It is observed that the spectral bands (440-470) and (480-510) are pruned along the spectral axis and these spectral bands are not decomposed into spatial-frequency subbands. However, the spectral bands of 430 and 440 are decomposed into subbands in spatial-frequency axis.

The extracted 12 features are then ranked by four different feature selection algorithms and fed into the linear classifier incrementally.

- Fisher Distance Based Feature Selection(FFS)
- Correlation Based Feature Selection(CFS)
- PCA Based Feature Selection(PCA)
- Wrapper Based Feature Selection

In contract to FFS and CFS, PCA does not work in inremental way and uses all the features to project to the new space. The wrapper model is just selects the feature combination giving the best classification.The FFS and CFS algorithms ordered the extracted features as in Figure 7.5. The darkness and the number on nodes indicate the relevance of the features in those nodes. The order of features may vary depending of the feature selection algorithm and this selection may effect the classification accuracy.

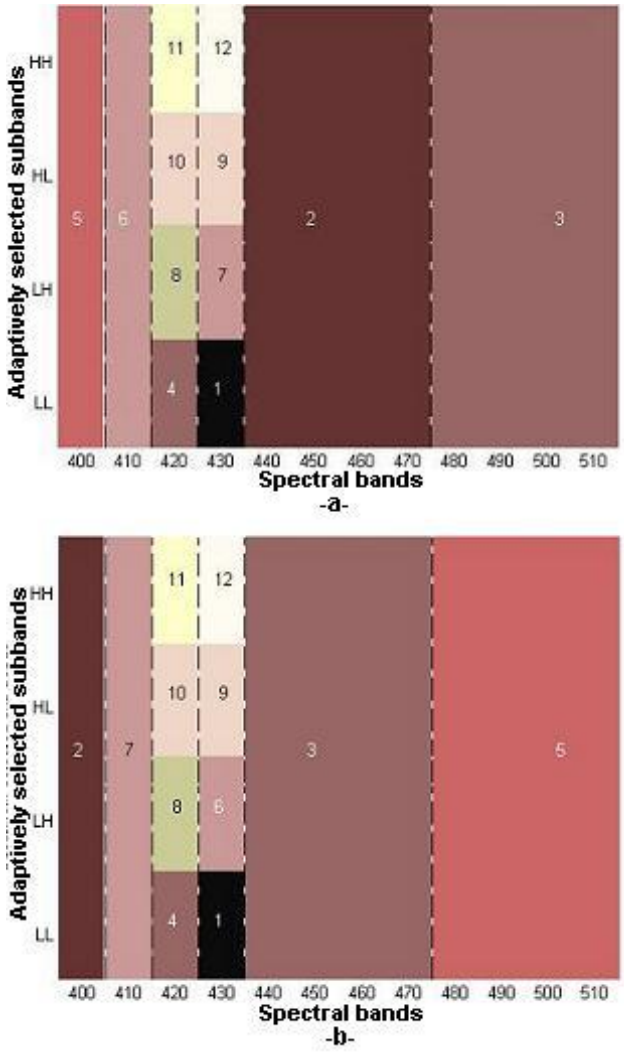

Figure 7.5: Spectral Spatial-Frequency feature map of SRT hazelnut data ranked by a) by FFS, b) by CFS algorithm

The selected features are added one by one to find out the optimal number of features for classification. The minimum classification error is obtained with the two features by PCA; four features by wrapper and five features by CFS and FFS (Table 7.1, Figure 7.6). In contrast to other feature selection algorithms, the feature number in PCA methods (Table 7.1) is the number of projected eigenvectors.

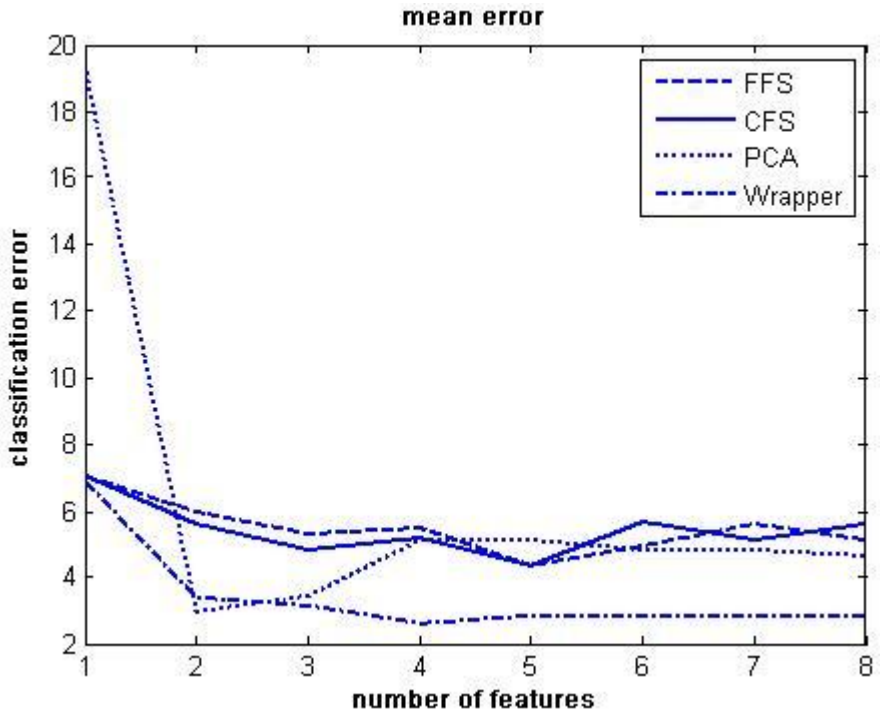

Figure 7.6: The classification error curves on FFS, CFS, PCA and Wrapper based selected ranked features

Table 7.1: Minimum classification error obtained by four feature selection algorithms. The number of features of methods giving the error is shown in brackets

	FSS(5)	CFS(5)	PCA(2)	Wrapper(4)
Error(%)	4.35	4.35	3.00	2.60

For a practical sorter system, it is preferable to reach to lowest error with fewer number of features. The lowest error is achieved by four wrapper based selected features. It is possible to get good results with PCA ordered features. However, It is impractical to use the PCA-processed features because the PCA uses all the features at hand for all unique projection although it gives lower classification error.

When the classification results with five FFS ordered features are analyzed, it observed that 10 of 181 *SRT_Cont* hazelnut and 3 of 104 *SRT_UnCont* hazelnuts were misclassified. However none of the misclassified *SRT_Cont* hazelnuts contain aflatoxin. The mean aflatoxin level of the test set including hazelnut from *SRT_Cont* and *SRT_UnCont* group is 608 ppb and the algorithm classified the kernels in to two classes whose aflatoxin contamination levels are 1095 ppb and 0.7 ppb.

The feature extraction step (Figure 4.7), which is the focus of proposed study, positively affects the success of the feature selection algorithm by providing the most discriminative features in hyperspectral data. This statement is validated (Figure 7.7, 7.8 and 7.9) by comparing the classification results when feature selection algorithms (CFS, FFS and PCA) are applied after feature extraction or applied to candidate feature set in the 192 dimensional space. This comparison could not be performed with wrapper model because of the extensive computation due to the high number of feature subset combination.

Lower classification error curves are obtained when working with extracted feature set than those with candidate feature set by all these feature selection algorithms. It is observed from the Figures 7.7, 7.8 and 7.9 that the 2D feature extraction algorithm generates high discriminative features by pruning both in spectral and spatial-frequency domains. It also enables us to select the sufficient spectral band by eliminating the irrelavant ones. This will dicrease the image acquisition and processing cost of the food inspection and sorter systems.

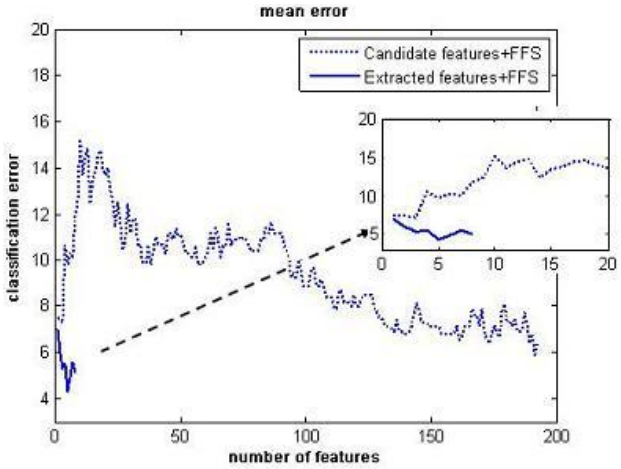

Figure 7.7: The classification error curves with the features selected from candidate and extracted features by FFS algorithm

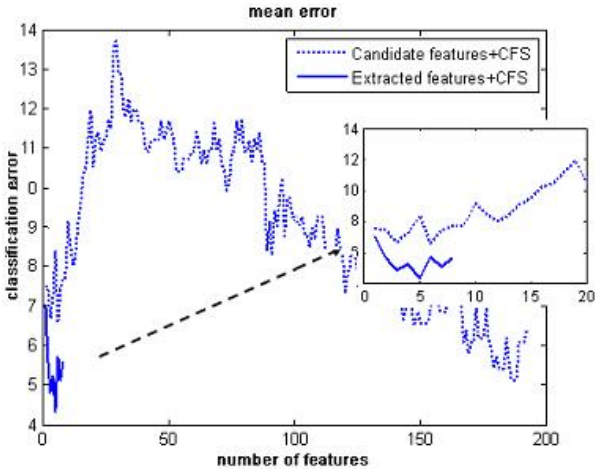

Figure 7.8: The classification error curves with the features selected from candidate and extracted features by CFS algorithm

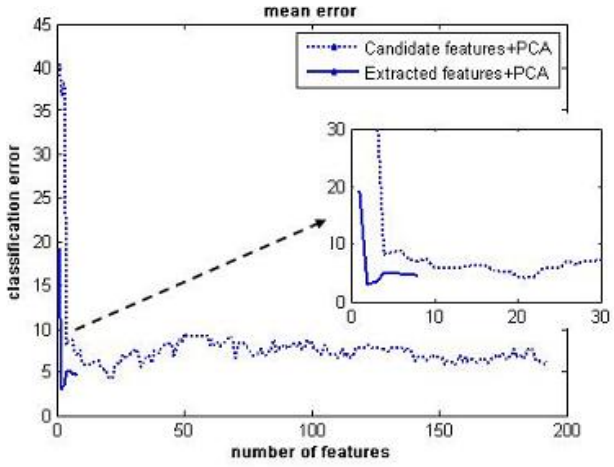

Figure 7.9: The classification error curves with the features selected from candidate and extracted features by PCA algorithm

7.2 Problem 2: Classification of *SRT_Afla+* and *SRT_Afla-* Hazelnuts

In this problem, the SRT hazelnuts are categorized by assigning the ones over 4 ppb aflatoxin concentration to SRT_Afla+ and the remaining ones to SRT_Afla- groups. The average aflatoxin level of 96 SRT_Afla+ and 189 SRT_Afla- group hazelnuts are 1883 ppb and 0.06 ppb respectively. Same procedure in the first classification problem (Section 7.1) was applied for the new data set. The spectral pruning in feature extraction step pruned the spectral bands of 420-430, 440-450 and 480-510 but kept the spectral bands of 400, 410, 460, 470 nm (Figure 7.10) ntact. The subbands in spatial-frequency axis of all spectral bands are completely pruned except the 420-430 nm spectral band.

The extracted features are then ranked by feature selection algorithms and used in linear classifier. The extracted feature map whose features are ranked by FFS and CFS algorithms are given in Figure 7.10. The darkness and the number on the nodes indicate the relevance of the features in those nodes.

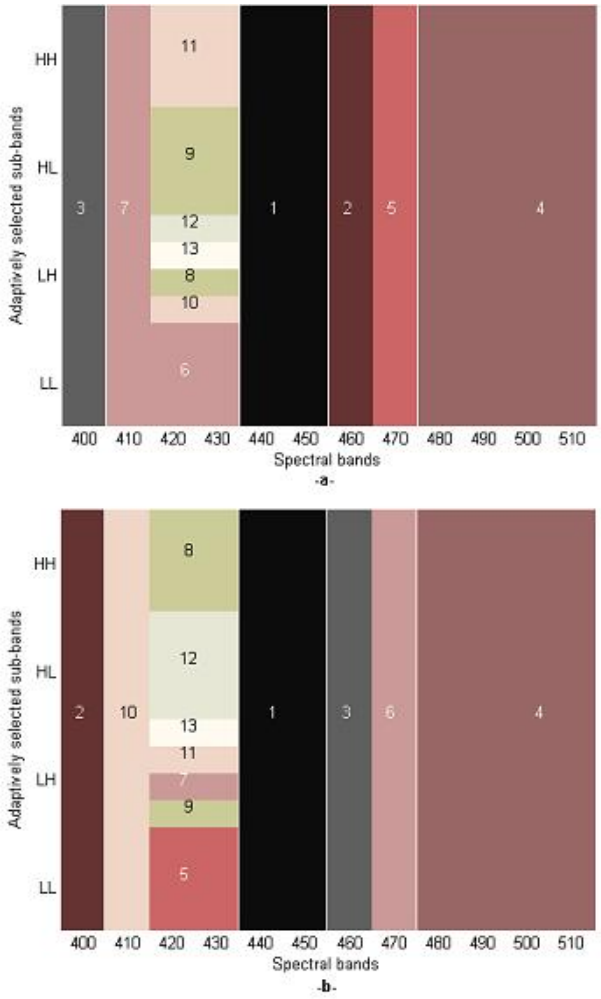

Figure 7.10: Spectral Spatial-Frequency feature map of SRT_Afla+ and 189 SRT_Afla- data which were ranked by a) by FFS, b) by CFS algorithm.

The selected features are fed into the linear classifier in four fold validation as in Problem 1. However, lower classification accuracies are obtained compared to the classification of SRT_Cont and SRT_UnCont classes. The minimum classification error is obtained with the 6 features by PCA; 3 features by wrapper and four features by CFS and FFS (Table 7.2, Figure 7.11). The spectral pruning in feature extraction step pruned the spectral bands of 420-430, 440-450 and 480-510 but kept the spectral bands of 400, 410, 460, 470 nm (Figure 7.10) for the new data set.

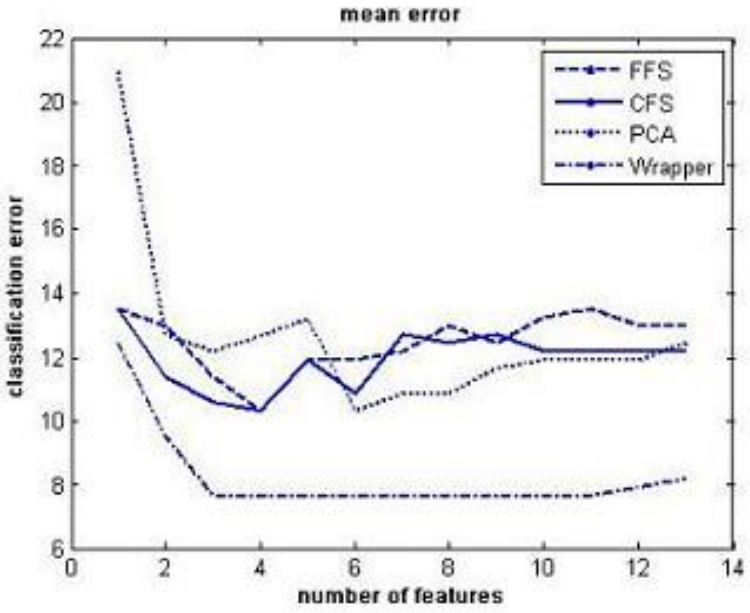

Figure 7.11: The classification error curves of SRT_Afla+ and SRT_Afla- data by FFS, CFS, PCA and Wrapper based selected features

Table 7.2: Minimum classification error obtained by four feature selection algorithms.

	FSS(4)	CFS(4)	PCA(6)	Wrapper(3)
Error(%)	10.34	10.34	10.34	7.69

The lowest error of 7,69% is achieved with three features selected by Wrapper model. When the classification results with 4 FFS ordered features are analyzed, it is observed that the algorithm misclassified 3 of the 96 SRT_Afla+ hazelnuts and 39 of the 189 SRT_Afla- hazelnuts. Two of the 3 misclassified SRT_Afla+ hazelnuts are from SRT_UnCont; the remaining misclassified kernel is from $SRT\_WaterCont$ group, originally. Whereas, 38 of the 39 misclassified SRT_Afla- hazelnuts are from $SRT\_WaterCont$, one of the 39 is from SRT_UnCont class, originally.

The effect of feature extraction step in the proposed algorithm can also be observed with SRT_Afla+ and SRT_Afla- data set with three different feature selection algorithms (Figure 7.12, 7.13 and 7.14). It is observed that better classification error curves are obtained with extracted (pruned) features than candidate features.

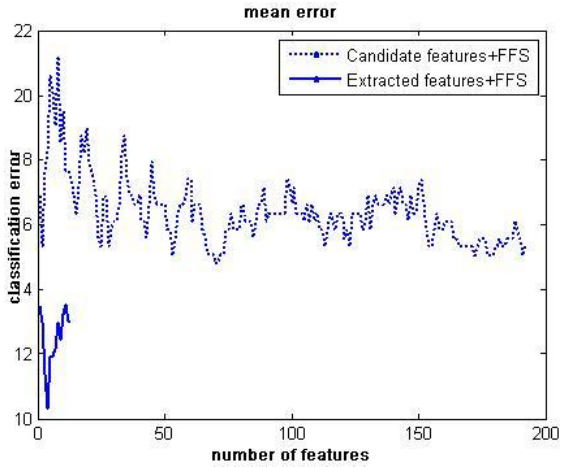

Figure 7.12: The classification error curves with the features selected from candidate and extracted features by FFS algorithm

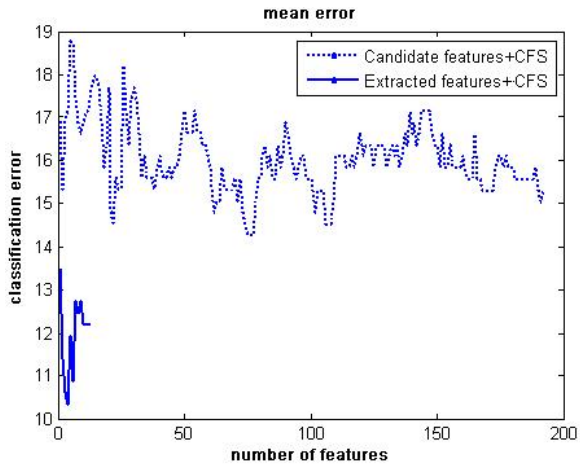

Figure 7.13: The classification error curves with the features selected from candidate and extracted features by CFS algorithm

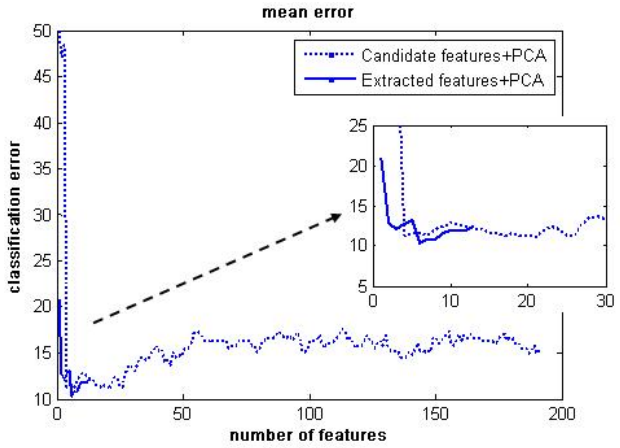

Figure 7.14: The classification error curves with the features selected from candidate and extracted features by PCA algorithm

The CFS based feature selection algorithm has similar performance compared to the FFS feature selection algorithm (Figure 7.6 and Figure 7.11). When the classification problems P1 and P2 of SRT hazelnuts are compared, better results are obtained in classifying SRT_Cont and SRT_UnCont kernels. The aflatoxin level of the SRT hazelnuts decreased to 0.7 ppb from 608 ppb by removal of the SRT_Cont hazelnuts and decreased to 0.84 ppb from 608 ppb by removal of the SRT_Afla+ hazelnuts. It is recommended to separate SRT_Cont kernels from hazelnut lots to decrease aflatoxin level because the contaminated kernels $SRT\_WaterCont$ are likely contain aflatoxin. These nuts are also not preferred by consumers because of bad taste and appearance.

7.3 Problem 3: Classification of SHD_Cont and SHD_UnCont Hazelnuts

In this problem, the Shelled hazelnuts,SHD category, are divided into mold contaminated SHD_Cont and uncontaminated SHD_UnCont groups wihtout considering the aflatoxin concentration. The average aflatoxin level of the 81 SHD_UnCont and 150 SHD_Cont group hazelnuts are 0.36 ppb and 938 ppb respectively. Same procedure in the first classification problem (Section 7.1) was

applied for the new data set. The hyperspsctral images of the SHD category hazelnuts are lower then the SRT category hazelnuts. In contrast to SRT hazelnuts, we used the spectral band images of 550nm and 600 nm because of their positive effects on classification results of SHD hazelnuts. Recall that these spectral bands have higher FWHM range compared to the other spectral bands between 400 nm and 510 nm. Moreover, in contrast to the SRT hazelnuts, the algorithm did not prune the subbands both in spectral and spatial-frequency axis. The pruning algorithm only pruned the spectral bands of 460 and 470 nm. However, the algorithm pruned the subbands in LL and HH region of spatial-frequency axis of images (Figure 7.15). Figure 7.15 also shows the extracted feature location obtained 2D pruning algorithm and the features that is ranked by FFS based feature selection algorithm. The CFS algorithm ranked the features similar to FFS algorithm in that they selected the same features for the first 10.

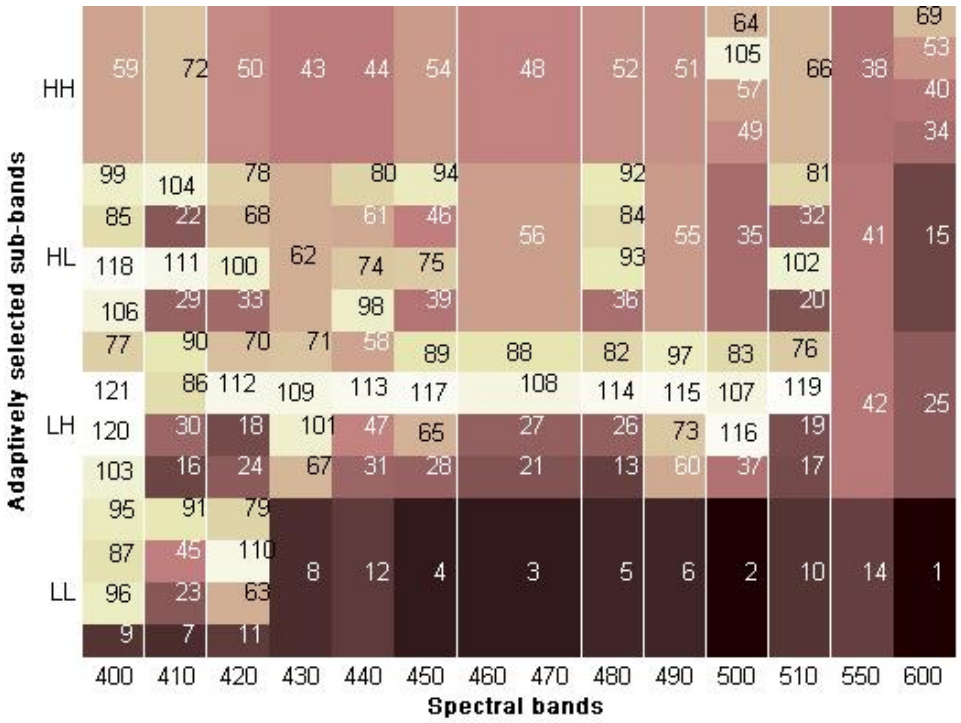

Figure 7.15: Spectral Spatial-Frequency feature map of *SHD_Cont* and *SHD_UnCont* data which were ranked by a) by FFS algorithm

Recall that the numbers and the color darkness on the map shows the order

of the selected features. It is observed that most discriminative feature is the LL subband of the spectral bands of 600 nm. When the classification results with the feeatures ranked by FFS, CFS and PCA algorithm are compared, high classification errors are obtained with the first a few features and the addition of new features marjinally effects the error (Figure 7.16).

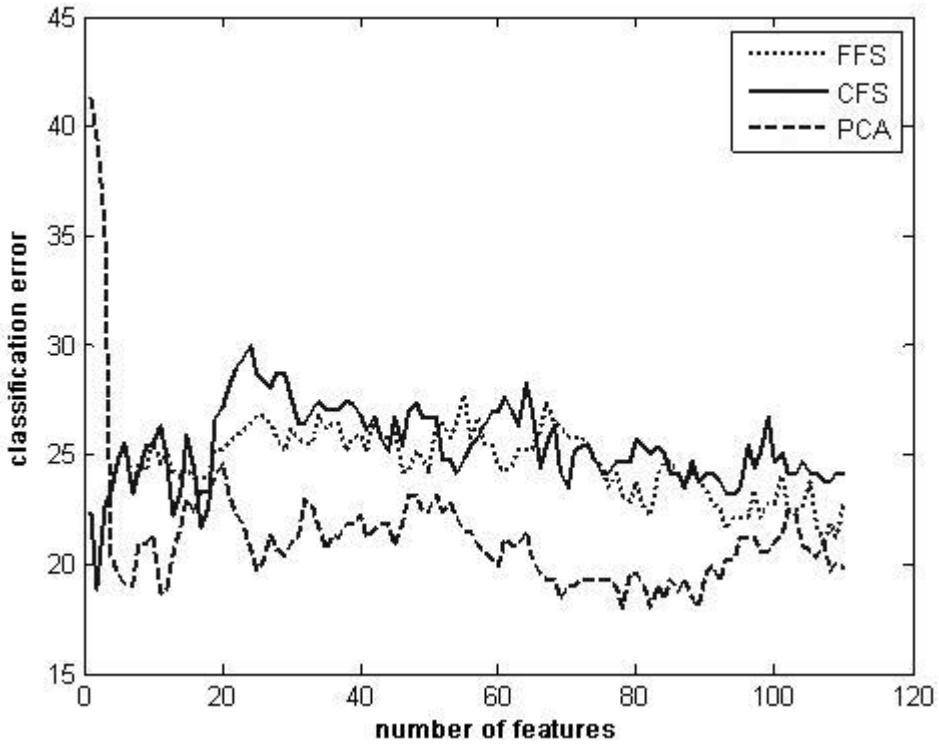

Figure 7.16: The classification error curves of SHD_Cont and SHD_UnCont data by FFS, CFS and PCA based selected features

The minimum classification error is obtained with the 78 PCA ranked; two wrapper, CFS and FFS ranked features (Table 7.3). The algorithm missclassified 10/81 SHD_UnCont and 37/150 SHD_Cont hazelnuts with FFS ranked features. However wrapper based selected features give better classification accuracy of 15.85% compared to other methods.

Table 7.3: Minimum classification error of SHD_Cont and SHD_UnCont data obtained by four feature selection algorithms. The number of features of methods giving the error is shown in brackets

	FSS(2)	CFS(2)	PCA(78)	Wrapper(2)
Error(%)	18.88	18.88	18.02	15.85

The effect of feature extraction step for classifying the SHD_Cont and SHD_UnCont data set with three different feature selection algorithms can be seen in Figures 7.17, 7.18 and 7.19. It is observed that better classification error curves are obtained with extracted (pruned) features than candidate features.

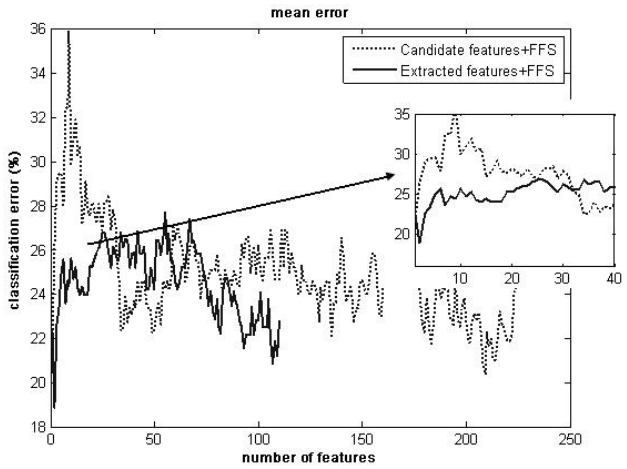

Figure 7.17: The classification error curves with the features selected from candidate and extracted features of SHD category hazelnuts by FFS algorithm

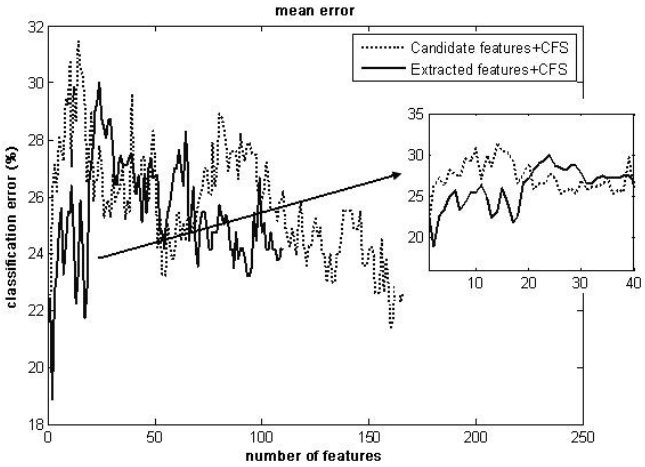

Figure 7.18: The classification error curves with the features selected from candidate and extracted features by of SHD category hazelnuts CFS algorithm

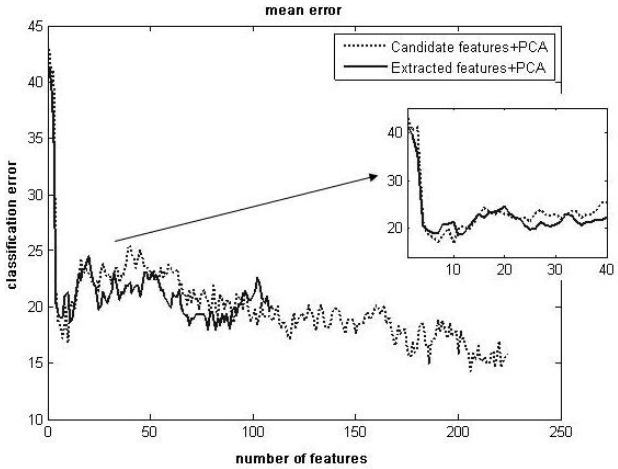

Figure 7.19: The classification error curves with the features selected from candidate and extracted features by of SHD category hazelnuts PCA algorithm

7.4 Problem 4: Classification of SHD_Afla+ and SHD_Afla- Hazelnuts

In this problem, the SHD hazelnuts are categorized by assigning the ones with 4 ppb aflatoxin concentration to SHD_Afla+ and the remaining ones to

SHD_Afla- groups. The average aflatoxin level of 53 SHD_Afla+ and 179 SHD_Afla- group hazelnuts are 3146 ppb and 0.05 ppb respectively. The algorithm pruned the spectral bands of 480 and 490 nm in spectral axis. Similarly, all the spatial-frequency subbands of the 450, 510 and 550 nm images are completely pruned(Figure 7.20). Figure 7.20 also shows the order of the features that are selected by FFS algorithm. As in stated before the algorithm does not make a comprehensive pruning to the low quality images (such as SHD hazelnut images). The most discriminative feature in the map is located in the spectral band of 510 nm.

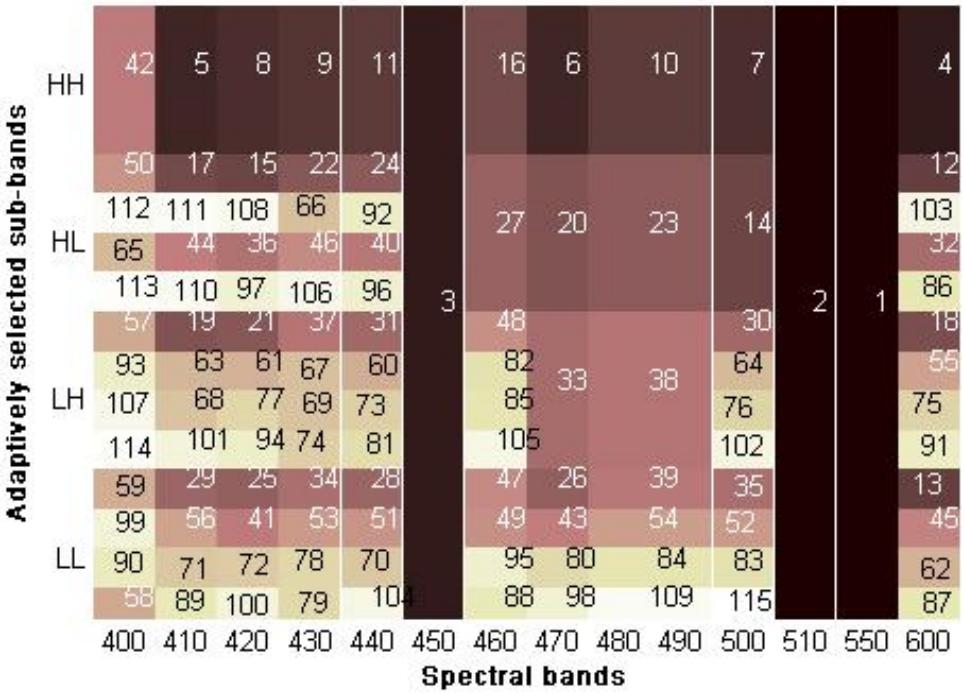

Figure 7.20: Spectral Spatial-Frequency feature map of SHD_Afla+ and SHD_Afla- data which were ranked by a) by FFS algorithm

The lowest classifiation error of 17% is obtained with the features that are selected by wrapper approach. The CFS and FFS algorithm results similar error curve which are worst then the curve obtained by PCA selected features(7.21). Minimum classification error for SHD_Afla+ and SHD_Afla- data set is obtained with 115 PCA ranked, 95 FFS ranked, 18 CFS ranked and two wrapper

ranked features (Table 7.4).

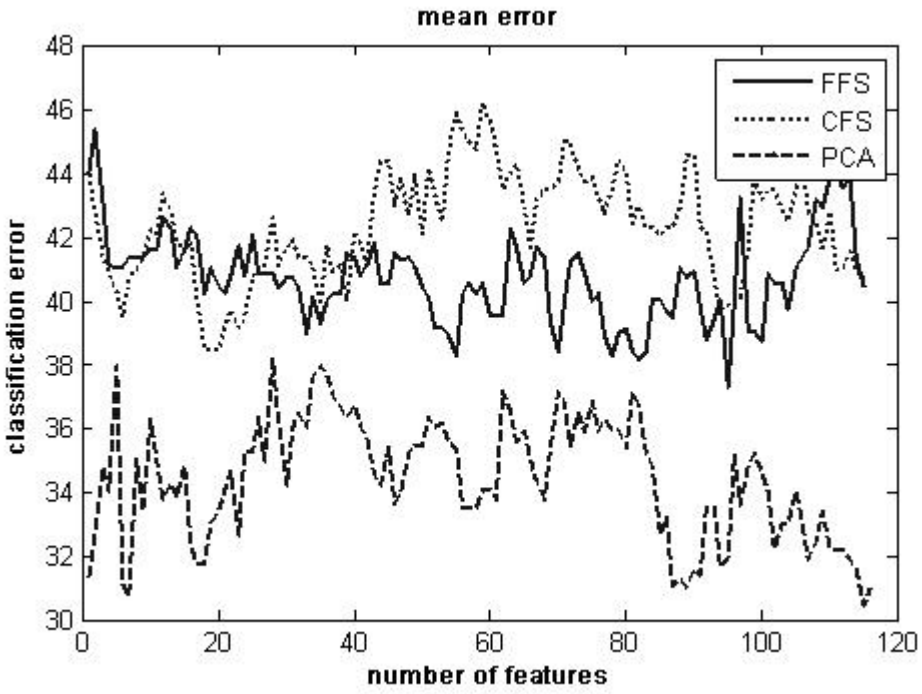

Figure 7.21: The classification error curves of SHD_Afla+ and SHD_Afla- data by FFS, CFS and PCA based selected features

Table 7.4: Minimum classification error of SHD_Afla+ and SHD_Afla- data obtained by four feature selection algorithms. The number of features of methods giving the error is shown in brackets

	FSS(95)	CFS(18)	PCA(115)	Wrapper(2)
Error(%)	37	38	30	17

The feature extraction step in the algorithm does not positively effects the performance of feature selection algorithm at classification of the SHD_Afla+ and SHD_Afla- hazelnuts (Figure 7.22, 7.23 and 7.24). This is thought to be from the low quality of images. The decrease in quality may suppress the possible discriminative features in the images.

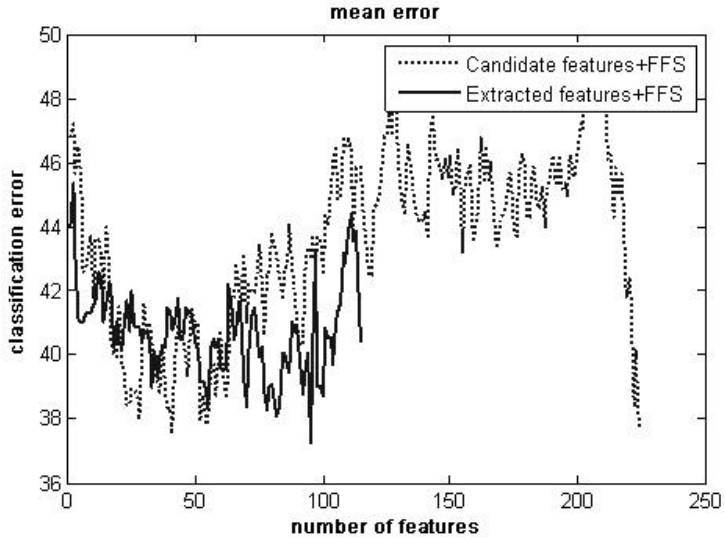

Figure 7.22: The classification error curves with the features selected from candidate and extracted features of SHD category hazelnuts by FFS algorithm

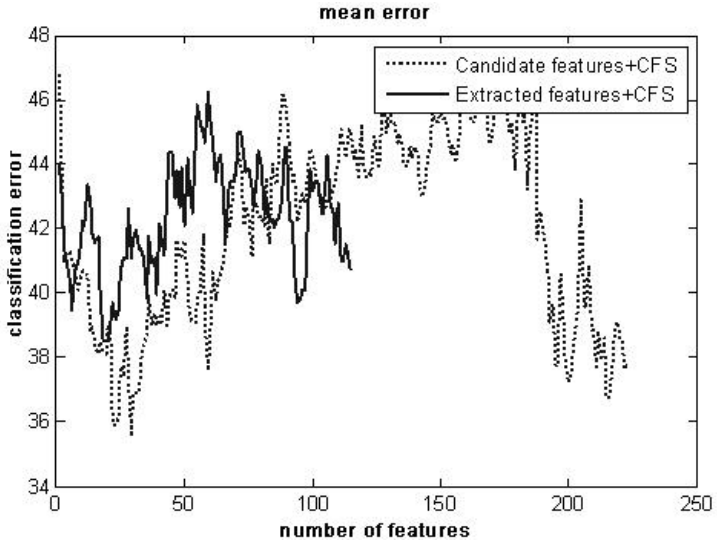

Figure 7.23: The classification error curves with the features selected from candidate and extracted features of SHD category hazelnuts by CFS algorithm

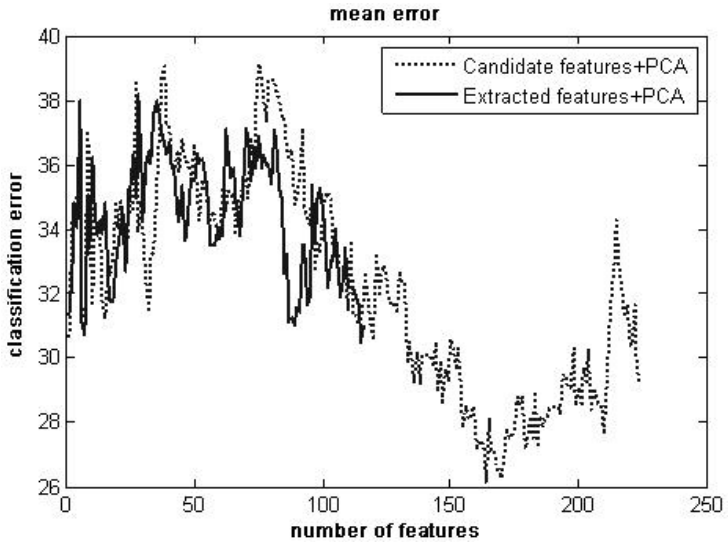

Figure 7.24: The classification error curves with the features selected from candidate and extracted features of SHD category hazelnuts by PCA algorithm

CHAPTER 8

Conclusions

In this thesis, an algorithm is develeoped to extract discriminative features from acoustic and hyperspectral data by using Local Discriminant Bases search. The original LDB algorithm is adapted to two dimensional searches to extract the most discriminant features in data. The feature extraction process decreases the feature dimension by both eliminating the irrelevant ones and/or by merging the ones that do not provide extra information on their own. Another dimension reduction is performed by selecting the extracted features by various feature selection algorithms. Our aim is to achieve high classification accuracy with fewer number of features. The number of extracted feature for mimimum error error is obtained by classification accuracy and a basic LDA classifier is used to get this accuracy. One can try other non-linear classifiers, like neural networks or Support Vector Machine, to achieve better classification accuracies with the extracted features.

The developed algorithm is implemented on both impact acoustic and hyperspectral data of hazelnut kernels for classification. This application is stemmed from the need of separating contaminated or potentially contaminated hazelnut kernels by non-invasive and fast methods that can perform real time in practical systems. The usage of fewer number of features with less amouth of data enables the production of low cost and high thoughput sorting systems.

We conducted an experimental study on detecting the effect of hazelnut shell on aflatoxin contamination and it observed that shell of hazelnut form a strong barrier against mold contamination. However, any damage on shell eliminates this capability. Therefore the hazelnuts with cracked shell should be separated from the regular shell hazelnut by using impact acoustic signal. The relevant features in acoustic signal are extracted by searching the local discriminant bases

first in time, then in frequency axis. The extracted features are then selected by feature selection algorithms and used in linear classifier. A classification accuracy of 96.5% is obtained with 64 LBD features. We observed that the most discriminative feature locations were concentrated in the high frequency bands corresponding to the early and post impact regions as indicated in Figure 6.3.The LDB based features give better classification accuracy compared to other types of features. In addition, the features obtained by feature extraction step positively effect the classification compared to candidate feature set. The developed algorithm can be implemented to real-time sorting devices due to its high throughput up to 25 nuts/sec. This limitation in throughput stemmed from the time required for each acoustic signal, not from the computation time.

Unlike to InH hazelnuts, the risk in SHD and SRT category hazelnuts can not be eliminated by impact acoustic. We used hyperspectral imaging for classification in shelled (SHD) and shelled&roasted (SRT) categories. Two different classification problems are defined for each category hazelnuts. The first problem is based on classifying contaminated (*Cont*) or uncontaminated (*UnCont*); second one is on classifying aflatoxin contaminated (*Afla+*) or aflatoxin free (*Afla-*) hazelnuts. The developed algorithm for hyperspectral images starts by obtaining a candidate feature set by generating two feature trees on spectral and spatial-frequency axis in order. The features trees are then pruned to get the most discriminative ones in spectral and spatial-frequency axis.

For the separation problem of *Cont* and *UnCont* group hazelnuts in SRT category, the candidate feature set of 192 dimensions is decreased to 12 by adaptive pruning in both axes. Four different feature selection algorithms are performed on extracted feature set to decrease the feature dimension if possible. A classification accuracy of 95.6% is achieved by the first five CFS or FFS ranked features. A better accuracy of 97.4% is achieved by the first four wrapper based ranked features. The most discriminant feature is defined as the LL subband of the spectral bands of 430 nm. For aflatoxin *Afla+* versus *Afla-* separation problem in the same category, the algorithm decreased to feature dimension from 192 to 14 in which the most discriminative one is the pruned form of the spectral bands of 440 and 450 nm. Relatively poor classification accuracies are obtained compared to

the first problem of this category. A classification accuracy of 89.66% is obtained by FFS, CFS and PCA ordered features. However, better accuracy of 92.31% is obtained by the first wrapper based ranked features. The extracted features positively affect the classification accuracies compared to candidate feature set. These can be observed from the Figures 7.7- 7.9 and Figures 7.12-7.14. The aflatoxin level of the SRT hazelnuts decreased to 0.7 ppb from 608 ppb by removal of the SRT Cont hazelnuts and decreased to 0.84 ppb from 608 ppb by removal of the *SRT_Afla+* hazelnuts. It is recommended to separate *SRT_Cont* kernels from hazelnut lots to decrease aflatoxin level because the contaminated kernels are high risk ones and these nuts are also not preferred by consumers because of bad taste and appearance.

The system does not produce good results for the SHD category hazelnuts as with the SRT category hazelnuts. As stated in Chapter 5, the hazelnuts in SHD category do not reflect sufficient light with existing hyperspectral imaging system under UV illumination even at high exposure times. Therefore, the images of SHD category hazelnuts are very low quality compared to SRT category hazelnuts. We included the images of the spectral bands at 550 and 600 nm to increase the information we have. For the *UnCont* and *Cont* group classification problem of SHD category hazelnuts, the feature extraction procedure did not decrease the feature dimension to reasonable levels. The most discriminative features are concentrated on LL region of spectral bands. Minimum classification accuracy of 18% is achieved with two FFS and CFS ordered features, whereas the same accuracy is obtained with 78 PCA ordered features. The lowest accuracy of 15.85 % is achieved with two wrapper based ranked features. The extracted features marginally decreased the error curves compared to candidate feature set (Figure 7.17-7.19). For the *SHD_Afla+* and *SHD_Afla-* classification problem, worse classification accuracies around 30% are achieved with CFS, FFS and PCA ranked features. The lowest classification accuracy 17% for *SHD_Afla+* and *SHD_Afla-* classification is achieved with two wrapper based selected features.

8.1 Future work

The limitations in this study originated from the hyperspectral imaging system with UV illumination. The existing illumination conditions are not suitable for SHD category hazelnuts. These nuts can be illuminated by light sources performing in IR, NIR or VIS region.

We used a rotating filter wheel to skip to other filters of same FWHM. The reflectance of a combined filter is estimated by combining the reflectance of individual filters. An electronically tunable filter with tunable FWHM may help taking more spectral images at any pass band region. This may help to identify the best spectral bands for any specific classification problem.

Final classification accuracy of the system is obtained with the selected features among the extracted feature set. The feature extraction procedure did not take the correlation between features in the data into account. The feature-feature correlation is considered in feature selection step. The feature selection and extraction algorithm may be combined to get most discriminant as well as independent features.

The developed algorithm is fast, robust and can be applied to real-time food grading and sorting systems by just using the identified filters for imaging.

The feature extraction algorithm can be applied to other hyperspectral data and we are also working on satellite images as well as other food items.

REFERENCES

[1] **Hsu, P.**, 2004. Feature Extraction of HyperSpectral Images Using Matching Pursuit, *Proceedings of the XXth ISPRS Congress, Istanbul*.

[2] **Landgrebe, D.A.**, 2003. Signal Theory Methods in Multispectral Remote Sensing, *John Wiley & Sons*.

[3] **Lee, C. and Landgrebe, D.**, 1993. Analyzing High-dimensional Multispectral Data, *IEEE Trans. Geoscience and Remote*, **31**, 792–800.

[4] **Jolliffe, I.**, 2002. Principal Component Analysis, second ed, *Springer*.

[5] **Jia, X. and Richards, J.**, 1999. Segmented Principal Components Transformation for Efficient Hyperspectral Remote-Sensing Image Display and Classification, *IEEE Trans Geoscience and Remote Sensing*, **37(1)**, 538–542.

[6] **Coifman, R. and Wickerhauser, M.V.**, 1992. Entropy-based Algorithms for Best Basis Selection, *IEEE Trans. Inform. Theory*, **38**, 713–719.

[7] **Saito, N. and Coifman, R.R.**, 1994. Local Discriminant Bases, in Mathematical Imaging: Wavelet Applications in Signal and Image Processing II, *Proceedings of the SPIE*, **2003**, 2–14.

[8] **Ince, N.**, **Tewfik, A. and Yagcioglu, S.**, 2005. Classification of Movement EEG With Local Discriminant Bases, *Proceedings of the IEEE ICASSP*.

[9] **Ince, N.**, **Arica, S. and Tewfik, A.**, 2006. Classification of Single Trial Motor Imagery EEG Recordings With Subject Adapted Non-dyadic Arbitrary Time-frequency Tilings, *J. Neural Eng*, **3**, 235–244.

[10] **Yang, H.**, **S.V.Vuuren and Hermansky, H.**, 1999. Relevance of Time-Frequency Features for Phonetic Classification Measured by Mutual Information, *Proceeding of IEEE ICASSP*.

[11] **Kumar, S.**, **Ghosh, J. and Crawford, M.**, 2001. Best-Bases Feature Extraction Algorithms for Classification of Hyperspectral Data, *IEEE Trans Geoscience and Remote Sensing*, **39**, 1368–1379.

[12] **Cheriyadat, A. and L.M.Bruce**, 2003. Why principal component analysis is not an appropriate feature extraction method for hyperspectral data, *Proceedings of the IEEE IGARSS*, **6**, 3420–3422.

[13] **C.R.Dichter**, 1984. Risk Estimates of Liver Cancer Due to Aflatoxin Exposure from Peanuts and Peanut Products, *Food Chemistry and Toxicology*, **22(6)**, 431–437.

[14] **Jimenez, L. and Landgrebe, D.**, 1999. Hyperspectral Data Analysis and Feature Reduction Via Projection Pursuit, *IEEE Transactions on Geoscience and Remote Sensing*, **37(6)**, 2653–2667.

[15] **Jain, A.**, **Duin, R. and Mao, J.**, 2000. Statistical Pattern Recognition: A Review, *IEEE Trans. Pattern Analysis and Machine Intelligence*, **22(1)**, 4–37.

[16] **Hall, M.A.**, 1998. Correlation-based Feature Selection for Machine Learning, *PhD Thesis, Hamilton, NZ: Waikato University, Department of Computer Science*.

[17] **Zhao, J.**, **Wang, G.**, **Wu, Z.**, **Tang, H. and Li, H.**, 2002. The Study on Technologies for Feature Selection, *Proceedings of the International Machine Learning and Cybernetics*.

[18] **L.Talavera**, 2005. An Evaluation of Filter and Wrapper Methods for Feature Selection in Categorical Clustering, *Lecture Notes in Computer Science, Springer Berlin / Heidelberg*, **3646**.

[19] **Peng, H.**, **Long, F. and Ding, C.**, 2005. Feature Selection Based on Mutual Information:Criteria of Max-Dependency, Max-Relevance, and Min-Redundancy, *IEEE Transactions on pattern analysis and machine intelligence,*, **27 (8)**, 1226–1238.

[20] **Ince, N.**, **Tewfik, A. and Arica, S.**, 2007. Extraction Subject-specific Motor Imagery Time-frequency Patterns for Single Trial EEG Classification, *Computers in Biology and Medicine*, **37(4)**, 499–508.

[21] **Saito, N.**, 2002. Discriminant Feature Extraction Using Empirical Probability Density and A Local Basis Library, *Pattern Recognition*, **35**, 1842–1852.

[22] **Coifman, R.R. and Donoho, D.**, 2002. Translation Invariant De-noising, Wavelets and Statistics, *Lecture Notes in Statistics, Springer-Verlag*, 125–150.

[23] **Gyaourova, A.**, **Kamath, C. and Fodor, I.**, 2002. Undecimated Wavelet Transforms for Image De-Noising, *LLNL technical report, UCRL-ID-150931.*

[24] **Stefanou, H.**, **Kakouros, S.**, **Cavouras, D. and M.Wallace**, 2005. Wavelet-based Mammographic Enhancement, *Proceedings of the 5th International Network Conference (INC).*

[25] **Figueiredo, M. and Nowak, R.**, 2007. An EM Algorithm for Wavelet-based Image Restoration, *IEEE Transaction on Image Processing*, **12(8)**.

[26] **Unser, M.**, 1995. Texture Classification and Segmentation Using Wavelet Frames, *IEEE Transactions on Image Processing*, **4(11)**.

[27] **Duda, R. and Hart, P.**, 1973. Pattern Classification and Scene Analysis, *John Wiley & Sons, Inc.*

[28] **Pearson, T.**, **Wicklow, D.**, **Maghirang, E.**, **Xie, F. and Dowell, F.**, 2001. Detecting Aflatoxin in Single Corn Kernels by Using Transmittance and Reflectance Spectroscopy, *Transactions of the ASAE*, **44(5)**, 1247–1254.

[29] **Hirano, S.**, **Okawara, N. and Narazaki, S.**, 1998. Near Infra Red Detection of Internally Moldy Nuts, *Bioscience, Biotechnology, and Biochemistry*, **62(1)**, 102–107.

[30] **T.W.Tayson and R.L.Clark**, 1974. An Investigation of Ilorescence Properties of The Aflatoxin -Infected Pecans, *Transactions of the ASAE*, **17**, 942–944.

[31] **Fersaie, A.**, **McClure, W.F. and Monroe, R.J.**, 1978. Development of Indices for Sorting Iranian Pistachio Nuts According to Fluorescence, *Journal of Food Science*, **43(5)**, 1550–1552.

[32] **Wicklow, D.**, 1999. Influence of Aspergillus Flavus Strains on Aflatoxin and Bright Greenish Yellow Fluorescence of Corn Kernels, *The American Phytopathological Society,Plant Disease*, **83(2)**.

[33] **Steiner, W.E.**, **Rieker, R.H. and Battaglia, R.**, 1988. aflatoxin Contamination in Dried Figs: Distribution and Association with Fluorescence, *J. Agric. Food Chem.*, **36(1)**.

[34] **Doster, M.A. and Michailides, T.J.**, 1998. Production of Bright Greenish Yellow Fluorescence in Figs Infected by Aspergillus Species in California Orchards, *The American Phytopathological Society, Plant disease*, **82(6)**.

[35] **Hadavi, E.**, 2005. Several Physical Properties of Aflatoxin-Contaminated Pistachio Nuts: Application of BGY Fluorescence for Separation of Aflatoxin-Contaminated Nuts, *Food Additives and Contaminants*, **22(11)**, 1144–1153.

[36] **Steiner, W.E.**, **Brunschweiler, K.**, **Leimbacher, E. and Schneider, R.**, 1992. Aflatoxins and Fluorescence in Brazil Nuts and Pistachio Nuts, *J. Agrlc. Food Chem.*, **40**, 2453–2457.

[37] **Bothast, R.J. and Hesseltine, C.W.**, 1975. Bright Greenish-Yellow Fluorescence and Aflatoxin in Agricultural Commodities, *Applied MICROBIOLOGY*, 337–338.

[38] **Jacks, T.**, 2005. Evaluation of Kojic Acid for Determining Heme and Non-heme Haloperoxidase Activities Spectrofluorometrically, *Analytical Letters*, **38**, 921–927.

[39] **Pearson, T.C.**, 1987. Separating Early Split From Normal Pistachio Nuts For Removal of Nuts Contamination On The Tree With Aflatoxin, *Ms Thesis, University of California*.

[40] **Pearson, T.C.**, 1996. Machine Vision System for Automated Detection of Stained Pistachio Nuts, *Lebensm.-Wiss. u.-Technol.*, **29**, 203–209.

[41] **Pearson, T.C. and Schatzki, T.F.**, 1998. Machine Vision system for Automated Detection of Aflatoxin-Contaminated Pistachios, *Journal of Agric. Food Chem.*, **46**, 2248–2252.

[42] **Kalkan, H.**, **Yardimci, Y.**, **Ince, F.**, **Tewfik, A.**, **Senyuva, H.**, **Arici, M.**, **Pearson, T.**, **Cetin, E. and Onaran, I.**, 2007. Separation of Damaged Shell Hazelnut by Impact Acoustics, *XII International IUPAC Symposium on Mycotoxins and Phycotoxins, Istanbul*.

[43] **Cetin, A.**, **Pearson, T. and Tewfik, A.**, 2004. Classification of Closed-And Open- Shell Pistachio Nuts Using Voice-Recognition Technology, *Transaction of the ASAE*, **47(2)**, 659–664.

[44] **Onaran, I.**, **Dulek, B.**, **Pearson, T.**, **Yardimci, Y. and Cetin, E.**, 2005. Detection of Empty Hazelnuts From Fully Developed Nuts by Impact Acoustics, *13th EUSIPCO, Antalya*.

[45] **Kalkan, H. and Yardimci, Y.**, 2006. Classification Of Hazelnut Kernels By Impact Acoustics, *IEEE MLSP, Dublin*.

[46] **Taylor, S.K. and McCure, W.F.**, 1989. Measuring the Distribution of Chemical Components, *Proceedings of the Second International NIR Conference,Tsukuba, Japan*, 393–404.

[47] **Zeringue, H. and Shih, B.**, 1998. Extraction and Separation of the Bright-Greenish-Yellow Fluorescent Material from Aflatoxigenic Aspergillus spp. Infected Cotton Lint by HPLC-UV/FL, *Agric. Food Chem.*, **46(3)**, 1071–1075.

[48] **Park, B.**, **Chen, Y.R. and Nguyen, M.**, 1998. Multi-spectral Image Analaysis Using Neural Network Algorithm for Inspection of Poultry Carcasses, *Journal of Agricultural Engineering*, **69**, 351–363.

[49] **Park, B.**, **Lawrance, K.C.**, **Windham, W.R. and Smith, D.P.**, 2002. Multi-Spectral Imaging System for Fecal and Ingesta Detection on Poultry Carcasses, *J. Food Proc. Engr.*, **27(5)**, 311–327.

[50] **Mehl, P.M.**, **Chen, Y.R.**, **Kim, M.S. and Chan, D.E.**, 2004. Development of Hyperspectral Imaging Technique for the Detection of Apple Surface Defects and Contaminations, *Journal of Food Engineering*, **61**, 67–81.

[51] **Dharwarkar, G.**, 2005. Using Temporal Evidence and Fusion of Time-Frequency Features for Brain- Computer Interfacing, *Ms Thesis, Waterloo, Ontario, Canada*.

[52] **Saito, N. and Coifman, R.R.**, 1994. Local discriminant bases, *Mathematical Imaging: Wavelet Applications in Signal and Image Processing II Proc. of SPIE*, **2303**, 2–14.

[53] **Wickerhauser, M.**, 1994. Adapted Wavelet Analysis from Theory to Software, *Massachusetts: A.K. Peters*.

CURRICULUM VITAE

Habil Kalkan was born in Erzincan in 1979. He graduated from Ege University, Department of Electrical and Electronics Engineering in 2002. He received his M.S. degree from METU, Informatics Institute in 2005. He has started to his PhD education in Informatics Institute in 2005 and he has worked as a visiting researcher at University of Minnesota, Department of Electrical Engineering and Kansas, USDA-ARS-GMPRC in 2006. Since 2002, he has been working as research assistant in METU. His current research interests are in the field of signal and image processing, pattern recognition and machine learning.

IDENTIFICATION OF DAMAGED WHEAT KERNELS AND CRACKED-SHELL HAZELNUTS WITH IMPACT ACOUSTICS TIME-FREQUENCY PATTERNS

N. F. Ince, I. Onaran, T. Pearson, A. H. Tewfik, A. E. Cetin, H. Kalkan, Y. Yardimci

ABSTRACT. *A new adaptive time-frequency (t-f) analysis and classification procedure is applied to impact acoustic signals for detecting hazelnuts with cracked shells and three types of damaged wheat kernels. Kernels were dropped onto a steel plate, and the resulting impact acoustic signals were recorded with a PC-based data acquisition system. These signals were segmented with a flexible local discriminant bases (F-LDB) procedure in the time-frequency plane to extract discriminative patterns between damaged and undamaged food kernels. The F-LDB procedure requires no prior knowledge of the relevant time or frequency indices of the impact acoustics signals for classification. The method automatically finds all crucial time-frequency indices from the training data by combining local cosine packet analysis and a frequency axis clustering approach, which supports individual time and frequency band adaptation. Discriminant features are extracted from the adaptively segmented acoustic signal, sorted according to a Fisher class separability criterion, post-processed by principal component analysis, and fed to a linear discriminant classifier. Experimental results establish the superior performance of the proposed approach when compared to prior techniques reported in the literature or used in the field. The new approach separated damaged wheat kernels (IDK, pupal, and scab) from undamaged wheat kernels with 96%, 82%, and 94% accuracy, respectively. It also separated cracked-shell hazelnuts from those with undamaged shells with 97.1% accuracy. The adaptation capability of the algorithm to the time-frequency patterns of signals makes it a universal method for food kernel inspection that can resist the impact acoustic variability between different kernel and damage types.*

Keywords. *Adaptive time-frequency analysis, Food kernel inspection, Impact acoustics, Kernel classification.*

Food kernel damage caused by insects, fungi, and mold is a major source of quality degradation. For instance, *Fusarium graminearum*, a fungus found in wheat, creates "scab" damage and may lead to toxins known to cause cancer (Christensen and Meronuck, 1986). Internal insect infestation degrades the quality and value of wheat and is one of the most difficult kernel defects to detect. This type of kernel damage occurs when an adult female insect chews a small hole in the kernel, deposits an egg, and then seals the egg with a mixture of mucus. The egg plug is the same color as the wheat surface, so it is nearly impossible to detect by visual inspection. When the egg hatches, the insect larvae feeds on the kernel endosperm and then exits the kernel by chewing an exit tunnel and forming what is called an "insect-damaged kernel" (IDK). Insect infestations cause grain loss by consumption, nutritional losses, and degradation in the end-use quality of flour (Pederson, 1992). Separation of damaged from undamaged wheat kernels is crucial for quality and proper grading of wheat loads. Therefore, the percentage of insect-damaged kernels in the production/market is controlled by the USDA and industry standards. For example, in the U.S., U.S. No. 1 to U.S. No. 5 grades only allow up to 31 damaged wheat samples per 100 g. Damaged samples exceeding this number are graded as U.S. Sample grade (USDA, 2008).

A similar problem occurs in hazelnut production. Environmental conditions and processing procedures may decrease nut quality by causing cracks on the shell. Damage to the shell of the nut kernel increases the likelihood of fungi infecting the kernels, since the mold spores have unabated access to the kernel. Fungal infestation can cause aflatoxin formation, which is a type of mycotoxin that is linked to various health problems including liver cancer (Dichter, 1984). Therefore, it is crucial to detect hazelnuts with damaged shells and separate them from undamaged nuts.

In this study, two important food inspection problems are addressed using a novel adaptive time frequency segmentation technique:

- Detection of damaged wheat kernels.
- Detection of hazelnuts with cracked shell.

Submitted for review in May 2007 as manuscript number IET 7006; approved for publication by the Information & Electrical Technologies Division of ASABE in August 2008. Presented at the 2007 ASABE Annual Meeting as Paper No. 074152.

The authors are **Nuri F. Ince,** Post-Doctoral Associate, Department of Electrical and Computer Engineering, University of Minnesota, Minneapolis, Minnesota; **Ibrahim Onaran,** Research Assistant and Doctoral Student, Department of Electrical and Electronics Engineering, Bilkent University, Ankara, Turkey; **Tom C. Pearson, ASABE Member Engineer,** Agricultural Engineer, USDA Agricultural Research Service, Manhattan, Kansas; **Ahmed H. Tewfik,** Professor, Department of Electrical and Computer Engineering, University of Minnesota, Minneapolis, Minnesota; **A. Enis Cetin,** Professor, Department of Electrical and Electronics Engineering, Bilkent University, Ankara, Turkey; **Habil Kalkan,** Research Assistant, Doctoral Student, and **Yasemin Yardimci,** Professor, Informatics Institute, Middle East Technical University, Ankara, Turkey. **Corresponding author:** Nuri F. Ince, Department of Electrical and Computer Engineering, 4-147C EE/CSCI Building, 200 Union St. SE, University of Minnesota, Minneapolis, MN 55455; phone: 612-625-5006; fax: 612-625-4583; e-mail: firat@umn.edu.

Impact Acoustics for Food Inspection

Because the proportion of damaged kernels is small compared to the total number of undamaged wheat kernels, a low false positive error rate (identification of an undamaged kernel as damaged) is crucial for an economically feasible detection system. Several methods have been studied to tackle the problem of detecting insect-damaged wheat kernels, including x-ray imaging (Karunakkaran et al., 2003), NIR spectroscopy (Maghirang et al., 2003; Dowell et al., 1998), and carbon dioxide measurements (Bruce et al,. 1982). However, these methods are slow, expensive, and do not provide the required accuracy in classification. Hence, these types of wheat kernel inspection methods have not found widespread application in industry.

In hazelnut production, farmers separate the empty hazelnuts from fully developed ones before selling the nuts. A mechanical device using an air fan is utilized for this purpose. The air fan removes immature or empty hazelnuts with lower weight, and the remaining hazelnuts are accepted as fully developed. This system is unable to remove the nuts with cracked shells because hazelnuts with cracked shells have weights and densities that are very similar to hazelnuts with undamaged shells.

The drawback of these methods of wheat and hazelnut inspection led researchers to explore new techniques. Recently, impact acoustic emission has been proposed to separate pistachios with closed shells from those with split shells (Pearson, 2001). In this system, as depicted in figure 1, the nuts are projected onto a steel plate and the resulting acoustic signals are analyzed. With this method, the classification accuracy was approximately 97% with a throughput of 40 nuts per second. This same strategy was applied to wheat inspection, and successful results were obtained for detection of IDK from undamaged kernels (Pearson et al., 2005). Although the mechanical structure was similar, Pearson et al. (2005) reported that the signal features used for pistachio classification, such as the integrated absolute value of microphone output signal and the gradient of the signal at manually selected time intervals, did not work well in wheat inspection. They improved the system by including a combination of time and frequency domain features individually. To be more specific, variances and maximum values extracted from short time windows were used as time features. In addition, signal modeling was performed with a three-step transformation. As an initial step, the signal was rectified by computing its absolute value at all time points. Then a non-linear filter replaced the center data point with the maximum value in a seven-point window. Finally, a non-linear estimation of the four parameters of the Weibull function was implemented. These parameters were used as features for classification. The frequency domain features were: the frequency index corresponding to the peak DFT magnitude of the signal, 30 normalized DFT magnitudes centered about the peak DFT, the entire set of 128 DFT magnitudes, and the 32 magnitudes of the differential spectrum. The reader is referred to Pearson et al. (2005) for details. Although these feature combinations provided good results for IDK separation, the authors also reported poor results on other types of kernel damage, such as scab and infested kernels at the pupal stage, where the insect was still inside the kernel. The same impact acoustics based system was also recently extended to separate cracked hazelnut shells from undamaged ones (Kalkan and Yardimci, 2006) and immature hazelnuts from fully developed hazelnuts (Onaran et al., 2006). Specifically, Kalkan and Yardimci (2006) reported a classification accuracy of 91.8% in cracked and healthy hazelnut shell separation by using the energy in the frequency subbands of impact acoustics.

The results of Pearson et al. (2005), Kalkan and Yardimci (2006), and Onaran et al. (2006) emphasized the importance of signal processing methods for the impact acoustic signal to achieve higher accuracies in food kernel inspection. These improvements were obtained by extracting frequency and time domain features separately. Generally, a subset of these

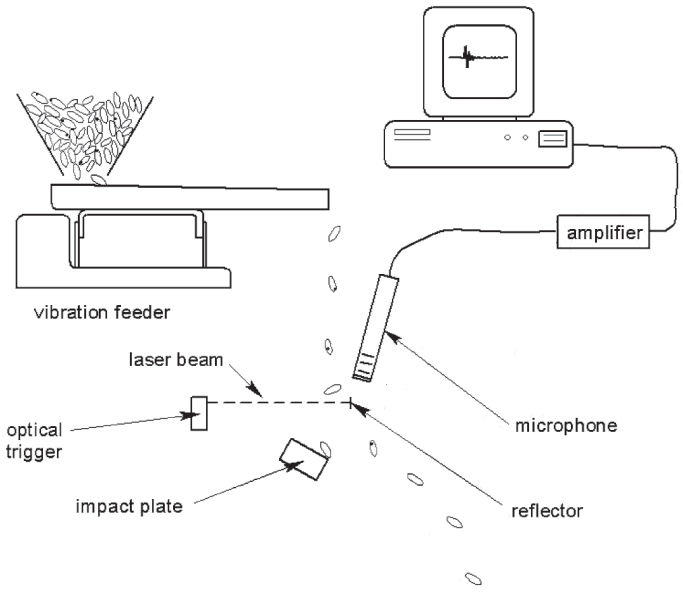

Figure 1. Schematic of food kernel sorter based on acoustic emissions. This system was used for sorting pistachios and wheat kernels by Pearson (2001) and Pearson et al. (2005).

features was selected using traditional stepwise discriminant analysis for classification. In the presence of variability of acoustic waveforms due to different kernel damages, it is cumbersome to extract relevant features and adapt them to changing conditions.

The objective of this study was to investigate a detection method for cracked hazelnuts and wheat kernel damage based on an adaptive time-frequency (t-f) analysis of the impact acoustic signals emitted by wheat kernels or hazelnut shells when dropped from a fixed height onto a steel plate. The proposed approach requires no prior knowledge of the relevant time or frequency indices of the impact acoustics signals. It implements an arbitrary time and frequency tiling with a flexible local discriminant bases algorithm (Ince et al., 2006) to find the most relevant indices automatically. This algorithm is obtained by combining local cosine packet (LCP) analysis (Mallat, 1999; Wickerhauser, 1994) with a frequency axis clustering approach that supports individual time and frequency band adaptation. The time and frequency segmentation steps produce too many features. Furthermore, these features are generally correlated. Therefore, the adaptively extracted t-f features are processed by principal component analysis to reduce the number of features and combine correlated features. Finally, the PCA post-processed feature set was classified with linear discriminant analysis.

Material and Methods

A schematic diagram describing the overall signal processing and classification system is shown in figure 2. As indicated previously, the time-frequency features extracted from impact acoustic signals are used for the identification of damaged wheat kernels and hazelnuts with cracked shells. The time-frequency features are computed by windowing the acoustic signal in adapted time segments and then applying a spectral analysis to estimate the frequency spectrum. After computing the features, they are sorted with Fisher's discriminative criterion to select the most parsimonious ones and post-processed by PCA. Finally, linear discriminant analysis is used to identify damaged food kernel acoustics. The next sections provide a detailed description of the data acquisition system used to record the impact acoustics and perform the signal processing steps.

Impact Acoustics Data Acquisition

The same experimental setup of Pearson et al. (2005) was used to record the impact acoustics. A schematic of the experimental apparatus for singling wheat kernels and hazelnuts, which consisted of dropping the nuts/kernels onto the impact plate and then collecting the acoustic signals from the impact, is shown in figure 1. A vibration feeder (F-TO-C, FMC-Syntron, Homer City, Pa.) was used to transform the wheat kernels into a single-file stream, which consisted of a vibrating bulk hopper and a V-shaped steel trough. The wheat kernels were impacted onto a polished stainless steel plate with dimensions of approximately $75 \times 50 \times 100$ mm. The drop distance from the feeder to the impact plate was 400 mm, and the plate was inclined at 30° above the horizontal. This angle was determined by trial and error in order to prevent bounces. Flatter angles of incline produced a stronger signal, but the kernels tended to bounce twice before falling off of the plate. This was not conducive to high-speed sorting.

A microphone (4939 L with 2669 L pre-amp, Bruel and Kjaer North America, Norcross, Ga.), sensitive to frequencies up to 100 kHz, was used to capture audible and ultrasonic acoustic emissions from the impact of the wheat kernels with the steel plate. The end of the microphone was placed 25 mm from the point where kernels impacted the plate. The microphone output was further amplified (2690 NEXAS, Bruel and Kjaer North America, Norcross, Ga.) at 1 V/Pa to ensure that the system had the required dynamic range to capture the acoustic emissions. Microphone signals were digitized using a sound card (Waveterminal 192X, Ego Sys, Seoul, South Korea) at a sampling frequency of 192 kHz with 16-bit resolution. This sound card does not have the 20 kHz low-pass filter that most consumer sound cards use. The data acquisition was triggered using an optical sensor (QS30LLPC, Banner Engineering Corp., Minneapolis, Minn.). In the wheat kernel experiment, 600 undamaged (UD), 600 IDK, 600 pupal, and 400 scab kernels were used.

To evaluate the performance of the proposed algorithm in discrimination of cracked shell hazelnuts from undamaged ones, the dataset of Kalkan and Yardimci (2006) was used. A setup similar to that used for the wheat experiment was constructed to record the hazelnut impact acoustic signals with undamaged and cracked shells. A stainless steel plate with dimensions of $75 \times 150 \times 20$ mm was used as the impact plate. The impact plate was fixed to the ground at a 120° angle to prevent nuts from making multiple impacts. A microphone (AT9100, Audio-Technica U.S., Inc., Stow, Ohio), sensitive to frequencies up to 20 kHz, was placed 50 mm from the impact plate. The impact acoustic signal was sampled at 44.1 kHz with a standard sound card attached to the computer. 'Levant' type hazelnuts, which were collected from an orchard in Akcakoca, Turkey, in August 2003, were used in this study. The weights of the hazelnuts were measured, and those less than 0.9 g were taken as empty or undeveloped nuts. Hazelnuts with weights over 0.9 g were accepted as fully developed. This value was found empirically by inspecting the weight of several empty, underdeveloped, and fully developed hazelnuts. The hazelnut shells were visually inspected and were further

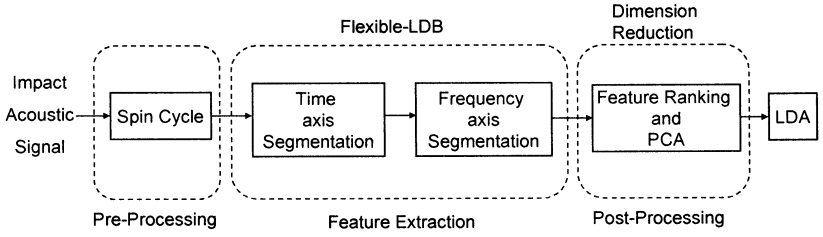

Figure 2. Block diagram of the proposed signal processing and classification system.

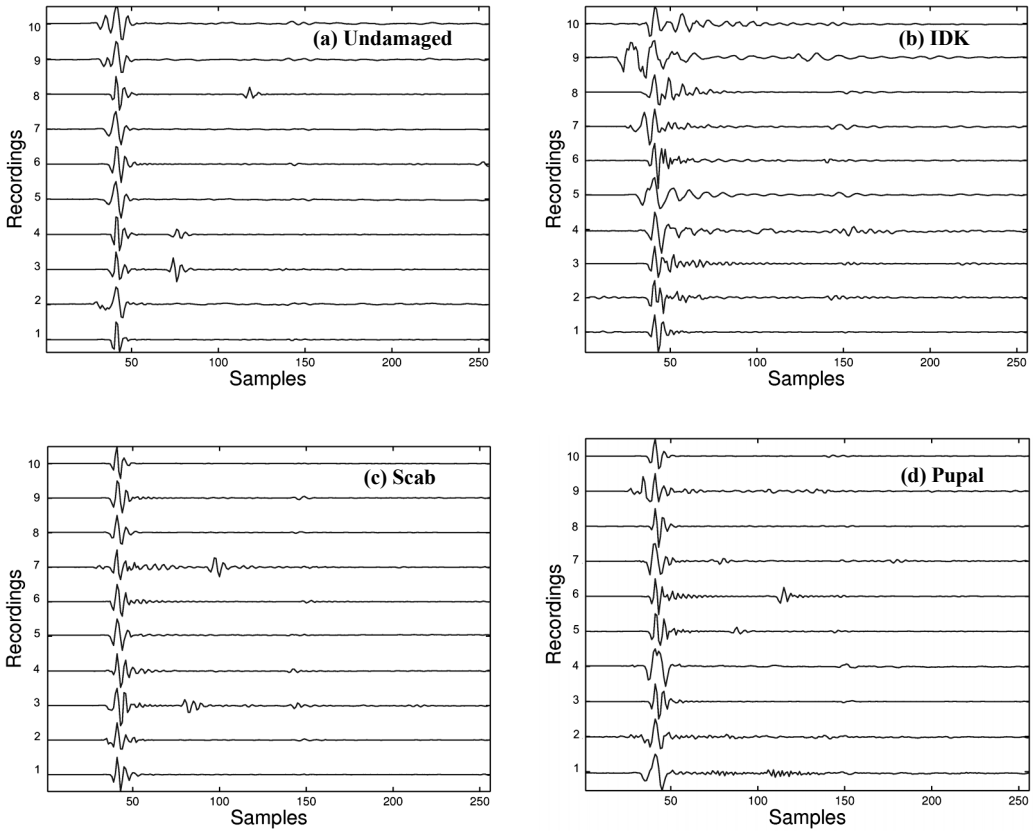

Figure 3. Sample waveforms of wheat kernel impact acoustics for the types studied in this article (N = 10): (a) undamaged kernels, (b) insect-damaged kernels (IDK) with exit holes, (c) fungi damage (scab), and (d) kernels with hidden damage at the pupal stage where the insect is still in the kernel.

classified into nuts with regular shell and nuts with cracked shell. For each undamaged and cracked class, 180 signals were recorded. Representative impact acoustic signals of wheat and hazelnut kernels recorded with these systems are presented in figures 3 and 4, respectively.

Signal Processing

Transient features in a signal may carry significant information for classification. Such features are sometimes omitted due to their low energy or improper analysis that ignores temporal information. As shown in figures 3 and 4, the impact acoustic signals also contain transient waveforms that may carry information for discrimination. In order to extract such localized information, time-frequency methods are widely used (Mallat, 1999; Vetterli, 2001). A time-frequency analysis explores the time-varying characteristic of a signal by windowing it in consecutive time segments, generally overlapping, and then applying a spectral analysis to estimate energy distribution of the signal in the frequency domain. The width of the time window determines the resolution of the spectral analysis. While longer windows provide higher spectral resolution, they provide poor time localization, vice versa. Therefore, it is desirable to adjust the time windows to adapt to the time-varying characteristic of the signal. In this study, the flexible local discriminant bases (F-LDB) algorithm of Ince

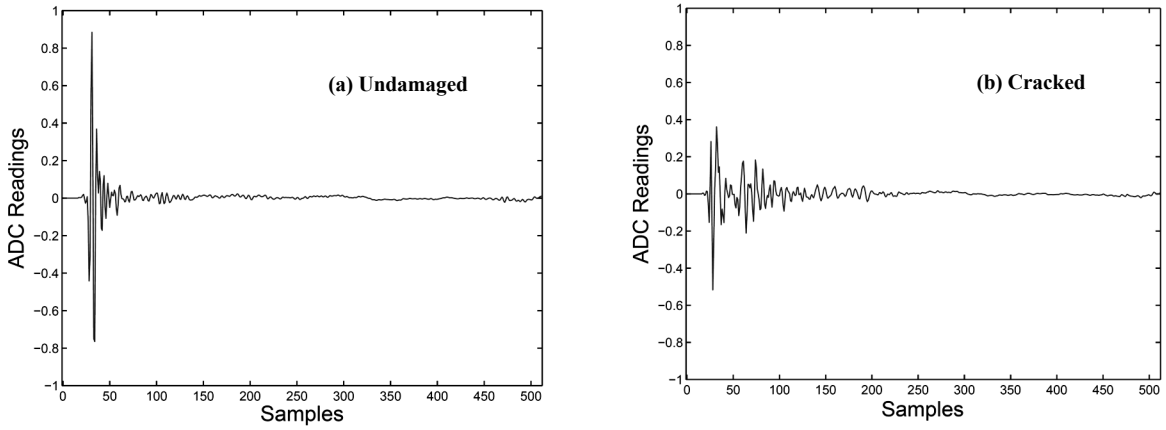

Figure 4. Typical (a) undamaged and (b) cracked shell hazelnut acoustics records.

et al. (2006) was used to adaptively segment the time-frequency plane and extract relevant features from the impact acoustic signal for classification. The adaptive time-frequency plane feature extraction procedures and pre- and post-processing steps are discussed below.

Adaptive Time-Frequency Segmentation

The F-LDB algorithm expands the signal into orthonormal bases using cosine packets, a local trigonometric transform, in consecutive time segments, and finds those segments with a merge/divide strategy, where the distance between the spectra of different classes is maximum. This iterative procedure adjusts the width of time windows to increase the distance between signals. Once the signals are segmented along the time axis, they are represented by local cosine transform. In the next step, the merge/divide strategy is repeated along the frequency axis to group consequent discriminative frequency indices. Here, consecutive frequency indices were merged only if their union had larger discrimination power than that of the individual indices treated separately. The procedure described above is basically a clustering approach by cost function maximiza–tion and produces adaptive frequency segmentation suitable for discrimination in each time segment. The reader is referred to Ince et al. (2006) for detailed description of the algorithm.

Although the acoustic recordings were triggered with optical sensors, temporal variability exists in the observed signals due to different travel time of the food kernels from the feeder to the impact plate. Since the cosine packet transform is not shift invariant, this temporal variability may cause variance in the extracted features for classification. For instance, small shifts of the signal in the time axis cause abrupt changes in local cosine packet coefficients. In order to deal with this problem, the ”spin cycle” procedure of Ince et al. (2006) and Saito et al. (2002) was applied to the training and test data, as indicated in figure 2, prior to the time and frequency segmentation step. The spin cycle procedure generates several copies of a signal by shifting it to the left and right for a number of given samples. In this study, a one-sample spin cycle procedure was implemented, and as a result three copies of each record were created: the original signal, and one-sample left and right shifted copies of it. This expands the dataset with several instances of each record to simulate the temporal variability in the time axis. Each of these records is processed separately by the time-frequency analysis method for feature extraction and used in the final classification. By using this procedure, the overall algorithm becomes more robust against the temporal variability in the recorded signals. The reader is referred to Saito et al. (2002) and Ince et al. (2006) for further details.

There are various choices for distance measures to be used in constructing the time segmentation. This study used the Euclidean distance between the cumulative probability distributions of each expansion coefficient under class 1 and class 2, respectively, estimated via a histogram.

Dimension Reduction and Classification

Once the t-f segmentation was completed, the Fisher class separability criterion was used for sorting the features:

$$F = \frac{(\mu_1 - \mu_2)^2}{\sigma_1^2 + \sigma_2^2} \quad (1)$$

where μ and σ are the mean and standard deviation, respectively, of the feature they correspond to. This step is referred to as class separability criterion based sorting (CS). This enabled us to filter out features that have small discrimination power and use those with higher discrimination information for the final decision.

Although the CS step eliminates most of the irrelevant features, there is still need to compact the top rank of the feature set to remove the correlations between features and reduce the dimensionality. As a last step, principal component analysis (PCA) was implemented on the top discriminant feature set returned from the CS step. The PCA-processed top feature set was input to a linear discriminant analysis (LDA) function.

Since the one-sample spin cycle procedure was used in the pre-processing stage, there were three multiple instances of a particular signal, i.e., shifted to the left and right by one sample along with the original recording with no shifts. In the classification stage, these multiple instances of the signal were classified separately, and a majority voter scheme was implemented for the final decision. For example, when an impact signal was recorded, it was first shifted by one sample to the left and one sample to the right. Then, for each of these instances, the features were calculated for the learned t-f segments and fed to the classifier. Finally, a majority voter post-processed the classification outputs for all shifts. The majority voter simply counted the classification outputs (votes) for each shift for a particular signal and assigned the signal to the class with the maximum number of votes.

As indicated in the previous sections, the F-LDB procedure creates t-f segmentation for two-class problems. Since there are four classes (UD vs. IDK, pupal, and scab) in the wheat kernel inspection problem, the following strategy was used:

- All damaged wheat kernel types are classified versus UD in a single step.
- Each damaged wheat kernel type is classified versus UD in a pairwise manner.

The impact acoustic signals corresponding to wheat kernels (UD, IDK, scab, and pupal) were 1024 samples long, while those corresponding to cracked and healthy hazelnut shells were 960 samples long. The minimum window size used for the time axis segmentation with the F-LDB procedure was selected to be 16 samples for wheat and 32 samples for hazelnuts. After a visual inspection, it was observed that the impact acoustics patterns for wheat records have very short living transients compared to hazelnut records (figs. 3 and 4). Therefore, shorter windows were selected in the analysis of wheat signals. The smooth overlapping part of the windows was set to half of the minimum window size. A one-sample spin cycle procedure was used before processing the signals. After completing the time-frequency segmentation with F-LDB, the features were converted to log scale, normalized, and sorted by the F criterion. The top 128 features were processed by PCA and sorted according to the corresponding eigenvalues in descending order. A 2×2-fold cross-validation was implemented to estimate the classification error. First, the dataset was randomly distributed. Half of the record set was used in the training stage to find most the discriminant t-f features, PCA and LDA weights. The remaining set was used to test the performance of the learned parameters. This

experiment was repeated twice. In order to compare the efficiency of the proposed algorithm, the features used by Pearson et al. (2005) were also extracted and referred to as the reference approach (RA). These features were extracted from the short time variances of signal segments, maximum signal amplitudes, spectral peak locations, and the parameters of a Weibull function approximation of the envelope of the impact signal parameters. The same features were used in the wheat and hazelnut experiments for comparison purposes.

In order to asses the efficiency of extraction time-frequency features with adaptive tilings in the classification of impact acoustic signals, experiments with fixed time-frequency tilings were conducted. In particular, the time-frequency features were computed by segmenting the signals into fixed-width time windows (W) with 32 or 64 sample lengths and then calculating 4 or 8 subband (SB) features in each time window with equal bandwidth. The extracted feature set was post-processed with PCA and fed to LDA for final decision, as in the previous experiments.

Results and Discussion

Wheat Classification

Table 1 shows the classification results when undamaged (UD) wheat kernels were classified against all IDK, scab, and pupal damaged kernels with a one-against-all strategy. In particular, single time-frequency plane segmentation and a single LDA classifier were constructed to discriminate between undamaged and all damaged wheat kernels. The algorithm yielded high accuracy for IDK (95.9%) and scab types (91.2%). However, it resulted in poor classification accuracy (61%) for pupal damaged kernels. Based on these results, time-frequency segmentations and classifiers were designed to discriminate between undamaged kernels vs. IDK, undamaged kernels vs. scab, and undamaged kernels vs. pupal. In this scheme, the final classification can be done in a cascaded classification strategy. In particular, a new observed acoustic signal can be tested for IDK damage, then scab damage, and finally for pupal damage.

As indicated previously, paired discrimination is recognized as a one-against-other classification strategy (Hastie et al., 2001; Alpaydin, 2004). The results of using such a technique are presented in table 2. The pairwise approach provided improvements in classification of pupal damaged kernels. In particular, using the paired classification strategy, the classification accuracy rate for pupal damaged kernel improved from 62% to 81%. Note that the classification accuracies of undamaged and scab types are slightly higher in the paired classification strategy. Also note that time-frequency plane feature extraction and the classification algorithm outperformed the reference approach (RA), especially for the scab and pupal damaged kernels. The paired classifier using adaptively segmented time-frequency plane features significantly outperformed the RA in all UD vs. IDK, UD vs. scab, and UD vs. pupal discriminations ($p = 2.3 \times 10^{-7}$, $p = 2.7 \times 10^{-8}$, $p = 8.5 \times 10^{-7}$, t-test, respectively).

The results discussed above suggest that the pupal class has features distinct from the IDK and scab classes. To understand why the F-LDB approach yields better results than the RA approach with the paired classification technique, the scab and pupal damaged data were studied in more detail. Consider the time-frequency locations/features selected by the F-LDB method shown in figure 5 for UD vs. scab and UD vs. pupal kernel classification. Interestingly, the moment of impact where maximum signal amplitude was observed and several time-frequency locations on the tail of the signal were selected by the algorithm. These post-impact features appeared to be the most discriminative features and resulted in a lower error rate. It is possible that the features on the tail of the signal might be related to the vibration of the metal plate or turbulence in the air. Note that different time-frequency segmentations were constructed in the impact and post-impact regions. The time windows were quite short in the early impact region, while wider windows and narrow frequency indices were selected in the post-impact region. Furthermore, the time-frequency maps partly explain the degradation in performance in the one-against-all classification strategy. As seen in figures 5a and 5b, the time-frequency locations selected for pupal and scab damaged kernels are different. A rapid transition from lower to higher bands in scab features was observed. Contrary to pupal kernel discrimination, mostly higher bands were utilized by the algorithm. The capability of the algorithm to adjust the time-frequency segmentations for a given damage type can be critical for obtaining good results. Also note that, for both scab and pupal kernel classification, post-processing with PCA resulted in lower error rates, as indicated in figures 5c and 5d. Recall that the CS ordered features are post-processed with PCA for dimension reduction and decorrelation of the top rank. This final signal processing step slightly improved the final classification accuracy.

These results indicate that using the one-against-other strategy provides higher recognition accuracies for damaged wheat kernels. To preserve the high classification accuracy for all types, a cascaded discrimination strategy, as indicated in figure 6a, could therefore be used in practice. The cascaded classification engine integrates three paired classifiers (UD vs. IDK, UD vs. scab, and UD vs. pupal). Specifically, when a new impact acoustic signal is observed, the system first tests for IDK damage. If the system decides that no IDK damage is present, it tests for scab damage. If no scab damage is detected, it finally checks for pupal damage. In the current system, the least accurate classifier is the one that detects pupal damaged kernels. A receiver operating characteristic (ROC) curve for the UD vs. pupal damaged classifier is plotted in figure 6b. The current operating point is shown with a solid arrow. In order to improve the true positive rate to 95%, a high false positive rate (dashed arrow) must be tolerated as well.

Table 1. Classification accuracies obtained with F-LDB in separating undamaged kernels (UD) from damaged kernels in a single step.

	UD	IDK	Scab	Pupal
F-LDB	90%	95.9%	91.2%	61%

Table 2. Classification accuracies obtained with F-LDB and reference approach (RA) in separating undamaged kernels (UD) from damaged kernels. The results belong to paired classifications.

	UD vs. IDK	UD vs. Scab	UD vs. Pupal
F-LDB	96% to 95.7%	93.9% to 96.9%	84% to 81.2%
RA	92% to 82.3%	68.4% to 66.3%	69.8% to 66.5%

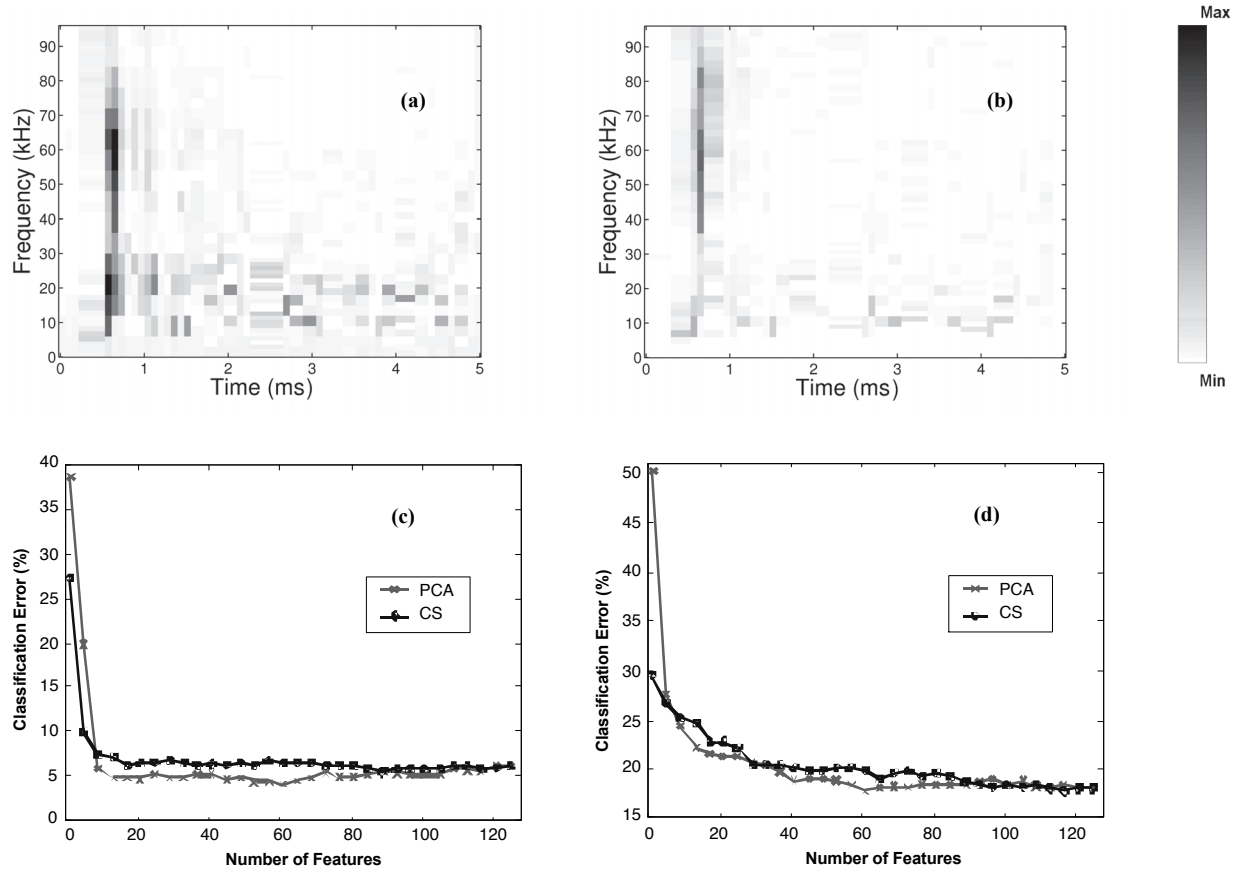

Figure 5. The t-f features selected for (a) UD vs. scab and (b) UD vs. pupal classification. The darker features have more discrimination power. Both graphs are visualized with the same scale to emphasize the difference in the discrimination power of extracted features. The bottom row shows the classification error versus the number of features that were sorted by a class separability criteria (CS = F) and PCA. The error curves belong to (c) UD vs. scab and (d) UD vs. pupal. Note the lower error rates for PCA with a smaller number of features.

Hazelnut Classification

The proposed system achieved 97.1% classification accuracy in separating the undamaged hazelnut shells from cracked shells. In particular, the undamaged and cracked shell hazelnuts were recognized with 99.2% and 95% accuracies, respectively. A classification accuracy of 91.8% was reported by Kalkan and Yardimci (2006) on this same dataset by manually selecting the most discriminative subbands and using their energies for classification. These results suggest that adaptively segmented time-frequency plane features significantly outperformed the results of Kalkan and Yardimci (2006) ($p = 0.0061$, t-test). The discriminant time-frequency features selected by the algorithm are shown in figure 7a. This figure indicates that the most discriminant features are located in high-frequency bands following impact. Kalkan and Yardimci (2006) also

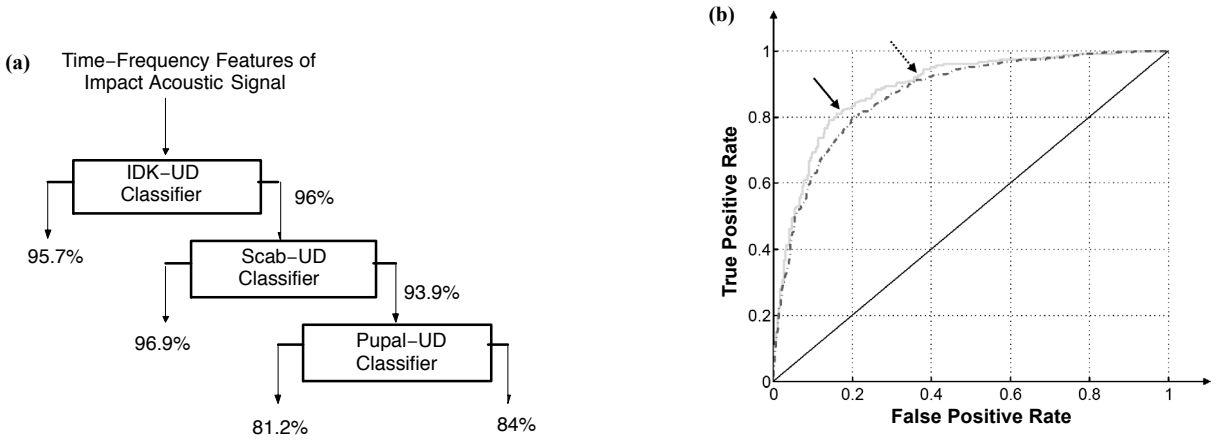

Figure 6. (a) Cascaded classification strategy and (b) ROC curve of UD vs. pupal classifier output. The solid curve was obtained with the spin cycle procedure, and the dashed curve was obtained without the spin cycle. Note that improving the classification accuracy above 90% involves higher false positive rates. Note also that the spin cycle preprocessed classifier has higher accuracy.

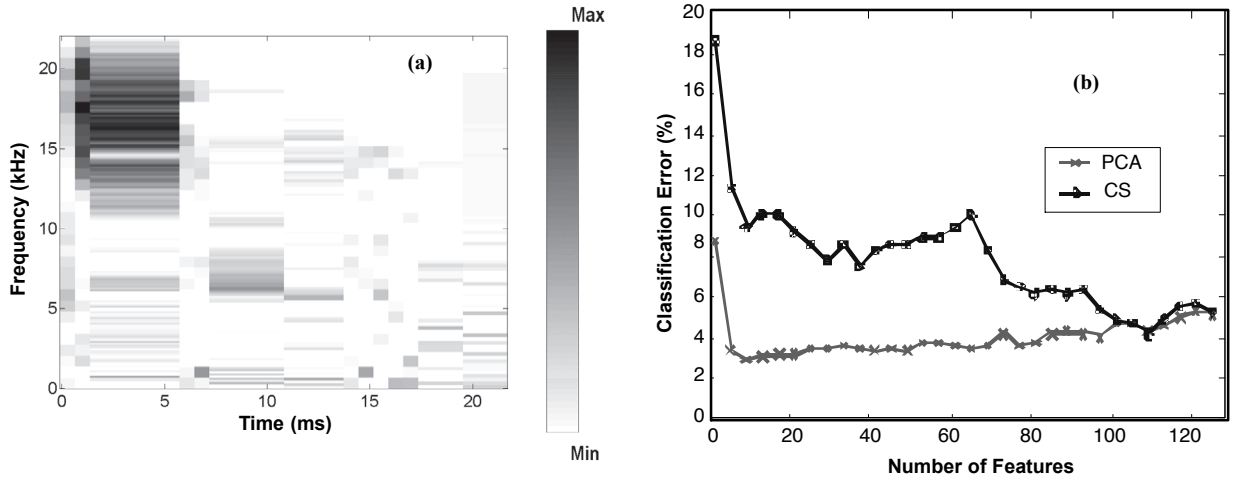

Figure 7. (a)The t-f features selected for separation of cracked hazelnuts from undamaged nuts. The darker features have more discrimination power. Note that the higher frequency band is primarily selected by the algorithm. (b) The classification error curve obtained with and without PCA post-processing. Note that PCA provides lower error rates with a minimal number of features.

reported higher bands as crucial frequency indices after manually inspecting several subbands with wavelet transform. The algorithm proposed in this article learned these indices automatically from the data.

As in the wheat classification results, the PCA post-processing step improved the classification accuracies. In figure 7b, the classification error curves versus the number of features for PCA and CS are given. Here, the use of PCA improved the classification accuracy from 96% to 97.1% with a small number of features. This shows the importance of post-processing the t-f features sorted by the F criterion, which does not account for the correlation or interaction between extracted features.

Experiment with Fixed Resolution Features

Table 3 shows the classification results for wheat and hazelnuts computed using time-frequency features with fixed resolution. Note that the classification accuracies obtained with fixed resolution were quite poor for wheat kernel classification. For hazelnut classification, the fixed resolution results were slightly lower than adaptive arbitrary tilings. In general, an improvement in classification accuracies was observed when shorter time windows were utilized in wheat kernel classification. Interestingly, it has been observed that the undamaged kernels were better discriminated when longer windows were used in UD vs. scab kernel discrimination. When shorter windows (32 samples) were used with eight subbands, the undamaged kernel recognition accuracy dropped to 82.4% from 87.6%. In contrast, the scab kernel recognition accuracy was improved from 75.5% to 79.1%. Similar results were observed for pupal kernel classification. When the number of subbands increased from 4 to 8 with 32 sample long time windows, the undamaged kernel recognition accuracy dropped from 76.4% to 74.7%. In contrast, the pupal kernel recognition accuracy slightly increased.

For the hazelnuts, the classification accuracies obtained with arbitrary and fixed time-frequency tilings were similar. The arbitrary tilings provided slightly better results (97.1%) than fixed tilings (96.5%). Note that the adaptive time-frequency plane tilings for hazelnuts were not as complex as for wheat kernels (figs. 6 and 7). Therefore, nearly the same discriminant information can be captured with fixed tilings. Note also that larger windows provided better results, and the number of subbands did not have much effect on the recognition accuracy.

The results obtained indicate that different kernels can be discriminated with distinct time-frequency segmentations. Furthermore, when the segmentations are adapted to the problem, the classification accuracies dramatically increase.

Computational Complexity

The t-f segmentation steps are completed off-line. After learning the most discriminative segments in an off-line manner, it is only necessary to process the impact acoustics data at the selected time-frequency locations in real time. The processing includes calculating the expansion coefficients in the learned time segments, merging the coefficients in the frequency domain, projecting the resulting features onto the principal components, and feeding the results into LDA.

The spin cycle procedure, which is used to eliminate the lack of translation invariance of local cosine packets, adds additional complexity to the proposed system, since it entails estimating the expansion coefficients for several shifts of the

Table 3. Classification accuracies obtained with fixed resolution time-frequency patterns for wheat kernels and hazelnuts (W = length of time windows in number of samples, and SB = number of subbands computed in each time windows).

	Wheat			Hazelnut
	UD - IDK	UD - Scab	UD - Pupal	UD - Cracked
W = 64, SB = 4	87.2% - 83.0%	73.4% - 67.5%	71.2% - 72.6%	98.7% - 93.1%
W = 64, SB = 8	88.2% - 87.1%	87.6% - 75.5%	74.4% - 73.8%	98.9% - 93.6%
W = 32, SB = 4	90.9% - 86.5%	76.9% - 73.5%.	76.4% - 74.0%	97.8% - 93.1%
W = 32, SB = 8	89.5% - 89.5%	82.4% - 79.1%	74.7% - 74.5%	98.9% - 92.3%

recorded data. For real-time applications, the average of expansion coefficients for consecutive shifts might be used instead. Another solution could be using transformations that satisfy the translation invariance condition. Although the system can classify wheat samples with higher accuracies, the need to recalculate features in the paired hierarchical classification strategy can be a drawback. This may boost the computations required by the system, resulting in lower processing speeds. In order to evaluate the processing speed of the proposed approach, the speed of the algorithm was tested on a desktop PC equipped with 1.8 GHz processor and 512 MB of memory. Processing of a single wheat sample took approximately 0.027 s. This corresponds to a processing speed of nearly 37 samples per second on the top node of the classification system. Since at least three steps are required for UD wheat kernel recognition, they cannot be processed with a speed of more than 12 kernels per second. The processing speed for hazelnuts was 77 kernels per second. Since the classification was implemented in a single step and minimal error was achieved with small number of features, the processing speed was quite fast for cracked hazelnut separation.

Conclusion

In this article, an adaptive time-frequency plane feature extraction and classification technique to discriminate between damaged and undamaged food kernels by analyzing related impact acoustics signals was investigated. In particular, the study focused on the problems of detecting damaged wheat kernels and hazelnuts with cracked shells. The procedure requires no prior knowledge of the relevant time-frequency indices of the impact acoustics signals for classification. The method automatically learns all crucial time-frequency indices from the training data by implementing individual time and frequency band adaptation. Discriminant features were extracted from the adaptively segmented acoustic signal, sorted according to a Fisher class separability criterion, post-processed by principal component analysis, and fed to linear discriminant classifier for final decision. The approach achieved classification accuracies in paired separation of undamaged wheat kernels from insect-damaged kernels with exit holes, kernels with hidden damage at the pupal stage, and scab damaged kernels of 96%, 82%, and 94%, respectively. For the cracked shell vs. undamaged hazelnut separation, the overall accuracy was 97.1%. The results indicate that adaptive time-frequency features extracted from impact acoustic signals provide improved accuracies in damaged food kernel inspection when compared to baseline methods, which used features from the time or frequency domain with fixed resolution. The adaptation capability of the algorithm to both the time and frequency content of signals makes it a universal method for food kernel inspection that can resist the impact acoustic variability between different kernels and damage types, even though in certain cases it may have a relatively high computational complexity.

Acknowledgment

This work was supported by the scientific and technological research council of Turkey (TUBITAK) under the grant 106E057.

References

Alpaydin E. 2004. *Introduction to Machine Learning*. Cambridge, Mass.: MIT Press.

Bruce, W. A., W. M. Street, R. C. Semper, and D. Fulk. 1982. Detection of hidden insect infestations in wheat by infrared carbon dioxide gas analysis. ARS Bulletin AAT□S-26. Washington, D.C.: USDA-ARS.

Christensen, C. M., and R. A. Meronuck. 1986. *Quality Maintenance in Stored Grains and Seeds.* Minneapolis, Minn.: University of Minnesota Press.

Dichter, C. R. 1984. Risk estimates of liver cancer due to aflatoxin exposure from peanuts and peanut products. *Food Chemistry and Toxicology.* 22(6): 431-437.

Dowell, F. E., J. E. Throne, and J. E. Baker. 1998. Automated nondestructive detection of internal insect infestation of wheat kernels by using near-infrared reflectance spectroscopy. *J. Econ. Entomol.* 91(4): 899-904.

Hastie, T., R. Tibshirani, and J. Friedman. 2001. *The Elements of Statistical Learning*. New York, N.Y.: Springer.

Ince, N. F., S. Arica, and A. H. Tewfik. 2006. Classification of single trial motor imagery EEG recordings by using subject adapted non-dyadic arbitrary time-frequency tilings. *J. Neural Eng*. 3(3): 235-244.

Kalkan, H., and Y. Yardimci. 2006. Classification of hazelnuts by impact acoustics. In *Proc. IEEE Machine Learning for Signal Processing Congress.* Piscataway, N.J.: IEEE.

Karunakkaran, C., D. S. Jayas, and N. D. G. White. 2003. Soft x-ray inspection of wheat kernels infested by *Sitophilusoryzae. Trans. ASAE* 46(3): 739-745.

Maghirang, E. B., F. E. Dowell, J. E. Baker, and J. E. Throne. 2003. Automated detection of single wheat kernels containing live or dead insects using near-infrared reflectance spectroscopy. *Trans. ASAE* 46(4): 1277-1282.

Mallat, S. 1999. *A Wavelet Tour of Signal Processing.* 2nd ed. San Diego, Cal.: Academic Press.

Onaran, I., T. C. Pearson, Y. Yardimci, and A. E. Cetin. 2006. Detection of underdeveloped hazelnuts from fully developed nuts by impact acoustics. *Trans. ASABE* 49(6): 1971-1976.

Pearson, T. C. 2001. Detection of pistachio nuts with closed shells using impact acoustics. *Applied Eng. in Agric.* 17(2): 249-253.

Pearson T., A. E. Cetin, A. H. Tewfik, and R. P. Haff. 2005. Feasibility of impact-acoustic emissions for detection of damaged wheat kernels. *Digital Signal Proc*. 17(3): 617-633.

Pederson, J. 1992. Insects: Identification, damage, and detection. In *Storage of Cereal Grains and Their Products.* D. B. Sauer, ed. St. Paul, Minn.: American Association of Cereal Chemists.

Saito, N., R. R. Coifman, F. B. Geshwind, and F. Warner. 2002. Discriminant feature extraction using empirical probability density and a local basis library. *Pattern Recog.* 35(12): 1842-1852.

USDA. 2008. Official U.S. standards for grain. Washington, D.C.: USDA-GIPSA. Available at: www.gipsa.usda.gov/GIPSA/webapp?area=home&subject=grpi&topic=sq-ous.

Vetterli, M. 2001. Wavelets, approximation, and compression. *IEEE Signal Proc. Magazine* (Sept.): 59-73.

Wickerhauser, M. V. 1994. *Adapted Wavelet Analysis from Theory to Software*. Wellesley, Mass.: A.K. Peters.

Hindawi Publishing Corporation
EURASIP Journal on Advances in Signal Processing
Volume 2008, Article ID 247643, 11 pages
doi:10.1155/2008/247643

Research Article

Classification of Hazelnut Kernels by Using Impact Acoustic Time-Frequency Patterns

Habil Kalkan,[1] Nuri Firat Ince,[2] Ahmed H. Tewfik,[2] Yasemin Yardimci,[1] and Tom Pearson[3]

[1] *Informatics Institute, Middle East Technical University, 06531 Ankara, Turkey*
[2] *Department of Electrical and Computer Engineering, University of Minnesota, MN 55455, USA*
[3] *Agricultural Research Service, United States Department of Agriculture, KS 66502, USA*

Correspondence should be addressed to Yasemin Yardimci, yardimy@ii.metu.edu.tr

Received 17 January 2007; Revised 7 July 2007; Accepted 8 October 2007

Recommended by Hugo Van hamme

Hazelnuts with damaged or cracked shells are more prone to infection with aflatoxin producing molds (*Aspergillus flavus*). These molds can cause cancer. In this study, we introduce a new approach that separates damaged/cracked hazelnut kernels from good ones by using time-frequency features obtained from impact acoustic signals. The proposed technique requires no prior knowledge of the relevant time and frequency locations. In an offline step, the algorithm adaptively segments impact signals from a training data set in time using local cosine packet analysis and a Kullback-Leibler criterion to assess the discrimination power of different segmentations. In each resulting time segment, the signal is further decomposed into subbands using an undecimated wavelet transform. The most discriminative subbands are selected according to the Euclidean distance between the cumulative probability distributions of the corresponding subband coefficients. The most discriminative subbands are fed into a linear discriminant analysis classifier. In the online classification step, the algorithm simply computes the learned features from the observed signal and feeds them to the linear discriminant analysis (LDA) classifier. The algorithm achieved a throughput rate of 45 nuts/s and a classification accuracy of 96% with the 30 most discriminative features, a higher rate than those provided with prior methods.

1. INTRODUCTION

Tree nuts are extensively used in the food industry. Environmental conditions and processing procedures may decrease nut quality by causing cracks or damage to the shell. Damage to the shell of the nut kernel increases the likelihood that fungi will infect the kernels. Fungal infestation can cause aflatoxin formation, which is a type of mycotoxin that is linked to various health problems including liver cancer [1]. Therefore, nuts with shell damage should be separated from nuts with regular shells. This same problem affects many different types of tree nuts such as almonds, pecans, hazelnuts, pistachio nuts, and so on. Initial attempts at separation of fungal damaged food items from undamaged ones go back to the studies of Pearson [2]. For pistachio nuts, Pearson showed that nearly all the aflatoxin contaminated pistachios are either caused by bird damage or insects before harvesting or due to early split. Pearson [3] used a machine vision system to classify pistachio nuts into 3 categories such as stained (caused by early splitting), unstained, or moderately stained, with an average classification error of 11%. After removing stained pistachio nuts from unstained ones, the aflatoxin contamination level of pistachio nut is reduced from 4.8–8.6 range to 0.04–2.5 ppb [4].

In another application of tree nut sorting, a high speed sorter based on impact acoustics was developed to separate the pistachio nuts with closed shells from the ones with cracked shells by using the features that were extracted from impact sound signals [5]. This system was improved by using the eigenvalues of mel-cepstrum coefficients and sound amplitudes [6] resulting in a classification accuracy of 97.8%. While this system was primarily designed for separating open and closed shell pistachio nuts, it was shown to provide a feasible method for detecting hazelnuts with cracked shells [7] as well.

Hazelnut quality in the market is mainly measured by the ratio of inner kernel weight to the shell weight. Hence farmers separate the empty hazelnuts from fully developed ones before selling the nuts. A mechanical device working with an air fan is used for this purpose. The air fan deflects

the hazelnuts with lower weight and the rest of the hazelnuts are accepted as fully developed. This system is unable to determine the nuts with cracked shells because hazelnuts with cracked shell have weights that are very similar to hazelnuts with regular shell. The acoustic sorter system described above is used to separate empty hazelnuts from fully developed nuts in [7] and 97.5% of these hazelnuts are correctly classified by using 70 features. These features are extracted from the short time variances of signal segments, maximum signal amplitude, spectral peak locations, and the parameters of a Weibull distribution approximation of the envelope of the impact signal parameters. The same features were used for cracked and regular shell hazelnut separation and 94.47% classification accuracy was obtained. However, this type of algorithm is computationally complex and therefore hard to implement in real time. The results obtained in [7] show the importance of time and frequency features in impact acoustics classification. In order to reduce computational complexity and achieve error rates similar to [7], we recently used an undecimated wavelet transform to classify hazelnuts with regular shell and cracked shell [8]. The most discriminative subbands are manually selected and their energies are used for classification in [8]. A 91.8% classification rate is achieved with nearly 20 features. Although the computational complexity is reduced with this approach, the classification accuracy is poor compared to [7].

In this study, we propose an adaptive time-frequency (t-f) analysis approach based on a local discriminant basis algorithm similar to that used in [9–11] to select the most relevant time segments and subbands to maximize classification performance. For this purpose, we combine local cosine packets and wavelet transform which are subsequently used for time and frequency plane feature selection. A schematic diagram summarizing our approach is given in Figure 1. In particular, the local cosine packet analysis is used along the time axis with a pyramidal tree to segment the signals such that the spectral distances in the selected time windows are maximized between classes. A Kullback-Leibler distance was used to estimate the distance between the spectrum of cracked and undamaged hazelnut acoustics. In the next step in each selected time segment, an undecimated wavelet transform is implemented to select the most discriminant subbands. Unlike the algorithm proposed in [10, 11] that uses fixed frequency bands, we enhance the frequency axis segmentation by using an undecimated wavelet transform in each adapted time segment. Accordingly, the proposed technique requires no prior knowledge of the relevant time and frequency locations. All these segmentation procedures are executed automatically in an offline manner. As a final step the t-f features are sorted according to a cost function and fed to a linear discriminant. In order to asses the efficiency of different feature selection approaches, we compare two different methods. In particular, the resulting t-f features are sorted by using Fisher discrimination on the pruned tree or processed by the correlation-based feature selection algorithm of [12] implemented on the full tree. The features selected by both algorithms are then fed into the linear discriminant analysis classifier.

The paper is organized as follows. In the next section, the data acquisition system and sample selection procedure are given. The procedures for constructing the time-frequency plane segmentations and the advantages of using undecimated wavelet transform are described in Section 3. Experimental results and conclusions are given in Sections 4 and 5, respectively.

2. MATERIALS

2.1. System description

The impact acoustic recording system (Figure 2) consists of a pipe, an impact plate, and a microphone. Hazelnut kernels are dropped on an impact plate through the pipe. The impact acoustic signal generated by the system is captured by a microphone and processed by a PC. A stainless steel plate with dimensions $7.5 \times 15 \times 2$ cm is used as the impact plate. The impact plate is fixed to the ground at a 120° angle. This angle prevents the nuts from making multiple impacts. The microphone is sensitive to frequencies up to 20 kHz and is placed 5 cm from the impact plate. The impact acoustic signal is sampled at 44.1 kHz.

2.2. Collection of samples

"Levant"-type hazelnuts collected from an orchard in Duzce, Turkey, in August 2006, are used in this experimental study. Developed hazelnuts are first selected by a standard air fan system and resorted using their measured weights. Hazelnuts less than 0.9 g are accepted as empty and removed from the fully developed class. The shells of fully developed hazelnuts are visually inspected and are further classified as nuts with regular shell and nuts with cracked shell. Each selected hazelnut is dropped on the metal plate and the resulting acoustic signals (Figure 3) are recorded. Averaged time-frequency maps of cracked and open hazelnut acoustics are given in Figures 3(c) and 3(d).

3. METHODS

Before explaining the details of the proposed signal processing and classification system, let us summarize the overall algorithm. The proposed method implements an offline learning step to extract the most discriminative time-frequency features. This is achieved by first segmenting the training signals along the time axis with a pyramidal tree. In particular, the segmentation is calculated by pruning the pyramidal tree from bottom to top to maximize the Kullback-Leibler distance between the expansion coefficients of good and cracked hazelnuts in each segment. The expansion coefficients in each segment are obtained from local cosine packets that provide local spectral representations. Then, each adapted time segment is decomposed into subbands by an undecimated wavelet transform. The subbands are represented in a binary tree format and are pruned to find the most discriminative subbands along the frequency axis. Finally a time-frequency map is computed by extracting the

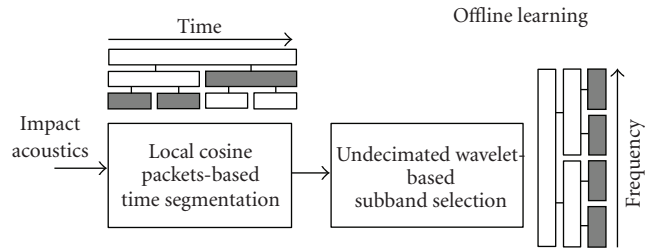

Figure 1: The block diagram of the offline learning step of the proposed algorithm.

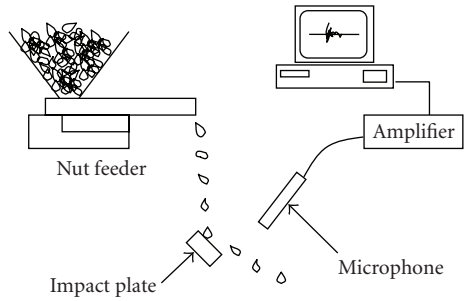

Figure 2: Schematic of experimental apparatus for collecting acoustic emissions from hazelnut kernel.

most relevant features. An LDA classifier is trained with these features and tested using data that was not used for training.

The main contribution of the proposed approach is the systematic and automatic extraction of the relevant features during the training step so as to improve classification accuracy. In the remainder of this section we describe that step in detail.

3.1. Local discriminant bases

In previous studies, impact acoustic classification is performed by combining the features obtained from the time and frequency domains as indicated in [7]. Here, we explore a different approach that is based on extracting features from the time-frequency plane. The local discriminant bases (LDBs) method was developed to extract such local information [9] for classification. The LDB algorithm basically expands the signal by using wavelet packets or local trigonometric bases over a pyramidal-binary tree as shown in Figure 1. This tree is then pruned from bottom to top to maximize a predefined cost function which measures the discrimination power of each node. The pruning operation adapts the tree for classification task. The original algorithm implements adaptation either in time or frequency. It has been shown that adaptation along both axes is crucial [10, 13]. Once the segmentation is accomplished the time-frequency features are sorted according to a cost measure and fed to a classifier for final decision. Since the time-frequency plane is a high-dimensional space, a postprocessing step is implemented by several authors to boost the classification performance [10, 14]. Depending on the problem, this step can be principal component analysis or a Mel-Scale-based approach to get band features.

Here, we utilize the local cosine packets and wavelet transform sequentially. As a first step to adapt to the temporal variability between the cracked and undamaged hazelnut acoustics, we use local cosine packets which provide time axis segmentation with smooth windows. Local cosine packets are widely used in signal processing to segment signals with time varying characteristic [15]. Once we obtain the time axis segmentation, we use wavelet transform to select the most relevant subbands for the final feature extraction. Since our purpose is to discriminate between signals coming from different classes, we use a dissimilarity criterion to obtain the segmentations along both the time and frequency axis. Now let us describe the distance measure and algorithms used for time and frequency segmentation in detail.

3.2. Dissimilarity measure

Various types of dissimilarity measures were tested and the following ones were selected and used. Let p and q be the spectral energy distributions of signals belonging to class1 and class2, respectively. The distance measure can be:

(i) the symmetric Kullback-Leibler distance, which is also called J-divergence:

$$J(p,q) = I(p,q) + I(q,p),$$
$$I(p,q) = \sum_{i=1}^{n} p_i \log \frac{p_i}{q_i}, \tag{1}$$

or

(ii) Euclidean distance:

$$D(p,q) = \|p-q\|^2 = \sum_{i=1}^{n} (p_i - q_i)^2. \tag{2}$$

We have used the J criterion for time segmentation and D for subband selection in each adapted segment. As shown in Figure 4(a), the averaged spectrum of cracked and regular hazelnut shells has most of its energy in midbands. However, when the distance between these two spectra is calculated, we noticed that the J criterion emphasizes higher bands more than the D criterion. During our experimental studies, we observed that the most discriminant locations are located in higher frequency bands. Therefore, using J for time segmentation provided better results.

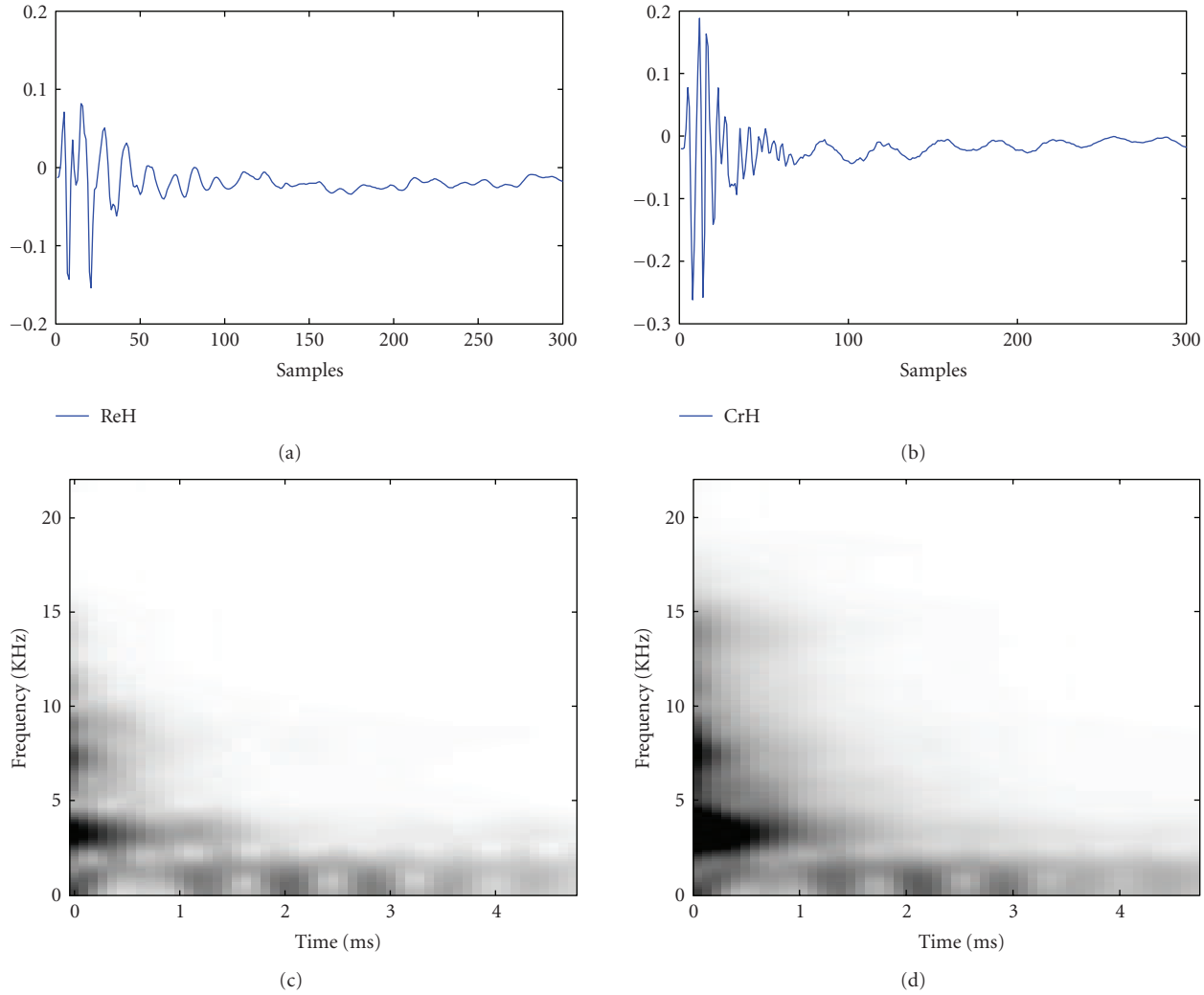

FIGURE 3: Typical impact acoustic signals of (a) fully developed hazelnuts with regular shell (ReH), (b) fully developed hazelnuts with cracked shell (CrH), and averaged spectrogram of (c) ReH and (d) CrH signals.

3.3. Time segmentation with local cosine packets

The impact acoustic signals have different characteristics in the impact, postimpact, and late impact phases. Therefore, impact signals should be analyzed locally. In general, local information of the signal is extracted by a short time Fourier transform (STFT). Some researchers used local cosine packets (LCPs) because of its advantages over the STFT [9, 11]. Local cosine packets (LCPs) is preferred in this study and used to partition the time axis in a pyramidal tree structure of Figure 1.

Local cosine packets partition the time axis by using smooth bells [15] that are constructed using cut-off functions $r(t)$ that satisfy

$$\begin{aligned} &|r(t^2)| + |r(-t)^2| = 1 \quad \forall\ t \in R, \\ &r(t) = \begin{cases} 0 & \text{if } t \le -1, \\ 1 & \text{if } t \ge 1. \end{cases} \end{aligned} \tag{3}$$

An example of such a function $r(t)$ is

$$r(t) = \begin{cases} 0 & \text{if } t \le -1, \\ \sin\left[\dfrac{\pi}{4}\left(1 + \sin\left(\dfrac{\pi t}{4}\right)\right)\right] & \text{if } -1 < t < 1, \\ 1 & \text{if } t \ge -1. \end{cases} \tag{4}$$

First, all signals are represented with local cosine packets within smooth windows (as in (4) in the tree structure. The resulting expansion coefficients are squared and then averaged over the signals in the given class. This provides an averaged energy spectrum of each class in a given time segment within the pyramidal tree. Let p_i and q_i be the mean energy spectra of cracked and regular classes, in a given time segment, respectively. The distance between the average spectra is calculated with the criterion J where "n" in (1) corresponds to the total number of time samples in a given node. This way, the distance is accumulated along the spectrum within

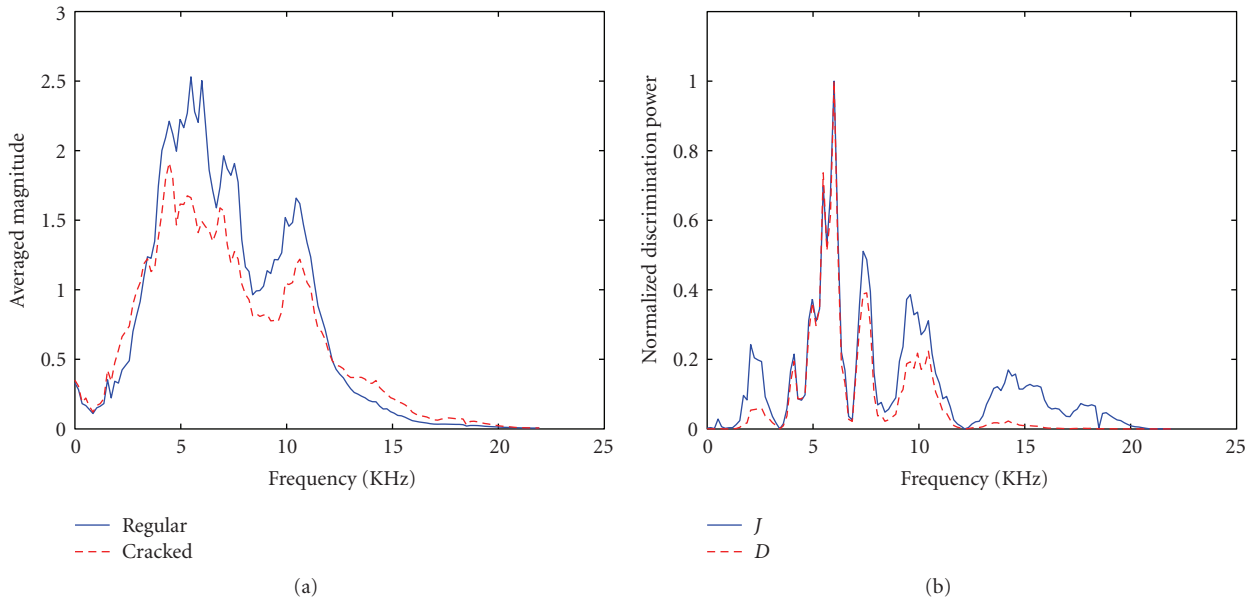

FIGURE 4: (a) The averaged magnitude spectrum of cracked and regular hazelnut impact acoustic signals related to the first 128 samples. (b) The J and D distance between two spectra.

If $J_{\text{mother}} \geq (J_{\text{child1}} + J_{\text{child2}})\, x\ \varphi$,
keep mother,
else
keep children.

ALGORITHM 1: Pruning algorithm.

all subspaces to get a single value representing each node of the tree. The resulting binary tree is then pruned from bottom to top according to the rule in Algorithm 1 to find the nodes with maximum discrimination power:

Here J_{mother} and J_{child} are the discrimination power of the mother and children nodes and are computed by the Kullback-Leibler distance criteria and φ is an empirically selected constant. It is experimentally found that $\varphi = 0.95$ preserves discriminative information while leading to robust segmentation. The algorithm keeps the mother if it captures 95% of the discriminative power of the children, otherwise it keeps the children.

3.4. Frequency segmentation

We have observed time jitter in the recorded signals which is due to variances in the travel time to the steel plate. Therefore, a shift invariant decomposition is highly desirable for processing the signal. The importance of shift invariance for classification is also emphasized in [9–11]. The undecimated wavelet transform (UDWT) has the shift-invariance property. It was first used for texture classification in [16]. In this study, a similar approach is taken to analyze the impact signals for classification. A filter $f(n)$ with a z-transform $F(z)$ that satisfies the quadrature mirror filter condition

$$F(z)F(z^{-1}) + F(-z)F(-z^{-1}) = 1 \tag{5}$$

is used to construct the pyramidal filter bank (Figure 5). The high-pass filter $g(n)$ is obtained by shifting and modulating $f(n)$. Specifically, the z transform of $g(n)$ is chosen as

$$G(z) = zF(-z^{-1}). \tag{6}$$

The subsequent filters in the filter bank are then generated by increasing the width of $f(n)$ and $g(n)$ at every step, for example,

$$\begin{aligned} F_{i+1}(z) &= F(z^{2^i}), \\ G_{i+1}(z) &= G(z^{2^i}), \quad i = 0, 1, \ldots, N. \end{aligned} \tag{7}$$

In the signal domain, the filter generation can be expressed as

$$\begin{aligned} f_{i+1}(k) &= [f]_{\uparrow 2^i}, \\ g_{i+1}(k) &= [g]_{\uparrow 2^i}, \end{aligned} \tag{8}$$

where the notation $[]_{\uparrow m}$ denotes the up-sampling operation by a factor of m.

The resulting filter bank of which the second level frequency response is demonstrated at Figure 6 is used to extract the subband signals at the nodes. It is observed that the signal has different energy distribution in each subband.

The Euclidean distance between cumulative probability distributions (cdf) of subband energies in (2) is chosen as the discriminative measure. We selected to use cdf over pdf because it is easier to calculate. One can also use pdf instead. The resulting pyramidal subband tree is pruned from bottom to top by the rule, shown in Algorithm 2.

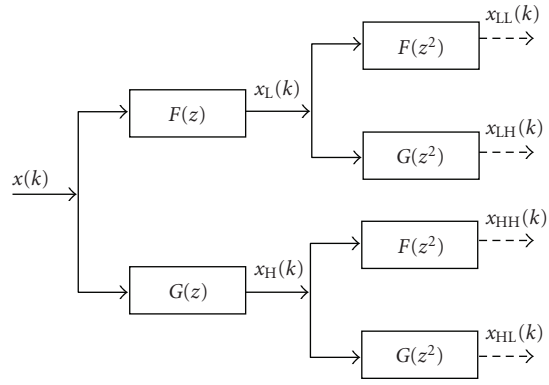

Figure 5: Pyramidal filter tree up to second level. L and H stand for low and high bands, respectively.

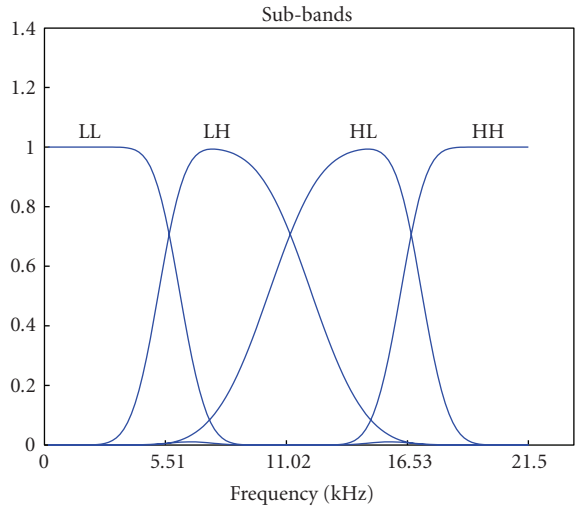

Figure 6: Frequency response of the 2nd level filters.

If $d_{\text{mother}} < \max\{d_{\text{child1}}, d_{\text{child2}}\}$,
set $\max\{d_{\text{child1}}, d_{\text{child2}}\}$ as mother,
else
remove children.

Algorithm 2: Pruning algorithm.

Where d_{child1} and d_{child2} are the Euclidian distances of subbands nodes of mother node where as d_{mother} is the distance of the mother node.

4. RESULTS

One thousand cracked and one thousand uncracked hazelnut kernels are used in this study. Each hazelnut is dropped on the metal plate and the resulting acoustic signal consisting of 768 time samples is recorded. We analyzed the signal up to a tree depth of 4 resulting in a smallest segment size of 48 time samples in the time domain. We empirically found that this level provides a healthy balance between focus on to transient waveforms and the required spectral resolution to distinguish between subbands with different behavior. The signals were first represented by using LCP over the pyramidal tree structure. The pyramidal tree was pruned by using the algorithm of Section 3.3 and the adaptive time segmentation for classification purpose was obtained for different sets of signals as indicated in Figure 7. It was observed that different sets of signals may cause different segmentation in time. We used the segmentation of Figure 7(a) in our simulations. In this case, the time axis is divided into 7 segments.

In each time segment, the signal was decomposed into subbands up to the 4th wavelet decomposition level and the most relevant subbands were detected by using the procedures of Section 3.4.

A discriminative time-frequency map was generated in Figure 8 by combining the adaptively pruned trees both in time and frequency to visualize the most crucial t-f patterns. In our application, the algorithm usually generates a t-f map with around 70 subbands for various training data sets. For every signal in each training set, the energy value for each subband was computed resulting in two sets of feature vectors corresponding to cracked and healthy shell classes.

The 70 features obtained were sorted in descending order according to their discrimination power and then used for classification. Fisher's discrimination measure is used for feature selection. We observed with all training data sets that the most discriminative feature locations were concentrated in the high frequency bands corresponding to the early and post impact regions as indicated in Figure 8. Among the 70 subbands, the 25 most discriminative ones are indicated by different shades of gray, with darker shades corresponding to higher discrimination levels.

4.1. Classification

In order to assess the efficiency of the proposed algorithm, a comparison is made with the features of [7] and those features of our previous work [8] which used nonadaptive subbands and different order statistical features. Recall that in [7], 70 features were extracted from the short time variances of signal; maximum signal amplitude, spectral peak locations, and Weibull distribution fit to the envelope of the impact signal and all are used for classification. In the subband-based algorithm [8], features were extracted from subband signals and the 20 most relevant features and the subbands including these features were manually selected. The time segmentation of Figure 7(a) is employed to obtain a total of 28 statistical features including mean absolute energy, variance, skewness, and kurtosis on each of the seven time segments.

The one thousand acoustic signals for each class are randomly divided into 5 nonoverlapping sets, each consisting of 200 records. Five pairs of uncracked and cracked sets are then randomly formed. Each pair is used to construct the adaptive t-f segmentation and select features. The features identified are then used with the remaining 1600 acoustic signals to determine the performance of the classifier. This procedure is repeated five times with the five different pairs of uncracked and cracked sets.

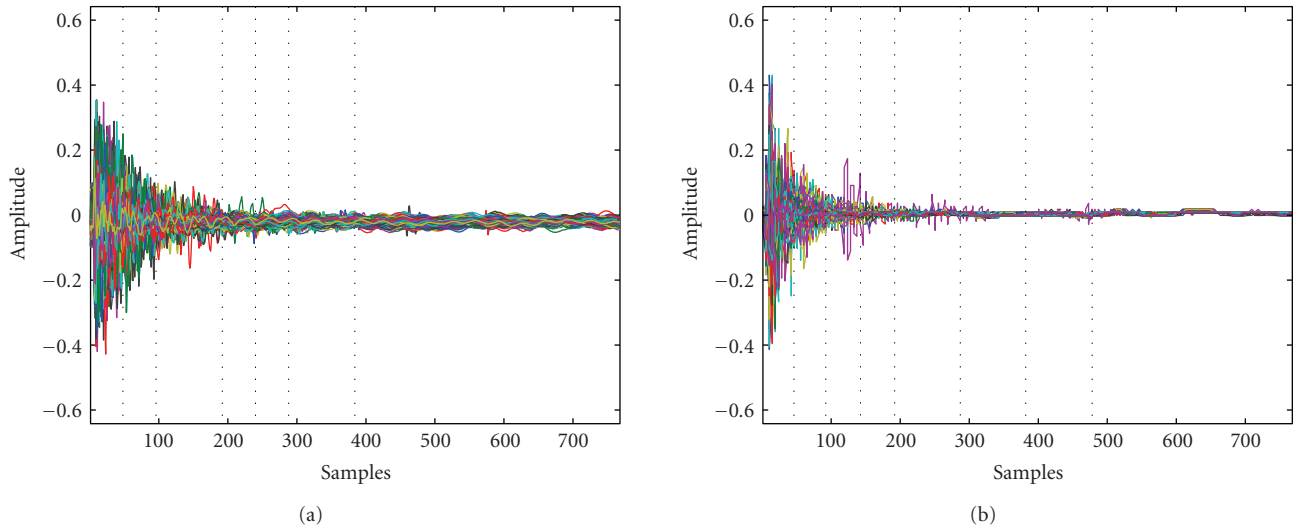

FIGURE 7: The adaptive time segmentation grids (dotted lines) of (a) set1 and (b) set2.

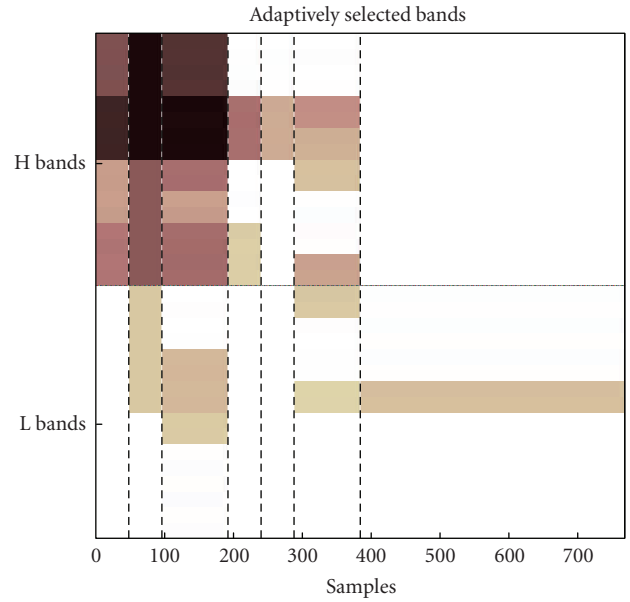

FIGURE 8: The time-frequency discrimination map of impact acoustic data. Darker regions indicate higher discrimination power.

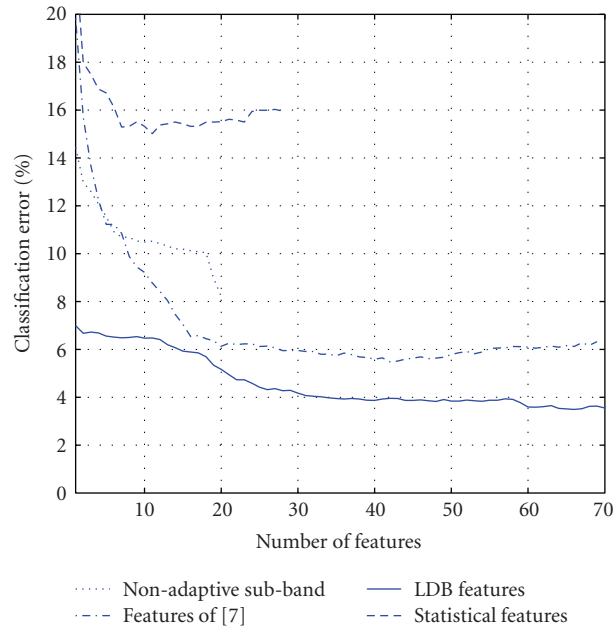

FIGURE 9: The classification error rates with various numbers of features.

The optimal number of features for classification was investigated by adding features one by one according to Fisher's discrimination criterion. This step is repeated for all four methods. Related classification error curves are presented in Figure 9.

We noticed that the lowest classification error is achieved with our proposed approach. The minimal classification error rates achieved by each method are given in Table 1. It is observed that the lowest error is achieved by the first 64 features with an error level of 3.5% by our proposed approach. For the method of [7], 43 out of 70 time and frequency domain features provided the minimum error level. Similarly, 20 nonadaptive subband features are used for the method of [8]. The statistical features gave poor classification error rates compared to other methods. The lowest error rate occurred when the first 7 features are used. Our proposed approach reaches an error rate around 4% after the first 30 features. Increasing the number of features provided marginal improvement of the error rate.

The ROC curves for the three methods are presented in Figure 10. It is observed that 64- and 30-dimensional LDB features provide higher detection of cracked hazelnuts for a given false alarm rate.

Table 1: Classification rate comparison of proposed LDB-based method against the previously developed algorithms.

Method	Accuracy(%)
43 features of method of [7]	94.47
7 statistical features	85.00
20 nonadaptive subband features	91.80
64 LDB-based feature	**96.51**

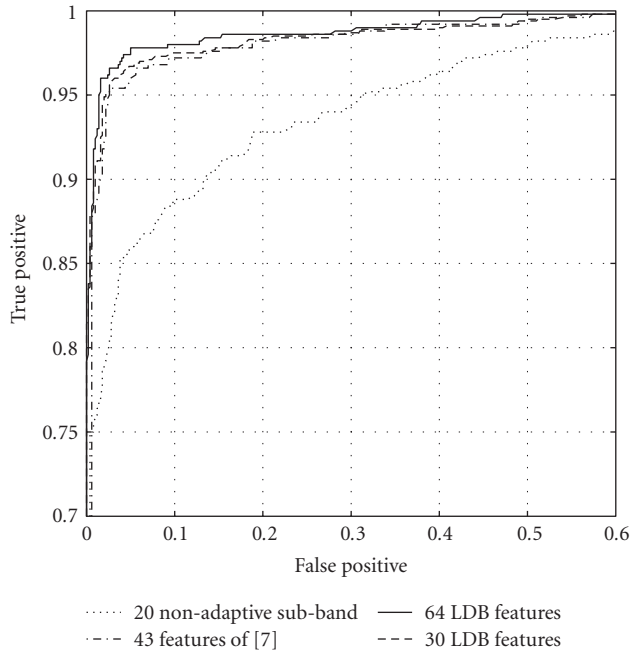

Figure 10: Receiver operating characteristics (ROCs) curves.

4.2. Filter selection

Various types of wavelet filters (Daubechies, Coiflet, and Sym) are used for decomposition of the frequency axis, and their effects on classification accuracy are observed. In Figures 11(a) and 11(b), the classification accuracy of Daubechies and Coiflet wavelets is depicted in contour graphics format. The x-axis indicates the total number of features retained after sorting. The y-axis indicates the filter type used in subband decomposition. The higher filter types correspond to higher-order filters. The darker regions in the contour graph give lower classification accuracy. It is observed that better classification error rates (< 4%) are obtained when approximately 40 or more features are retained after decomposition with high-order wavelet filters (Db12–Db15 and Coif3–Coif5). We selected one of the high-order wavelet filters, Coiflet 4, for further analysis. The discriminant band distribution of Figure 8 may slightly change depending on the wavelet filter.

4.3. Effect of noise on classification

In order to asses the robustness of our methods against disturbing effects, a zero mean Gaussian noise at various SNR levels is added to the signal, and classification performances are compared as shown in Figure 12. It is observed that the algorithm performs well for reasonable noise levels. The algorithm usually selects low level subbands nodes when the signals are disturbed by high-level noise. This can be justified by fact that the energy of the impact acoustics is concentrated in the mid and lower bands of the spectrum as indicated in Figure 4. In order to keep the efficiency in classification, the algorithm selects features from lower bands with increasing noise level. This also results a decrease in classification accuracy.

4.4. Effect of shift-invariance to classification

As indicated in the previous sections the main motivation for using UDWT against DWT is the shift invariance property of the UDWT In order to justify our selection we compared the UDWT results with those obtained from the DWT and spin-cycle procedure of [17]. The spin-cycle procedure is introduced by [17] to overcome the lack of shift invariance of the DWT and LCP. In particular, a signal is shifted to the left and right for a selected number of spins. For each shift, the signal is expanded into its DWT coefficients. These coefficients are either averaged or processed individually. It has been shown that the spin-cycle procedure provides many improvements over the direct use of the DWT or LCP [13, 17]. In Figure 13, we show the classification curves obtained from the DWT, the DWT with spin-cycle, and the UDWT methods.

As expected, the results obtained from DWT were poor. Interestingly the DWT with spin-cycle provided results as good as the UDWT. We note that the minimum error of spin-cycle method was slightly lower than UDWT but used more features. However, one should note that the computational complexity of spin-cycle method is 3 times higher than that of UDWT. In real-time applications, it is difficult to obtain fast processing by this method.

4.5. Feature selection

A total of 210 features corresponding to 210 time-frequency band are obtained before frequency axis pruning operation. Recall that when Fisher criterion is used for feature sorting, the frequency tree is pruned as a prior step to obtain an uncorrelated subband feature set. Here, we investigate the efficiency of the proposed approach by comparing it to the correlation-based feature selection (CSF) procedure of [12]. The CSF uses the feature-to-class and feature-to-feature correlations to select a subset of features from a redundant set. Since it can account for the feature-to-feature correlations, we presented the unpruned full feature dictionary to CSF method. The subset returned by the CSF method was used for classification. In Figure 14, we show the classification curve of CSF and compare it with the curve of our algorithm based on Fisher's criterion on the pruned set. The CSF method achieved to minimal error of 4% with around 70 features. Although a redundant feature dictionary was presented to the algorithm, it successfully selected a subset without any pruning step.

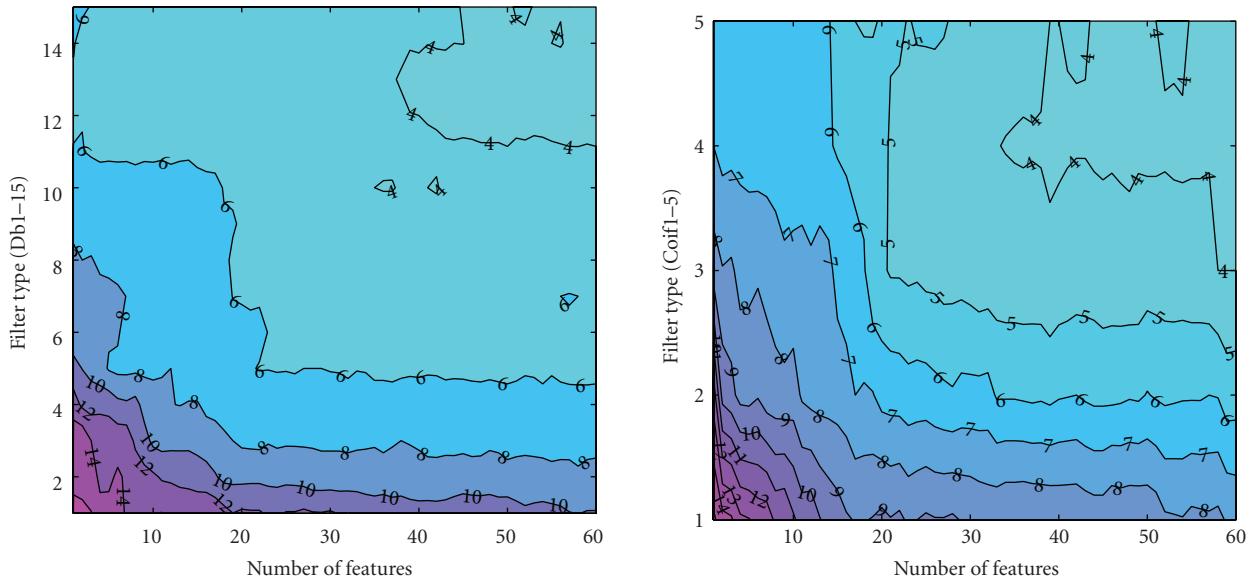

Figure 11: The effect of selected wavelets and feature dimension on classification accuracy; (a) Daubechies, (b) Coiflet.

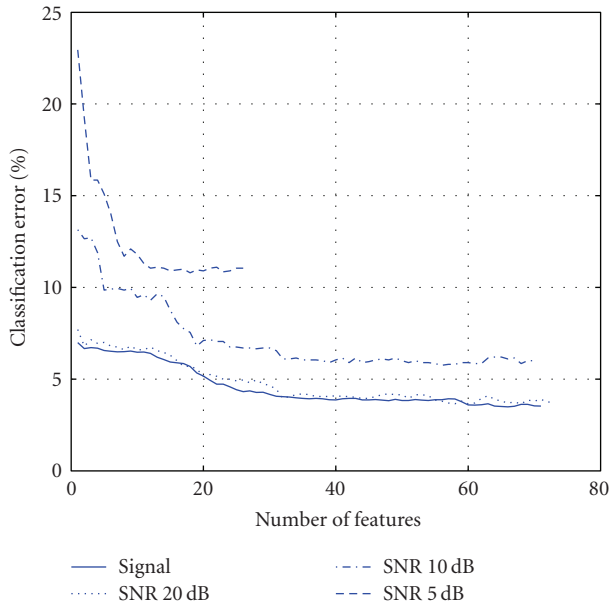

Figure 12: The classification error curves for noise disturbed impact acoustic signals.

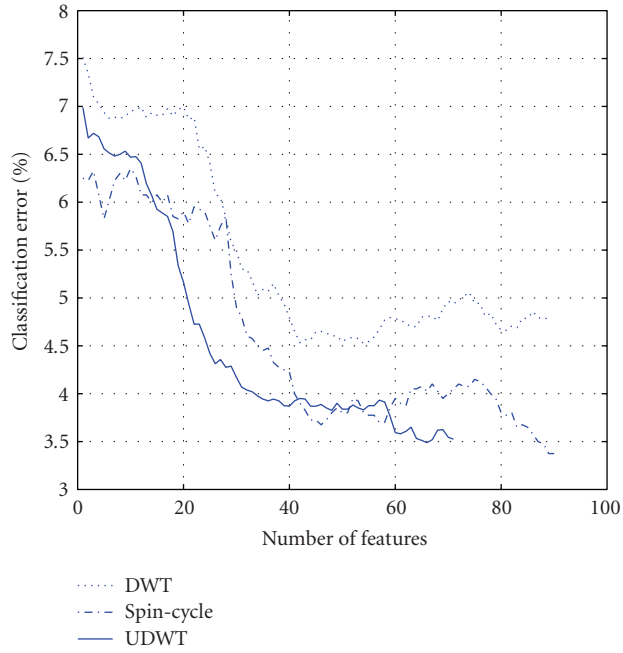

Figure 13: The classification error curves for evaluating the efficiency of shift invariance property. The spin-cycle curve stands for the results obtained from DWT supported 1-Spin-cycle procedure.

It is observed that the classification error increased after 70 features. Interestingly within the first 10 features, the CSF provides a lower error rate than Fisher's criterion. However, with increasing number of features the Fisher-based sorting procedure over the pruned subband tree provided lower error rates. The pruning algorithm in our method automatically eliminated two third of these features. The error curve (Pruned tree, Fisher) in Figure 14 indicates that the pruning and Fisher criteria combination is successful at detecting relevant features in acoustic signals.

4.6. Computational complexity

Determining the best time-frequency segmentation of the signals and the bands to be retained for classification is relatively computationally demanding but this step has to be carried out only once, offline. For online processing, the throughput of the algorithm in terms of nuts processed per second depends on the number of features used in

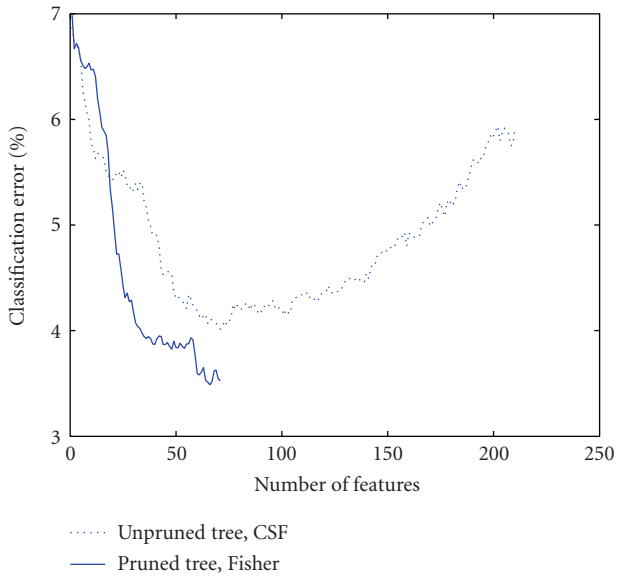

Figure 14: The classification error curves of CSF method and our proposed approach.

classification. When the first 64 features providing the best classification rate is employed, all 768 samples need to be processed. In this case 17.4 milliseconds are required for signal acquisition of a single nut at a sampling rate of 44.1 kHz. The computations for feature extraction and classification require 13.1 milliseconds on a dedicated P4 3 GHz processor. In this case, up to 32 nuts can be processed in a second with classification error of 3.5%. In case an extra 0.5% classification error is tolerable, up to 45 nuts can be processed in a second with 30 features. We observed that only the first half of the signal is required to compute the first 19 features. The classification error achievable at this case is 5.3% and the throughput can be as high as 119 nuts/s provided that the mechanical sorter system is able to keep up with signal processing.

5. CONCLUSION

In this study, an adaptive time frequency plane feature selection algorithm is introduced to separate cracked hazelnuts from regular hazelnuts. The adaptation in time and frequency is achieved by combining local cosine packets and an undecimated wavelet transform. The impact signal is adaptively segmented in the time domain with LCP. Similarly the signals in each resulting time segment are decomposed into subbands by an undecimated wavelet transform. The subband tree is pruned from bottom to top according to the discrimination power of its nodes. The resulting t-f map is used to extract the best features for classification. Interestingly, higher bands are selected by the algorithm. Finally, the hazelnuts are classified by LDA. The proposed approach is robust, adaptive to signal type and provides superior classification results. The algorithm can work in a real time automatic sorter with a processing speed of 45 nuts/s.

ACKNOWLEDGMENTS

This work is supported by National Science Foundation (NSF) and by the Project EEEAG-106E057 and Program 2214 of National Scientific Research Council of Turkey.

REFERENCES

[1] C. R. Dichter, "Risk estimates of liver cancer due to aflatoxin exposure from peanuts and peanut products," *Food and Chemical Toxicology*, vol. 22, no. 6, pp. 431–437, 1984.

[2] T. Pearson, "Separating early split from normal pistachio nuts for removal of nuts contamination on the tree with aflatoxin," M.S. thesis, University of California, Berkeley, Calif, USA, 1987.

[3] T. Pearson, "Machine vision system for automated detection of stained pistachio nuts," *Lebensmittel-Wissenschaft und-Technologie*, vol. 29, no. 3, pp. 203–209, 1996.

[4] T. Pearson and T. F. Schatzki, "Machine vision system for automated detection of aflatoxin-contaminated pistachios," *Journal of Agricultural and Food Chemistry*, vol. 46, no. 6, pp. 2248–2252, 1998.

[5] T. Pearson, "Detection of pistachio nuts with closed shells using impact acoustics," *Applied Engineering in Agriculture*, vol. 17, no. 2, pp. 249–253, 2001.

[6] A. E. Cetin, T. Pearson, and A. H. Tewfik, "Classification of closed- and open-shell pistachio nuts using voice-recognition technology," *Transactions of the American Society of Agricultural Engineers*, vol. 47, no. 2, pp. 659–664, 2004.

[7] I. Onaran, B. Dulek, T. Pearson, Y. Yardimci, and E. Çetin, "Detection of empty hazelnuts from fully developed nuts by impact acoustics," in *Proceedings of the 13th European Signal Processing Conference (EUSIPCO '05)*, Antalya, Turkey, September 2005.

[8] H. Kalkan and Y. Yardimci, "Classification of hazelnuts by impact acoustics," in *Proceedings of the 16th IEEE Signal Processing Society Workshop on Machine Learning for Signal Processing (MLSP '06)*, pp. 325–330, Maynooth, Ireland, September 2006.

[9] N. Saito and R. R. Coifman, "Local discriminant bases," in *Wavelet Applications in Signal and Image Processing II*, vol. 2303 of *Proceedings of SPIE*, pp. 2–14, San Diego, Calif, USA, July 1994.

[10] N. F. Ince, A. H. Tewfik, and S. Arica, "Classification of movement EEG with local discriminant bases," in *Proceedings of IEEE International Conference on Acoustics, Speech and Signal Processing (ICASSP '05)*, vol. 5, pp. 413–416, Philadelphia, Pa, USA, March 2005.

[11] N. F. Ince, A. H. Tewfik, and S. Arica, "Extraction subject-specific motor imagery time-frequency patterns for single trial EEG classification," *Computers in Biology and Medicine*, vol. 37, no. 4, pp. 499–508, 2007.

[12] M. A. Hall, "Correlation-based feature selection for machine learning," Ph.D. dissertation, Department of Computer Science, Waikato University, Hamilton, New Zealand, 1998.

[13] N. F. Ince, S. Arica, and A. H. Tewfik, "Classification of single trial motor imagery EEG recordings with subject adapted non-dyadic arbitrary time-frequency tilings," *Journal of Neural Engineering*, vol. 3, no. 3, pp. 235–244, 2006.

[14] K. Englehart, B. Hudgins, P. A. Parker, and M. Stevenson, "Classification of the myoelectric signal using time-frequency based representations," *Medical Engineering and Physics*, vol. 21, no. 6-7, pp. 431–438, 1999.

[15] M. V. Wickerhauser, *Adapted Wavelet Analysis from Theory to Software*, A. K. Peters, Natick, Mass, USA, 1994.
[16] M. Unser, "Texture classification and segmentation using wavelet frames," *IEEE Transactions on Image Processing*, vol. 4, no. 11, pp. 1549–1560, 1995.
[17] N. Saito, R. R. Coifman, F. B. Geshwind, and F. Warner, "Discriminant feature extraction using empirical probability density estimation and a local basis library," *Pattern Recognition*, vol. 35, no. 12, pp. 2841–2852, 2002.

EURASIP Journal on Wireless Communications and Networking

Special Issue on Wireless Network Security

Call for Papers

Recent advances in wireless network technologies are growing fast, evidenced by wireless location area networks (WLANs), wireless personal area network (WPANs), wireless metropolitan area networks (WMANs), cellular networks, ad hoc networks, mesh networks, vehicular networks, and sensor networks. However, wireless network security is a major obstacle to successfully deploy these wireless networks. The effort to improve wireless network security is linked with many technical challenges including compatibility with legacy wireless networks, complexity in implementation, and practical values in real market, etc. The need to address wireless network security and to provide timely solid technical contributions establishes the motivation behind this special issue.

This special issue focuses on the novel and practical ways, but solid contributions, to improve the wireless network security. Papers that do not focus on wireless network security will not be reviewed. Specific areas of interest in above networks include (but are not limit to):

- Attacks, security mechanisms, and security services
- Authentication
- Access control
- Data confidentiality
- Data integrity
- Nonrepudiation
- Encryption and decryption
- Key management
- Fraudulent usage
- Wireless network security performance evaluation
- Wireless link layer security
- Tradeoff analysis between performance and security
- Authentication and authorization for mobile service network
- Wireless security standards
- Forensics

Authors should follow the EURASIP Journal on Wireless Communications and Networking manuscript format described at the journal site http://www.hindawi.com/journals/wcn/. Prospective authors should submit an electronic copy of their complete manuscript through the journal Manuscript Tracking System at http://mts.hindawi.com/, according to the following timetable:

Manuscript Due	January 1, 2009
First Round of Reviews	April 1, 2009
Publication Date	July 1, 2009

Guest Editors

Yang Xiao, Department of Computer Science, The University of Alabama, Tuscaloosa, AL 35487, USA; yangxiao@ieee.org

Hui Chen, Department of Computer Science, Virginia State University, Petersburg, VA 23806, USA; huichen@ieee.org

Shuhui Yang, Department of Computer Science, Rensselaer Polytechnic Institute, Troy, NY 12180, USA; yangs6@rpi.edu

Yi-Bing Lin, Department of Computer Science and Information Engineering, National Chiao Tung University, 30050 Hsinchu, Taiwan; liny@csie.nctu.edu.tw

Ding-Zhu Du, Department of Computer Science, University of Texas at Dallas, Department of Computer Science, Richardson, TX 75083, USA; dzdu@utdallas.edu

Extraction of Discriminative Features from Hyperspectral Data

Habil Kalkan *Yasemin Yardımcı*

Informatics Institute, Middle East Technical University, Ankara, Turkey
habil@ii.metu.edu.tr *yardimy@ii.metu.edu.tr*

Abstract

This paper presents a method to discover the discriminative patterns or features in hyperspectral data for classification. The proposed method searches the data space along both spectral and spatial frequency axis and combines the adjacent spectral and spatial frequency bands so that a simpler but more effective feature set is achieved. The algorithm is tested on hyperspectral images of hazelnut kernels. The detected features were evaluated for classifying contaminated and uncontaminated hazelnut kernels. The developed algorithm is adaptive, robust and can be applicable to other type of hyperspectral data.

1. Introduction

Hyperspectral imaging involves imaging the object under inspection at a large number of frequency bands. The spectral richness of hyperspectral data is often accompanied by redundancy and irrelevant information due to high correlation between spectral bands [1]. The increase in data dimension (number of spectral bands) not only increases the computational complexity but also decreases the classification accuracy when a limited number of training data is available [2, 3]. Due to the limitation of gathering high number of training samples, the researchers preferred to reduce the hyperspectral data dimension by eliminating the irrelevant ones or by combining the bands that do not provide extra information on their own.

The current dimensionality reduction algorithms are usually classified into two categories; feature extraction and selection. Feature extraction is defined as transforming to m dimensional feature space from n ($m<n$) dimensional measured data space by using various transformation methods like Principal Component Analysis (PCA), Decision Boundary Feature Extraction [4], Best Bases Feature Extraction [5], Segmented Principal Component Transformation (SPCT) [6], etc.. In SPCT, the highly correlated adjacent bands in hyperspectral data are grouped together. The principal components in each group are computed and each group is represented by a few components (eigenvectors) with high eigenvalues. The eigenvectors are then pruned according to their Bhattacharya distance between classes.

Unlike feature extraction, feature subset selection does not distort the original data by transformation and aims to reduce the feature dimension by eliminating the irrelevant ones as much as possible. In this way, the irrelevant features are not collected in the first place.

In this study, the authors propose a method which searches the spectral and spatial frequency axis to discover the most discriminative features in hyperspectral images. The images are obtained from hazelnut kernels illuminated by UV light source. The developed algorithm adaptively combines the spectral domain feature fusion and frequency domain subband decomposition to discover the relevant features in this data. The feature extraction step is followed by filter based feature selection algorithm in order to minimize the data dimension. The usefulness of the extracted and selected features is evaluated for detecting contaminated hazelnut kernels by using their hyperspectral images.

Section 2 gives the details of the proposed method and Local Discriminant Analysis (LDB) algorithm which the proposed method inspired from. Section 3 contains an overview on aflatoxin contamination on food stuff, the hyperspectral data acquisition and the preprocessing of the spectral images. The results and conclusions are presented in Section 4 and Section 5, respectively.

2. LDB Based Discriminant Bases Search

Coifman and Wickerhauser [7] developed the Best-Basis algorithm to get the best bases for signal representation and compression. This method first expands the signal into a library of orthogonal bases in

binary tree structure by using wavelet or trigonometric bases. Each node in the binary tree represents the orthogonal subspaces of the signal at different time-frequency localization. The binary tree is then pruned from leaf node to root node by using a cost function. They used entropy to measure the information content of the signal subspaces. A parent node in binary tree is compared to its subband (child) nodes and it survives if its entropy is higher than sum of its child nodes.

The Best-Bases algorithm is extended to classification problems [8] to get the Local Discriminant Bases (LDB) for classification. Instead of using the entropy a dissimilarity cost function is used to maximize the difference between the bases. The LDB algorithm decomposes the time axis by Local Cosine Packets or frequency axis by wavelet packets. However, Ince et al [9] showed that decomposition in both time and frequency axes is crucial for localizing the discriminative subbands. The LDB algorithm is also adapted to hyperspectral images [5,10,11] by accepting the hyperspectral curve of pixels as one-dimensional signal.

The main objective of this study is to extract the discriminative features from spectral – spatial frequency domain by using LDB algorithm. The algorithm consists of three steps. The discriminative bases searches in both spectral and spatial-frequency axis by pruning are the two major steps of the proposed algorithm (Figure 1). The discriminant bases (features) are then selected before classification at the third step.

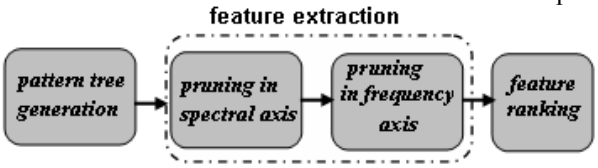

Figure 1. Block diagram of the proposed LDB based discriminative feature extraction algorithm.

2.1 Pattern Tree Generation

The algorithm starts with generating two pattern trees on spectral and spatial-frequency axis in order. The reflectance energies of $N(\leq 2^k)$ spectral images were placed to the k^{th} level of the binary tree from left to right. Figure 2 shows an illustration to *k=4* levels binary spectral band tree for a maximum *N=16* spectral band images. For the case of $N(< 2^k)$, the remaining $(2^k - N)$ nodes at the k^{th} level can be set to null in order to complete the binary tree. The energy value of the mother nodes at the high levels were computed by averaging the feature values of their branch nodes.

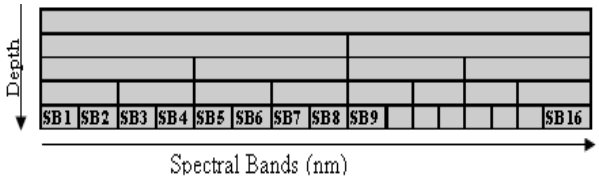

Figure 2: *k=4* levels binary spectral band tree.

The second pattern tree was generated by decomposing the raw spectral images into *h* level full wavelet subbands in quad tree structure as in Figure 3. Wavelet transform retains the original image information and completely represents the image in **A**pproximation, **H**orizontal Detail, **V**ertical Detail and **D**iagonal Detail subbands.

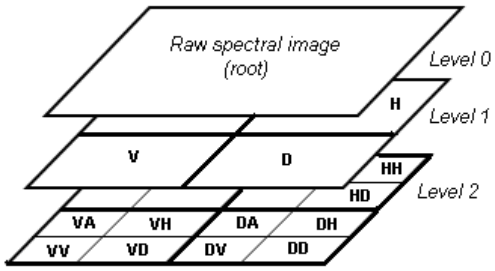

Figure 3. Full wavelet decomposition quad tree up to *h=2* levels. The images (**A**, **V**, **H**, **D**) at Level 1 are decomposed into subbands(**_A**, **_V**, **_H**, **_D**) at Level 2

The energy in each subband is computed and used as features for further analysis.

2.2 Pruning in Spectral Axis

The obtained pyramidal spectral band tree (Figure 2) is pruned from bottom to top by the following rule:

Pruning algorithm

If $d_{mother} < max\{ d_{child1}, d_{child2}\}$,

set max $\{ d_{child1}, d_{child2}\}$ *as mother,*

else

remove children.

where d_i is the discrimination potential of the i^{th} node between classes and it is computed by the Euclidean distance between cumulative probability distribution (cdf).

$$d = \|p - q\|^2 = \sum_{j=1}^{J} (p_j - q_j)^2 \qquad (1)$$

where p and q are the cdf of the i^{th} node of each classes. Other distance metrics (Fisher, Kullback-Leibler, Bhattacharya, etc) can be used as well.

The algorithm prunes the spectral bands (branch node) if their discrimination potential is lower than their mother node. This process fuses some of the spectral band for better classification accuracy. The frequency subband energies of the pruned spectral bands are averaged in parallel before pruning in frequency axis.

2.3 Pruning in Spatial-Frequency Axis

The pruning algorithm in Section 2.2 is modified to four children mode because of the quad tree structure (Figure 3) in spatial-frequency axis and applied to prune the quad tree in a bottom-up manner. The algorithm keeps the mother node if its discrimination potential, d_i, is higher than any of its four children nodes. Otherwise the children nodes survive as the nodes with high discrimination potential. As an illustration to pruning in the frequency axis, the frequency subbands of the image at can be pruned as in Figure 4.

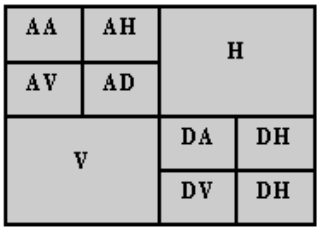

Figure 4. Frequency subband pruning of a spectral band image. Note that "A" and "D" nodes in the first level are preferred to branch while the "H" and "V" nodes are remained.

2.4 Discriminant Bases Ranking

The pruning operation both in the spectral and frequency axis by distance cost function revealed the discriminant data pattern in hyperspectral data. The discriminant features were also sorted according to their discrimination potential and incrementally included feature vectors by using the Correlation Based Feature Selection (CFS) algorithm [13]. The CFS generates a feature set involving the features that are highly correlated with the class and uncorrelated with each other. A linear classifier is used for classification and the desired number of features in classification is obtained when the minimum classification error is reached.

3 Hazelnut Hyperspectral Data Acquisition

3.1 Aflatoxin in Agricultural Products and Sample Preparation

Many agricultural products (hazelnut, pistachio nut, red pepper, corn, almond, etc...) are prone to external and internal insect or mold infestation that degrades quality. The Aspergillus types of molds may cause aflatoxin formation in foods during harvesting, processing and storage stage. Aflatoxins are known as a reason for liver cancer [14]. The regulations limited the Aflatoxin contamination to be 4 ppb (ng/g) and 20 ppb in EU countries and USA, respectively. The aflatoxin contaminated food items should be identified and removed from the lot so these contamination levels can be met. Several researchers used hyperspectral imaging for inspecting the quality of food items. They selected a few relevant spectral bands and used for classification. Mehl [15] used the spectral images taken at 686 and 675 nm for determining the main contamination and defect in apple. Pearson used the 630 and 690 nm spectral bands for detecting infected pistachios [16].

In this study, hyperspectral images of hazelnut kernels (Figure 5) were used for analysis.

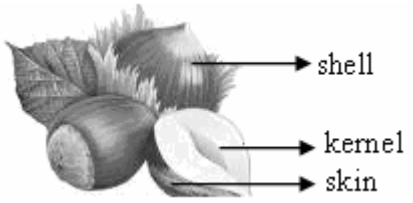

Figure 5: Hazelnuts

Shelled hazelnut kernels were arbitrarily divided into two groups. The first group was reserved for uncontaminated class whereas the second group was for contaminated class. Some of the hazelnut kernels in the second group were directly contaminated by aflatoxin producing molds and the remaining kernels at the second group was incubated with pure water and kept in suitable conditions for mold infestation. The hazelnuts kernels were then roasted to remove the skin over them. These hazelnuts were chemically analyzed for aflatoxin contamination after hyperspectral image acquisition. The chemical analysis results showed high level of aflatoxin contamination at mold incubated hazelnuts (~2227 ppb) and respectively low level of aflatoxin at the pure water incubated hazelnuts (~7,47 ppb). The mean aflatoxin level of the uncontaminated group is 0.7 ppb which is below the allowed aflatoxin limit (4 ppb).

3.2 Hyperspectral Data Acquisition of Hazelnut Kernels

The hyperspectral imaging system (Figure 6) consisting of an Imaging Source VIS DFK 41AF02 digital CCD camera, two Spectroline UV-A Lamps (peak intensity at 365 nm), a cabin to function as dark room, a filter wheel with 12 filter holders and computer for data acquisition and processing is used for visualize samples under UV radiation. The filter set consists of band pass filters from 400 nm to 510 nm with 10 nm FWHM (Full Width Half Maximum). The kernels were also visualized with filters of which center frequencies are 550 nm (70 nm FWHM) and 600 nm (40 nm FWHM) but these data were not included in the spectral binary tree because their FWHM values are different and they require different exposure durations.

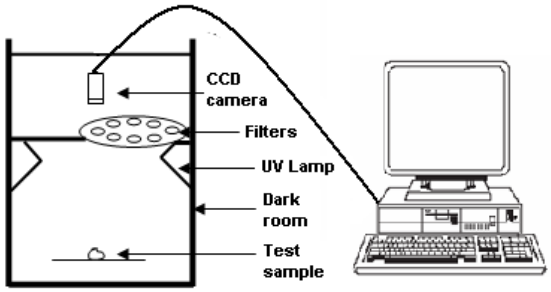

Figure 6. Hyperspectral imaging system with a rotating filter wheel.

A total of 172 contaminated and 105 uncontaminated hazelnut kernels were used for data acquisition. Figure 7 shows some of the spectral band images of hazelnut kernels from two classes.

The first two columns from left show the highly contaminated kernels which were incubated with Aspergillus type molds whereas following two columns show the contaminated kernels which were incubated with pure water. The last two columns show the uncontaminated hazelnut images.

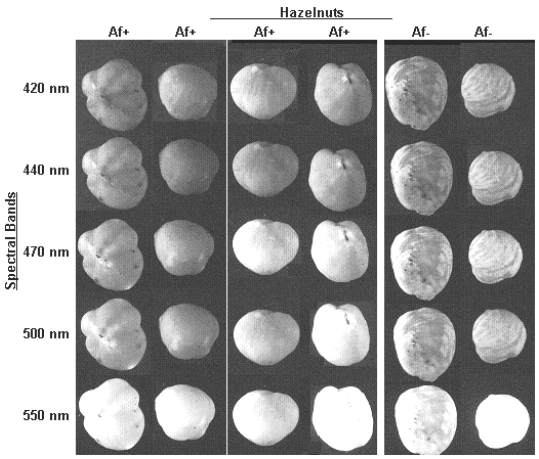

Figure 7. A few spectral band images for aflatoxin contaminated and uncontaminated group.

3.3 Preprocessing the spectral images

A median filter was used to remove the noise on the spectral images (Figure 8-a). Secondly, a binary mask was generated by thresholding followed by morphological operation to extract the hazelnut from background. The generated mask removes both the background and the pixels of the region which the inner skin was not removed during roasting. The spectral image at 550 nm was used for mask generation due its clear distinction between sample, background and unskinned region (Figure 8-a).

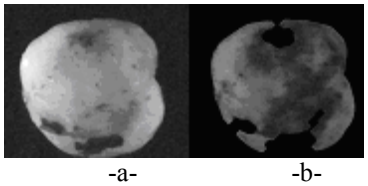

-a- -b-

Figure 8. a) A noise removed spectral band image with unskinned region at the surface, b) a sample to masked image at 430 nm spectral band

The masked spectral images were divided into regions of 91x91 pixels and each region is regarded as an independent samples. They were later on used for voting on the class membership of a given hazelnut kernel. The hazelnuts are classified according to "majority voting" principle.

4. Results and Discussions

The hyperspectral data set is randomly divided into four sets for four fold classification. The algorithm is developed with three sets (training) and the performance of the extracted features is tested with the remaining set. Recall that the hazelnut images are divided into small windows of 91x91. These windows are independently classified and the results used for voting the hazelnut kernels into contaminated or uncontaminated classes.

Initially, pattern trees are generated in spectral and spatial frequency axis in order. The reflectance energies of 12 spectral images (400-510) were placed on the 4th level of the binary tree from left to right (Figure 2). The remaining four spectral band nodes (SB13-SB16) at the 4th level were set to null in order to complete the binary tree. In parallel, the spatial frequency quad pattern tree is generated by decomposing the spectral bands by full wavelet transform (Figure 3). We used Daubechies 8 tap filter for decomposition. Other wavelets can be used as well. For each spectral image, a total of 21 subband images are constructed by a two level decomposition (Figure 3). A total of 252 spatial frequency patterns are obtained on 12 spectral bands. The nodes in trees are represented by their energies and evaluated as features. The pruning operation is performed on spectral and spatial frequency axis in order. The binary energy tree is pruned by comparing the discrimination power of the mother nodes in the tree with their children's. Figure 9 shows the spectral band pruning. The spatial frequency domain features (Figure 2) of the spectral bands are averaged according to the pruning in Figure 9 before pruning in spatial frequency axis.

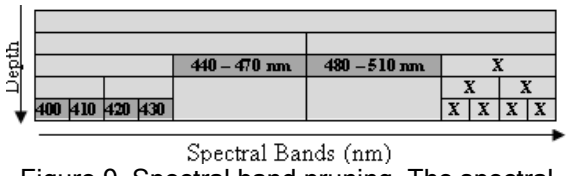

Figure 9. Spectral band pruning. The spectral bands (440-470) and (480 -510) are pruned. The null bands in the tree were ignored at pruning

Next, the frequency subbands nodes in quad tree structure are pruned by using a similar pruning algorithm in Section 2.2 in that a mother node is compared to its four children nodes. The pruning in both axes revealed the location of the most discriminative features of the hyperspectral data. A total of 12 spectral-frequency features were obtained after pruning operation. This operation also decreased the feature dimension from 252 to 12. These 12 discriminative features are then ordered by the CFS algorithm and used for evaluating the classification accuracy on a linear classifier. It is observed that the maximum classification accuracy (95.17%) is achieved by the first three features (Figure 10). The accuracy of 93.4% and 93.6% are achieved by the 12 extracted features and 252 features, respectively. The addition of new features decreases classification accuracy because of the correlation between features.

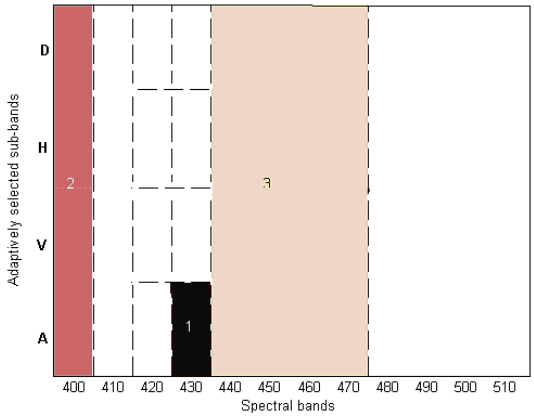

Figure 10. The location of the most discriminative features of the hyperspectral hazelnut data.

It is observed that the spectral bands (440-470) and (480-510) are pruned along the spectral axis and these spectral bands and the bands of 400 and 410 nm were not decomposed into spatial frequency subbands. However, the spectral bands of 430 and 440 were decomposed into subbands in spatial frequency axis. The most discriminant feature is located at the **A**pproximation band of the spectral band image of 430 nm.

5. Conclusions and Future Work

A two dimensional LDB based algorithm is developed to search the discriminative feature location in spectral- spatial frequency axis of hyperspectral data. The algorithm searches the data first along the spectral axis then along the spatial frequency axis.

The algorithm is tested for classifying contaminated and uncontaminated `hazelnut kernels and 95.17% correct classification accuracy is obtained by the proposed algorithm. This feature extraction method can be applied to other hyperspectral data and

we are also applying these techniques on satellite images as well as other food items.

6. Acknowledgement

This work is supported by National by the National Scientific Research Council of Turkey (TUBITAK) project EEEAG-106E057. The authors thank Dr. Pervin Basaran and Meltem Ozcan (Suleyman Demirel University) for incubation of hazelnut samples and Dr. Hamide Senyuva (TUBITAK-ATAL) for conducting the HPLC analysis.

7. References

[1] A. Jain and D. Jongker, "Feature Selection: Evaluation, Application and Small Sample Performance", *IEEE Trans. Pattern Anal. and Machine Intelligence*, 19(2): 153-158, 1997

[2] P. H. Hsu, "Feature Extraction of HyperSpectral Images Using Matching Pursuit", *Proceedings of the XXth ISPRS Congress*, Istanbul, 2004

[3] D. A. Landgrebe, "Signal Theory Methods in Multispectral Remote Sensing", *John Wiley & Sons*, 2003

[4] C. Lee, D.A. Landgrebe, "Analyzing High-dimensional Multispectral Data", *IEEE Trans. Geoscience and Remote Sensing*, 31(1993),792 - 800

[5] S. Kumar, J. Ghosh, M.M. Crawford, "Best-bases feature extraction algorithms for classification of hyperspectral data", *IEEE Trans. Geoscience and Remote Sensing,* 39 (2001) 1368—79

[6] X. Jia, J. Richards, "Segmented principal components transformation for efficient hyperspectral remote-sensing image display and classification", *IEEE Trans Geoscience and Remote Sensing,* 1999; 37(1): 538–542

[7] R.R. Coifman and M. V. Wickerhauser, *Entropy-based algorithms for best basis selection*, IEEE Trans. Inform. Theory, vol. 38, pp. 713–719, Mar. 1992.

[8] N. Saito and R. R. Coifman, *Local discriminant bases, in Mathematical Imaging: Wavelet Applications in Signal and Image Processing*, in Proc. SPIE, v:2003, 1994, pp. 2–14.

[9] Nuri F. Ince, Sami Arica and Ahmed H. Tewfik, *Classification of single trial motor imagery EEG recordings with subject adapted non-dyadic arbitrary time–frequency tilings*, *J. Neural Eng.* **3** 235-244 , 2006.

[10] P.H. Hsu, Y.H.Tseng, *Feature extraction of hyperspectral data using the Best Wavelet Packet Basis* Proc. IEEE Geoscience and Remote Sensing Symposium (IGARSS), 2002.

[11] A. Cheriyadat, L. M. Bruce, *Decision Level Fusion with Best-Bases for Hyperspectral Classification*. IEEE Workshop on Advances in Techniques for Analysis of Remotely Sensed Data, 2003, USA

[12] H. Kalkan, F. Ince, A.Tewfik, Y. Yardimci, *Classification of Hazelnut Kernels byUsing Impact Acoustic Time- Frequency Patterns*, EURASIP Journal on Advances in Signal Processing, Volume 8 , Issue 1, 2008.

[13] M. A. Hall, *Correlation-based Feature Selection for Machine Learning, Ph.D Diss.*,Hamilton, NZ: Waikato University, Department of Computer Science, 1998.

[14] C.R.Dichter. "Risk Estimates of Liver Cancer Due to Aflatoxin Exposure from Peanuts and Peanut Products", *Food Chemistry and Toxicology*. Vol.22(6):431-437, 1984.

[15] P. M. Mehl, Y. R. Chen, M. S. Kim and D. E. Chan, "Development of Hyperspectral Imaging Technique for The Detection of Apple Surface Defects and Contaminations", *Journal of Food Engineering* (2004) ,61,67-81

[16] T. Pearson, "Machine Vision System for Automated Detection of stained Pistachio Nuts". Lebensm.-Wiss. u.-Technol. Vol. 29:203-209,1996.

CLASSIFICATION OF HAZELNUT KERNELS BY IMPACT ACOUSTICS

Habil Kalkan[1], Yasemin Yardımcı[1]

[1] Informatics Institute, Middle East Technical University

ABSTRACT

An automated hazelnut classification system is developed using sub-band information of impact acoustic signal taken from hazelnut kernels. It is observed that hazelnuts emit different acoustic signals when they impact on a metal plate. Impact acoustic signal of nuts are decomposed with undecimated wavelet transform. Each sub-band is divided into non-overlapping time segments and a feature vector is constructed using the energy values calculated for each segment. A maximum likelihood classifier is used to classify the hazelnut kernels into three groups: *i)* empty or undeveloped kernels *ii)* fully developed nuts with regular shell and *iii)* fully developed nuts with cracked shell. A two stage classification scheme is developed in this study. Hazelnuts kernels are first classified into two classes *i)* empty or undeveloped and *ii or iii)* fully developed classes with 98.20% accuracy. The fully developed hazelnuts are then classified into cracked shell and regular shell classes at the second stage. The developed algorithm detected 95.26% of cracked shells at the second stage.

1. INTRODUCTION

Automated screening systems are frequently used for evaluating quality of manufactured items. With the increased performance and decreased cost of computer technology such systems are also being developed for food quality and safety applications such as detecting infected or low quality fruits, grains, three nuts, etc..[1, 2, 3, 4]. Tree nuts are extensively used in the food industry. Environmental conditions or processing procedures may decrease the nut quality by causing crack or damage to the shell of nuts. These nuts are most prone to molding. Mold infestation can cause aflatoxin formation which is a type of mycotoxin that is linked with various health problems including liver cancer [5]. This phenomenon effects many different types of tree nuts such as walnuts, almonds, pecan, hazelnuts and pistachio nuts, etc.. For pistachio nuts, Pearson showed [6] that nearly all the aflatoxin contaminated pistachios are either damaged by birds or insects before harvesting or are early split ones. The damage at the shell of the kernels allows mold to diffuse into the kernels and cause aflatoxin. Pearson [1] used a machine vision system to classify pistachios nuts as stained (caused by early splitting), unstained or moderated stained with an average of 11% classification error rates. By removal of stained pistachio nuts aflatoxin contamination level of pistachio nut is reduced from 4.8-8.6 interval to 0.04-2.5 ppb [2]. An acoustic sorter system is also developed to separate pistachio nuts with closed shells from the nuts with open shells [7] by using the features extracted from gradient of impact sound signal. In this system, nuts are dropped on a metal plate and the generated impact sound is recorded, processed and used for classification. The classification accuracy of this system is 97%. The same sorting system is used by replacing the sound gradient based features by eigenvalues from PCA of mel-ceptrum coefficients and sound amplitudes [8]. This system correctly classified 96.8% of closed shell pistachios and 98.8% of open shell pistachios. Hazelnut kernels are affected by physiological (plant stress, lack of nutrients) and physical disorder (insect, mold) during maturation, harvesting and processing stages [9]. These disorders decrease the quality of hazelnuts by causing mycotoxin production in kernels and also preventing the maturation of kernels. Hazelnut quality in the market is mainly measured by the ratio of inner kernel weight to the shell weight. Hence farmers separate the empty hazelnuts from fully developed ones before selling the nuts. A mechanical device working with an air fan is used for this purpose. Air fan throws the hazelnuts at lower weight and the rest of the hazelnuts are accepted as fully developed. This system is unable to determine the nuts with cracked shell because hazelnuts with cracked shell have weights that are very similar to hazelnuts with regular shell. A crack or damage at the shell increases the probability of aflatoxin contamination. Therefore, these hazelnuts should be separated from the hazelnuts with regular shell. Hence there is a significant need for a system which is capable of classifying hazelnuts as empty, cracked (fully developed with cracked shell) and regular (fully developed with regular shell) nuts. An acoustic sorter system is used to separate empty hazelnuts from fully developed nuts in [9] and 97.5% of the fully developed kernels and empty kernels are correctly classified by using a combined feature vector of length 78. These features were extracted by five different methods. In the time domain, four parameters of the Weibull function, short-time variances of the original signal and the maximum values in short time windows are used. Frequency domain parameters such as spectral peak

locations and line spectral frequencies are also employed. This binary separation system only separates full hazelnuts from the empty ones and it is not capable of separating the full hazelnuts with regular shells from those with cracked shell. In this paper, an algorithm based on the wavelet features is developed and the mechanical system in [9] is used for classifying the hazelnuts into three classes: i) empty or undeveloped, ii) fully developed with regular shell and iii) fully developed nuts with cracked shell in this paper. This system correctly classified 98.51 % of the fully developed hazelnuts (FuH), and 99.37% of the empty or undeveloped kernels (EmH) for two category case. The LHH sub-band of undecimated wavelet transform is used for this purpose. At the second stage, instead of the LHH sub-band the H sub-band is used and fully developed nuts with cracked shell (CrH) are separated from fully developed nuts with regular shell (ReH). 92.65% of fully developed hazelnuts with regular shells, 95.31% of fully developed hazelnuts with cracked shells are correctly classified at this stage.

2. MATERIAL AND METHODS

2.1 System description

A system is designed to take impact acoustic data. The system (Fig. 1) consist of a pipe through which the hazelnuts slide in, an impact plate that the hazelnuts are dropped on, a microphone for impact sound acquisition and a PC for recording and processing the signals.

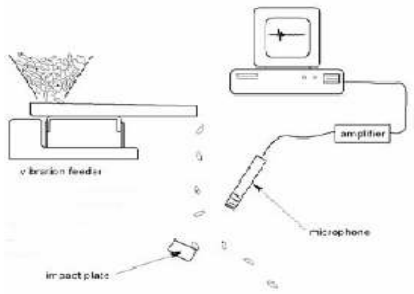

Figure 1: Schematic of experimental apparatus for collecting acoustic emissions from hazelnut kernels.

A stainless steel plate with dimensions 7.5 x 15 x 2 cm is used as the impact plate. The impact plate is fixed to the ground with 1200. This angle prevents the nuts from making multiple impacts. A microphone, sensitive to frequencies up to 20 kHz, is placed 5 cm from the impact plate. The impact acoustic signal is sampled at 44.1 kHz.

2.2 Collection of Samples

'Levant' type hazelnuts which were collected from an orchard in Akcakoca, Turkey in August 2003 are used in this study. The weights of the hazelnuts are measured and the ones less than 0.9 gram are taken as empty or undeveloped nuts. Hazelnuts with weights over 0.9 grams are accepted as fully developed. The shells of these nuts are visually inspected they are further classified as nuts with regular shell and nuts with cracked shell. The weight histogram of the nuts is depicted in Figure 2.

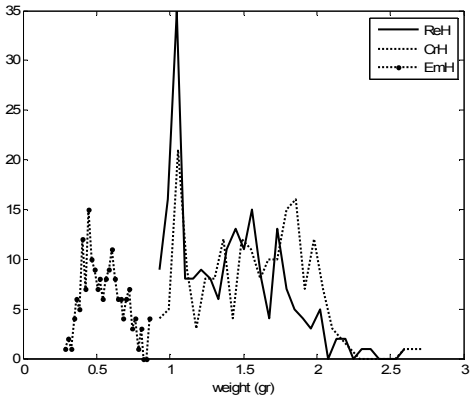

Figure 2: Weights of 'EmH', 'CrH' and 'ReH' hazelnuts.

It is seen that the fully developed nuts with cracked shell have similar weights with the fully developed nuts with regular shell. We randomly selected 183 empty hazelnuts, 190 fully developed nuts with cracked shell and 204 nuts with regular shell from the lot that was already classified into empty or fully developed classes by the standard air fun system and resorted them using their measured weights.

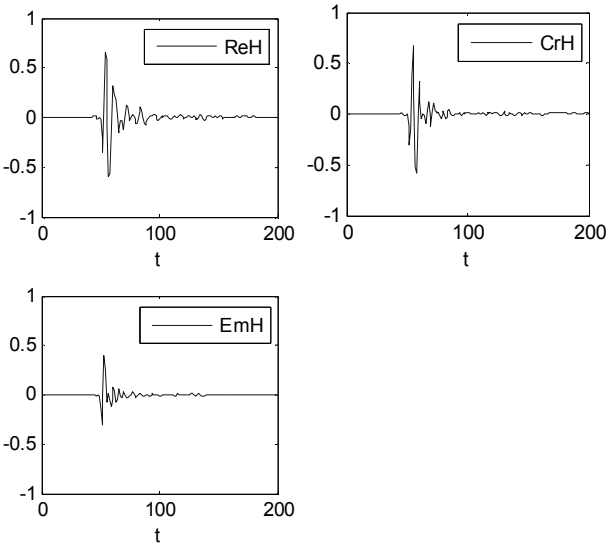

Figure 3: Typical impact acoustic signals of fully developed hazelnuts with regular shell (ReH), fully developed hazelnuts with cracked shell (CrH), empty hazelnuts (EmH).

Typical signals of an empty or undeveloped hazelnut (EmH), a full hazelnut with regular (ReH) and cracked

shell (CrH) are shown in Figure 3. It is observed that empty hazelnuts generate weak signals with respect to fully developed ones (FuH) and their impact signals computed by Equation 1 tend to have lower energy values. The cracked hazelnut impact sounds have similar energy values to those with regular shell indicating similar weights but the cracked impact signals usually have a longer decay time due to the oscillations caused by the crack. We also observed that the characteristic of the impact sound varies significantly between trials on the same hazelnut depending on the impact location on the shell. We decided to use features that allow evaluation of signal characteristics in both time and space. The wavelet family is suitable for this task.

2.3 Feature Extraction

Each hazelnut is dropped on the metal plate and the generated acoustic signals are recorded. This operation is repeated three times for each nut. The acoustic signals of only the first impact are used for classification except when voting is employed for classification.

Figure 5 shows that there is significant correlation between the nuts' weights and the total energy of the impact acoustic signal, x(j), of the nuts computed by

$$e = \sum_{j} |x(j)| \qquad \text{j=1, 2,.. M} \qquad (1)$$

where M is the total number of samples. Hence, signal energy can be used to classify the hazelnuts as empty or fully developed nuts. However, this is not valid for separation of ReH and CrH because they have similar weights and energy values. Therefore more advanced signal processing techniques should be used to extract the relevant features for classification of ReH and CrH. We used Daubechies-8 wavelet filters and 4-level undecimated sub-band decomposition (Fig. 4) to compute the impact acoustics sub-signals.

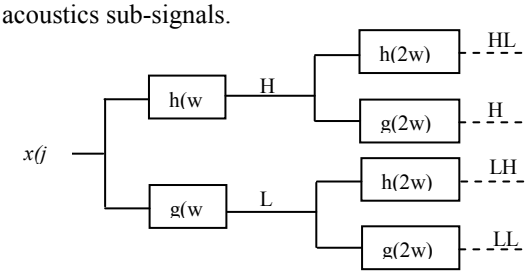

Figure 4: Undecimated wavelet decomposition up to 2 levels. H and L stand for the sub-bands which include high and low frequency components, respectively.

Each sub-signal is divided into K non-overlapping segments that include equal number of samples (L) over time. For the k^{th} segment and the i^{th} sub-signal, the corresponding energy value is computed using

$$e_{ik} = \left[\frac{1}{L} \sum_{j=1}^{L} |x_{ik}(j)| \right]^{t} \qquad (2)$$

i = 1, 2. ..N k=1, 2. . . K

The exponent t , $0 < t \leq 1$, is used to weigh the energy values of individual segments. With N sub-bands and K segments in each sub-band, a KN dimensional feature vector $\underline{v}$ is constructed:

$$\underline{v} = [e_{11}\ e_{21} \ldots e_{K1}\ ,\ e_{12}\, e_{22} \ldots . e_{K2}\ ,\ e_{1N}\, e_{2N} \ldots .\ e_{KN}]^{T} \qquad (3)$$

where ^{T} denotes the transpose operation.

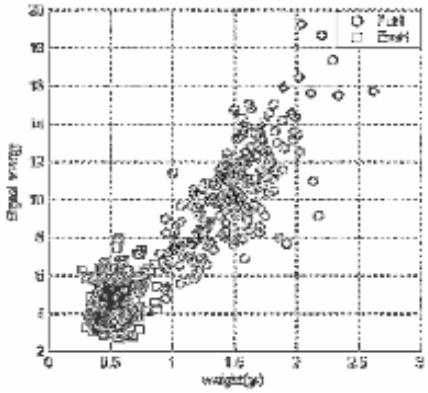

Figure 5: Signal energy of hazelnuts at various weights.

We tried various numbers of segments and sub-bands to be included in the feature vector. It turned out that H band is critical for separation of ReH and CrH. However, LHH sub-band is more effective for separating the empty EmH and fully developed FuH hazelnuts. Inclusion of other sub band energy values to H and LHH sub-band increased the processing time but did not increase classification accuracy. Therefore only the H and LHH sub-bands are used. Most of the energy is contained in the first 80 samples of the signal so this region is divided into 20 segments and the feature vector in Equation 3 is constructed with energy values in Equation 2. The starting point of the signal is taken as the instant with absolute measured value that is greater than 0.01.

The weighting factor, t, essentially limits the effect of segments with very high energy values in the total decision statistic. Its effect on the classification rate between EmH and FuH classes using the LHH band is shown in Figure 6. It is seen that the classification accuracy is higher for $0.50 < t < 0.68$. We used t=0.60 for classifying empty and fully developed hazelnuts in this paper. For the CrH and ReH classification using the H band with t=0.38 gives best results.

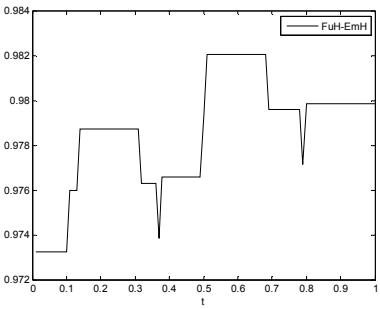

Figure 6: The effect of the energy weighting exponent t on the classification rates between ReH and CrH classes using the H-band.

3. CLASSIFICATION AND RESULTS

The available data in Section 2.2 is partitioned into set1 and set2 each having equal number of samples. In the first set of trials, set1 is used for training and set2 is used for testing. In the second set of trials, the functions of set1 and set2 are reversed for two-fold cross validation. The average classification accuracy of the two trials is determined as classification rate and presented in this study. The feature vector of each set is obtained as described above and the sample mean vectors and sample covariance matrices corresponding to EmH, FuH, CrH, ReH classes are computed.

To test the algorithm, pair wise log- likelihood ratio is used assuming a Gaussian prior distribution, i.e. the likelihood ratio between class a and class b

$$\lambda_{ab} = \log\left(\frac{P(\underline{v} \mid s_a)}{P(\underline{v} \mid s_b)}\right) \qquad (4)$$

is compared to zero where

$$P(\underline{v} \mid s_a) = \frac{1}{(2\pi)^{d/2}|C_a|^{1/2}} \exp\left[-\frac{1}{2}(\underline{v}-\underline{\mu}_a)^T C_a^{-1}(\underline{v}-\underline{\mu}_a)\right] \qquad (5)$$

and μ_a is the mean vector and C_a is the covariance matrix corresponding to ath class. Feature vector $\underline{v}$ is assigned to class ***a*** *if* λ_{ab} >0, else $\underline{v}$ is assigned to class ***b***.

A two stage classification system as in Figure 6 is proposed in this study. Hazelnuts are first subjected to test1 and empty hazelnuts are separated from fully developed ones at this stage. The accepted hazelnuts (fully developed ones) are then subjected to test2 to determine whether they have cracked or regular shell.

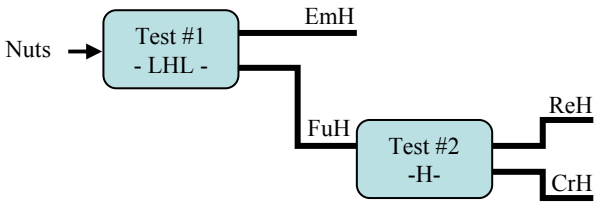

Figure 7: Two stage testing scheme

3.1 Separation of Empty and Fully Developed Hazelnuts

As depicted in Figure 2, only the raw impact signal energy can be effective to segregate empty hazelnuts from fully developed nuts. We used this classifier as the benchmark. The samples are assumed independent and the feature vector v is one-dimensional. The one-dimensional sample mean and sample variance are used for each class in Equation 5 instead of a mean vector and covariance matrix. The classification accuracy even with such a simple feature vector was 96.10 % as shown in Table 1. The energy discrimination is increased to 98.03% when we use the average energy of three acoustic signals of each nut (Table 2). The weights of the misclassified fully developed nuts are observed to be less than 1 gr. which is close to the 0.9gr threshold.

	FuH (Est)	EmH(Est)
FuH (Act)	95.95	4.05
EmH(Act)	3.79	96.21

Table1: Classification rates for EmH and FuH using raw signal energy values. Average rate is 96.10%.

	FuH (Est)	EmH (Est)
FuH (Act)	97.22	2.78
EmH(Act)	1.16	98.84

Table2: Classification rates for EmH and FuH using the average energy of three impact signals for each nut kernel. Average rate is 98.03%.

However, it may be impractical to design an acoustic sorter system which is capable of taking three impact signals for each single nut. Alternatively, classification can be improved by using the LHH sub-band of first impact signals instead of the raw energy values (Table 3).

	FuH (Est)	EmH(Est)
FuH (Act)	98.03	1.97
EmH(Act)	1.63	98.37

Table 3: Classification rates for EmH and FuH by using the LHH sub-band energies with t=0.6. Average rate is 98.20%.

When the LHH band is used with no weighting (t=1.0) only a slight drop in the classification rates will take place as seen in Figure 6. The results for the EmH-FuH classification are summarized in Table 4. The results for the H-band are included because using this sub-band has lower computational complexity and it still gives high classification rates. Furthermore, it is useful for segregation of fully developed nuts as regular and cracked shell nuts as will be demonstrated in Section 3.2 and can be used as the basis for a ternary classification scheme of empty, cracked and regular nuts

METHOD USED	FuH	EmH	Aver.
Classification based on a single pass with raw signal energy values only	95.95	96.21	96.08
Three passes are made and average of raw enery values of passes are used	97.22	98.84	98.03
Single pass decision with LHH sub-band energies and t=0.6	98.03	98.37	98.20
Triple pass decision voting with LHH sub-band energies t=0.6	98.51	99.37	98.94
Single pass decision with H sub-band energies and t=0.38	98.03	96.17	97.10
Single pass decision with H sub-band energies and with t=1.0	96.17	97.80	96.97

Table4: Summary of correct classification rates for EmH and FuH hazelnuts using different techniques.

3.2 Separation of Fully Developed Hazelnuts as Regular and Cracked Shell Nuts

In the second stage of the scheme in Figure 7, fully developed hazelnuts are classified as nuts with regular shell and cracked shell. Very poor classification rates are obtained by using raw signal energies only as shown in Table 5 because the nuts in ReH and CrH classes have impact signals with similar energy.

	ReH (Est)	CrH(Est)
ReH(Act)	70.19	29.81
CrH(Act)	63.16	36.84

Table 5: Classification rates for CrH and ReH using raw signal energy values. Mean rate is 53.51%.

H sub-band was more effective for classifying regular and cracked shell hazelnuts. Again, cross validation tests are made by using half of the first impact acoustic signals of both classes for training and testing. On average, a classification accuracy of 90.12 % is achieved when the other half is used for testing as shown in Table 6.

	ReH (Est)	CrH(Est)
ReH (Act)	86.21	13.79
CrH(Act)	5.88	94.12

Table 6: Classification rates for CrH and ReH using the H band energies with t=0.38. Average rate is 90.12%

Similar classification rates are obtained when the second and third set of impact acoustic signals are used for testing. In practice most of the hazelnuts the system encounters will be with regular shell. The false positives that are classified as cracked shell even though they are regular shell will reduce the number of accepted nuts. The correct classification rates for regular shell nuts can be increased by using majority voting of three individual decisions as shown in Table 7.

	ReH (Est)	CrH(Est)
ReH (Act)	91.18	8.82
CrH(Act)	4.74	95.26

Table 7: Classification rates for CrH and ReH based on majority voting. Average rate is 93.22%.

The LHH band is not suitable for CrH and ReH classification. The mean classification rates are between 73-76% with various t values.

3.3 Ternary Classification

The final goal of the study is to determine the empty, cracked and regular hazelnuts. The highest rates for one step ternary classification of hazelnuts into these three categories are obtained using the H band because this band is effective for both EmH-FuH and ReH-CrH classification. The results are tabulated in Table 8.

	ReH(Est)	EmH(Est)	CrH(Est)
ReH (Act)	86.21	1.47	12.31
EmH (Act)	1.63	94.00	4.37
CrH (Act)	6.40	0.00	93.60

Table 8: Classification rates for EmH, CrH and ReH using H band with t=0.38 using ternary classification.

When the two-step procedure of Figure 7 with LHH band and t=0.60 is followed by the H band and t=0.38, slightly higher classification rates are obtained.

	ReH(Est)	EmH(Est)	CrH(Est)
ReH (Act)	86.21	0.98	12.80
EmH (Act)	1.63	96.18	2.17
CrH (Act)	5.88	1.57	92.54

Table 9: Classification rates for EmH, CrH and ReH using LHH band(t=0.6) followed by H band with (t=0.38)

These results indicate high detection rates for EmH and FuH classes but somewhat high false positives for ReH and CrH classification. This problem is partially alleviated when decision voting based on three measured signals is used as depicted in Table 10.

	ReH(Est)	EmH(Est)	CrH(Est)
ReH (Act)	91.17	0	8.82
EmH (Act)	1.63	96.18	2.18
CrH (Act)	4.73	0.00	95.26

Table 10: Classification rates majority voting for EmH, CrH and ReH using LHH band(t=0.6) followed by H band with (t=0.38).

3.4 Discussion of Results

The algorithm described here consists of two stages. At the first stage in which the empty hazelnuts are separated from the fully developed ones, very high classification rates are obtained. The LHH or the H bands can be used for this purpose. Slightly lower correct classification rates are obtained for separating regular and cracked shell hazelnuts due to similarity of the impact signals. Majority voting is especially useful for reducing the false alarm rates for CrH and ReH classification. If making multiple measurements for the same hazelnut is impractical, it is possible to modify the decision threshold in Equation 4 so that fewer regular hazelnuts are classified as cracked at the expense of missing some cracked shells. This is an economical decision weighting the health risks against the increased price.

4. CONCLUSIONS

New algorithms for segregating regular, cracked and empty hazelnuts are proposed in this study. The algorithm follows a two step procedure in which first the development level of the hazelnut is evaluated and then the fully developed ones are further classified as regular or cracked shell. The algorithm uses LHH and H sub-band energy values weighted nonlinearly to construct the feature vector. A linear classifier is employed for decision making. Over 90% mean classification rates are obtained. Slight improvement is achieved by decision voting that can be employed for multiple measurements.

As future work, the effect of multiple passes of the already classified lots for verification of results will be evaluated. Gaussian Mixture Model and Support Vector Machines will be examined in detail. Classification via audio-visual signals which will be achieved by using impact acoustic signal in conjunction with multispectral band images will be implemented. Impact acoustic signal separation will be tried to increase the nut throughput by allowing multiple nut signals to be captured simultaneously.

5. ACKNOWLEDGEMENTS

This work is partially supported by BAP-08-11-DPT02-K120510 and Tubitak-EEEAG 106E057. The authors would like to thank Tom Pearson, Enis Cetin and Firat Ince for valuable comments and suggestions.

6. REFERENCES

[1] T. Pearson, Machine Vision System for Automated Detection of stained Pistachio Nuts. Lebensm.-Wiss. u.-Technol. Vol. 29:203-209,1996

[2] T. C. Pearson and T. F. Schatzki. Machine Vision system for Automated Detection of Aflatoxin-Contaminated Pistachios. Journal of Agric. Food Chem. Vol. 46:2248-2252,1998.

[3] Dowell, F.E. 1990. An intelligent automated system for determining peanut quality. IEEE International Workshop on Intelligent Robots and Systems, IROS '90, pp. 237-241.

[4] Wang, D., Ram, M.S., Dowell, F.E. 2002. Classification of Damaged Soybean Seeds Using Near-Infrared Spectroscopy. Transaction of ASAE Vol. 45(6):1943

[5] C.R.Dichter. "Risk Estimates of Liver Cancer Due to Aflatoxin Exposure from Peanuts and Peanut Products." Food Chemistry and Toxicology. Vol.22(6):431-437, 1984.

[6] T. Pearson, Separating Early Split From Normal Pistachio Nuts For Removal of Nuts Contamination On The Tree With Aflatoxin. Master Thesis, University of California, 1987.

[7] Pearson, T.C. 2001. Detection of pistachio nuts with closed shells using impact acoustics. Applied Engineering in Agriculture 17(2):249-253.

[8] Cetin, A.E., Pearson, T.C., and Tewfik, A.H. 2004. Classification of Closed- And Open- Shell Pistachio Nuts Using Voice-Recognition Technology. Transaction of the ASAE, Vol. 47(2): 659-664.

[9] I. Onaran, B. Dulek, T. Pearson, Y. Yardımcı and E. Çetin. "Detection of empty hazelnuts from fully developed nuts by impact acoustics." EUSIPCO2005.

Bozulmuş Fındıkların Multispektral Görüntüleme ile Tespit Edilmesi

Detection of Contaminated Hazelnuts by Multispectral Imaging

Habil Kalkan, Yasemin Yardımcı

Enformatik Ensitüsü, Orta Doğu Teknik Üniversitesi
{habil,yardimy}@ii.metu.edu.tr

Özetçe

Tarımsal gıdalarda(fındık, fıstık, incir, mısır, vs) hasat öncesi gelişme; hasat sonrasında ise işleme ve depolama aşamalarında kanserojen etkiye sahip olan aflatoksin oluşabilmektedir. Bu çalışmada yapay olarak aflatoksin bulaştırılmış olan fındık örneklerinin temiz olanlardan multispektral görüntüleme ile ayırt edilmesi üzerinde durulmuştur. Aflatoksinli ve aflatoksinsiz grubundan alınan fındık örneklerinin farklı spektral bantlardaki görüntüleri alınmış ve yapılan incelemeler sonucunda istatistiksel olarak en iyi ayrımı yapan frekans bantları tespit edilmiştir. Fındık örneklerinin 460 ile 500 nm arasında yer alan bantlarındaki yansıma görüntülerinin en yüksek ayrımsallığı verdiği tespit edilmiştir.

Abstract

Agricultural products (hazelnuts, peanuts, figs, corn etc.) can be effected by aflatoxin producing molds on the growing, processing and storage stages. In this study, a method based on multi-spectral imaging is developed to separate the contaminated hazelnut kernels from the healthy ones. The multispectral images of the hazelnuts of contaminated and uncontaminated classes are analyzed and the bands that give the best statistical difference are determined. It is observed that the reflectance images at 460 to 500 nm are the most discriminative bands for aflatoxin contamination.

Giriş

Tarımsal gıdalar (fındık, fıstık, biber, incir, v.s.) gelişme, hasat ve hasat sonrası yapılan işlemler sırasında çeşitli küflere maruz kalmaktadır. Uygun nem ve sıcaklık koşullarında çoğalan küfler gıdada toksik madderin oluşumuna sebep olmaktadırlar. Bu toksinlerden biri olan aflatoksin *Aspergillus* türü küfler tarfından oluşturulmakta olup; belirli miktarların üzerinde alınması canlılarda karaciğer kanserine yol açmaktadır [1]. Avrupa Birliği ülkelerinde kabul edilen oran 4 ppb iken ABD'de 20 ppb'dir. Halihazırda aflatoksin tespiti kimyasal yöntemlerle yapılmakta olup analizi yapılan ürün tekrar kullanıma sunulamamaktadır. Bunun yanısıra kimyasal yöntemler pahalı, çok zaman alan işlemlerdir. Gelişen teknoloji ile gıda örneklerinin tahribatsız yöntemlerle incelenmesi mümkündür. Bu çalışmada multispektral görüntüler kullanılarak aflaoksin içeren fındıklar tespit edilmiştir.

Pearson yaptığı incelemede aflatoksin içeren Antep fıstıklarının tamamına yakınının erken çatlamış veya kabuğu böcekler tarafından zarar görmüş olduğunu tespit etti [2]. Erken çatlayan fıstıkların uç kısmının normal fıstıklara göre daha koyu renkte olduğundan yola çıkarak bilgisayarlı görü ile bu fıstıkları ayıklamış ve çalıştığı fıstık grubunun mevcut aflatoksin seviyesini 4.8- 8.6 aralığından 0.04-2.5 ppb seviyelerine düşürmüştür [2]. Geçmişte araştırma grubumuzun fındık üzerine yaptığı çalışmalarda kabuğun küfe karşı koruyucu özellikte olduğu ve kabuğu çatlak veya kırık olan fındıkların sağlam olanlara nispeten daha fazla aflatoksin içerdiği tespit edildi [3]. Kabuğu çatlak olan fındıklar sağlam olanlardan çarpma seslerine bakılarak ayrıştırıldı[4].

Akustik sinyallerin yanısıra gıda imgeleri de aflatoksin tespitinde kullanılabilmektedir. Pearson [5] spektral yansıma oranlarını (R735 nm/R1005 nm) kullanarak yüksek oranda (>100 ppb) aflatoksin içeren mısırları düşük oranda (<10ppb) içerenlerden %95'lik bir başarım oranı ile ayırabilmiştir. Hirano [6] ise geçirgenlik oranlarını kullanarak (T700 nm/T1100 nm) aflatoksin içeren fıstıkları tespit edebilmiştir. Aspergillus küfleri floresan özelliğe sahip olan kojik asit salınımı

yapabilmektedir. Bu asit mor ötesi (UV) ışık altında floresan ışınımı yapmaktadır. Bu özellik Tyson and Clark [7] tarafından cevizlerde aflatoksin tespiti için kullanılmıştır. Tyson aflatoksin bulaştırılmış cevizleri 320 nm'de ışık veren UV kaynağı altında incelemiş ve örneklerin 440nm ve 490nm'deki yansıma oranlarını aflatoksin ayrımı için kullanmıştır.

Bu çalışmada da yapay olarak aflatoksine bulaştırılmış fındık örnekleri multispektral görüntüleme ile incelendi. UV ışık altındaki fındık örneklerinin 400 nm'den başlayıp 600 nm' ye kadar uzanan bir spekrumdaki görüntüleri 14 farklı bantta alındı. Buna ek olarak fındık öornekleri herhangi bir filtre kullanılmadan da görüntülendi. Bu görüntülerin yansıma gücü histogramından elde edilen ortalama yoğunluk ve değişinti değerleri öznitelik olarak alındı ve iki sınıf arasında en iyi ayrımı yapabilecek olan spektral bantlar tespit edilerek sınıflandırma yapıldı.

1. Örnek Hazırlanması

Temelde sınıflandırma problemi olan bu ayrıştırmayı yapabilecek bir sistem geliştirilmesi için elimizde aflatoksin içeren ve içermeyen fındıklar olması gerekmektedir. Bu fındıkların temini için yapay olarak aflatoksine sebep olacak şekilde küflendirilmesi işlemine gidildi. Küflenme için aflatoksine sebep olan A. Parasiticus türü küf sporu çoğaltılmış ve 1. grup iç fındık örnekleri küfe bulaştırıldıktan sonra 28 C^0 sıcaklık ve %90 nem içeren ortamda 9 gün bekletildi. Bu fındıkların yanısıra 2. bir fındık grubu ise hiç küfe bulaştırılmadan aynı şartlar altında bekletilmiştir. Dokuz günlük sürenin sorunda bu fındıklar ve kontrol amacıyla kullanılacak olan 3. grup fındıklar (herhangi bir işleme tabi tutulmamış) üzerlerindeki zardan kurtulmak amacıyla 130 C^0 15 dakika kavrulmuştur. Kavurma prosedürü tüketim amacıyla piyasaya sürülen kavrulmuş fındıklara uygulanan kavurma prosedürü ile aynı tutulmuştur. Kavrulma işlemi sonrasında görüntüsü alınan fındıklar hemen kimyasal analize tabi tutularak aflatoksin içeriği tespit edilmiştir. Yapılan analizler neticesinde küfe bulaştırılan fındıklarda aflatoksin miktarı 2500–4200 ppb aralığında değişirken küfe bulaştırılmadan nemli ortamda bekletilen fındıklarda ise bu rakam yine standartların üstünde olan 9-185 ppb aralığındadır. Bu durumda ilk iki grup birleştirilerek "aflatoksinli" grup oluşturulmuştur. Kontrol grubundaki fındıklar ise aflatoksinsiz fındık grubu olarak belirlenmiştir.

2. Multispektral Görüntüleme

Multispektral görüntülemede gıda örnekleri birden fazla frekans bandında gürüntülenmektedir. Elde edilen görüntü seti çeşitli amaçlar (sınıflandırma, izleme, inceleme v.s.) için zengin bilgi içeriğine sahip olmaktadır. En yaygın uygulaması sınıflandırma problemlerinde olan multispektral görüntüler çoğunlukla uzaktan algılama [8, 9] amacıyla kullanılmaktadır.

Gıda güvenliğinde kullandığımız multispektral görüntüleme sistemi (Şekil 1); ccd kamera, UV ışık kaynağı, filtreler ve bunların takıldığı filtre platformu, karanlık ortam sağlayan UV kabin ve bilgisayardan oluşmaktadır.

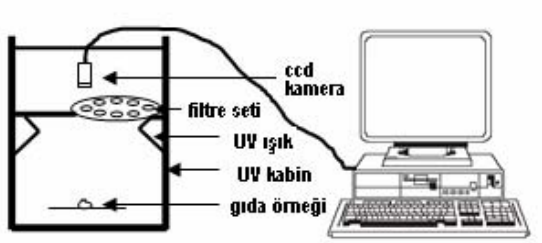

Şekil 1. Multispektral görüntüleme sistemi

Kabin içerisindeki fındık örnekleri filtresiz ve 400 nm'den 510 nm ye kadar 10 nm'lik geçirme bandına sahip filtreler kullanılarak görüntülendi. Bunlara ek olarak merkez ferkansı ve geçirme bandı (550-70nm), (600-40nm) olan filtrelerde kullanılmıştır. Aflatoksinli ve aflatoksinsizler sınıfından rastgele seçilmiş ikişer adet fındık örneğine ait bazı multispektral görüntüler Şekil 2'de verilmiştir.

3. Deneyler ve Sonuçlar

Çalışmada 106 adet aflatoksinsiz, 57 adet de aflatoksinli fındık kullanılmıştır. Multispektral görüntüsü alınan fındıklar hemen kimyasal analize tabi tutulup aflatoksin içeriği belirlenmiştir. Tüm görüntüler öncelikle mercek ve filtre üzerinde biriken toz taneciklerine karşı gürbüzlük sağlamak amacıyla ortanca filtreden (7x7) geçirilmiştir. Kavrulma işlemi sırasında bazı fındıkların yüzeyinde kahverengi zarın tam olarak uzaklaştırılamadığı tespit edilmiştir. Bu bölgeler

farklı yansıtma özelliklerinden dolayı sınıflandırma işlemlerinde ön plana çıkacağından zarlı bölge ve arkaplandan arındırıldı. Fındığı zarlı bölgelerden ve arkaplandan ayırt etmek için 550 nm dalgaboyundaki görüntüsü kullanıldı [Şekil 3-a]. Bu görüntü öncelikle deneysel çalışmalarla tespit ettiğimiz 120 yeğinlik eşiğine göre ikili imge şekline getirildi ve sonrasında görüntü kemirme işlemi ile istenmeyen kısımları ve arkaplanı yok eden maske elde edildi [Şekil 3-b]. Aynı fındığın bütün görüntüleri bu maske kullanılarak zarlı bölge ve arkaplandan arındırıldı [Şekil 3-c].

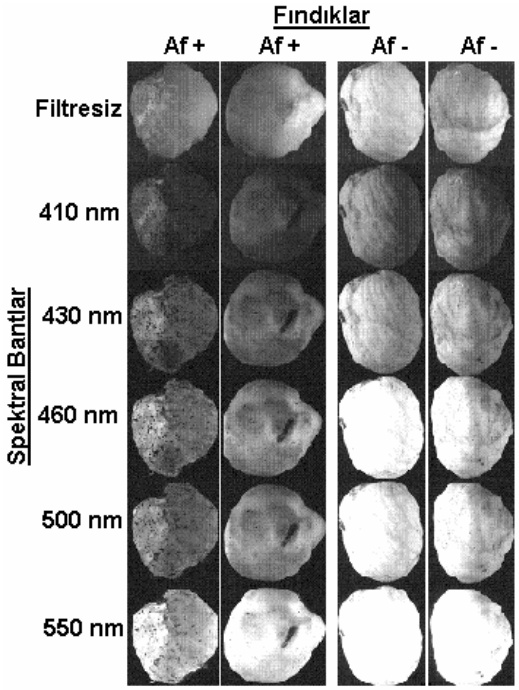

Sekil 2. Aflatoksinli (Af+) ve aflatoksinsiz (Af-) fındıkların değişik dalgaboylarındaki görüntüsü

-a- -b- -c-

Şekil 3. a-) Fındığın 550 nm dalgaboyundaki görüntüsü, b-) maske, c-) maskelenmiş görüntü

3.1 Öznitelik çıkarımı

Temizlenen fındık görüntülerinin histogramları iki farklı eşik değeri (t_1, t_2) kullanılarak 3 farklı bölgeye (B0_t_1, Bt_1_t_2, Bt_2_255) bölündü. Her spektral bantın yeğinlik dağılımı birbirinden farklı olduğundan herbiri için Tablo 1'deki eşik değerleri histogram üzerinde belirlenerek histogramlar bölgelere bölündü.

Bantlar (nm)	t_1	t_2
Filtresiz, 400,420 510,550,600	120	180
410,430,440,450, 460,470,480,490	60	90
500	230	250

Tablo 1: Multispektral görüntülerin deneysel olarak tespit edilen histogram eşik değerleri.

Histogramdaki her üç bölgedeki örneklerin ortalama değeri , μ_s^b , ile değişinti değeri , υ_s^b , öznitelik olarak hesaplandi. Burada ***b*** histogram bölgesini; ***s*** ise spektral bantı göstermektedir. Bu değerler kullanılarak hesaplanan 96 boyutlu öznitelik vektörü ***f*** karekökü alındıktan sonra normalize edildi ve sınıflandırmada kullanıldı.

$$f = \left\{\mu_{400}^1, \mu_{400}^2, \mu_{400}^3, \ldots \mu_{600}^3; \upsilon_{400}^1, \upsilon_{400}^2, \upsilon_{400}^3, \ldots \upsilon_{600}^3\right\}^{1/2} \quad (1)$$

3.2 Sınıflandırma

Herbir fındık örneği için oluşturulan ***f*** öznitelik vektörünün elemanları aralarında ayrımsallığı en yüksek olandan en düşük olana göre Fisher uzaklıkları, ***d***, kullanılarak sıralandı.

$$d = \frac{|\mu_1 - \mu_2|}{\left(\sigma_1^2 + \sigma_2^2\right)} \quad (2)$$

Sıralama sonunda en iyi ilk 6 özniteliğin 450,460 ve 490 nm bandından geldiği tespit edildi. Veriler eğitim ve test seti olarak 2 gruba bölündü ve iki aşamalı bir deney yapıldı. Sınıflandırıcı olarak doğrusal sınıflandırıcı kullanıldı. Uygun sayıdaki öznitelik sayısını tespit etmek amacıyla eğitim ve test gruplarındaki öznitelik vektörlerine sıralanmış öznitelikler birer birer eklendi ve sistem eğitilip test edildi. Deneyin ikinci aşamasında ise test seti eğitim için; eğitim seti ise test için kullanıldı. İki deneyin sonucunun ortalaması sınıflandırma başarımı olarak alındı (Şekil 4).

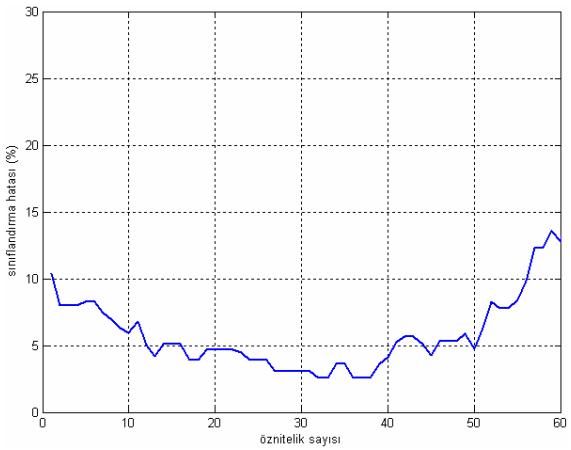

Şekil 4. Değişik sayıdaki öznitelikler ile elde edilen ortalama sınıflandırma hataları.

Şekil 4'de görüleceği üzere öznitelik değerlerinin eklenmesi sınıflandırma hatasını her zaman düşürmemektedir. İlk 32 öznitelik ile en düşük sınıflandırma hatası değeri olan %2.5'e ulaşıldı. Sonrasında öznitelik vektörüne eklenen öznitelikler sınıflandırma hatasını yükseltildi. Bunda öznitelikler arasındaki ilintinin etkili olduğu düşünülmektedir. İlk 32 öznitelik incelendiğinde bunların çoğunluklukla 450, 460, 470, 480, 490, 500 ve 550 nm merkez frekansına ait olan spektral bantlardan seçildiği tespit edildi. Fındıkların filtre kullanılmadan (görünür bant) alınmış görüntülerinden gelen öznitelikler düşük sınıflandırma özelliklerinden dolayı ilk 32 öznitelik arasında yer almamıştır. Sadece filtresiz görüntülerden gelen öznitelikler ile en düşük %8'lik sınıflandırma hatası elde edildi. Bu multispektral görüntülerin aflatoksin içeren fındıkların tespitinde önemli bilgiler içerdiğini göstermektedir.

4. Değerlendirme

Bu çalışmada aflatoksin içeren ve içermeyen zarlı iç fındıkların tespiti multispektral görüntüleri kullanılarak yapıldı. Elde edilen sonuçlar neticesinde spektral bantların sınıflandırma açısından önemli bilgiler taşıdığı görüldü. Doğrusal sınıflandırıcı ile yapılan sınıflandırmada fındıklar %97.5'lik bir doğru sınıflandırma oranı ile sınıflandırılabildi. Spektral bantlarda elde edilecek özniteliklerin çeşitlendirilmesinin sınıflandırma doğruluğunu artıracağı düşünülmektedir. Yapılan çalışma ile fındıkta kimyasal yöntemlerde tespit edilen aflatoksin içeriğinin tahribatsız yöntemlerle hızlı ve düşük maliyetli olarak belirlenebileceği tespit edildi. Sınıflandırmada faydalı bulunan 450-550 nm arasındaki bantları yerel ayırtaç tabanları (YTA-LDB) yöntemi [4] ile birleştirilerek daha az sayıda filtreye gerek duyan ve endüstride kullanılabilecek bir algoritma üzerinde çalışılmaktadır.

5. Teşekkür

Bu çalışma Tübitak EEEAG-106E057 no'lu proje tarafından desteklenmiştir. Çalışmaya katkılarından dolayı Karın Gıda A.Ş.'ye teşekkür ediyoruz.

6. Kaynakça

[1] C.R.Dichter. "*Risk Estimates of Liver Cancer Due to Aflatoxin Exposure from Peanuts and Peanut Products.*" Food Chemistry and Toxicology. Vol.22(6):431-437, 1984.

[2] T. Pearson, "*Separating Early Split From Normal Pistachio Nuts For Removal of Nuts Contamination On The Tree With Aflatoxin*". Master Thesis, University of California, 1987.

[3] H. Kalkan, Y. Yardimci, F. Ince, A. Tewfik, H. Senyuva, M. Arici, T. Pearson, E. Cetin, I. Onaran, "*Separation of damaged shell hazelnut by impact acoustics*" ", XII International IUPAC Symposium on Mycotoxins and Phycotoxins, Istanbul, 2007.

[4] H. Kalkan, F. İnce, A. Tewfik, Y.Yardımcı, "*Classification of Hazelnut Kernels by using Impact Acoustic time-Frequency patterns",* EURASIP Journal on Advanced in Signal Processing, V: 2008, Article ID 247643.

[5] T.C. Pearson, D.T. Wicklow, E.B. Maghirang, F. Xie "*Detecting Aflatoxin in Single Corn Kernels by Using Transmittance and Reflectance Spectroscopy*". Trans. of the ASAE. 2001.

[6] S. Hirano, N. Okawara and S. Narazaki, **"***Near Infra Red Detection of Internally Moldy Nuts***",** Bioscience, Biotechnology, and Biochemistry, 62, No. 1 pp.102-107, 1998.

[7] T.W.Tayson, R.L.Clark, "*An investigation of florescence properties of the aflatoxin –infected pecans".* Trans. ASAE, 17: 942-944, 948, 1974

[8] SF S. Kumar, J. Ghosh, M.M. Crawford: "*Best-bases feature extraction algorithms for classification of hyperspectral data".* IEEE Trans. Geos. and Remote Sensing 39, 1368—79, 2001.

[9] V.E. Brando, A.G. Dekker, "*Satellite hyperspectral remote sensing for estimating estuarine and coastal water quality"*, IEEE Trans. Geos. and Remote Sensing , 41(1378 - 1387), 2003

[10] M. Hall, "*Correlation-based Feature Selection for Machine Learning". Ph.D Diss.*, Hamilton, NZ: Waikato Univ., Depart. of Comp. Science, 1998.

Zaman-Frekans Düzleminde Sınıflandırma için En İyi Özniteliklerinin Elde Edilmesi

Extraction of Optimal Time-Frequency Plane Features for Classification

Habil Kalkan[1], Firat Ince[2], Ahmed Tewfik[2], Yasemin Yardimci[1], Tom Pearson[3]

[1]Enformatik Enstitüsü, Ortadoğu Teknik Üniversitesi, 06531, Ankara
[2]Elektrik ve Bilgisayar Mühendisliği, Minnesota Üniversitesi, MN 55455, ABD
[3]USDA – Zirai Araştırma Birimi, ABD

habil@ii.metu.edu.tr yardimy@ii.metu.edu.tr

Özetçe

Bu çalışmada sağlam ve çatlak fındıklara ait çarpma sesi sinyallerin sınıflandırılmasında kullanılacak en iyi sınıflama potansiyeline sahip olan özniteliklerin otomatik olarak zaman frekans düzleminden elde edilmesi amaçlı yeni bir yöntem anlatılmaktadır. İki farklı sınıfa ait olan akustik sinyaller öncelikle zaman ekseninde yerel kosinus dönüşümü ile sınıflar arasındaki uzaklığı artıracak şekilde bölütlenmiş ve zaman bölütü içerisindeki en ayırımcı frekans bantları indirgenmemiş dalgacık dönüşümü ile seçilmiştir. Oluşan zaman-frekans ayrımsallık haritası kullanılarak öznitelik çıkarımı yapılmış ve akustik sinyaller doğrusal ayrımcı analiz ile sınıflandırılmıştır. Geliştirilen algoritma sağlam ve çatlak fındıkları ayırmada 96% başarıya ulaşmış olup endüstriyel uygulamalar için umut vericidir.

Abstract

A method based on Local Discriminant Bases is developed to extract discriminanting features for classification from time-frequency pattern of one dimensional signals. Acustic signals from two classes are first divided into segments along the time axis according to their discrimination power. The signals in time segments are then decomposed into subbands in binary tree structure by using undecimated wavelet transform. The subband tree is then pruned by assessing the discirimination power of the nodes. The resulting time-frequency map indicates the location of the best features for classification. This map is then used to extract features to be used for classification. It is observed that the extracted features increase the classification accuracy compared to various features previously used for the same problem.

1. Giriş

Sınıflandırma problemlerinde ayrıştırma özelliğine sahip en iyi özniteliklerin belirlenmesi büyük önem taşır. Genelde n boyutlu olan veri uzayı, m boyutlu öznitelik uzayına ($m<n$) dönüştürülerek, sınıflandırma açısından gereksiz veya az öneme sahip olan ölçümlerden arındırmaktadır. Bu yaklaşım sınıflandırma probleminin çözümünü kolaylaştırdığı gibi hızını da artırmaktadır.

Sınıflandırma problemlerinde sinyallerin hem frekans hem de zaman bilgilerini taşıması açısından dalgacık öznitelikleri yaygın olarak kullanılmıştır[1-4]. Bu çalışmalarda genellikle sinyallerin altbantlarındaki dalgacık katsayıları veya bu katsayılardan elde edilen değerler öznitelik olarak kullanılmıştır. Fakat altbantlardaki bilgilerin sınıflandırma açısından önemsiz olduğu düşünüldüğünde bu altbantların kullanılmaması gerekir. EEG sinyallerinde vurgu (spike) tespiti üzerine yapılan çalışmada[3] sinyaller altbantlara ayrılmış, bu altbantlar kullanılarak orjinal sinyal tekrar elde edilmeye çalışılmıştır. Sinyalin geri elde ediminde gözle görülür bir katkısı olmayan altbantlar sınıflandırma için kullanılmamıştır. Benzer şekilde yapılan bir çalışmada yüksek dalgacık katsayısına sahip olan alt bantların sınıflandırmaya katkısı olduğu düşünülerek bu özellikteki bantlardan fazla sayıda öznitelik çıkarılmıştır[1]. Daha önce yaptığımız çalışmada kabuğu çatlak olan fındıkları sağlamlardan ayırt etmek için akustik sinyalleri kullanılmıştır [2]. Bu sinyaller 5. seviyeye kadar alt bantlara ayrılarak altbantların ayrı ayrı ve birbirleriyle olan kombinasyonlarının sınıflandırma oranına etkisi belirlenerek eleme yapılmıştır. Sonuçta bu ayrım için yüksek freakans altbantının yeterli olduğu görülmüştür. Kabuğu çatlak olan fındıkların akustik sinyaller kullanımı ile ayırt edilmesinde hem zaman hem de frekans düzlemindeki bilgilerin kullanılmasının önemi bu konuda yapılan çalışmalarla da belirtilmiştir [5]. Lakin bu çalışmalarda önemli olan alt bantlar deneme yanılma yöntemi ile seçildiginden işlemin yükü fazladır.

Sınıflandırmada kullanılacak olan bilgilerin konumunu otomatik olarak belirlemek amacıyla Yerel Ayırtaç Tabanları (Local Discriminant Bases) methodu geliştirilmiş [6] ve bu method geliştirilerek zaman-frekans düzlemi daha esnek bir şekilde bölümlere ayrılarak [7] elde edilen öznitelikler EEG sinyallerinin sınıflandırılmasında kullanılmıştır. Daha önce yapilan çalışmalar [7, 8] işaretten zaman ve frekans bölgesinde uyarlanabilir olarak öznitelik çıkarmanın onemini ortaya çıkarmıştır. Zaman bölgesindeki uyarlama yerel kosinüs dönüşümü ile gerçeklenmiştir. Daha sonra hez zaman bölgesi içerisindeki en önemli frekans bantları ayrımcı gruplama ile seçilmiştir.

Yerel Ayırtaç Tabanları (YAT) metodu temel alınarak yaptığımız bu çalışmada akustik sinyallerin sınıflandırılmasında önemli olan özniteliklerin zaman-frekans düzlemindeki konumu otomatik olarak tespit edildi. Frekans düzlemi üzerindeki uyarlama hesaplama yükü fazla olan gruplama yöntemi yerine indirgemesiz dalgacık dönüşümü ile hesaplandı. Bu konumlardan elde edilen öznitelikler de Fisher uzaklıklarına göre sıralanarak sınıflandırıcıda kullanıldı. Geliştirilen algoritma sağlam ve çatlak kabuklu fındıkların çarpma sesleri ile ayrımı problemine uygulandı.

2. Veri Toplama

Kabuğu çatlak olan fındık tanelerinde küflenme, kabuğu sağlam olanlara göre daha kolay içeri işleyebilmektedir.

Küflenen fındıklarda insan sağlığı açısından kanserojen etkiye sahip olan aflatoksin maddesi oluştuğundan bu fındık tanelerinin ayırt edilmesi ve ayrı bir ortamda muhafaza edilmesi gerekmektedir. Bu sebeple her iki sınıftan 180 adet fındık tanesi metal bir yüzeye çarptırıldı ve elde edilen akustik sinyaller (Şekil 1) bir mikrofon vasıtası ve 44.1kHz lik örnekleme frekansı ile kaydedildi.

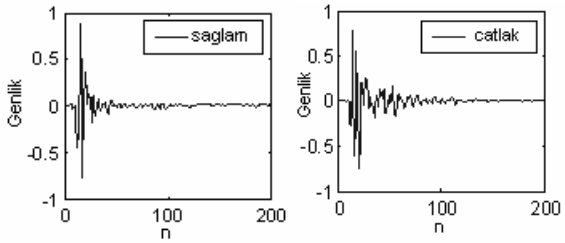

Şekil1: Kabuğu sağlam ve kabuğu çatlak olan fındıklara ait akustik örnek sinyaller.

3. Yöntem

Yerel Ayırtaç Tabanları (YAT) metodu en iyi tabanlar algoritmasının [9] bir uzantısı olarak geliştirilmiş ve ilk olarak Saito ve Coifman tarafından sınıflandırma amaçlı kullanılmıştır[10]. Bu yöntemde sinyaller dalgacık paketleri veya yerel trigonometrik tabanlar kullanılarak agaç yapısında dikgen tabanlara bölünür. Daha sonra bu ağaç belirlenen bir ceza fonksiyonu kullanılarak budanır ve böylece sınıflandırma için gerekli olan tabanlar elde edilir. Sınıflandırma problemlerinde ceza fonksiyonu olarak benzemezlik ölçütü kullanılmıştır. Bu çalışmada YAT yöntemine dayalı olarak sinyaller ilk önce zaman düzleminde bölütlendi ve oluşan bölütler belirlediğimiz bir benzemezlik ölçütü kullanılarak birleştirildi. Oluşan bölütler frekans düzleminde altbantlara bölündü ve sınıflandırma açısından zaman-frekans düzleminde en iyi bölütleme tespit edildi.

3.1. Benzemezlik ölçüsü

Benzemezlik ölçütü zamanda elde edilen bölütler ve herbir bölüt içerisinde oluşan altbantların ayrımsallık potansiyellerini hesaplamak için kullanılabilir. Bu problemde çeşitli ayrımsallık ölçüleri denendi ve aşağıdaki ölçüler seçilip kullanıldı. İki farklı sınıfa ait düzgelenmiş enerji dağılımları p ve q olarak ifade edildiğinde iki sınıf arasındaki uzaklık (benzemezlik) ölçüsü aşağıdaki gibidir.

- Simetrik Kullback Leibler uzaklığı (J ayrımı)

$$J(p,q) = I(p,q) + I(q,p)$$
$$I(p,q) = \sum_{i=1}^{n} p_i \log \frac{p_i}{q_i} \quad (1)$$

- Euclidean uzaklığı

$$D(p,q) = \|p_i - q_i\|^2 = \sum_{i=1}^{n} (p_i - q_i)^2 \quad (2)$$

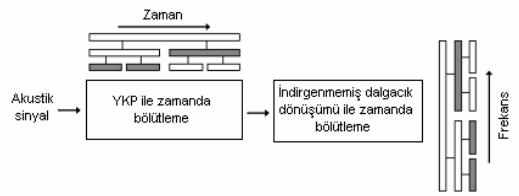

Şekil 2: Zaman-frekans düzleminde bölütleme şeması

3.2. Zaman düzleminde bölütleme

Yapılan incelemelerde akustik sinyallerin çarpma anı, çarpmadan hemen sonraki ve daha sonraki bölümlerinde farklı özellikler gösterdiği için akustik sinyallerin yerel olarak incelenmesi gerektiği sonucuna varıldı. Sinyallerdeki yerel inceleme için araştırmacılar genellikle kısa pencereli Fourier dönüşümünü kullanmışlardır. Bu pencereler çoğunlukla üst üste binecek şekilde seçilirler. Böyle bir analiz *n* boyutlu sinyal uzayını daha da büyütüp gereğinden fazla dönüşüm katsayısı sağladığından sınıflamada kullanılması verimli değildir. Fakat sonrasında yapılan çalışmalarda [6,7] yerel kosinüs paketlerinin (YKP) üst üste binen pencereler ile kullanımının daha avantajlı olduğu görülmüştür. YKP üst üste düşen pencereler kullanmasına rağmen işareti gereğinden fazla dönüşüm katsayısı yaratmadan (complete) temsil edebilmektedir. Bu yüzden bu çalışmada sinyaller YKP kullanılarak zaman ekseninde ağaç yapısıyla (katmanlar halinde) bölümlere ayrıldı (Şekil. 2).

YKP zaman eksenini yumuşak çan şekilli ve üst üste binen pencereler kullanarak bölütler [11]. Bu pencereler aşağıdaki özellikteki kesme fonsiyonu r(t)'den oluşturulur.

$$\left|r(t)^2\right| + \left|r(-t)^2\right| = 1 \quad t \in R$$
$$r(t) = \begin{cases} 0, & t \le -1 \\ 1, & t \ge 1 \end{cases} \quad (3)$$

Örnek bir r(t) fonksiyonu aşağıdaki gibidir.

$$r(t) = \begin{cases} 0, & t \le -1 \\ \sin\left[\frac{\pi}{4}\left(1 + \sin(\frac{\pi t}{4})\right)\right], & -1 < t < 1 \\ 1, & t \ge 1 \end{cases} \quad (4)$$

Öncelikle her iki sınıftan sistemin eğitimi için kullanılacak olan sinyaller, ağaç yapısındaki her bir boğum için uygun büyüklükteki YKP ile temsil edildi. Sonra her bir boğumdaki açılım katsayılarının karesi alındı ve kendi sınıfları içerisinde düzgelendi. Her iki sınıfa ait bütün boğumlardaki ortalama enerji spektrumu hesaplandıktan sonra sınıflar arasındaki mesafe Kullback Leibler uzaklığı ölçütü kullanılarak hesaplandı. Sonra her bir boğum içerisindeki uzaklık değerleri toplanarak boğumlar tek bir uzaklık değeri ile ifade edildi. Sonuçta oluşan ağaç yapısı en yüksek ayrımsama gücüne sahip olan boğumları belirlemek için aşağıdan yukarıya aşağıdaki algoritma kullanılarak budandı.

1.budama algoritması

Eğer $J_{anne\ boğum} >= (J_{\textbf{çocuk1}} + J_{çocuk2})\ x\ \varphi$,

anne boğumu koru
değilse
çocuk boğumları koru

Burada J_i her iki sınıftaki i. boğumlar arasındaki Kullback Leibler (1) uzaklığıdır. Formüldeki φ deneysel olarak belirlenmiş bir katsayı olup bölütlemenin daha gürbüz olması açısından yapılan deneyler neticesinde 0.95 olarak belirlendi. Algoritma, çocukların toplam ayrımcılığının %95'ine sahip olması durumunda anne boğumu korur. Aksi takdirde anne boğumun bölünmesine karar vererek çocuk boğumları korur.

3.3. Frekans düzleminde bölütleme

Yaptığımız gözlemlerde fındıklardan elde edilen akustik sinyallerin zamanda düzgün hizalanmadığı ve aralarında faz farkı olabildiği gözlendi. Bu yüzden işareti temsil ederken kaydırma karşı değişimsiz dönüşümlere ihtiyaç duyulmaktadır. Sınıflandırma problemlerinde kaydırma karşı değişimsiz dönüşümlerin önemi yapılan çalışmalarlada tespit edilmiş[6-8] ve bu sistemlerden bir tanesi olan indirgenmemiş dalgacık dönüşümü de sınıflandırma problemlerimde kullanılmıştır [12].

Bu çalışmada da frekans düzleminde bölüntüleme için indirgenmemiş dalgacık dönüşümü kullanıldı. Zaman düzleminde oluşan her bir bölüm frekans düzleminde ekseninde 4. seviyeye kadar altbantlara bölündü ve oluşan oluşan ağaç şeklindeki yapının her bir boğumu (altbant) içerdiği dalgacık katsayılarının enerjisinin toplanması ile elde edilen tek bir sayı ile ifade edildi. Herbir boğumun düzgelenmiş enerji dağılımı hesaplandı ve her iki sınıfta birbirine karşılık gelen dağılımlar arası mesafe Euclidian uzaklığı (*d*) ile belirlendi. Daha sonra boğumlar aşağıdaki algoritma ile budandı.

2.budama algoritması

Eğer $d_{anne\ boğum} > maks\ \{d_{\textbf{çocuk1}}, d_{çocuk2}\}$

maks $\{d_{\textbf{çocuk1}}, d_{çocuk2}\}$*' u anne ata değilse*
çocuk boğumları söndür

4. Deneyler ve Sonuçlar

Kabuğu sağlam ve çatlak olan fındıklardan elde edilen sinyallerin ilk 758 örneği alındı ve ilk önce zaman düzleminde en kısa boğumda 48 örnek olacak şekilde 4. seviyeye kadar bölütlendi. Oluşan ağaç yapısındaki bölütleme Bölüm 3.2' de belirtilen algoritma ile budandı ve ayrımsama gücü en yüksek olan bölütleme elde edildi. Yapılan deneylerde farklı setlerin zamanda farklı bölütlemeyi tercih ettiği görüldü (Şekil.3). Bu da algoritmanın farklı veri setlerine sağladığı uyumun göstergesidir.

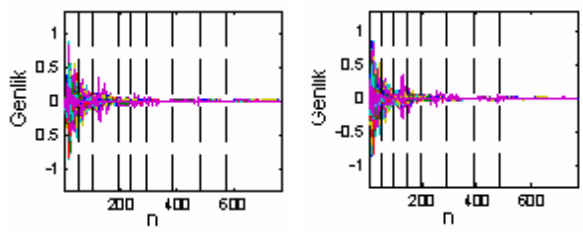

Şekil 3. İki farklı veri setinin zamanda bölütlemesi

Zaman ekseninde oluşan her bir bölüt frekans ekseninde 4. seviyeye kadar indirgenmemiş dalgacık dönüşümü ile ağaç şeklinde alt bantlara bölündü ve sınıflandırma için en gerekli alt bantlar Bölüm 3.2' deki algoritma ile budandı. Zaman eksenindeki ilk iki bölütte seçilen altbantlar Şekil 4' de verilmektedir.

Şekil 4.(a) birinci ve (b) ikinci zaman bölütünde seçilen altbantlar

Zaman ve frekans ekseninde yapılan bölütlemeler birleştirildiğinde bir zaman-frekans ayrımsallık (ZFA) haritası elde edildi. Kullandığımız veri setlerinde yaklaşık olarak 90 altbantlık ZFA haritası oluşdu. Öznitelik çıkarımı bu harita doğrultusunda yapıldı ve sadece haritada belirtilen altbantlardaki sinyal enerjileri öznitelik olarak seçildi. Son aşama olarak bu özniteliklerin olasılık dağılım fonksiyonları hesaplandı ve iki sınıfa ait dağılımın Euclidian mesafesi alınarak sınıflandırma potansiyeli belirlendi. Öznitelikler elde edilen bu değere göre büyükten küçüğe (en yüksek ayrımsama potansiyelinden en küçüğe doğru) doğru sıralandı. Elde edilen bu 90 öznitelikten 25 tanesi konumları ve ayrımsallık potansiyelinin görülmesi açısından Şekil 5.'de verildi.

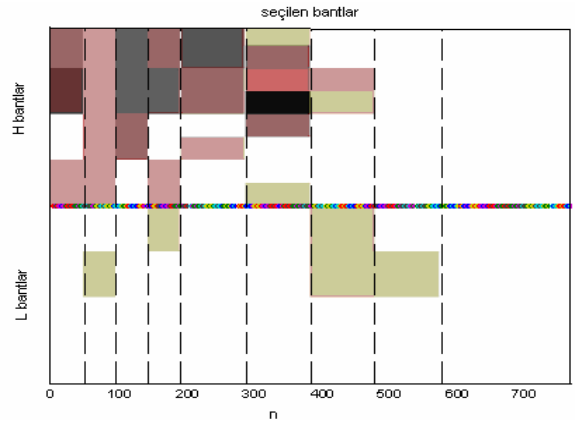

Şekil 5. ZFA haritası. Koyuluk özniteliğin önemine işaret etmektedir.

Şekilde görüldüğü üzere kabuğu sağlam ve kabuğu çatlak olan fındıkların ayırt edilmesinde en önemli ayırt edici bilgiler fındık sesinin çarpma ve çarpma sonrası bölgedeki yüksek frekanslarında bulunmaktadır.

Oluşan ZFA haritası kullanılarak bütün sinyallerden öznitelikler çıkarıldı ve doğrusal ayırtaç sınıflandırıcı ile test edildi. İhtiyaç duyulan en iyi öznitelik sayısının belirlenmesi açısından öznitelikler öznitelik vektörüne teker teker eklenerek sınıflandırıcıda kullanıldı (Şekil 6).

Altbant ayrışımında Daubechies ve Coiflet dalgacık ailesi kullanılmıştır. Yüksek sınıflandırma oranına sebep olan en uygun dalgacık fonksiyonunun tespiti açısından Daubechies 1-10 dalgacıkları ve de Coiflet 1-5 dalgacıkları incelendi ve en iyi sınıflandırma oranı Coiflet 5 tipi filtre ve 24 boyutlu öznitelik vektörü; Daubechies 9 tipi filtre ve 14 boyutlu öznitelik vektörü ile elde edildi.

Şekil 6'da YAT metodu ile elde ettiğimiz öznitelikler aynı problemin çözümümünde kullanılan altbant dalgacık öznitelikleri[2] ve ses işleme öznitelikleri[5] ile karşılaştırıldı. Altbant dalgacık öznitelikleri en iyi sınıflandırma oranına sahip olan alt bantların ve bu bantlardaki en iyi özniteliklerin denemelerle test edilmesiyle belirlenen 20 öznitelikten en yüksek ayrımcılığı olan 12'si ile en düşük sınıflandırma

oranına erişildi. Ses tanımaya dayalı geliştirilen yöntemde sinyalin kısa zamanlı değişintilerinden, maksimum genliğinden, spectral tepe konumlarından, Weibull dağılımı genliği ve ölçekleme parametrelerinden çıkarılan 70 adet öznitelikden en ayrımcı 25 öznitelik ile en düşük sınıflandırma hatasına erişildi. Bizim geliştirdiğimiz yöntemde ise elde edilen 90 öznitelikten 24 tanesi ile en düşük hata oranına ulaşıldı(Tablo 1).

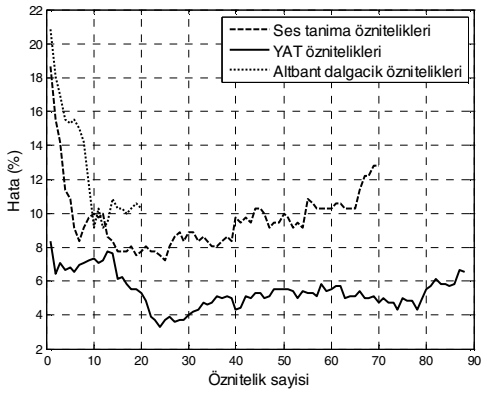

Şekil 6: Farklı öznitelikler ile sınıflandırma hata oranı

Her üç metodunda en iyi sınıflandırma oranlarına bakıldığında (Tablo 1) geliştirdiğimiz YAT algoritmasından elde edilen özniteliklerle çok daha yüksek sınıflandırma oranına erişilmiştir.

Yöntem	Kesinlik (%)
Altbant dalgacık öznitelikleri (12)	90.83
Ses tanıma öznitelikleri (25)	92.77
YAT öznitelikleri (24)	96.66

Tablo 1: YAT öznitelikleri ile ulaşılan sınıflandırma oranlarının diğer yöntemlerle elde edilen sonuçlarla karşılaştırılması.

4. Değerlendirme

Bu çalışmada zaman-ferakans düzleminden otomatik öznitelik seçimi yapılarak kabuğu sağlam olan fındıklar kabuğu çatlak olanlardan ayırt edilmiştir. Özniteliklerin belirlenmesi için sinyaller önce zaman düzleminde yerel kosinüs paketleri kullanarak ağaç yapısında bölütlere bölündü. Bu ağaç yapısındaki boğumlar ayrımsallık kriteri göz önüne alınarak budandı. Zaman düzlemindeki her bir bölüntü frekans düzleminde indirgenmemiş dalgacık dönüşümü ile alt bantlara bölündü ve oluşan altbantlar gene ayrımsallık kriteri baz alınarak budandı. Oluşan zaman-frekans ayrımsallık haritası kullanılarak öznitelikler belirlendi ve doğrusal ayırtaç sınıflandırıcı ile sınıflandırma yapıldı. Önerilen özellik çıkarma ve sınıflama sistemi %96.6 sınıflama başarımına ulaştığı gözlemlendi. Yapılan çalışmada kullanılan veri seti için en iyi ayrıştırıcı özniteliklerin uyarlanabilir olarak yüksek frekans bölgelerinden seçildiği görüldü. Geliştirilen metod sanayide sağlam ve çatlak fındık ayrımını daha yüksek hassasiyet ile ayırabilecek sistemlerin geliştirilmesi icin umut vericidir.

5. Teşekkür

Bu çalışma NSF (National Science Foundation) ve Tübitak EEEAG-106E057 no'lu proje tarafından desteklenmiştir.

6. Kaynakça

[1] S. Pittner and S.V. Kamarti, "Feature Extraction From Wavelet Coefficients for Pattern Recognition Tasks". *IEEE Trans. On Pattern Analysis and Machine Intelligenc*e. Vol:21(1), 1999

[2] H.Kalkan, Y Yardimci, "Classification of hazelnuts by impact acoustics". *IEEE MLSP 2006.*

[3] T.Kalayci and Ö.Özdamar, "Wavelet Preprocessing for Auomated Neural Network Detection of EEG Spikes", *IEEE Engineering in Medicine and Biology*, Vol:14, 1995.

[4] J. N. Gowdy and Z. Tufekci, "Mel-scaled discrete wavelet coefficients for speech recognition," *Proc. of IEEE Acoustics, Speech, and Signal Processing*, vol.3, 2000.

[5] I. Onaran, B. Dulek, T. Pearson, Y. Yardımcı and E. Çetin. "Detection of empty hazelnuts from fully developed nuts by impact acoustics*." EUSIPCO2005*.

[6] N. Saito, R.R. Coifman, "Local discriminant bases", *Proc. SPIE*,2303,2-14,1999.

[7] Nuri F. Ince, Sami Arica and Ahmed H. Tewfik, "Classification of single trial motor imagery EEG recordings with subject adapted non-dyadic arbitrary time–frequency tilings". *J. Neural Eng.* **3** 235-244 , 2006.

[8] R.R. Coifman and M. V. Wickerhauser, "Entropy-based algorithms for best basis selection" *IEEE Trans. Inform. Theory*, vol. 38, pp. 713–719, Mar. 1992.

[9] N. Saito and R. R. Coifman, "Local discriminant bases, in Mathematical Imaging: Wavelet Applications in Signal and Image Processing II," *in Proc. SPIE*, vol. 2303,1994.

[10] Wickerhauser M V 1994 "Adapted wavelet analysis from theory to software" (Massachusetts: A.K. Peters).

[11] Nuri F. Ince, Ahmed H. Tewfik and Sami Arica, "Extraction subject-specific motor imagery time–frequency patterns for single trial EEG classification", Computers in Biology and Medicine : *Special issue on wavelet algorithms in medical problems, Elsevier*

[12] M. Unser, "Texture Classification and Segmentation Using Wavelet Frames", IEEE *Trans. on Image Processing*, 4(11) 1995.

XII International IUPAC Symposium on Mycotoxins and Phycotoxins

Abstract 1:

Separation of damaged shell hazelnut by impact acoustics

Habil Kalkan, Yasemin Yardimci, Firat Ince, Ahmed Tewfik, Hamide Senyuva, Muhammed Arici, Tom Pearson, Enis Cetin, Ibrahim Onaran

In this presentation, techniques for noninvasive detection of hazelnuts with damaged shells will be described. We will first present the HPLC results of aflatoxin measurements on A. Parasiticus contaminated hazelnuts with different levels of damage to the shell. These results show that intact shells form strong barriers against A. Parasiticus contamination during storage but any crack or damage on the shell eliminates this capability. Motivated with this result, we developed new techniques based on impact acoustics to segregate hazelnuts with cracked or broken shells from intact ones. The acoustic system processes the sound signals generated by the impact of the hazelnuts on a metal plate and determines the hazelnuts with intact and cracked or broken shells with over 95 percent accuracy. Such nuts with damaged shells are more prone to A. Parasiticus contamination and these nuts can be separated from the rest of the lot by a pneumatic system. This segregation will largely limit the spread and infusion of A.Parasiticus.

Abstract 2:

A Novel Prospective Technological Approach: Machine Vision Techniques for Noninvasive Aflatoxin Detection in Chilly Peppers

Habil Kalkan, Pelin Beriat, Meltem Özcan, Yasemin Yardımcı, Pervin Basaran

In this presentation, machine vision techniques for noninvasive and rapid detection of aflatoxin contamination in Maraş peppers will be described. Modern signal processing techniques based on texture analysis and image fusion will be evaluated. This approach will use both local and global distribution of reflectance energy under various illumination (UV and visible bands). Therefore it will provide more detail about the food sample under investigation. The correlation between the image features and aflatoxin levels will be investigated.

TÜBİTAK
PROJE ÖZET BİLGİ FORMU

Proje No: 106E057

Proje Başlığı:

Tahribatsız ve Hızlı Yöntemlerle Gıdalarda Kalite Kontrolü

Proje Yürütücüsü ve Araştırmacılar:

Prof.Dr.Yasemin Yardımcı (Yürütücü)

Yrd. Doç.Dr. Pervin Başaran (Yrd. Araştırmacı)

Projenin Yürütüldüğü Kuruluş ve Adresi:

Enformatik Enstitüsü, 06531, ODTÜ, Ankara

Destekleyen Kuruluş(ların) Adı ve Adresi:

Projenin Başlangıç ve Bitiş Tarihleri: 01.07.2006- 31.12.2008

Öz (en çok 70 kelime)

Bu projede fındık ve kırmızı biberlerin kanserojen aflatoksin maddesi barındıranlarının görüntü ve ses işlemeye dayalı yöntemlerle tespit edilmesi üzerine algoritmalar geliştirilmiştir. Kabuklu fındıklar için kabuğu sağlam ve çatlak olanlar çarpma sesine dayalı olarak; iç fındıklar (kavrulmuş veya naturel) ve kırmızı biberler ise hiperspektral görüntülerine dayalı olarak ayırt edilmiştir. Bu ayrıştırma için alınan ses ve görüntü sinyallerinden çeşitli öznitelikler çıkartılmış ve en yüksek başarımı verenler tespit edilmiştir. Geliştirilen algoritma ile kabuklu fındıklar %96, kavrulmuş fındıklar %97, naturel fındıklar %85, kırmızı biberlerde %80 lik başarım oranları ile sınıflandırılmıştır.

Anahtar Kelimeler:

Hiperspektral görüntü işleme , akustik sinyal işleme, öznitelik çıkarımı ve seçimi, gıda güvenliği

Fikri Ürün Bildirim Formu Sunuldu mu **Evet** ☐ **Gerekli Değil** ☒

Fikri Ürün Bildirim Formu'nun tesliminden sonra 3 ay içerisinde patent başvurusu yapılmalıdır.

Projeden Yapılan Yayınlar:

- H. Kalkan, Y. Yardimci *"Feature Extraction from Hyperspectral Data by 2D Local Discriminant Bases"*, Submitted to Pattern Recognition (Elsevier)
- H. Kalkan, F. Ince, A.Tewfik, Y. Yardimci, T. Pearson *"Classification of Hazelnut Kernels by Using Impact Acoustic Time- Frequency patterns"*, EURASIP Journal on Advances in Signal Processing, V: 2008, Article ID 247643
- N. Ince, I. Onaran, T. Pearson, A.Tewfik, A.E.Cetin, H.Kalkan, Y.Yardimci, Identification of Damaged Wheat Kernels and Cracked Hazelnuts with Impact Acoustics Time Frequency Patterns, Transactions of the ASABE, 51(4): 1461-1469, 2008.
- H. Kalkan, Yasemin Yardımcı, "Extraction of Discriminative Features from Hyperspectral Data", IEEE SSTDM Workshop on International Conference on Data Mining 2008,Pisa, Italy.
- H. Kalkan, Y. Yardımcı, *"Classification of Hazelnut Kernels by Impact Acoustics"*, IEEE MLSP 2006, Dublin
- Nuri F. Ince ,I. Onaran , A. H. Tewfik , H.Kalkan, T. Pearson, A.E. Cetin, Y.Yardimci, *"Wheat and Hazelnut Inspection with Impact Acoustics Time-Frequency Patterns"*, 2007 ASABE Annual

International Meeting, Minneapolis, USA

- H. Kalkan, M. Özcan, Y. Yardımcı, P. Basaran,P. Beriat, *"A Novel Prospective Technological Approach: Machine Vision Techniques for Noninvasive Aflatoxin Detection in Chilly Peppers"*, XII International, IUPAC Symposium on Mycotoxins and Phycotoxins, Istanbul,2007
- H. Kalkan, Y. Yardimci, F. Ince, A. Tewfik, H. Senyuva, M. Arici, T. Pearson, E. Cetin, I. Onaran, *"Separation of damaged shell hazelnut by impact acoustics"*"", XII International IUPAC Symposium on Mycotoxins and Phycotoxins, Istanbul, 2007
- H. Kalkan, F. Ince, A. Tewfik ,Y. Yardimci, T. Pearson, "Extraction of Optimal Time-Frequency Plane Features for Classification", IEEE SIU, Eskisehir, 2007
- H. Kalkan, Yasemin Yardımcı. "Detection of Contaminated Hazelnuts by Hyperspectral Imaging", IEEE SIU, Didim, 2008